



The University of
Nottingham

UNITED KINGDOM • CHINA • MALAYSIA

The Development and Application
of an Antibody Microarray as a
Diagnostic Platform for COPD

By

Senthooran Selvarajah

BSc, MSc

Thesis submitted to the University of Nottingham for the degree of
Doctor of Philosophy (PhD)

February 2013

Abstract

According to the Global Initiative for Chronic Obstructive Lung Disease (GOLD) Management Guidelines (2001), the definition of COPD is “a disease state characterised by airflow limitation that is not fully reversible. The airflow is usually progressive and associated with inflammatory responses of the lungs to noxious particles and gases.” It is becoming an increasing prevalent problem worldwide, with the incidences of morbidity and mortality continually increasing and promoting a lower quality of life in individuals that continue to suffer from it.

To date, there is still an incomplete understanding of the pathogenesis of the disease resulting in poor diagnosis and treatment plans for COPD that are insufficient in preventing a decline in lung function. In recent years, research has focussed on discovering a set of biomarkers that could improve our understanding of pathogenesis of disease. The ability to measure a vast array of biomarkers simultaneously is highly desirable however the cost associated is somewhat prohibitive. Current methods centre on measuring the presence or absence of multiple biomarkers in patient samples compared to controls.

As COPD is a multi-component disease which encompasses diseases such as emphysema and chronic bronchitis, it may be necessary to look at biomarker patterns within each disease category. A variety of immune effector cells are known to lead to the pathophysiology of COPD including neutrophils, macrophages and CD8 T-lymphocytes that are all documented to be increased in number and contribute to the inflammatory process.

Protein microarrays are used as a measurement tool to determine and quantify the presence or amount of proteins that exist in biological samples (i.e. blood, sputum,

urine etc). The wide use of protein microarray technology has advanced diagnosis and management of multifactorial diseases such as cancer, autoimmunity and allergy.

At present, multiple microarray kits are available to researchers at a large cost which make it impractical for most research groups to investigate multiple biomarkers of interest simultaneously. Here we show development, validation and implementation of our bespoke in-house microarray platform enabling quantitative and simultaneous analysis of multiple protein biomarkers at a reasonable cost. The methodology is based on the traditional sandwich ELISA; antibodies are immobilised on poly-L-lysine coated glass and signals amplified and quantified through fluorescence. The accuracy and reproducibility of the in-house microarray was investigated using the guidelines outlined by the Food and Drug Administration (FDA) for pharmacokinetic assay validation. The assay was shown to have high reproducibility with assay accuracy between 80-120% and precision within 20% coefficient of variation, except in very low abundant cytokines such as IL-10, where the CVs were higher due to the variation at the lowest concentrations in sera. Importantly there were no significant differences between ELISA and microarray.

This microarray platform was then used to study a selection of healthy controls (n=12), healthy smoking controls (n=36) and COPD patients (n=60) to see if there was a difference in the expression of the 16 biomarkers tested. The overall analysis of the 16 biomarkers investigated in this study, a significant increase in expression of eotaxin-2 was observed in the sera those that have COPD compared to healthy controls and healthy smoking controls. This suggests that eotaxin-2 may potentially be responsible for the recruitment and activation of multiple cytokines which in turn lead to the inflammatory cascade observed in COPD.

COPD severity is divided into four categories according to international guidelines outlined by the Global Initiative for Chronic Obstructive Lung Disease (GOLD). This is often known as stage 1 (mild), stage 2 (moderate), stage 3 (severe) and stage 4 (very severe). This is based on the forced expiratory volume per second (FEV-1%).

Interestingly when investigating the different severities of GOLD in COPD, it was observed that at the highest stage of GOLD (stage 4), the expression of 15 of the 16 biomarkers had dropped significantly in comparison to the other stages. This may suggest that at this point of the disease process, the immune system may in fact be suppressed in alliance to hypoxia experienced by an individual.

Additionally it has to be acknowledged that the medication that the COPD patients were on were not available prior to analysis. It has to be taken into account that patients at GOLD stages 3 and 4 could be likely to be on a high dose of inhaled corticosteroids, which are immunosuppressive which would lead to drop in the 15 cytokines observed. However without the information available, it cannot be definitive to make such conclusions.

Hence this work offers an understanding into the development of a bespoke microarray platform that is capable of investigating protein biomarkers in any disease setting.

Declaration

The work presented in this thesis was performed between 2010 and the end of 2012 in the School of Molecular Medical Sciences, University of Nottingham, UK. Apart from the help and advice mentioned in the Acknowledgements, the work described here is totally my own. This thesis has not been previously submitted for any other degrees.

Senthooran Selvarajah

August 2013

Acknowledgments:

I would like to thank my supervisors Dr Fairclough and Dr Tighe for giving me an opportunity to undertake this interesting and challenging project. Their advice and expertise in their respective research fields was invaluable to me in both my lab and writing-up periods. I thoroughly enjoyed many “educational” supervision meetings where I feel I have not only learnt about my research field but also many other aspects of life which perhaps I wouldn’t have envisaged at the beginning of my PhD!

Additionally I would like to thank Dr Ian Todd for his measured and valuable input he had in my PhD. I don’t think he would have imagined the boy he lectured at 18 at undergrad level would go onto study for a PhD! I feel thoroughly privileged to work under all three of my supervisors who have all been inspirational in their individual ways.

I would like to thank Tim Harrison for his clinical input and vision he had in setting up the start of the PhD and his financial contribution in enabling this PhD to be completed. I am grateful to the Nottingham BRU for funding this work. I’m deeply indebted to Charlotte Bolton in providing the clinical samples for me to use for this project.

I want to acknowledge Dr Ola Negm whose friendship and expertise when I joined the group was invaluable in enabling me to find my feet quickly. The manner in which she conducted her research in the lab was the template which I incorporated into my own work. I would like to thank the remainder of the MBTI research group whose banter over the course of the last three years kept me sane and focussed.

I would like to thank Sameer, Osman, Arpit and the JLS crew whose calls, skypes and messages enabled me to keep me going in hard times. I would sincerely like to thank Pooja for being my regular punch-bag of frustration. She has understood my emotions and kept me focussed and determined as ever to make this PhD a success.

Last but not least, I would like to thank my family especially my mum, dad and sister who have kept encouraging me continuously and always believed that I could go on to greater things when perhaps I lacked that belief myself. Without their love and support I would not have made it through.

I hope I made all of you proud.

Table of Contents

Chapter 1: General Introduction	1
1.1: Chronic Obstructive Pulmonary Disease	1
1.1.1 COPD general introduction and definition	1
1.1.2: Pathophysiological symptoms	1
1.1.3: Diagnosis	4
1.1.4: Treatment	6
1.1.5: Smoking Risk factors	7
1.1.6: Non-Smoking Risk factors	10
1.2. Immune Cells Involved in COPD	11
1.2.1: Macrophages	12
1.2.2: Neutrophils	12
1.2.3: T-Lymphocytes	13
1.2.4: Epithelial Cells	16
1.3 Biomarkers in COPD	19
1.4 Cytokines as biomarkers	28
1.4.1 Proinflammatory Cytokines	31
1.4.2 Immunomodulatory Cytokines	32
1.4.3 Eosinophil Chemokines	32
1.4.4 Neutrophil Chemokines	33
1.4.5 Lymphokines:	33
1.4.6 Macrophage Chemokines	34
1.4.7: Growth Factors	36
1.5 Microarray Overview	37
1.5.1 Microarray Slide Surfaces and Immobilisation	39

1.5.2 Slide Noise and Spot Background	41
1.5.3 Spot Size and Morphology	41
1.5.4 Signal Detection and Generation	42
1.6 Introduction to Assay Validation	44
1.6.1: Assay Validation Parameters	51
1.6.2: Accuracy	51
1.6.3: Precision	51
1.6.4: Intra assay	53
1.6.5: Inter Assay	53
1.6.6: Specificity	53
1.6.7: Limit of Detection	54
1.6.8: Limit of Quantification	55
1.7 Aims and Hypothesis:	56
Chapter 2: Materials and Methods	57
2.1: Materials	57
2.1.1: Chemicals and Reagents	57
2.1.2: Antibodies	60
2.2 Methods	62
2.2.1: Biomarker Study Population	62
2.2.2: Slide Surfaces and Print Buffer	63
2.2.3: ELISA protocol	67
2.2.4 Generating Microarray Standard Curves; Initial Protocol	69
2.2.5 Final Optimised Microarray Array Protocol	71
2.2.6: Amplification	72
2.3 Printing	73

2.4: Microarray Validation	75
2.4.1 Intra and Inter-Assay	75
2.4.2: PBS Spikes and Serum Spikes.....	75
2.4.3 ELISA Vs Microarray Comparison	76
2.4.4: Lower Limit of Detection, Lower Limit of Quantification (LLoQ) and Upper Limit of Quantification (ULoQ)	76
2.5 Statistical Analysis.....	77
Chapter 3: Optimisation of an Antibody Microarray Platform.....	78
3.1: Introduction	78
3.2: Materials and Methods	81
3.3: Results	83
3.3.1 Epoxysilane.....	83
3.3.2 Aminosilane	89
3.3.3 Poly-L-Lysine	94
3.3.4 Nitrocellulose.....	100
3.3.5: Milk and NAP Blocking Buffer.....	107
3.3.6 Establishing the optimum capture antibody concentration for printing on poly-L-lysine slides	110
3.3.7 Poly-L-Lysine Standard Curve Reproducibility	112
3.3.8 Sensitivity at the lower end of a standard curve	114
3.3.9 Amplification.....	116
3.3.10: Time Course Experiment to Optimise Cytokine Standard Curves	118
3.3.11 Printing Conditions on Poly-L-Lysine slides.....	120
3.3.12: Cy5 and the Long terms effects on the slide surface	126
3.3.13: The Effects of Blocking Buffers in Serum/Plasma.....	128
3.3.14: Large and low abundance cytokines.....	136

3.4 Discussion.....	138
3.4.1: Printing Buffers	138
3.4.2: Slide Surfaces	139
3.4.3: Blocking Buffers.....	143
3.4.4 Amplification.....	145
3.4.5 Time Course.....	146
3.4.6: Printing	147
3.4.7 Cy5 Detection	147
3.5 Conclusion:	148
Chapter 4: Validation of an Antibody Microarray Platform.....	149
4.0 Introduction	149
4.2 Materials and Methods	154
4.3 Results	157
4.3.1 Limits of Detection and Quantification	157
4.3.2: Cross Reactivity.....	160
4.3.3 PBS and Serum Spike recovery	167
4.3.4 Target Concentration Spiked in PBS or Serum	169
4.3.5: Intra and Inter assay precision	175
4.3.6 Comparison of Microarray technology with ELISA	177
4.4 Discussion.....	184
Chapter 5: Application of an Antibody Microarray as a Diagnostic Platform for COPD	187
5.1 Introduction	187
5.2 Materials and Methods	189
5.3: Results	190

5.3.1: The effect of COPD on cytokine levels in Non Smoking Controls, Smoking Controls and COPD individuals	190
5.3.2: The effect of smoking status on the likelihood of developing COPD	195
5.3.3: The correlation between cytokine expression and FEV% in those with COPD.....	198
5.3.4: The effect of gender on the cytokine expression in those with COPD....	203
5.3.5: The GOLD stages of COPD	204
5.3.6: Relationship between Age and FEV-1%	210
5.3.7: The effect of Age on COPD	211
5.3.8: Clustering of Microarray Data.....	215
5.3.9 False Discovery:	218
5.4 Discussion.....	220
5.4.1 Biomarkers in COPD	220
5.4.2: Gender differences in COPD	226
5.4.3: Age differences in COPD	227
Chapter 6: General Discussion, Future Work & Conclusion.....	229
6.1 General Discussion	229
6.2: Future Work.....	235
6.3 Concluding Remarks	240
Bibliography	241

Table of Figures:

FIGURE 1: COPD IS A MULTIPLE COMPONENT DISEASE SETTING WHICH IS A COMBINATION OF SMALLER DISEASES SUCH AS EMPHYSEMA AND CHRONIC BRONCHITIS.	2
FIGURE 2: THE PATHOGENESIS OF COPD.	3
FIGURE 3: THE FLETCHER-PETO GRAPH OUTLINING THE BENEFITS OF SMOKING CESSATION. .	8
FIGURE 4: CYTOKINES AND CHEMOKINES PLAY A KEY ROLE IN THE PATHOGENESIS OF COPD.	18
FIGURE 5: A SYSTEMIC VIEW ON THE POTENTIAL BIOMARKERS OF INTEREST THAT COULD BE INVESTIGATED IN COPD FROM THOSE IN THE LUNGS TO THOSE IN PERIPHERAL BLOOD.	21
FIGURE 6: SOME OF THE INFLAMMATORY MEDIATORS INVOLVED IN COPD.	29
FIGURE 7: A MODIFIED REPRESENTATION OF MONOCYTE MIGRATION IN RESPONSE TO A CHEMOATTRACTANT.	35
FIGURE 8: AN EXAMPLE OF ONE TYPE OF PROTEIN MICROARRAY USING A NITROCELLULOSE SLIDE.	37
FIGURE 9: METHODS OF DETECTION AND SIGNAL GENERATION.	43
FIGURE 10: THE VALIDATORY EXPERIMENTS THAT HAVE TO BE PERFORMED ON AN ANTIBODY MICROARRAY FOR BOTH QUALITATIVE AND QUANTITATIVE APPROACHES.	47
FIGURE 11: THE THREE KEY STAGES INVOLVED IN VALIDATION.	49
FIGURE 12: THE RELATIONSHIP BETWEEN ACCURACY AND PRECISION.	52
FIGURE 13: THE RELATIONSHIP BETWEEN THE LOD, LLOQ AND ULOQ FROM A STANDARD CURVE.	55
FIGURE 14: ILLUSTRATING THE PRINTING BUFFER /SLIDE SURFACE EXPERIMENT OVERVIEW.	64
FIGURE 15: THIS IS AN ILLUSTRATION WHICH SHOWS THE DISTRIBUTION OF HOW EACH 16 PAD SLIDE IS SET UP.	65
FIGURE 16: ILLUSTRATES THE ELISA PROCEDURE.	68
FIGURE 17: ILLUSTRATES THE INITIAL MICROARRAY METHOD.	70
FIGURE 18: THE AMPLIFICATION PROCEDURE AND THE EFFECT IT HAS ON A STANDARD CURVE.	72
FIGURE 19: THE LAYOUT OF THE PRINT EXPERIMENT.	74
FIGURE 20: SIGNAL INTENSITY OF 8 PRINTING BUFFERS ON EPOXYSILANE SLIDES.	85
FIGURE 21: SPOT MORPHOLOGY EPOXYSILANE SLIDES WHEN TESTED WITH 8 COATING BUFFERS.	86
FIGURE 22: SIGNAL INTENSITY OF EPOXYSILANE SLIDES PROCESSED IMMEDIATELY OR DELAYED.	88
FIGURE 23: SIGNAL INTENSITIES OF 8 PRINTING BUFFERS ON AMINOSILANE SLIDES.	90
FIGURE 24: SPOT MORPHOLOGY AMINOSILANE SLIDES WHEN TESTED WITH 8 COATING BUFFERS AND BLOCKED WITH 3% BSA.	91
FIGURE 25: SIGNAL INTENSITY OF AMINOSILANE SLIDES PROCESSED IMMEDIATELY OR DELAYED.	93
FIGURE 26: SIGNAL INTENSITIES OF 8 PRINTING BUFFERS ON POLY-L-LYSINE SLIDES.	96

FIGURE 27: SPOT MORPHOLOGY AMINOSILANE SLIDES WHEN TESTED WITH 8 COATING BUFFERS AND BLOCKED WITH 3% BSA.	97
FIGURE 28: SIGNAL INTENSITY OF POLY-L-LYSINE SLIDES PROCESSED IMMEDIATELY OR DELAYED.	99
FIGURE 29: SIGNAL INTENSITY OF 8 PRINTING BUFFERS ON NITROCELLULOSE SLIDES.	102
FIGURE 30: IMAGE TO SHOW IRREGULAR SPOTTING AND SMEARING OF PRINT BUFFERS ON NITROCELLULOSE SLIDES WHEN BLOCKED WITH 3% BSA.	103
FIGURE 31: SIGNAL INTENSITY OF NITROCELLULOSE SLIDES PROCESSED IMMEDIATELY OR DELAYED.	106
FIGURE 32: CHOOSING THE OPTIMAL CONCENTRATION OF CAPTURE ANTIBODY THAT WAS PRINTED ON A POLY-L-LYSINE SLIDE SURFACE AND BLOCKED WITH 3 % BSA.	111
FIGURE 33: SHOWING THE EFFECT OF PROCESSING POLY-L-LYSINE SLIDES IMMEDIATELY AND DELAYED ON STANDARD CURVES USING SIX CYTOKINES: (A) TNF-A, (B) RANTES, (C) GMCSF, (D) MCSF, (E) IL-2 AND (F) IFN- γ RESPECTIVELY.	113
FIGURE 34: STANDARD CURVES FOR 6 CYTOKINES AT THE LOWER END OF THE STANDARD CURVE.	115
FIGURE 35: THE EFFECT OF BIO-RAD AMPLIFICATION IS THREE FOLD; IT ALLOWS THE RAISING OF THE STANDARD CURVE IN GENERAL ENABLING GREATER SENSITIVITY AT THE LOWER CONCENTRATION.	117
FIGURE 36: TIME COURSE EXPERIMENT TO OPTIMISE MICROARRAY PROTOCOL:	119
FIGURE 37: THE EFFECT OF DWELL TIME AND TARGET HEIGHT ON SPOT PRINTING.	122
FIGURE 38: THE EFFECT OF DWELL TIME AND TARGET HEIGHT ON SPOT DIAMETER/SIZE. ...	123
FIGURE 39: THE EFFECT OF DWELL TIME AND TARGET HEIGHT ON SIGNAL INTENSITY.	125
FIGURE 40: THE LONG TERMS EFFECTS OF CY5 ON SIGNAL INTENSITY.	127
FIGURE 41: VISUAL DIFFERENCE BETWEEN SERUM AND PLASMA WHEN BLOCKED WITH 3% BSA.	130
FIGURE 42: THE OVERALL S/N RATIO BETWEEN PLASMA AND SERUM SAMPLES FOR THE 8 CYTOKINES ANALYSED.	131
FIGURE 43: A/B: INVESTIGATING THE BEST BLOCKING BUFFER IN SERUM.	133
FIGURE 44: A/B: INVESTIGATING THE BEST BLOCKING BUFFER IN PLASMA.	135
FIGURE 45: IMAGE TO SHOW THE MICROARRAY INCORPORATING HIGH AND SMALL ABUNDANCE CYTOKINES.	137
FIGURE 46: CROSS REACTIVITY EXPERIMENT 1; A COMPLETE SELECTION OF CAPTURE ANTIBODIES ARE ADDED AND ONLY 1 PROTEIN STANDARD IS ADDED WITH A COMPLETE COCKTAIL OF DETECTION ANTIBODIES.	161
FIGURE 47: CROSS REACTIVITY EXPERIMENT 1; A GRAPHICAL REPRESENTATION OF THE EXPERIMENT WHERE A SELECTION OF CAPTURE ANTIBODIES ARE ADDED AND ONLY 1 PROTEIN STANDARD IS ADDED WITH A COMPLETE COCKTAIL OF DETECTION ANTIBODIES.	162
FIGURE 48: CROSS REACTIVITY EXPERIMENT; A COMPLETE SELECTION OF CAPTURE ANTIBODIES ARE ADDED WITH NO RECOMBINANT PROTEIN STANDARDS AND A COMPLETE COCKTAIL OF DETECTION ANTIBODIES.	163
FIGURE 49: CROSS REACTIVITY EXPERIMENT 2; A GRAPHICAL REPRESENTATION OF THE EXPERIMENT COMPLETE SELECTION OF CAPTURE ANTIBODIES ARE ADDED WITH NO PROTEIN STANDARDS AND A COMPLETE COCKTAIL OF DETECTION ANTIBODIES.	164

FIGURE 50: CROSS REACTIVITY EXPERIMENT 3; 16 CAPTURE ANTIBODIES ARE PRINTED AND ADDED WITH A COMPLETE SET OF 16 PROTEIN STANDARDS AND WITH A 15 DETECTION ANTIBODIES EXCEPT FOR EOTAXIN-1 ANTIBODY.....	165
FIGURE 51: CROSS REACTIVITY EXPERIMENT 3; A GRAPHICAL REPRESENTATION OF THE EXPERIMENT WHERE 16 CAPTURE ANTIBODIES ARE PRINTED AND ADDED WITH A COMPLETE SET OF 16 PROTEIN STANDARDS AND WITH A 15 DETECTION ANTIBODIES EXCEPT FOR EOTAXIN-1 ANTIBODY.....	166
FIGURE 52: MICROARRAY ASSAY VALIDATION USING PBS AND SERUM SAMPLES SPIKED WITH KNOWN CONCENTRATIONS OF CYTOKINES.....	168
FIGURE 53: ACCURACY AND PRECISION OF CYTOKINE CONCENTRATION DETERMINATION BY MICROARRAY ASSAY.	171
FIGURE 54: PBS AND SERUM WERE SPIKED AT THREE KNOWN CONCENTRATION ACROSS ALL 16 BIOMARKERS (A & B).....	172
FIGURE 55: THE OBSERVED MEAN CONCENTRATION WAS RECORDED AND COMPARED WITH THE EXPECTED CONCENTRATION TO CALCULATE THE MEAN ACCURACY.....	173
FIGURE 56: THE PRECISION OF THE ASSAY OF ALL 16 CYTOKINES ARE SHOWN WAS CALCULATED (A &B).	174
FIGURE 57: THE INTRA- AND INTER-ASSAY PRECISION.....	176
FIGURE 58: A-D: THIS SHOWS THAT MULTIPLEX MICROARRAY TECHNOLOGY SIGNIFICANTLY CORRELATES WITH THE “TRADITIONAL” ELISAS.	178
FIGURE 59: CORRELATION BETWEEN MICROARRAY AND ELISA TECHNIQUES.....	180
FIGURE 60: BLAND ALTMAN GRAPHS TO SHOW DIFFERENCE BETWEEN TWO ELISAS AND MICROARRAYS.....	181
FIGURE 61: DIFFERENCES IN CYTOKINE EXPRESSIONS IN SUBJECTS WITH COPD, HEALTHY SMOKING CONTROLS AND NON-SMOKING CONTROLS: IL-8, IL-6, IL-1B AND TNF-A (A-D, RESPECTIVELY).....	191
FIGURE 62: DIFFERENCES IN CYTOKINE EXPRESSIONS IN SUBJECTS WITH COPD, HEALTHY SMOKING CONTROLS AND NON-SMOKING CONTROLS: IFN-G, IL-17, IL-4 AND IL-10 (E-H, RESPECTIVELY).....	192
FIGURE 63: DIFFERENCES IN CYTOKINE EXPRESSIONS IN SUBJECTS WITH COPD, HEALTHY SMOKING CONTROLS AND NON-SMOKING CONTROLS: VEGF, EOTAXIN-1, EOTAXIN-2 AND RAGE (I-L, RESPECTIVELY).....	193
FIGURE 64: DIFFERENCES IN CYTOKINE EXPRESSIONS IN SUBJECTS WITH COPD, HEALTHY SMOKING CONTROLS AND NON-SMOKING CONTROLS: MCP-1, IP-10, TGF-B AND IL-23 (M-P, RESPECTIVELY).....	194
FIGURE 65: CORRELATION BETWEEN FEV-1 PREDICTED AND CYTOKINE CONCENTRATION: IL-8, IL-6, IL-1B AND TNF-A (A-D, RESPECTIVELY).....	199
FIGURE 66: CORRELATION BETWEEN FEV-1 PREDICTED AND CYTOKINE CONCENTRATION: IFN-G, IL-17, IL-4, IL-10 (E-H, RESPECTIVELY).	200
FIGURE 67: CORRELATION BETWEEN FEV-1 PREDICTED AND CYTOKINE CONCENTRATION: VEGF, EOTAXIN-1, EOTAXIN-2 AND RAGE (I-L, RESPECTIVELY).	201
FIGURE 68: CORRELATION BETWEEN FEV-1 PREDICTED AND CYTOKINE CONCENTRATION: MCP-1, IP-10, TGF-BETA AND IL-23 (M-P, RESPECTIVELY).	202

FIGURE 69: GRAPH TO SHOW HOW THE CONCENTRATION OF CYTOKINE VARIES WITH THE GLOBAL INITIATIVE FOR CHRONIC OBSTRUCTIVE LUNG DISEASE (GOLD) STAGE FOR IL-8, IL-6, IL-1B AND TNF-A RESPECTIVELY (A-D).....	205
FIGURE 70: GRAPH TO SHOW HOW THE CONCENTRATION OF CYTOKINE VARIES WITH THE GLOBAL INITIATIVE FOR CHRONIC OBSTRUCTIVE LUNG DISEASE (GOLD) STAGE FOR IFN-G, IL-17, IL-4 AND IL-10 RESPECTIVELY (E-H).....	206
FIGURE 71: GRAPH TO SHOW HOW THE CONCENTRATION OF CYTOKINE VARIES WITH THE GLOBAL INITIATIVE FOR CHRONIC OBSTRUCTIVE LUNG DISEASE (GOLD) STAGE FOR VEGF, EOTAXIN-1, EOTAXIN-2 AND RAGE RESPECTIVELY (I-L).....	207
FIGURE 72: GRAPH TO SHOW HOW THE CONCENTRATION OF CYTOKINE VARIES WITH THE GLOBAL INITIATIVE FOR CHRONIC OBSTRUCTIVE LUNG DISEASE (GOLD) STAGE FOR MCP-1, IP-10, TGF-BETA AND IL-23 RESPECTIVELY (M-P).....	208
FIGURE 73: DOT PLOT TO SHOW THE MEAN CYTOKINE EXPRESSION OF ALL 16 CYTOKINES ACROSS THE 4 STAGES OF GOLD.....	209
FIGURE 74: THE RELATIONSHIP BETWEEN “AGE” AND PREDICTED FEV-1% IN COPD INDIVIDUALS.....	210
FIGURE 75: CORRELATION BETWEEN “AGE” AND CYTOKINE CONCENTRATION: IL-8, IL-6, IL-1B AND TNF-A RESPECTIVELY (A-D, RESPECTIVELY).....	211
FIGURE 76: CORRELATION BETWEEN “AGE” AND CYTOKINE CONCENTRATION: IFN-G, IL-17, IL-4 AND IL-10 (E-H, RESPECTIVELY).....	212
FIGURE 77: CORRELATION BETWEEN “AGE” AND CYTOKINE CONCENTRATION: VEGF, EOTAXIN-1, EOTAXIN-2 AND RAGE (I-L, RESPECTIVELY).....	213
FIGURE 78: CORRELATION BETWEEN “AGE” AND CYTOKINE CONCENTRATION: MCP-1, IP-10, TGF-B, IL-23 (M-P, RESPECTIVELY).....	214
FIGURE 79: HEAT-MAP TO SHOW THE EXPRESSION OF ALL 16 BIOMARKERS ACROSS ALL THE SAMPLES WHICH ARE SUBDIVIDED INTO THE THREE PATIENT COHORTS.....	217

List of Tables:

TABLE 1: OUTLINES THE KEY STAGES OF COPD PROGRESSION IN ASSOCIATION WITH THE CHARACTERISTICS OF THE DISEASE WITH REFERENCE TO FEV1/FVC1 VALUES.....	5
TABLE 2: A SELECTION OF POTENTIAL BIOMARKERS TO WHICH HAVE BEEN REPORTEDLY ASSOCIATED WITH COPD:	22
TABLE 3: SHOWS ALL KNOWN INFORMATION ON COPD BIOMARKERS AND THE TISSUE TYPE ANALYSED.....	26
TABLE 4: SHOWS THE SUBCLASSES OF CYTOKINES/CHEMOKINES INVOLVED IN COPD.	30
TABLE 5: TO EXPLORE THE VALIDATORY QUESTIONS ASKED WHEN DEVELOPING AN ANTIBODY MICROARRAY METHOD.....	46
TABLE 6: THE INGREDIENTS INVOLVED IN THE FORMULATION OF 8 DIFFERENT COATING BUFFERS TESTED.	57
TABLE 7: THE DIFFERENT BLOCKING BUFFERS TESTED.....	58
TABLE 8: THE TYPE OF SLIDE SURFACE USED AND WHERE THEY WERE PURCHASED FROM....	59
TABLE 9: A LIST OF ALL THE ANTIBODIES USED FROM OPTIMISATION TO RUNNING PATIENT SAMPLES.....	61
TABLE 10: DEMOGRAPHIC AND SPIROMETRIC DATA OF THE STUDY PARTICIPANTS.	62
TABLE 11: SUMMARY OF THE OPTIMISATION TESTS PERFORMED ACROSS THE 5 SLIDE SURFACES.	109
TABLE 12: SHOWS THE LOD, LLOQ AND ULOQ FOR 16 CYTOKINES.....	159
TABLE 13: SUMMARY OF THE DATA FROM ALL THE VALIDATORY TESTS.	183
TABLE 14 INVESTIGATES THE EFFECT OF SMOKING STATUS OF DEVELOPING COPD IN HEALTHY NON-SMOKING INDIVIDUALS, EX HEALTHY SMOKERS, CURRENT HEALTHY SMOKERS, COPD EX-SMOKERS AND COPD CURRENT SMOKERS	196
TABLE 15: TO SHOW THE SIGNIFICANT ANALYSIS OF MICROARRAYS” OR “SAM” METHOD USED TO DISCOVER FALSE-POSITIVE RESULTS AMONGST ALL 16 CYTOKINES.....	219

List of Abbreviations

Ab	Antibody
AU	Arbitrary unit
AV	Adenovirus
BODE	BMI (Body Mass Index), Obstruction, Dyspnea, Exercise Capacity (health index)
BSA	Bovine serum albumin
BHR	Bronchial hyperresponsiveness
CCL	Chemokine (C-C motif) ligand
CD	Cluster of differentiation
COPD	Chronic Obstructive Pulmonary Disease
CRP	C-reactive protein
CV%	Coefficient of variation %
Cy5	Cyanine
DMSO	Dimethyl sulfoxide
DNA	Deoxyribonucleic acid
EGR-1	Epithelial growth receptor gene 1
ELISA	Enzyme-Linked Immuno-Sorbant Assay
Eot-1	Eotaxin-1
FDA	Food and Drug Administration
FEV-1	Forced expiratory volume in 1 second
FVC-1	Forced vital capacity in 1 second
GCSF	Granulocyte colony-stimulating factor
Glyc	Glycerol
GMCSF	Granulocyte-macrophage colony-stimulating factor
GOLD	Global Initiative for Chronic Obstructive Lung Disease
GRO-a	Growth regulated oncogene-alpha
HDACs	Histone deacetylases
HRP	Horseradish peroxidase
ICAM-1	Intercellular Adhesion Molecule 1
Ig	Immunoglobulin
IL	Interleukin
IFN-G	Interferon-gamma
IP-10	Interferon gamma-induced protein 10
LLoQ	Lower limit of quantification
LOD	Limit of Detection
LTB ₄	Leukotriene B ₄
MEV	MultiExperimentViewer
MIP	Macrophage inflammatory protein
MCP-1	Monocyte chemoattractant protein-1
MCSF	Macrophage-colony stimulating factor
MMP	Matrix metalloproteinase
NAP	Non-animal protein
NF-kB	Nuclear Factor-KappaB
NK-cells	Natural killer cells
NO	Nitric oxide
PBS	Phosphate buffered saline

PCR	polymerase chain reaction
PDGF	Platelet-derived growth factor
PMT	Photo-multiplier tube
PVA	Polyvinyl alcohol
QC	Quality control
RAGE	Receptor for advanced glycation end-products
RANTES	Regulated and normal T cell expressed and secreted
RV	Rhinovirus
SAM	Significant analysis of microarray
SD	Standard Deviation
SOD	Superoxide dismutase
S/N	Signal to Noise
TEER	Trans-epithelial electric resistance
TGF- β	Transforming growth factor beta
Th1	T-Helper cells-1
TIMPs	Tissue inhibitors of metalloproteinases
Tre	Trehalose
Treg	Regulatory T cells
Tw	Tween-20
TNF- α	Tumour necrosis factor-alpha
VEGF	Vascular endothelial growth factor
ULoQ	Upper limit of quantification

Chapter 1: General Introduction

1.1: Chronic Obstructive Pulmonary Disease

1.1.1 COPD general introduction and definition

Chronic obstructive pulmonary disease (COPD) can be defined as “a disease state characterised by airflow limitation that is not fully reversible. The airflow is usually progressive and associated with inflammatory responses of the lungs to noxious particles and gases” [1, 2]. COPD has become a major worldwide problem with the incidences of morbidity and mortality continually increasing and promoting a lower quality of life of the individuals that continue to suffer from it. In the United States, COPD has become the 4th highest cause of mortality and morbidity [3-6]. Additionally in the United Kingdom, COPD is said to be the 3rd highest cause of mortality and morbidity [7, 8] .

1.1.2: Pathophysiological symptoms

The sub-phenotype of COPD include emphysema and chronic obstructive bronchitis (Figures 1 and 2). Bronchitis causes a narrowing of the airway lumen which limits airflow. Emphysema causes a reduction in elasticity recoil due to damage of lung alveoli, which cause small pockets of air being trapped in the lungs, which gives rise to symptoms such as shortness of breath [5]. Some of the hallmarks of COPD include ineffective tissue repair, and a mass influx of inflammatory cells which in turn leads to increased cell death (apoptosis) [9, 10].

Two of the main symptoms observed in those that smoke and have COPD are breathlessness (during normal day activities) and a chronic cough. Additionally symptoms include reoccurring lung infections, weight loss and the use of accessory

muscles to breathe [11, 12]. The smaller airway diseases in smokers can persist for many years without exhibiting any clinical symptoms and can only be diagnosed through spirometry [13-15]

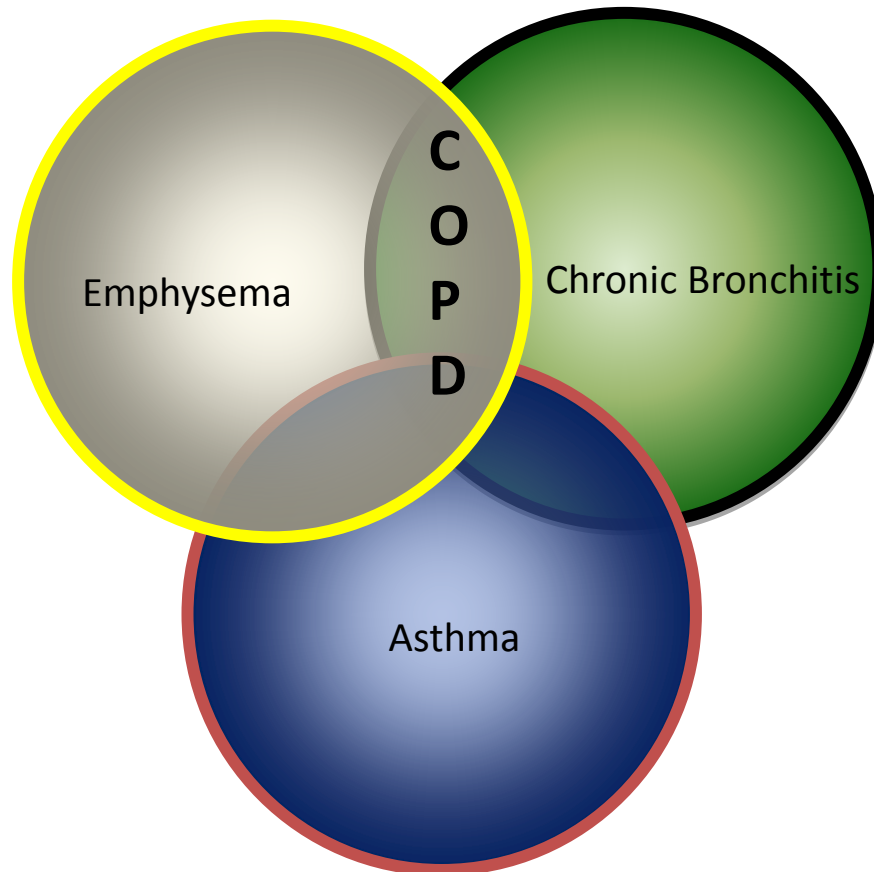


Figure 1: COPD is a multiple component disease setting which is a combination of smaller diseases such as emphysema and chronic bronchitis.

The symptoms that manifest from such diseases are used as possible indicators of the overall disease state. Asthma shares many of the clinical features of COPD such as wheezing and airflow obstruction. In many cases COPD is often misdiagnosed as asthma due to the close overlapping of clinical symptoms [16-18].

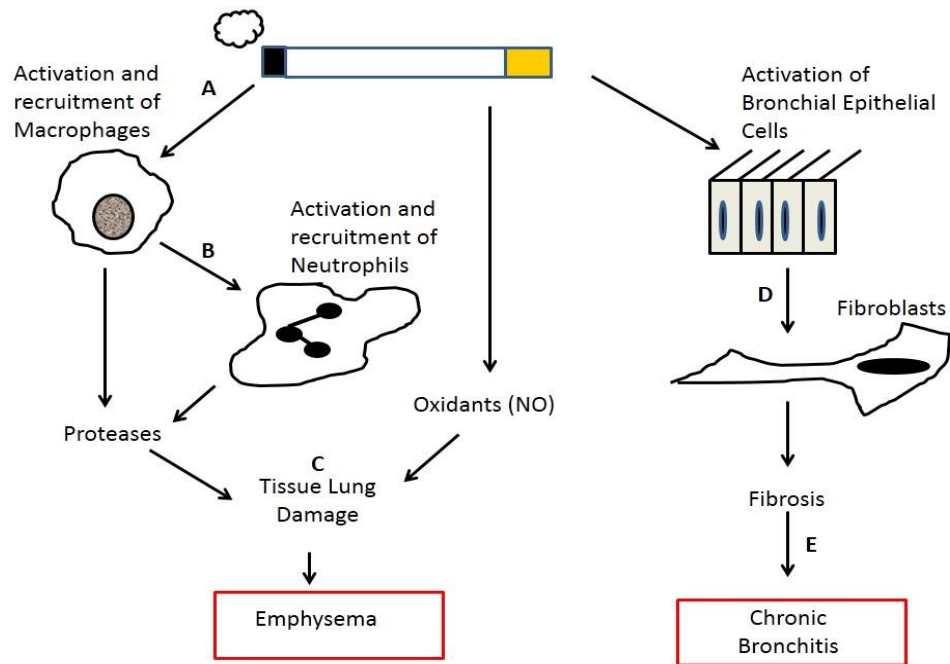


Figure 2: The pathogenesis of COPD.

Cigarette smoke leads to the activation of COPD (A) which in turn leads to the chemotactic recruitment and activation of neutrophils (B). This releases oxidants like NO which over time leads to tissue damage in the lungs (C) giving rise to emphysema. Activation of bronchial epithelial leads to fibroblast activity (D) leading to chronic bronchitis and bronchiolitis (E). Adapted from [19].

1.1.3: Diagnosis

In terms of diagnosis, spirometry is currently used to measure lung function. A key characteristic of COPD includes a reduced forced expiratory volume (FEV_1) which is partly due to a combination of emphysema as well as other airway diseases [20]. Furthermore, FEV_1 values are often used to grade the severity of COPD. If an individual has a FEV_1 value of 80%, it is thought their pathogenesis of the disease can be classified as being mild whilst, if the percentage drops down to 30%, then the individual has severe COPD (Table 1) [21].

Chest X-rays are used as possible indicators of those with emphysema but this technique is inconclusive as a predictor of the severity of COPD. An X-ray will point to pockets of trapped air which is associated with emphysema [22, 23]. Alternative tests for diagnosis include a normal exercise test (such as the 6 minute walk test), which indicate breathlessness and also there are questionnaires on the quality of life which indicates the states of mind with those that suffer from the disease [24, 25].

As the disease is progressive, there is a continuous decrease in airflow which, over a period of time, leads to disability and premature death. Environmental factors influence an individual's susceptibility to COPD including dust, gases, and in particular cigarette smoke which is the leading cause of the disease [26].

Table 1: outlines the key stages of COPD progression in association with the characteristics of the disease with reference to FEV₁/FVC₁ values.

<u>COPD Diagnostic Stages:</u>	<u>Characteristics of Disease</u>
1) Mild	FEV ₁ /FVC ₁ <0.70 FEV ₁ ≥80% predicted
2) Moderate COPD	FEV ₁ /FVC ₁ <0.70 50%≤FEV ₁ ≤80% predicted
3) Severe COPD	FEV ₁ /FVC ₁ <0.70 30%≤FEV ₁ ≤50% predicted
4) Very severe COPD	FEV ₁ /FVC ₁ <0.70 FEV ₁ ≤50% predicted plus chronic respiratory failure FEV ₁ ≤30% predicted

Spirometric classification of COPD severity based on postbronchodilator FEV₁ according to Global Initiative for Chronic Obstructive Lung Disease (GOLD) Management Guidelines 2011.

1.1.4: Treatment

Currently many of the treatments for COPD are insufficient in preventing a decline in lung function. The main treatment involves the cessation of smoking. In terms of pharmaceutical treatments, the leading drugs include nicotine inhibitors, bronchodilators and Bupropion which can relieve the craving symptoms associated with giving up smoking. Furthermore increasing the price of cigarettes as well as increased health warnings are being pursued in a bid to reduce the number of people smoking both nationally and worldwide [27] [28]. Treatment is often centred on treatment that is based primarily for asthmatics and hence not very specific for those with COPD [29-31].

Interestingly in terms of preventing chronic inflammation, anti-inflammatory drugs such as steroids are ineffective due to the resistance induced by macrophages producing peroxynitrate [32]. Additionally cytokines such as IL-8 and TNF- α can also induce steroid resistance. Theophylline is currently used to treat individuals with a more severe spectrum of the disease, often in combination with bronchodilators [33]. It has been found to be successful as it can reduce the number of neutrophils and also reduce the overall concentration of IL-8 which is a key chemoattractant in the recruitment of these cells of the immune system. Also Theophylline is thought to increase the activity of histone deacetylases (HDACs) which can regulate the transcription of inflammatory cells [34] [35].

It has been shown that bronchodilators can increase FEV₁ levels in those with COPD by up to 15-20% which is similarly observed in asthmatics. Those used specifically for COPD involve beta antagonists, anticholinergics and methylxanthines [36].

As COPD is an irreversible airflow disease, whilst there is an improvement in FEV₁ levels in such cases, lung function will never return to normal. Alternatively, oral

corticosteroids have been used to treat COPD patients [37]. The net effects of these drugs show improved spirometry results and better clinical outcomes in those with acute exacerbations of the disease [38]. In patients with COPD who are at a higher stage of the disease will be more likely to be on a higher dose of inhaled corticosteroids or other medications which can affect the immune system. Hence this has to be taken into account when measuring biological samples from patients.

1.1.5: Smoking Risk factors

Smoking is the leading cause of development of COPD. Approximately 25% of heavy smokers will at some point in their lives develop symptomatic COPD [39, 40] [41]. A cigarette contains many thousands of chemicals (including nicotine, tar and carbon monoxide) that serve to alter the mechanisms that are responsible for protection and repair of tissues that are regularly damaged by inhalation [42, 43].

Cigarette smoke in particular contains many oxidants and once inhaled into the lungs can cause an imbalance in the protective antioxidants that are present in lung tissue. Specifically reactive oxidative species include nitrogen oxide (NO) and peroxy-nitrate. NO can cause a dilatation of vascular and bronchiolar smooth muscle [44-46].

The primary antioxidant in the lungs is glutathione. Additionally there are superoxide dismutases (SODs) which are a group of enzymes whose function is to combat the threat of free radicals, which in this case would be from cigarette smoke [47, 48]. Specifically, manganese SOD is found in the alveoli, and in combination with other SODs, can convert highly reactive species, such as superoxide and nitrogen oxide, into less harmful substances that can be managed by the body. The activity of this enzyme is vastly increased in tissue samples of those who smoke and have COPD [49].

Individuals are encouraged to stop smoking as soon they are diagnosed with COPD. Many patients believe that once they have COPD the damage to the lungs has been done, that smoking cessation is not required. However as the Fletcher-Peto plot shows (Figure 3) the importance of smoking cessation could extend the number of years an individual can survive. However it has been noticed that despite the cessation of smoking, lung inflammation still persists in individuals, which could suggest that these reactive species may be present and or can be produced independent of cigarette smoke [50].

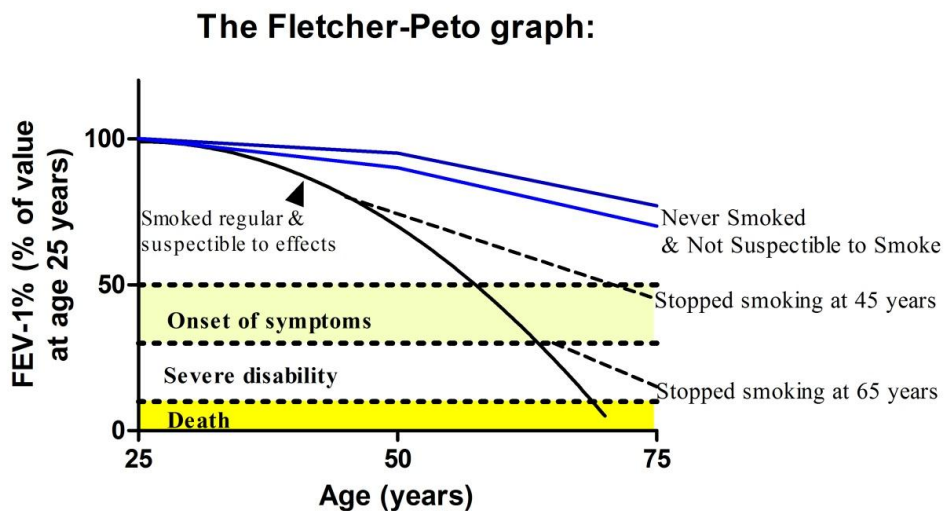


Figure 3: The Fletcher-Peto Graph outlining the benefits of smoking cessation.

The graph above clearly illustrates the importance of smoking cessation even at a late stage of COPD could extend the expected life span. Adapted from [51].

It is thought that histone deacetylase (HDACs) play a role in COPD. Multiple inflammatory genes are controlled by the acetylation of histones (to which DNA is wrapped around). Hence acetylation of key histones such as histone 4 allows transcription factors to become bound to the DNA and thus can begin transcription and eventually lead to the expression of inflammatory genes. This process is regulated by HDACs [52]. In those that smoke and have COPD, it is thought that this regulatory process is disrupted by the presence of peroxynitrate brought on by oxidative stress [53]. This in turn causes a decrease in HDAC activity which ultimately causes the release of inflammatory mediators in the lungs [54] [55].

The lung epithelium provides a protective barrier between the lung tissue and the external environment. It also provides a large surface area for the exchange of gases and in COPD it allows the transfer of cigarette smoke into the body. This smoke can cause damage to the lung tissue and thus the body responds by repairing and remodelling the epithelium to protect itself from subsequent injury [56] [57]. The inflammatory process leads to bronchiolar constriction through the release of mediators such as cytokines which has a direct effect on the airway smooth muscle cells. In addition to the mass infiltration of cells, the T-lymphocytes and neutrophils in the lung tissue cause a thickening of the airway walls which could conversely lead to airway narrowing, limiting airflow. The mechanism of infiltration depends upon tachykinins which recruit neutrophils through a chemotactic gradient and adhesion of neutrophils to the walls. This situation is worsened in conjunction with cigarette smoke which can accelerate the process. Additionally it has been observed there is an increase of number of goblet cells. Neutrophils cause goblet cells to degranulate through the release of elastase and cathepsin G [58].

1.1.6: Non-Smoking Risk factors

Whilst smoking is an established risk factor in COPD, it has emerged recently that up to 45% of patients with COPD have never smoked [59, 60]. Other factors which may cause onset of COPD include exposure to indoor and outdoor air pollutants, workplace exposure to dust and fumes and poor socioeconomic status [61]. In less developed countries, approximately half of all households and the vast majority of rural households use biomass fuel (such as charcoal and animal excrement) with coal as their main source of domestic energy. Many billions of people are exposed to second hand smoke from biomass fuel which may contribute as an increased risk factor to a variety of irreversible lung diseases. With approximately 3 billion people exposed to smoke from biomass fuels, it is now thought that biomass smoke is a leading worldwide risk factor for COPD [62, 63].

Due to the rising cost of energy bills in developed countries such as Australia, Canada and certain parts of USA, households have switched to using a variety of biomass fuels including wood and charcoal for heating purposes. In countries like Nepal, Pakistan and India, women use biomass fuel for cooking and have reduced respiratory function to those who do not use such fuels [64] [65].

Biomass is a poorly combustible fuel which is derived from both plant and animal sources. Due to poor combustion of the materials, highly toxic concentrations are enclosed in domestic households that are harmful to the health of those who are exposed to them [66] [67]. Chemicals released as a consequence of burning biomass fuel include carbon monoxide, sulphur dioxide and a variety of carcinogens [68].

Additionally it is suggested an increase in COPD is associated with occupational exposure to dust, fumes and toxic gases in the workplace [69]. It is thought that the effect of such exposure is worse than that of smoking [70-72]. Those who are

consistently exposed to such working conditions have a high prevalence for developing COPD than that of those who are sufficiently protected from such occupational hazards. For example railroad workers can inhale diesel exhaust fumes which once inhaled deep inside the lung leads to pulmonary inflammation [73]. Additionally chemical exposure as well as crop and animal farming are said to be risk factors associated with COPD [74].

Poor socioeconomic status is another risk factor that is associated with COPD. This often encompasses a variety of smaller factors, including poor nutrition whereby an individual is consuming insufficient antioxidants [75] [76].

1.2. Immune Cells Involved in COPD

A variety of immune effector cells are known to lead to the pathophysiology of COPD. There is a mass infiltration of cells like T-lymphocytes and neutrophils into the lung tissue that causes a thickening of the airway walls which could conversely lead to airway narrowing and limitation [77]. Additionally, macrophages and epithelial cells are thought to play a substantial role in the disease process (Figure 4).

One of the main differences between smokers with COPD and those without COPD is the intensity of the immune response rather than the nature of the inflammatory responses [78]. The key chemokines involved in the recruitment of T-cells include IL-1 β , MIP-1 α and IL-8 [79]. Additionally the presence and activation of these T-cells can contribute to emphysema. It has been shown that CD8 T-cells have the capability to produce cytokines and chemokines such as IFN- γ and IP-10 that upregulate metalloproteinases (such as MMP-12) that can effectively lead to emphysema [80]. Once the disease had been fully established the CD8⁺ subset of effector cells are selectively recruited, over neutrophils [81].

1.2.1: Macrophages

Macrophages are part of the innate immune system and are often one of the first immune cells involved in airways defence against infection and are thought to play a prominent role in COPD. Macrophages have several roles in COPD including the recruitment of neutrophils and activation of CD8 T-lymphocytes as well as releasing a host of chemotactic factors such as IL-8, CXCR3 and CCL2 etc. Additionally macrophages release TGF- β that are involved in airway remodelling and also can release IL-6 that induces hepatocytes to produce acute phase proteins [45, 82, 83].

1.2.2: Neutrophils

Neutrophils are documented to be increased in number and contribute to the inflammatory process in COPD. Additionally increased neutrophils levels have been observed in the sputum of those whom are α_1 -antitrypsin deficient compared to normal healthy subjects [84, 85]. A number of different chemotactic factors, such as IL-8, leukotriene B₄ and CXCL5, are involved in the recruitment of neutrophils which contributes to acute exacerbations in COPD. Neutrophils can lead to the activation of proteases such as elastases and matrix-metalloproteinases that can lead to excess mucus hypersecretion, proteolysis and TGF- β activation [86] [87] which in turn leads to inflammation and the release of proinflammatory cytokines and chemokines.

1.2.3: T-Lymphocytes

In COPD it is thought that the different subsets of T-lymphocytes; CD8⁺ T-cells, CD4⁺ T-cells, T-regulatory cells (Tregs) and TH-17 cells all could contribute to the pathogenesis of the disease.

In particular CD8⁺ T-cell lymphocytes are thought to participate in the inflammatory response in the airways of COPD patients of which there are two major mechanisms which contribute to CD8 T-cell cytotoxicity [88]. The first is dependent upon the release of cytotoxic proteins such as perforin and granzyme. These proteins cause cell lysis through the creation of pores in the lipid bilayer of target cells that disrupts their polarity and leads to immediate cell death. The second mechanism is through the expression of the Fas-ligand that is able to induce apoptosis by binding to the Fas receptor on target cells [89].

CD8 T-cells are found in elevated numbers at various sites in patients with COPD, including the draining lymph nodes, lung parenchyma and many of the blood vessels that lead to the lungs [4, 90].

An exacerbation of COPD could possibly occur due to infectious agents like bacteria and viruses that lead to lower respiratory tract infections. This could partly explain the reason for high numbers of CD8⁺ T-cells found in lung tissue. These T-cells cause alveolar damage and their homing to these sites are dependent upon cytokines, selectins and integrins. Even after infections, CD8 T-cells can still persist at these sites as memory cells [91] (Figure 4).

CD4⁺ T-cells are responsible for controlling downstream immune processes by activating cytokines that are involved in the amplification of the immune response in COPD. CD4⁺ T-cells are responsible for eliciting the development of the adaptive immune response as well as promoting the survival of CD8 T-cells [92]. It has been

shown in various publications that the ratio of CD4⁺/CD8⁺ T-cells is lower in those that have an exacerbation in COPD compared to those with stable COPD [93] [94] [95]. Additionally a publication by Gupta *et al* have shown there to a lower ratio of CD4⁺/CD8⁺ T-cells in COPD patients compared to healthy controls [96].

T-regulatory cells (Tregs) are a subset of CD4 lymphocytes have been thought to play a role in the immune regulation of COPD. There are two main lineages of CD4 + Tregs; natural Tregs (nTregs) and inducible Tregs (iTregs) [97].

In particular Tregs serve to provide protection to the body against overactive immune responses through the production of immune-modulatory cytokines such as IL-10 that inhibit T-cell proliferation [98, 99]. Additionally IL-10 is thought to suppress the production and induction of Th1 cytokines such as TNF- α and IL-6 and chemokines such as IL-8 and MIP-1 which are responsible for neutrophilia in COPD [100]. Tregs can also produce novel anti-inflammatory markers such as IL-35. In rodents it has been shown that IL-35 can inhibit Th17 production however this has not been shown in humans [101].

As COPD is an inflammatory disease, it was hypothesised that their numbers would be reduced in those with the disease. Interestingly, recent research has shown that increased levels of nTregs cells were found in patients who have an exacerbation in COPD and also those who have emphysema [102]. Overall there is growing evidence that whilst there is an increase in the number of Treg cells in those with COPD, however these cells are dysfunctional and are unable to alter the balance between pro- and anti-inflammatory cytokines. This is further justified where healthy smoking controls who do not have COPD, have elevated numbers of Tregs in their lungs but

the cells are more effective in regulating the level of inflammation in response to cigarette smoke [103].

Th17 (T-helper-17) cells are another subset of CD4 T-lymphocytes. Th17 cells are suggested to induce strong pro-inflammatory cytokines and chemokines such as IL-6 and IL-8 respectively. Cigarette smoke can directly lead to the upregulation of chemokines that are associated with Th17 cells which lead to the inflammation associated with COPD [104]. The main cytokine that is secreted by Th17 cells are IL-17. The IL-17 cytokine family has 6 cytokines in its family from IL-17A-F which are secreted from a variety of immune effector cells including antigen presenting cells and B-cells [105].

Two additional cytokines that are produced from Th17 cells are IL-21 and IL-22. Whilst IL-21 is said to be involved in a positive feedback loop that aids the amplification of Th17 cells, IL-22 is said to be involved in many autoimmune diseases as well as COPD [106].

IL-23 may also plays a role in the maintenance of Th17 cell through the induction and release of both IL-17 and IL-22 [107]. IL-23 is expressed in chronic inflammation and shown by immunohistology in those with stable COPD [108]. Work with murine models have shown there to be increased level of expression of IL-17 in the lungs upon exposure of cigarette smoke [104].

1.2.4: Epithelial Cells

The surface of airway epithelial is a mixture of basal cells, ciliated cells, Clara cells as well as goblet cells. The airway epithelium forms a rigid barrier through intracellular epithelial junctions. These junctions serve to protect against pathogens and noxious particles which are inhaled through the lungs [109].

When airway epithelial cells are exposed to cigarette smoke there is a reduction in the trans-epithelial electric resistance (TEER) [109]. This reduces the efficiency of the barrier function making it more prone to attack from pathogens. Cigarette smoking induces the upregulation of growth receptor gene 1 (Egr-1) in epithelial cells [110]. This in turn leads to the activation of pro-inflammatory cytokines such as TNF- α and IL-1 as well as leads to the production of IL-8 and mucins [111] (Figure 4).

Recent publications have shown that pathogens such as rhinovirus (RV) and adenovirus (AV) cause injury to the epithelial cell lining in the airways which cause a deterioration in lung function which in turn exacerbate the effects of COPD [112, 113].

The immune system responds to these viruses by producing a variety of different inflammatory chemokines and cytokines such as RANTES, GM-CSF and MCP-1. This leads further to the recruitment of other immune effector cells such as CD8+ T-cells and NK-cells which amplify the existing inflammatory processes that leads to pulmonary and systemic inflammation in the lungs [114].

A key feature of COPD in the lung is mucus hypersecretion. Normally mucus acts as a physical barrier to trap pathogens in the lungs and is cleared by the immune system. Cigarette smoke causes the apoptosis of ciliary epithelial cells, the activation of

capases and the IL-18R α dependant pathway which results on the oversecretion of mucus and the inability to clear the trapped pathogens [115]. This serves to exacerbate the symptoms of COPD with an increase in the level of inflammation and airway lung diseases.

COPD is involved in the airway remodelling of epithelial cells, in particular squamous metaplasia and mucous hyperplasia [116]. It is this remodelling that contributes to irreversible airflow obstruction which is a key symptom in COPD. Cigarette smoke cause the injury to epithelial cells and also disrupts the ability of the cell to regenerate and repair itself. Both TGF- β and matrix metalloproteinases (MMPs) are thought to be involved in the destruction and repair of epithelial cells [117]. In this process of regeneration, bacteria that exist in the lungs bind to cells that are undergoing repair. These bacteria release virulent factors which undermine the ability of the cell to regenerate, leaving it vulnerable to attack and unable to keep the epithelial barrier intact [118].

Overview of COPD:

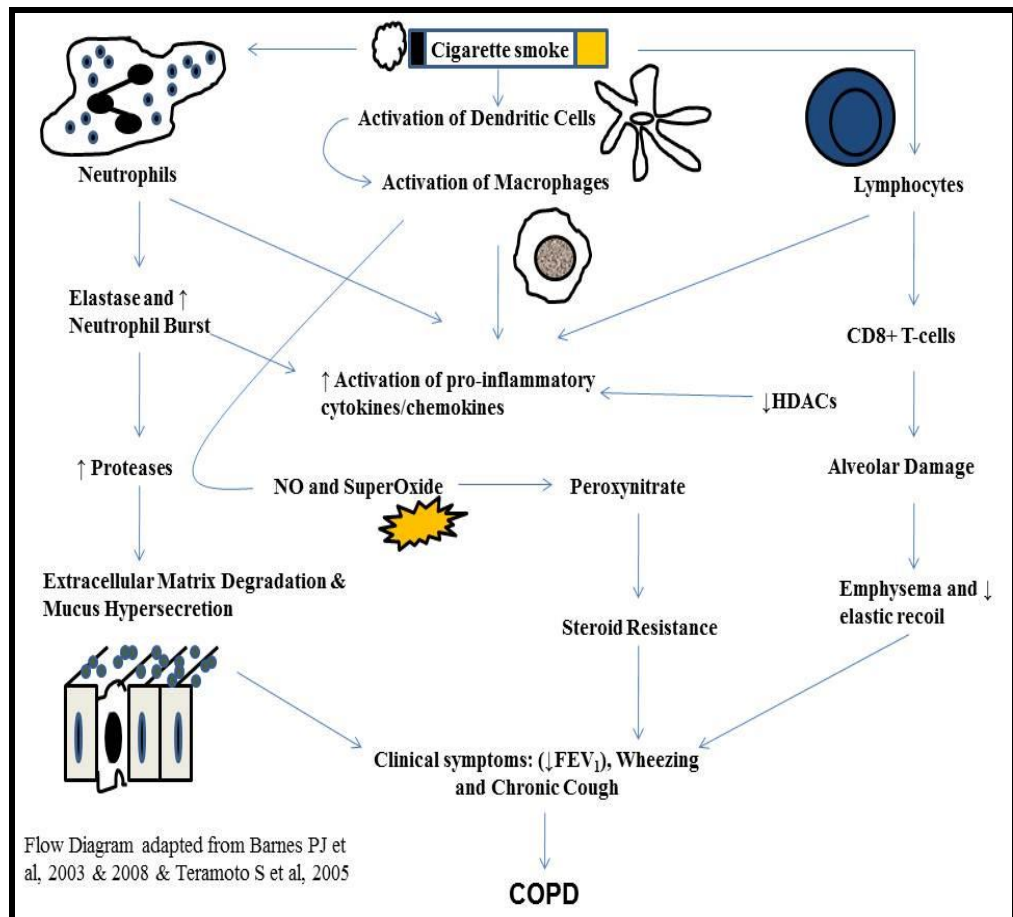


Figure 4: Cytokines and chemokines play a key role in the pathogenesis of COPD.

These include IL-8, TNF- α as well as IL-1 β , TGF- β and IL-17. Many of these cytokines serve to amplify the inflammatory process by recruiting key immune effector cells such as macrophages and neutrophils that contribute to the symptoms associated with COPD.

1.3 Biomarkers in COPD

A biomarker is defined as a “measurement of a molecule of interest which can indicate biological processes and thus can be used to predict disease process”, [119].

The key characteristics of a biomarker could be to show the pathophysiological process of a given disease, responses to changes in disease and possibly to indicate the phenotype at different stages of the disease [120].

FEV₁ is the only accepted marker that meets the FDA criteria for COPD as it characterises the severity of the disease and is a known predictor of mortality and morbidity. Rosenberg and Kalhan, *argue* the problem of using FEV₁ solely as a marker of COPD is that whilst it is both reproducible and easy to measure it, it doesn't correlate with the health status or symptoms of the patient [121]. Specifically, FEV₁ doesn't distinguish between the heterogeneity of the COPD with regard to two individuals who may have the same FEV₁ %, but display two different sub-phenotypes of COPD such as emphysema and small airways disease with varying levels of severity [122]. Hence the need to identify biomarkers in COPD that help improve the general understanding with regard to the complex nature of this disease.

It is thought that certain biomarkers will be more useful in the prognosis of the disease. In the case of COPD, which is a multifaceted disease involving many immune cells, enzymes and mediators (Fig 4 & Fig 5), there will be many biomarkers which could prove to be good indicators of the disease process. With the development of novel assays, such as microarrays, there is a possibility for a greater number of biomarkers to be studied with greater reproducibility and enhanced sensitivity [123] [124].

Frangogiannis, suggests at present there are two main approaches to identifying suitable biomarkers in disease setting. The first employs choosing a set of biomarkers based on the understanding of the pathophysiology of the disease. The second involves using an “unbiased” proteomic approach investigating multiple biomarkers which may be able to distinguish between the differential expression between normal and disease state individuals [125].

A further advantage of examining a spectrum of biomarkers is in drug development. At present pharmaceutical companies are producing drugs that are targeting inflammation in COPD. Hence there is a need to identify reliable biomarkers which can indicate the clinical effectiveness of anti-inflammatory therapy in those with COPD [126] [127].

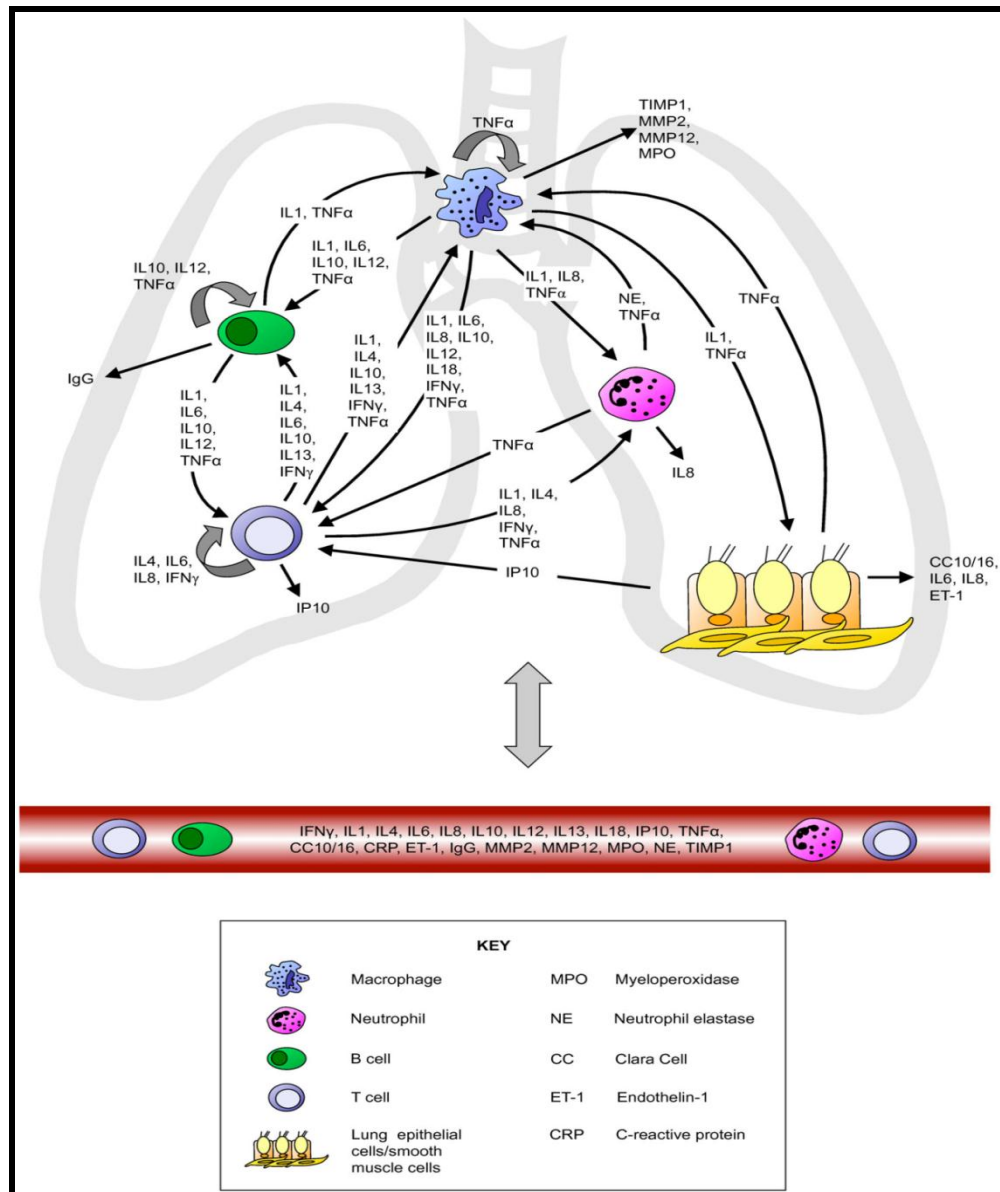


Figure 5: A systemic view on the potential biomarkers of interest that could be investigated in COPD from those in the lungs to those in peripheral blood.

Using one of the approaches Frangiannis, used to described to identifying biomarkers according to the present understanding of the pathophysiology of COPD, the figure above illustrates a potential vast array of biomarkers that could be produced by cells of the immune system ranging from macrophages to neutrophils to T-lymphocytes that could be investigated in the context of one another on a proteomic platform. Figure taken from [128].

When looking for biomarkers in COPD, taking into consideration pathophysiology of the disease, biomarkers can be split broadly into four distinct categories namely; i) chemo-attractants, ii) inflammatory mediators, iii) immune-modulatory iv) those involved in destruction and repair, all of which could play a role in disease progression (Table 2).

Table 2: A selection of potential biomarkers to which have been reportedly associated with COPD:

Type of Biomarker:						
Chemo-attractants	IL-8	Eot-1	MCP-1	Eotaxin-2	IP-10	
Inflammation	IL-1 β	TNF- α	IFN-G	IL-4	IL-6	RAGE
Destruction & Repair	TGF- β	VEG-F				
Immunomodulatory	IL-10					
Regulatory	IL-23	IL-17				

(Adapted from Pinto-Plata *et al.*)

Over the last four or five years there has been an increased emphasis in discovering new biomarkers that could contribute to improving the overall understanding of COPD. In 2007, a major study by Pinto-Plata investigated the profiling of serum biomarkers in those that had COPD using a protein microarray platform [129]. From well over a hundred biomarkers investigated it was shown that a panel of 24 biomarkers significantly correlated with FEV₁, BODE index as well as exacerbation frequency including IL-8, IL-17 and Eotaxin-2 (Table 3) [129].

In 2008, the ECLIPSE study was conducted to evaluate the phenotype and genetic parameters that would help define COPD as well as looking at potentially new biomarkers. This study was one of the biggest longitudinal studies in this research field looking at over 2000 COPD patients over a period of three years. Their research indicated that it was important to consider disease activity compared to disease severity when trying to investigate biomarkers in COPD. Their results showed that fibrinogen, serum surfactant protein D (SP-D) and CCL-18 could be considered potentially new biomarkers in COPD as they significantly correlated longitudinally with the disease as well with mortality [130] [131]. However they emphasised the need to not only investigate one biomarker in COPD but look for a variety of biomarkers that could serve to contribute at different stages of the disease.

A separate publication by Higashimoto *et al*, who also looked at serum biomarkers in COPD, found that CRP and MMP-9 were significantly correlated to lung function decline in those with COPD (Table 3) [127]. Interestingly their study showed that commonly sought biomarkers in COPD such as IL-8, IL-6 and TNF- α (often associated in the inflammatory stage of the disease) did not correlate with FEV₁ levels [127]. However it was shown in this publication that concentrations of IL-8 and

TNF- α were higher in those who smoked compared to non-smoking healthy controls [127].

In a more recent study by Garcia-Rio *et al*, looked at systemic biomarkers in COPD found that IL-8 and TNF- α were significantly higher than healthy controls whilst serum biomarker concentrations of IL-6 and albumin were linked to exercise tolerance [132]. Further studies by Rocke *et al*, [133] and Pinto-Plata *et al*, [134] have also shown a reoccurring theme whereby IL-6, TNF-A and CRP are significantly shown to be increased in COPD patients compared to healthy controls (Table 3).

Over the past four years, as there has become a clearer understanding of the role of regulatory T-cells in COPD, new investigations have looked at the role of cytokines that govern this subset of cells. Specifically studies conducted by Di Stefano *et al*, have shown there to be an increased expression of novel markers such as IL-17 and IL-23 in the sub-mucosa of those with COPD compared with healthy controls [135]. In addition, Gasse *et al*, have shown that IL-23 could be a key biomarker that could control part of the inflammatory pathway of COPD by inducing the production of IL-17 that leads to pulmonary inflammation in the disease [136].

Further publications have found “alternative” biomarkers that could contribute to the pathogenesis of COPD which include MCP-1 which is found to be higher in those with COPD than in healthy controls [137] whilst soluble receptor for advanced glycation endproducts (RAGE) were decreased in COPD [138, 139].

At present no single biomarker in COPD demands worldwide acceptance mainly due to the conflicting reporting of specific biomarkers in publications. Therefore instead of looking at just one biomarker in a clinical setting it is far more beneficial to see whether a pattern could exist when looking at a variety of biomarkers in the same clinical setting as one another. This could improve the overall understanding of the

disease to help differentiate the role each biomarker could play in the pathogenesis of the disease and also to ascertain whether one biomarker may be responsible for the increased or decreased expression of another biomarker. It would be interesting to see if there is a different biomarker pattern displayed by the three components that contribute to COPD (emphysema, chronic bronchitis and asthma) (Figure 1).

Therefore the following section will outline the role of prominent cytokines that have been chosen from recent publications and we will examine the function of these cytokines in COPD.

Table 3: Shows all known information on COPD biomarkers and the tissue type analysed

Type of Biomarker	Cytokines	References:	Tissue type:
Chemoattractants	IL-8	[140]	Epithelial Cells
		[141]	Plasma
		[107]	Sputum/Plasma
	Eotaxin-1	[142]	Bronchoalveolar lavage (BAL) Fluid
		[143]	Sputum
	MCP-1	[144]	Sputum
		[134]	Serum
	Eotaxin-2	[145]	Plasma/Sputum
		[129]	Serum
	IP-10	[146]	Serum
		[147]	Serum
Inflammation	IL-1- β	[148]	Epithelial Cells
		[149]	Epithelial Cells/Sputum
		[150]	Plasma
		[151]	Plasma
	TNF- α	[152]	Plasma
		[153]	Serum
		[154]	Sputum/Plasma
		[155]	Serum/Sputum
	IL-6	[156]	Plasma
		[157]	Sputum
		[158]	Plasma

	IL-4	[159] [160] [161]	Epithelial Cells Epithelial Cells Serum
	IFN- γ	[162] [163] [164]	Epithelial Cells Epithelial Cells/Plasma Plasma
	RAGE	[165] [138] [139]	Lung Tissue Serum Serum
	IL-23	[136] [132] [166]	Epithelial Cells Serum BAL Fluid
	IL-17	[135] [108] [105]	Endothelial Cells Plasma Plasma
Immunomodulatory	IL-10	[167] [168] [169]	Serum/Sputum Plasma Sputum/Serum
Destruction and Repair	TGF- β	[127] [170]	Serum Plasma
	VEGF	[171] [133]	Serum BAL Fluid/Serum/Sputum

1.4 Cytokines as biomarkers

Cytokines are small, extracellular signalling proteins (less than <75kDa) which are produced by a variety of cell types [172]. Cytokines are able to directly affect closely residing cells (paracrine) as well as target cells at a distance (endocrine/autocrine). Rarely are cytokines produced alone, often in association in one another. Hence when cytokines are produced together, patterns develop which can be used to characterize a type of disease.

The pathology of COPD shows chronic inflammatory reaction whereby a cycle of tissue damage and repair takes place in association with a mass influx of inflammatory cells regulated by a group of cytokines [173]. The recruitment of cells such as neutrophils, macrophages, T-cells and eosinophils to the site of inflammation is governed by a type of chemoattractant cytokines called chemokines [144]. Chemokines are smaller than cytokines and are primarily responsible for recruiting leukocytes to tissues (Figure 6).

Cytokines can be subdivided into the role they contribute to the pathology in COPD (Table 3 and 4) [172]. As can be seen there are a variety of cytokines such as IL-6, MCPs and RANTES that appear in more than one category indicating more than one role for this cytokines. Whilst the cytokines mentioned in Tables 3 and 4 all contribute to COPD, there is not a recognised pattern of cytokines that can be easily related to the disease.

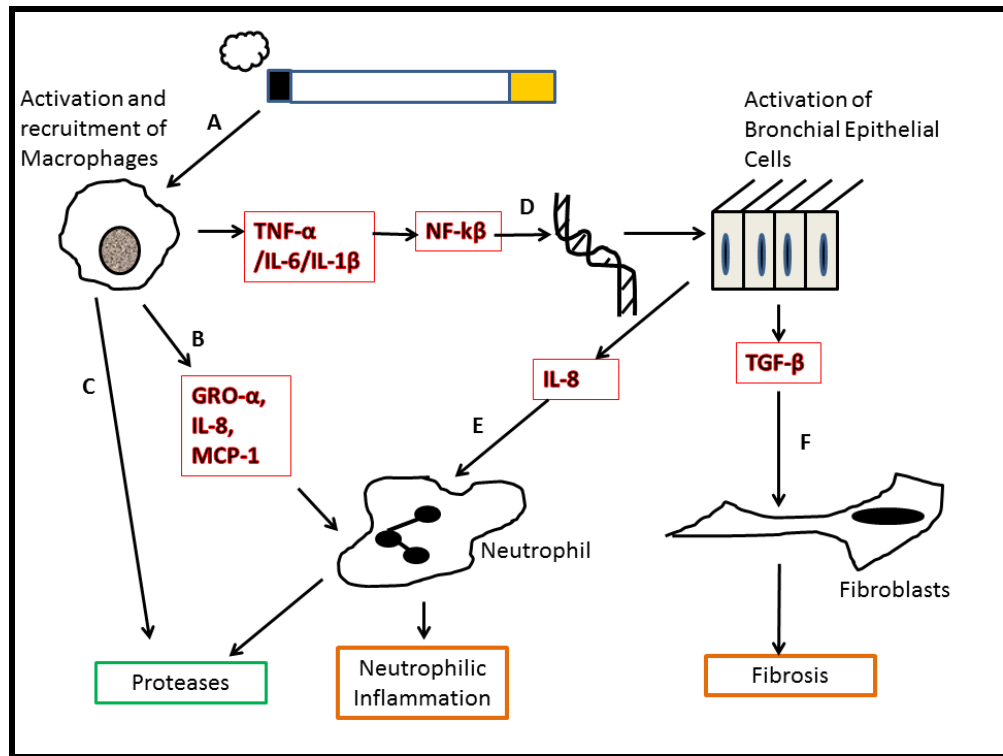


Figure 6: Some of the inflammatory mediators involved in COPD.

Cigarette smoke activates macrophages (A) which in turn secrete $IL-6$, $TNF-\alpha$ and a variety of other cytokines (B) as well as proteases (C). $TNF-\alpha$ promotes further gene transcription (D) that cause epithelial cells to release $IL-8$ (E) that leads to neutrophilic chemotaxis and further releases of proteases. Additionally epithelial cells produce $TGF-\beta$ (F) that is involved in tissue remodeling and repairs which eventually leads to fibrosis. Adapted from [19].

Family of Cytokine/Chemokine	Cytokine/Chemokine
Lymphokine	IL-4, IL-5, IL-6, IL-10, IL-13
Neutrophil Chemokine	IL-8, GRO- α , IL-1, TNF- α
Eosinophil Chemokine	RANTES, GMCSF, MCP-3/4
Macrophage Chemokine	RANTES, MCP-1, MIP-1 α , GRO- α
T-cells	MCP-1, RANTES, IL-16
Proinflammatory	IL-1 β , TNF- α , IL-6
Anti-Inflammatory	IL-10, IFN- γ
Growth Factors	TGF- β , PDGF, IGF

Table 4: Shows the subclasses of cytokines/chemokines involved in COPD.

The overlapping nature of certain cytokines and chemokine indicate more than one role in the pathogenesis in COPD affecting more than one subset of immune effector cells.

1.4.1 Proinflammatory Cytokines

Proinflammatory cytokines include IL-1, IL-6 and TNF- α . IL-6 is secreted by a variety of immune effector cells including macrophages, T-cells and B-cells. IL-6 has been recognised to be involved in exacerbation of COPD symptoms [153, 174, 175]. Specifically IL-6 contributes to the proliferation, survival and activation of T-cells in COPD [156, 158, 176]. IL-6 levels are known to be elevated in not only serum but also BAL fluid and sputum in the different stages of COPD [157]. IL-1 β has also been reported to have a primary role when investigated in rodents [148]. High expression of this cytokine was found in rat lung epithelia that eventually manifests into emphysema and airway remodelling [177]. It is possible IL-1 β exerts a similar type of effect in humans. Finally TNF- α is known to be an exceptionally potent mediator of inflammation. It is thought that the inhalation of cigarette smoke triggers the activation of TNF- α which in turn can lead to a cascade of reactions that result in further activation of other inflammatory cytokines like IL-6, IL-1 β , GM-CSF and G-CSF [178, 179].

1.4.2 Immunomodulatory Cytokines

IL-10 and IFN- γ are two such examples of anti-inflammatory cytokines that play a role in the inhibition of the production of inflammatory mediators mentioned above. Both IL-10 and IFN- γ play a role in the inhibition of CD4⁺ T-cell activity [180]. IFN- γ is thought to play a role in the inhibition of MMPs in COPD and thus activating TIMPs which are inhibitors of MMPs [181]. In the sputum of those with COPD, the level of IL-10 was found to be reduced whereas proinflammatory cytokines such as TNF- α and IL-1 β were up-regulated, ultimately leading to tissue damage. IFN- γ is a cytokine that plays a major role in COPD as it contributes to pulmonary emphysema [182, 183]. IFN- γ is thought to inhibit CCR2 expression in human monocytes hence act as an inhibitor against the recruitment of macrophages [184].

1.4.3 Eosinophil Chemokines

Eosinophils are thought to play an inflammatory process in the lung mucosa through the release of highly toxic proteins such as eosinophil cationic protein (ECP) that have been found to be in peripheral blood as well as BAL fluid in those with COPD [185]. Chemokines involved in this process include RANTES, eotaxin-1 & -2 as well as MCP-3 and MCP-4 [186] [142]. These cytokines are thought to be elevated in those with COPD compared to healthy controls and those with asthma indicating a role of cigarette smoke for inducing such changes [187]. These chemokines activate and attract eosinophils, in particular eotaxin-1 through the selective binding to the high affinity CCR3 receptor [187].

1.4.4 Neutrophil Chemokines

IL-8, IP-10 and MCP-1 are all but a few chemokines involved in the recruitment of neutrophils. They are expressed through either mesenchymal or inflammatory cells and can be stimulated by other cytokines including IL-6 and TNF- α [188] [147] . Additionally cigarette smoke is thought stimulate the production of IL-8 from both macrophages and bronchial epithelial cells [189] [190].

IL-8 is a potent neutrophilic chemokine that upregulates cell adhesion molecules such as ICAM-1 and e-selectin as well as increased production of LTB₄ that all contributes to neutrophils leaving the blood and migrating to the site of inflammation [191]. In addition to elevated serum levels of IL-8, an increased amount has been also observed in COPD sputum samples [192].

1.4.5 Lymphokines:

Lymphokines are a subset of cytokines that are produced by lymphocytes; in particular CD4⁺ T cells and CD8⁺ cells. These T cells are responsible for the regulation of the immune response through the signalling between cells [193-195].

Smoking can cause CD8 T-cells to release to IFN- γ which in turn up-regulates IFN- γ -inducible protein (IP-10). IP-10 can induce the production of matrix metalloproteinase 12 (MMP-12) that can lead to a reduction in elasticity recoil due to damage of lung alveoli [146]. Hence is its postulated IFN- γ , IP-10 and MMP-12 can work by a positive feedback loop in emphysema [44] [196].

Over the years, publications have shown that plasma cells in the submucosal glands of the lungs that express IL-4 can also lead to goblet cell hyperplasia [197] [198] [199]. It is thought that T-lymphocytes can secrete IFN- γ and the cytokine itself is responsible for the inhibition of cell proliferation and also contribute to the pathogenesis of the disease by augmenting the cytotoxic effects of TNF- α [76].

Research have shown that CD8 T-cells have the potential to be polarised towards a Tc2 profile; leading to production of cytokines such as IL-4 which lead to mucus hypersecretion [200].

1.4.6 Macrophage Chemokines

Growth-regulated protein alpha (GRO- α) and monocyte chemotactic protein-1 (MCP-1) play a similar role to IL-8 in the pathogenesis of COPD. Whilst both chemokines have been implicated as a potent neutrophilic chemoattractants, they have also been shown to be involved in a mass influx of macrophages that have been found in lung biopsies and sputum samples in COPD [144, 201]. Traditionally when there is saturated concentration of chemokine, the natural movement of cells is to bind to the cell surface slowing chemotaxis. However it has been noticed with GRO- α that even at high concentrations macrophages continue to migrate leading to a greater burden of these monocytes at the site of inflammation (Fig 7) [144].

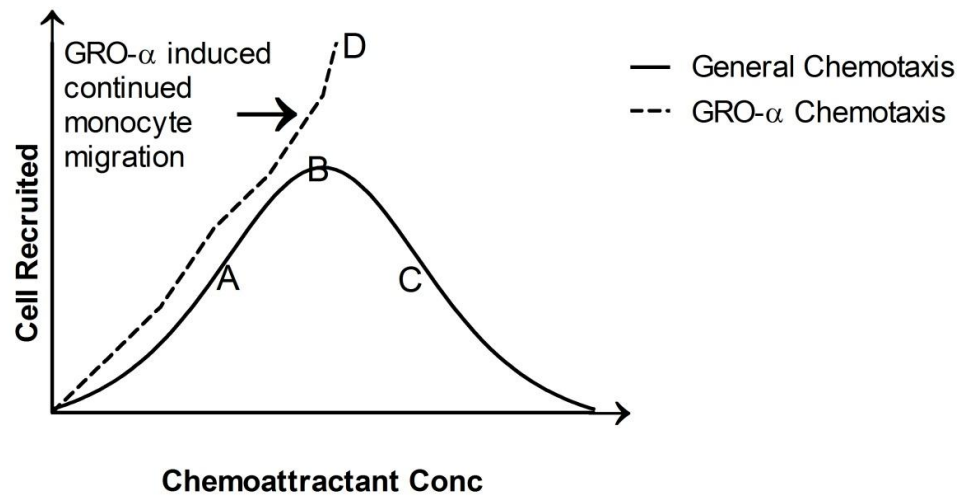


Figure 7: A modified representation of monocyte migration in response to a chemoattractant.

At low concentrations of chemoattractant there is a low gradient for cells to move efficiently (A). At the optimal concentration of chemoattractant the gradient is perfect for monocyte movement to the site of inflammation (B). As the concentration of chemoattractant increases, normally cells stick to the cell surface leading to reduced migration (C). However for chemokines like GRO- α , IL-8 and MCP-1 cell migration still continues leading to a greater number of macrophages observed in COPD (D). Figure originally adapted from [202].

1.4.7: Growth Factors

Growth factors such as TGF- β and platelet-derived growth factor (PDGF) induce the proliferation of structural cells; specifically airways smooth muscle cells and fibroblasts. TGF- β is a cytokine that is involved in cell proliferation and cell differentiation [203]. Airway smooth muscle cells of those who have COPD have been shown to express large amounts of this cytokine. Due to airway remodelling that occurs with those that smoke and have COPD, TGF- β is shown to be highly expressed [204]. Recent research has shown that TGF- β and its receptor TGF-R can enhance apoptosis of peripheral T-lymphocytes by preventing the progression of growth of these cells from the G1-S transition phase [205] [206].

1.5 Microarray Overview

Protein microarrays can be used as a measurement tool to determine and quantify the presence or amount of proteins that exists in biological samples (i.e. blood, sputum, or urine etc). This is a fairly novel approach (since early 2000s) which has many benefits in proteomic research. The most common protein microarray that is used is an antibody microarray. This is whereby capture antibodies are printed onto a small chip or slide which can be then used to detect proteins of interest in a biological sample (Figure 8).

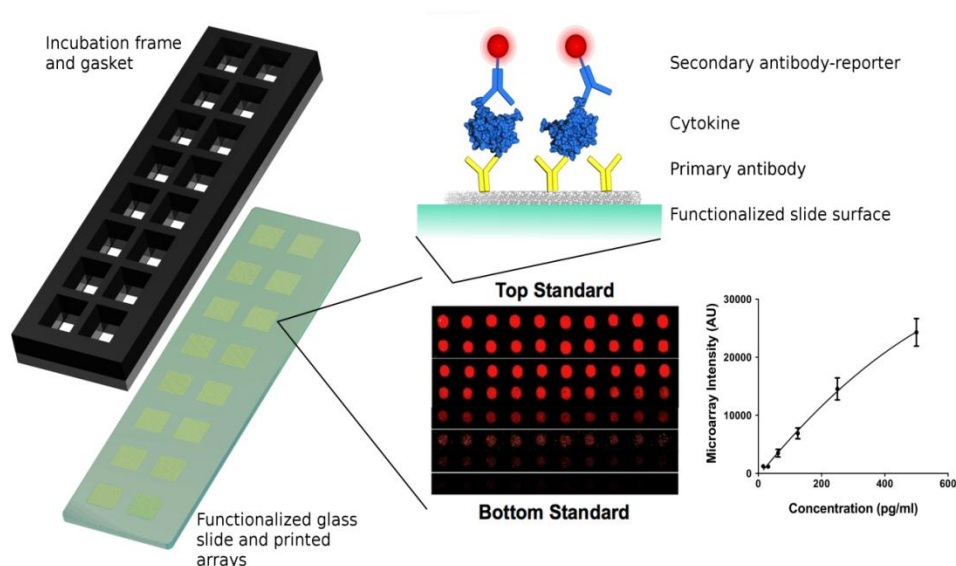


Figure 8: An example of one type of protein microarray using a nitrocellulose slide.

Antigens or proteins of interest can be detected using primary antibody and amplified further by the use of a secondary antibody which is tagged to biotin or alkaline phosphatase. The slide is subsequently scanned and standard curves are drawn to calculate the amount of protein present in a biological sample. (Figure courtesy of Dr Paddy Tighe).

Overall microarrays offer the potential to measure and evaluate a variety of inflammatory mediators including cytokines across a broad spectrum of concentrations, at a reduced overall cost compared to the traditional Enzyme-Linked Immuno-Sorbant Assay (ELISA). Despite the potential promise this technology brings to medical research; it is hindered by a lack of experience and reproducibility issues which require further validation and optimisation.

At present ELISAs are the “gold standard” for the measurement of inflammatory cytokines and is the best known method for measuring cytokines and other inflammatory mediators with both high levels of sensitivity and specificity. Recently there have been a lot of published studies that show the use of microarray technology in the quantification of cytokines in serum [207] [208] .

Microarrays also allow for multiple repeats to be performed on the same chip enhancing the validity of subsequent results.

The key advantages of microarrays over ELISAs involve:

- a) A smaller amount of sample required to run the assay
- b) The ability to detect and/or quantify more than one inflammatory mediator
- c) The ability to undertake multiple repeats of the same cytokine under the same experimental conditions
- d) The ability to detect a variety of proteins across a range of concentrations
- e) Reduced time and cost to run the assay

Antibody microarrays are regarded as the future of biomarker detection of disease [209] [210] [211]. At present protein microarrays have evolved from DNA microarray technology, however they are not as robust and as reliable as the latter. Sandwich ELISA microarrays allow for the analysis and quantification of a large variety of proteins which require a small volume.

1.5.1 Microarray Slide Surfaces and Immobilisation

One of the biggest obstacles to developing reproducible protein microarrays are slide surfaces. The surface chemistry of the slide dictates the immobilisation between the slide surface and the antibody or protein that is to be printed [212]. The physical interaction between proteins and the slide surface can occur by Van der Waals, covalent, ionic or hydrophobic interactions that need to be optimised depending on the nature of the protein of interest. In addition, the nature of the interaction should leave the protein functionally unaltered [213].

The adsorption of proteins to the surface of the slide can be engineered by either a combination of a large number of weak contacts (which could alter the shape and functionality of the protein) or small number of strong bonds which leaves the protein unchanged except for at the point of contact.

To enable this to occur, different types of slide surfaces have been developed. These can be divided into two broad classes. Firstly are 2D planar slides. These are coated by a variety of slide surface chemistries such as aminosilane, epoxysilane and poly-L-lysine [214]. These slide surface chemistries interact with the proteins of interest through either the formation of covalent bonds or electrostatic interactions. However the disadvantage of using such 2D surfaces is evaporation of the liquid environment that the antibodies are printed, which in turn can affect the 3D structure of the protein [215].

Another approach is to use a 3D surface such as a nitrocellulose or hydrophobic surfaces that bind to the protein via physical adsorption. The advantages of using such slide surfaces are that they can preserve the protein in its original conformation over a period of time. On the other hand there are large variations in signal intensities associated with using such slides [216]. More recently time has been invested developing slides with 3D surfaces such as hydrogels. It is thought that such a surface chemistry could provide a partially hydrated surface that would help maintain the functionality of the protein. Additionally the surface would allow a larger number of proteins to bind to the surface due to the increased surface area [217].

Ultimately the slide surface and the way they interacts with the protein of interest will govern the spot morphology/size, spot intensity and amount of antibody that binds with the surface. Therefore the key aspect of choosing the best slide surface with respect to slide surface chemistry must consider the following:

- 1) A high binding capacity
- 2) A high signal to noise ratio
- 3) The ability to bind to proteins securely whilst maintaining their functionality
- 4) A reduced variability between slides of the same surface chemistry

1.5.2 Slide Noise and Spot Background

Slide noise can be defined as “the fluorescent signal that appears on areas of the slide that have not been printed with antibody” [214]. Spot background can be defined as the signal that appears on the spot when there is no antigen bound during the experimental procedure. Therefore an increase in either slide noise or spot background can reduce the sensitivity of the assay especially at the lower spectrum of detection [217].

A possible reason for the increase in slide noise could be due to the denaturation of proteins used in the blocking phase of the procedure or alternatively non-specific binding of signal related proteins [218]. Spot background is due to non-specific binding of proteins to the slide which is influenced by the slide surface chemistry. Spot background may lead to the denaturation of the protein which can expose hydrophobic bonds which increases the likelihood of nonspecific binding.

1.5.3 Spot Size and Morphology

Often the spot size and morphology are dependent on either the slide surface chemistry or the printing buffer. Certain slide surfaces can prevent spot spreading, leading to a reduced spot diameter and better spot morphology [219]. The net result allows for more densely printed arrays. A poor slide composition can lead to poor spot morphology due to the inability of the surface to hold functionally active antibodies, which can ultimately lead to reduced signal intensities [214].

Another important question is to look at the spot size and the number of spots that can be printed into a defined area on a slide. Currently spot size varies in diameter from as little as 25 microns to 150 microns [214]. If the spot diameter can be reduced but can still maintain the same intensity this could lead to a greater number of spots being

printed in the same space. Clearly this has the advantage of permitting more proteins of interests to be studied on one slide.

1.5.4 Signal Detection and Generation

The sensitivity and detection step of an assay are the key factor in microarray technology [220]. Signal detection can be achieved in two main ways; A) directly by molecules of interest or B) indirectly without any modifications to the molecules of interest [221]. Direct labelling can occur through the labelling of the protein of interest which can involve biotinylation (Figure 9) [222]. The advantage of direct labelling allows all proteins to be labelled in exactly the same way however, the potential disadvantage of using this method could lead to high background due to nonspecific adsorption of proteins such as albumin in serum that could affect the sensitivity of the assay [223]. Indirect labelling involves the addition of a detection antibody either biotin conjugated or with the use of a tertiary antibody.

Fluorescent binding includes using Alexa, Oyster or Cyanine dyes. Fluorescence detection methods are currently the preferred choice in microarray detection as they are safe, have a high sensitivity limit as well as having a high resolution once scanned [224].

A major limitation that occurs with antibody microarrays is possible cross reactivity especially in a mixed antibody arrays where more than one marker is measured at one time. An important element of the detection process has been the advent of signal amplification enzymatically. This can occur through the use of biotin, alkaline phosphatase or tyramide signal amplification [225].

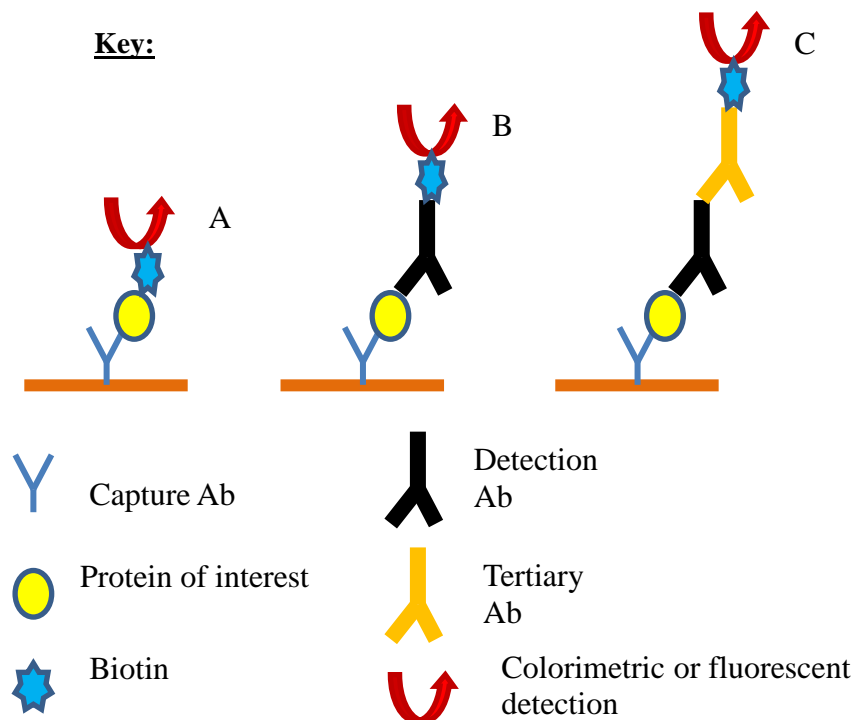


Figure 9: Methods of detection and signal generation.

The simplest way to generate a signal is to directly label the protein of interest through biotinylation (Fig A). The indirect approach involves the labelling of detection antibody (Fig B) or the labelling of tertiary antibody (Fig C). The latter approach takes away the need to chemically modify the nature of the detection antibody.

1.6 Introduction to Assay Validation

Assay validation is an evaluation of an experimental method to determine how well it fits for its specific use. In the validation process multiple parameters are investigated. Most importantly the use of validation enables the one to understand the limitations of the method and where it might be improved.

Validation is an on-going process where the design, development and establishment of a method, as well as optimisation and revalidation, are encompassed. However with many validatory procedures it is often limited by time constraints, resources and being able to have an assay that justifies the purpose of its needs [226].

Assay development is a major part of quality control and at present there are multiple guidelines provided by professional bodies, such as the FDA [227]. These guidelines provide the model of boundaries and limitations in assay.

Validation protocols have been published in recent literature with a variety of microarray concepts that have been developed by both major manufacturing companies (such as ThermoFisher and BIO-RAD) and in house microarray systems that have been used in research laboratories. The general definition of assay validation has been agreed to be the following “Assay validation involves documenting, through the use of specific laboratory investigations, that the performance characteristics of the method are suitable and reliable for the intended analytical applications. The acceptability of analytical data corresponds directly to the criteria used to validate the method.” [227].

A validation study can be described as a series of experiments that test the performance of an assay such as the accuracy, specificity and reproducibility of a system [228-230]. The major consideration taken in assay development is the intended purpose of the assay and how to construct a series of experiments that could answer the questions that could affect the assay [231].

One of the aims of this thesis is the validation of a microarray assay. In the antibody microarray system developed here, the purpose is to address the absence/ presence of proteins in biological samples. Specifically this requires the quantification of these proteins in biological samples. Hence in the validation of this microarray system we ask the following questions: i) can this microarray system accurately measure the exact concentration of a sample?, ii) what is the dynamic range of the assay and what would be the lowest reproducible value? and iii) is the assay accurate and precise when measured multiple times on the same day and on multiple days? (Table 5)

Table 5: To explore the validity questions asked when developing an antibody microarray method.

Test:	Purpose of Assay:	Questions asked of Assay:	Validation parameters tested:
Antibody Microarray	Measure/ detect/quantify the presence of absence of proteins in biological samples	a) Can assay accurately measure samples	Accuracy and Reproducibility
		b) What is the dynamic range?	Standard Curve & Range
		c) Can the assay be specific?	Specificity/Cross Reactivity
		d) Can assay be precise and accurate if repeated on the same day or multiple days?	Accuracy, reproducibility and precision (CV%)

The antibody microarray platform is used to measure and quantify proteins in biological samples. The key in being able to do this is to be accurate, precise and reproducible. A variety of different questions have to be answered by a variety of validity tests.

Antibody microarrays can be used to be both qualitative (ie measuring the presence or absence of a protein in a sample) and quantitative (ie measuring the actual amount of a substance). Hence figure 10 illustrates the types of experiments and parameters that have to be tested when measuring a microarray system when deciding to run a qualitative or quantitative approach. As seen with a quantitative approach, as used here more validity tests have to be performed to make sure the system is highly reproducible and accurate.

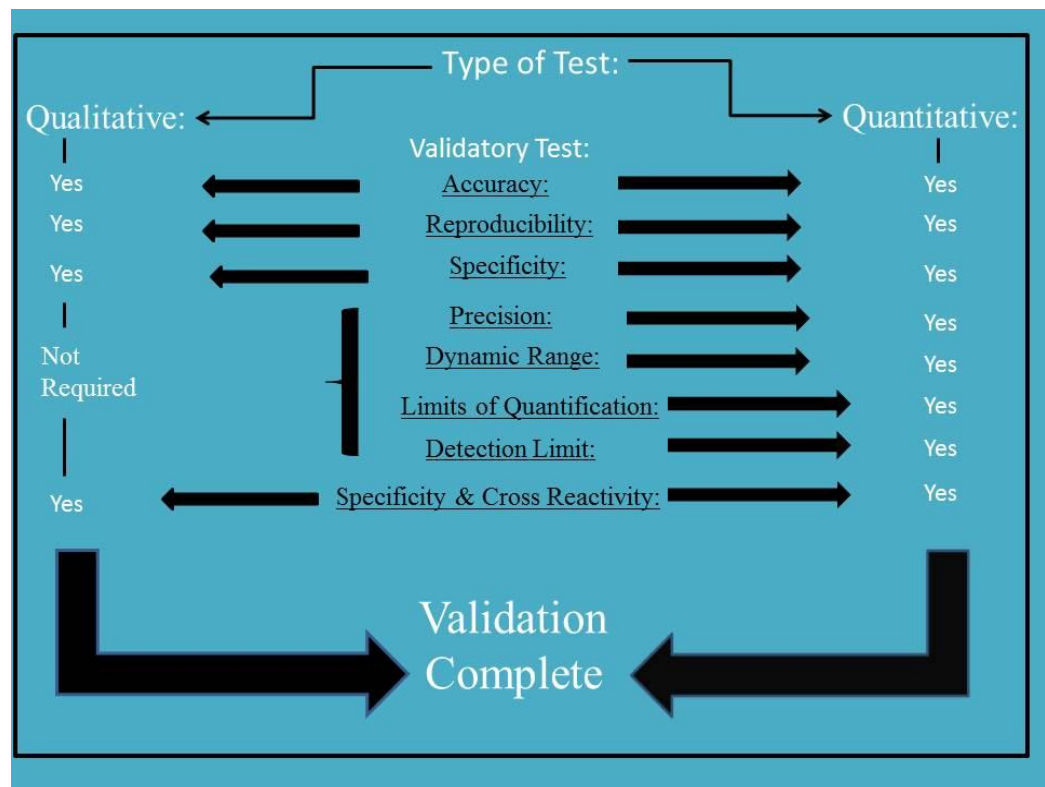


Figure 10: The validity experiments that have to be performed on an antibody microarray for both qualitative and quantitative approaches.

The qualitative approach allows for less validity experiments to be performed as the accuracy whilst needed is not as important as if a sample is to be quantified. In the quantitative approach multiple validity approaches have to be performed and implemented to make the system highly reproducible for everyday use.

The accepted standard procedure in running a validity process is to divide the nature of these experiments into different stages [232]. These stages include, i) Method selection: choosing the best way to quantify proteins in biological samples and how and best way to run the microarray system, ii) Development of the microarray system; this involves most optimisation including trying a variety of reagents, slides and buffers to enable the best combination that allows validation to take place (see Chapter 3) and iii) Measuring performance of the microarray; working out accuracy and reproducibility which involves repeatability, robustness and improving precision [233] (Figure 11). Often optimisation and validation are a joint process whereby improving one concept has an impact on the other and *vice versa*.

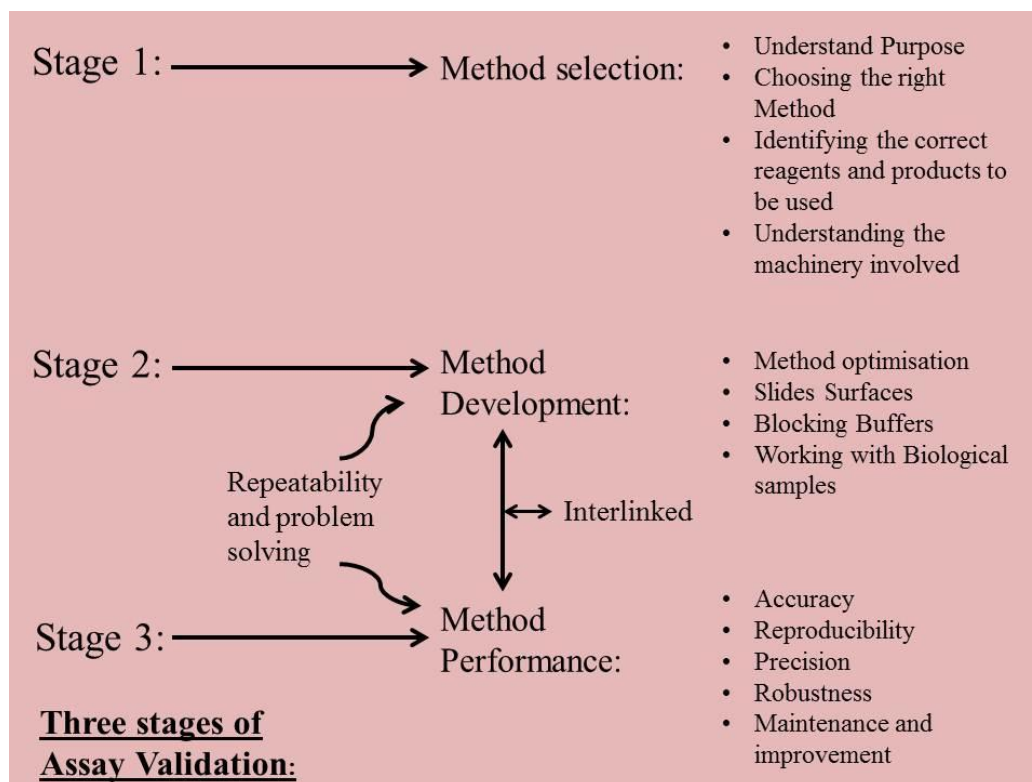


Figure 11: The three key stages involved in validation.

Stage 1 involves understanding the concept and choosing the right type of microarray procedure to run. Stage 2 involves the optimisation stage where the platform is built and initially tested with the biological samples to understand what is required from it. Thirdly, stage 3 is the main bulk of the validatory process where multiple experimental procedures are carried out to work out the accuracy and reproducibility of the platform and have a system in place that has no major issues which is ready to perform the initial hypothesis of the study.

If each stage is looked at in greater detail, one can understand why it is split into 3 different stages;

A) Method Selection; in this thesis the main aim was to build a methodology that is highly accurate and precise and allows for quantifiable detection of multiple biomarkers simultaneously across a variety of biological samples. For this reason the microarray approach was selected as the costs will be substantially reduced, requiring less sample and reagent than a traditional ELISA (which is limited to being able to measure one biomarker at one time). Furthermore microarrays have the capacity to deliver results quicker than an ELISA.

B) Method Development: Here the best conditions to run the microarray must be optimised, for example, what is the best print buffer? The best blocking buffer? The best slide surface? All these variables have to be investigated in depth and the best combination of these factors are then chosen together to move the microarray process forward. At this stage normal biological samples are tested and unknown concentrations of proteins are detected. However the reliability of these protein concentrations can only be checked in the performance stage.

C) Method Performance: This is where most of the validity tests are performed. Initially the limits of detection and quantification are defined. This will allow any further quantification work to fall within the boundaries of accurate quantification. Furthermore the performance of the assay can be tested by running a series of intra and inter assays over a period of days that show the accuracy and reproducibility of the system. In this investigation the guidelines for the parameters of the assay are based around the FDA Guidance on “Bioanalytical Method Validation” [227]. Here we compare the microarray system to the traditional ELISA. Once the methodology has been validated with the ELISA, clinical samples can be used in the assay.

1.6.1: Assay Validation Parameters

In all literature showing validation of an analytical method, parameters such as accuracy and precision have been identified and established to characterize the performance of an assay [234].

1.6.2: Accuracy

Accuracy can be defined as how exact the actual value obtained in an experiment is to the expected value [235]. This can be experimentally proven by applying the procedure to samples that can be prepared with a quantifiable accuracy (ie a series of “spikes”). Samples can be “spiked” to a known concentration and the amount detected in the assay is determined. Accuracy is often expressed as the % error between the observed concentration and the expected concentration. Whilst accuracy is an important parameter in validity testing, in certain examples such as qualitative measure accuracy cannot be required and instead can be replaced by sensitivity and specificity.

1.6.3: Precision

Precision is defined as the coefficient of variation (CV(%)) of multiple measurements or repeats [236, 237]. CV% is often calculated by dividing the standard deviation of multiple repeats by the mean of multiple repeats. Precision can be measured in a variety of ways, including repeatability of the same test, inter- and intra assays where experiments are performed multiple times on the same day or across multiple days.

Accuracy and precision are often misinterpreted as being same but in fact they are completely different to one another. The diagram (figure 12) below illustrates these concepts in relation to one another. For an analytical method to be successful it needs to be both highly precise and accurate:

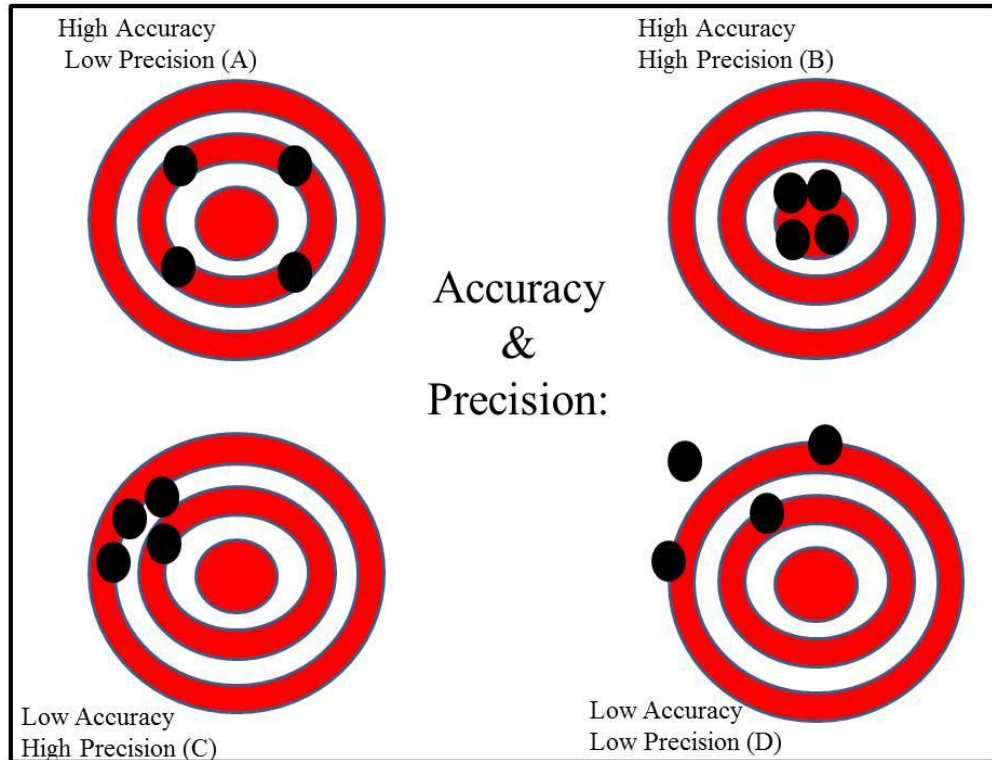


Figure 12: The relationship between accuracy and precision.

It is possible to have a high degree of accuracy and yet be imprecise across multiple measurements (A). Ultimately the aim of any assay is to be highly precise and highly accurate. This shows that from an experiment, the measured value is very close to the actual value (B). It is possible to have a set of data that is highly inaccurate but consistent for that experiment. This is again highly undesirable (C). Finally in the worst case scenario of microarray validation it is possible to be both imprecise and inaccurate giving rises to questions about the validity of the method which will have to be readdressed (D) [238].

1.6.4: Intra assay

Repeatability or the intra-assay can be defined as the precision obtained when the procedure or experiment is carried out under the same conditions within a short interval [239]. In the case of the microarray this is when the experiment is performed multiple times on the same slide. This serves as an indicator of how the precision is within the same day under normal working conditions.

1.6.5: Inter Assay

Inter assay where the experiment is carried out under the same experimental conditions across a few days. For example if a sample is taken and measured for any given protein on day 1, day 2 and day 3, one would expect the result to be consistent across the three days [240]. The precision is calculated and again serves as an indicator of how the effects of precision vary in slightly different external environments (i.e. change in room temperature, light, buffers/reagents etc). Often the precision is expected to be lower than that obtained in the intra assay.

1.6.6: Specificity

The specificity of a method, with reference to a microarray platform, is the ability to measure the presence of an analyte in the context of multiple analytes [241]. It is important that the microarray platform can be specific for individual analytes and show no cross-reactivity with other analytes in the same experiment.

Within specificity, both selectivity and recovery are two further parameters to be considered. Selectivity is defined as the presence or absence of a particular analyte in the context of complex sample mixture [242]. Recovery of an analyte is the amount detected from the total amount of a sample that has been added to a biological sample mixture. Often in recovery experiments these are run at three different concentrations; low, medium and high. The closer the recovery is to 100% the greater the precision of the assay.

1.6.7: Limit of Detection

The lower limit of detection (LOD), is defined as the lowest level that an analyte that can be detected but not be truly quantified [243] [244]. This is often presented as a concentration. In terms of the microarray the LOD is defined as a point that is above the level of the blank. Often the LOD is calculated as three times the standard deviation of the blank + the blank [243] [245].

1.6.8: Limit of Quantification

The limits of quantification are defined as the lowest (LLoQ) and highest (ULoQ) points in an assay that can be detected and quantified to an acceptable level of accuracy and precision [246-248]. Both the LLoQ and ULoQ, like the LOD, are expressed as a concentration. The LOD, LLoQ and ULoQ are all measured using standard curves. The LOD, LLoQ and ULoQ are all measured using standard curves. The LLoQ can be equal to the LOD but is often higher than the LOD. The LLoQ cannot however be lower than the LOD (Figure 13).

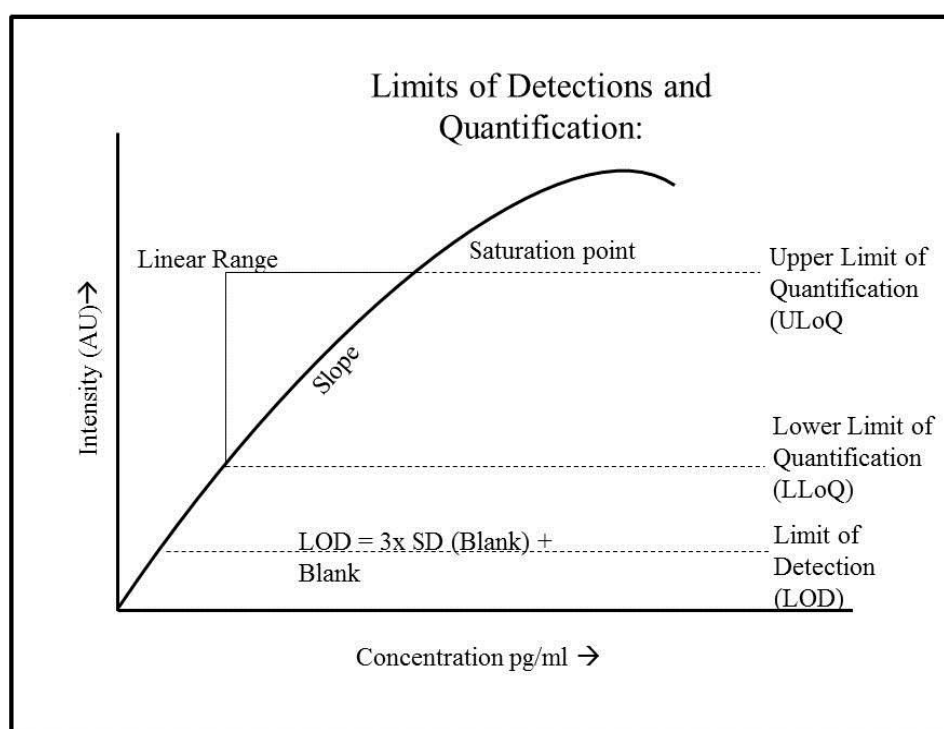


Figure 13: The relationship between the LOD, LLoQ and ULoQ from a standard curve.

The graph above illustrates the relationship of how the LOD, LLoQ and ULoQ can be determined from a standard curve. The LOD is often calculated to be 3 times the level of background intensity. Both the LLoQ and ULoQ are defined as the point in a standard curve which an analyte can be detected and quantified to an acceptable level of accuracy and precision.

1.7 Aims and Hypothesis:

The aim of this research is to develop a technique to enable a list of prominent biomarkers that allow for the early diagnosis of COPD. Additionally possible patterns of expression of biomarkers may help clinicians to categorise the severity of COPD. This would make it more beneficial and quicker to treat patients with this disease.

The wide use of protein microarray technology has allowed for the diagnosis and management of numerous diseases, such as cancer and autoimmunity. This ability to measure a vast array of biomarkers simultaneously is highly desirable. In the case of multifaceted diseases such as COPD which involves many immune cells, enzymes and mediators, microarray technology could detect biomarkers which could prove to be good indicators of the disease process. Sixteen prominent biomarkers are to be investigated in this study. All have been implicated in the disease process yet all 16 have yet to be investigated together.

The main hypothesis of the thesis was thus to build an antibody microarray platform that can be used as a diagnostic tool for the simultaneous quantification of inflammatory biomarkers in the sera of COPD patients. This has to be both reproducible and sensitive as compared to an ELISA (which is considered the “Gold standard” of inflammatory quantification). Once this is achieved the expression of these biomarkers will be compared between COPD patients and smokers with and without COPD to determine whether there are significant differences between the groups with relation to FEV₁, age or sex. Ultimately the aim is to use such a diagnostic tool to improve the prognosis, intervention and treatment of COPD.

Chapter 2: Materials and Methods

2.1: Materials

2.1.1: Chemicals and Reagents

2.1.1.1 *Printing Buffers*

A variety of *inhouse* coating buffers were made to identify the ideal buffer for printing antibody microarrays (Table 6):

Table 6: The ingredients involved in the formulation of 8 different coating buffers tested.

<u>Printing Buffers:</u>	<u>Ingredients:</u>
i) PBS	x1 PBS (Sigma) (v/v)
ii) PBS-Tween	x1 PBS (Sigma), 0.01% Tween-20(Sigma) (v/v)
iii) PBS-Glycerol	x1 PBS (Sigma), 5% Glycerol (v/v)
iv) PBS-Glycerol-Tween	x1 PBS (Sigma), 5% Glycerol, 0.01% Tween-20 (Sigma) (v/v)
v) PBS-Glycerol-Tween-Trehalose	x1 PBS (Sigma), 5% Glycerol, 0.01% Tween-20 (Sigma), 50mM Trehalose (v/v)
vi) PBS-Trehalose	x1 PBS (Sigma), 50mM Trehalose (v/v)
vii) PBS-Trehalose-Tween	x1 PBS (Sigma), 50mM Trehalose, 0.01% Tween-20 (Sigma) (v/v)
viii) DMSO	70% DMSO, 25% 0.2M sodium acetate pH 4.5, 5% Glycerol (v/v)

Abbreviations: i) PBS, ii) PBS-T, iii) PBS-GLYc iv) PBS-GLYc-Tw v) PBS-GLYc-TwTre vi) PBS-Tre vii) PBS-Tre-Tw and viii) DMSO

2.1.1.2: Blocking Buffers

A selection of blocking buffers were tested (Table 7):

Table 7: The different blocking buffers tested.

Blocking Buffers:	Purchased from:	Ingredients:
I Block	Tropix (Bedford, MA)	0.05g I Block in 25mL PBS-Tween-20 (0.05%) (Sigma)
3% BSA Block	Sigma, UK	Diluting 30% BSA in x1 PBS in 50mL
3% Milk Block	Marvel, UK	Diluting 3g dried milk powder in 100mL PBST (0.05% Tween-20)
NAP Block	G-Biosciences, MO	X2 Buffer diluted in 50mL of PBS
Smart Block	Candor Bioscience GmbH (Germany)	Used directly onto slides
PVA Block	Sigma, UK	Diluting 2g in 50mL in distilled water and heated until dissolved
Low Cross Block	Candor Bioscience GmbH (Germany)	Used directly onto slides

2.1.1.3: Wash Buffer (PBS-Tween 0.05%)

PBS (x10): tablets were diluted in deionised water and mixed with 0.05% Tween-20.

2.1.1.4: Reagent Diluent

Reagent Concentrate (x10) of 10% BSA solution (R&D systems, MN, USA) was diluted in 1:10 in deionized water before use.

2.1.1.5: Slide Surfaces

A selection of slide surfaces were tested (Table 8)

Table 8: The type of slide surface used and where they were purchased from.

Slide Surface	Purchased from:
Epoxysilane	ThermoFisher, UK Schott, Germany
Aminosilane	ThermoFisher, UK
Poly-L-Lysine	ThermoFisher, UK
Aldehyde	ThermoFisher, UK
Nitrocellulose	Grace Bio-Labs, OR, USA

2.1.2: Antibodies

2.1.2.1: Antibodies for print testing

The capture antibody used for the initial experiments was a monoclonal rat anti-mouse IgG1 (Cambridge Biosciences, UK). Detection antibodies were Alexa Fluor 488 labeled mouse IgG1, isotype control (BD Pharmingen, UK).

2.1.2.2 Antibodies for all ELISA and Microarray work

All antibodies were purchased as duosets kits from R&D systems with product numbers (MN, USA) (table 9).

Table 9: A list of all the antibodies used from optimisation to running patient samples.

Antibody	Product Number:
IL-8	DY208
IL-6	DY206
IL-1β	DY201
TNFα	DY210
VEGF	DY293b
Eotaxin-1	DY320
IFN-γ	DY285
IL-17	DY317
Eotaxin-2	DY343
IP-10	DY266
RAGE	DY1145
MCP-1	DY279
IL-4	DY204
IL-10	DY217B
TGFβ	DY240
IL-23	DY1290
GCSF	DY214
GMCSF	DY215
MIP-1β	DY271
RANTES	DY278
MCSF	DY216

2.2 Methods

2.2.1: Biomarker Study Population

Serum was obtained from 60 COPD patients, 37 healthy smoker volunteers and 13 age and gender matched non-smoking healthy controls. The study was approved by the local research ethics committee (Leicestershire, Northamptonshire, Rutland (LNR), REC 10/H0406/65. Samples were collected and stored at -70°C until use on the microarray to prevent repeated freeze-thaw cycles.

Table 10 displays patient demographics and spirometric measurements of the study participants.

Table 10: Demographic and Spirometric Data of the Study Participants.

	Age Mean (Range)	Gender	FEV-1% Mean (Range)
COPD (n=60):	67 (46-84)	35 Females 25 Males	72% (17-80%)
Gold Stage 1 (n=7)			
Gold Stage 2 (n=37)			
Gold Stage 3 (n=13)			
Gold Stage 4(n=3)			
Healthy Smokers (n=36)	65 (42-80)	16 Females 20 Males	76% (30-115%)
Control Non Smokers (n=12)	55 (41-65)	7 Females 5 Males	103.6% (87-122%)

Values are expressed as mean and (range). FEV1% - Percentage of Expected FEV1.

2.2.2: Slide Surfaces and Print Buffer

The capture antibody for the initial experiments were diluted serially from 250µg/ml across 10 dilutions in 8 different coating buffers (Figure 14) and all detection antibodies were used at 1:500, 1:1000 and 1:5000 dilution (PBS containing 3% BSA). Slides outlined in Table 8 were purchased and were processed immediately and after 1 week in storage in a vacuum.

2.2.2.1 Protocol for Print Production for Slide Surface and Print Buffer testing

Diluted capture antibody was loaded onto a 384 well plate (Genetix), and arrayed onto the different slides using a Biorobotics Microgrid II arrayer (Microgrid) and silicon contact pins (Parallel Synthesis Technologies, USA). The array chamber has a humidifier which was set at 58% humidity and run at room temperature during printing. The distance between spots was set to 315 microns and dwell time limited to 0.400s and target height printed was -0.184mm. The average spot diameter varied between 50-150 microns.

After printing slides were left overnight on the arrayer before being processed immediately or stored under vacuum or in air until use. Printed slides were blocked for 1 hour in 3% BSA, I-Block, 3% milk block or NAP block on a shaker. After blocking, slides were washed three times with PBST (containing 0.05% Tween-20) and incubated in solutions containing detection antibody conjugated with fluorescent dye for 1 hour at room temperature on a shaker.

Slides were washed with PBST (as described above) and rinsed briefly in ultrapure water. Slides were dried by spinning at 1200 rpm for 5 min and scanned a 4200 AL microarray scanner (Axon GenePix®).

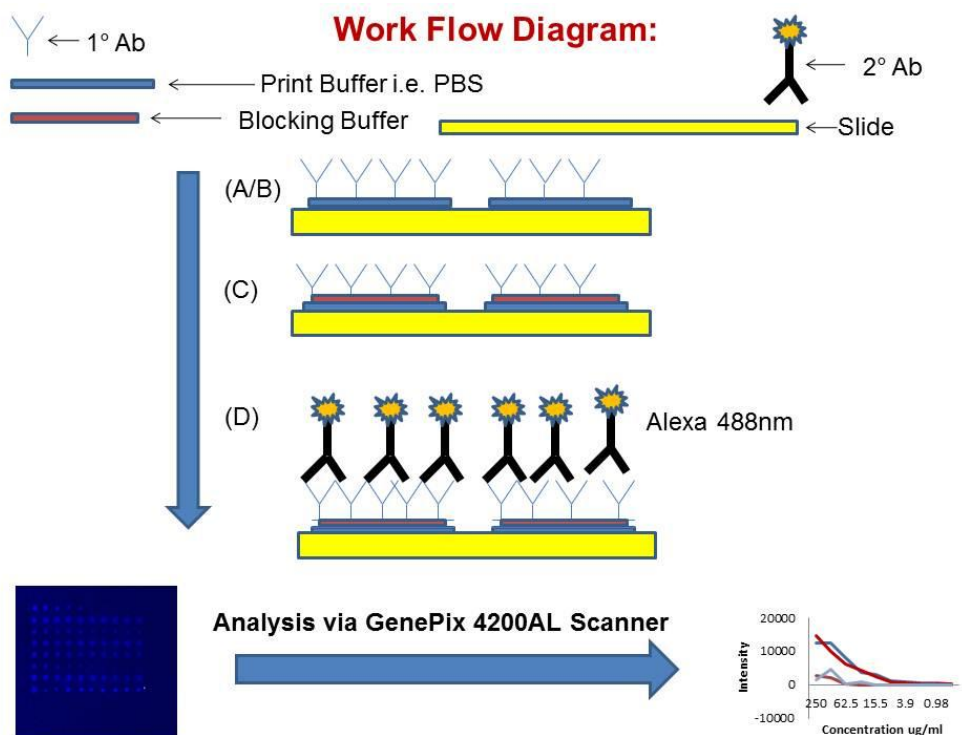


Figure 14: Illustrating the printing buffer /slide surface experiment overview.

Antibodies were printed on a slide surface (A & B), blocked (C) and then probed by detection antibodies tagged with Alexa 488 (D) and scanned.

2.2.2.2 Data Analysis

For a 16 pad slide, half of the slide is used for the construction of the standard curve. Often the top left well is used as a blank control well and the remainder of the left hand side of the slide is used to process the samples of interest. Each well on the microarray slide is equivalent to a well on an ELISA plate (Figure 15):

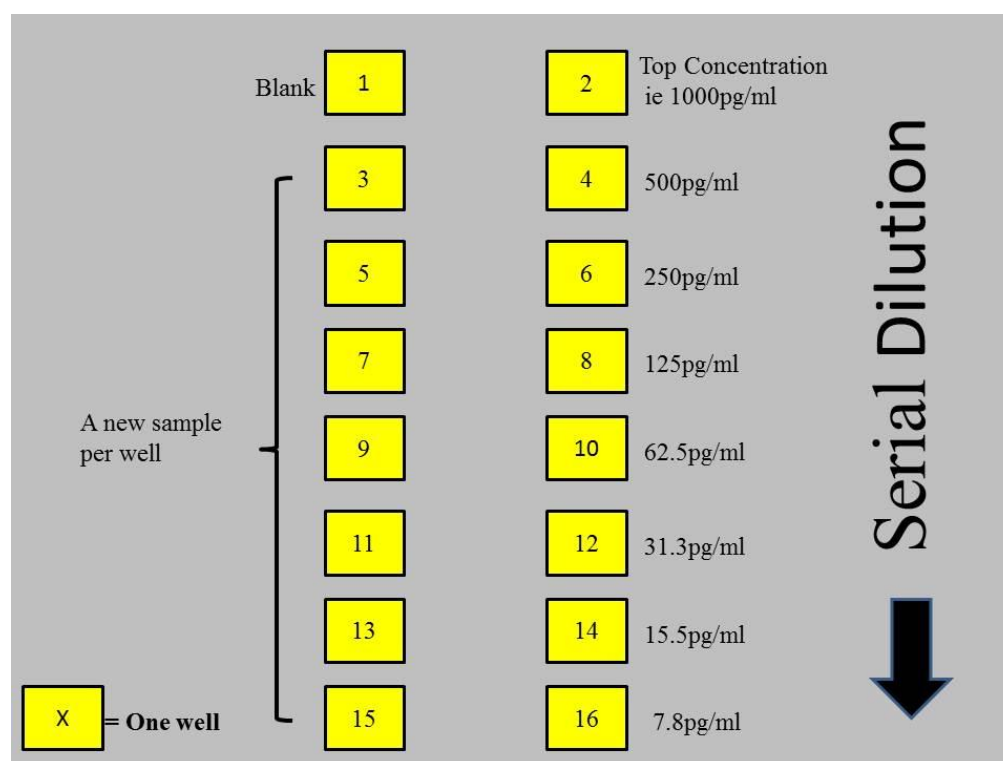


Figure 15: This is an illustration which shows the distribution of how each 16 pad slide is set up.

On the right hand side the standard curves are constructed with each concentration point in each well. On the top left hand slide is the negative control or blank. The remainder of the left hand of the slide is used for processing biological samples.

For the analysis undertaken in this thesis, the median value of the spot is considered as compared to the mean of the spot. When choosing between the median and mean of the spot the following has to be considered. “The mean intensity is defined as the average intensity of the signal pixel”, where the median is defined as the “intensity value that splits the distribution of the signal pixels in half” [249] [250]. The number of pixels above the spot should be the same as the number of pixels below the spot. The advantage of choosing the median value over the mean value lies in the ability of the median to take into account the outliers of within the spot. Contamination is a major issue in the microarray printing and processing. Contamination occurs due to dust and impurities that are present on the spot result in brighter pixels present on the image. Hence contamination introduces outliers in spot that are processed. If the software is incapable of correctly identifying the signal of the spot, taking into account the background and removing contaminated pixels, the median is often the preferred choice over the mean. In the majority of the experiments contamination of spots were rarely seen and hence to overcome this issue replicate spots are printed taking the average median of all the spots to give a signal. The median-background was taken in all experiments to take into account potential irregular spots and maintain consistency in the data with regard to possible contamination that may occur in the spots. This was used to construct a standard curve for each cytokine tested. From the standard curve, unknown concentrations of cytokines were calculated.

2.2.3: ELISA protocol

ELISA plates (96 wells) were purchased from Nunc-Immuno plate Maxisorp (Nunc, Denmark). ELISA duoset kits were purchased from R&D systems (Minneapolis, MN) and performed as described by the manufacturer's instructions (Figure 16).

Briefly, plates were coated with 1-4 μ g/ml of capture antibody and incubated overnight at room temperature. The plates were washed 3 times with PBS-Tween 0.05% (Sigma) and blocked with Reagent Diluent (1% BSA in PBS) for 1 hour and washed three times. Standards were made in Reagent Diluent at the top concentration (according to kit instructions) and diluted 2 fold (across seven points) at 100 μ l per well in duplicates for 2 hrs. The plate was washed three times and 50 μ l of appropriately diluted biotinylated detection antibody was added to each well for 2hrs. After washing three times with washing buffer, 50 μ l of diluted streptavidin-HRP was added and incubated at room temperature for 30 mins in the dark. Wells were washed three times and the enzyme substrate peroxidase chromogen was added. After incubation for 30 mins at room temperature the reaction was stopped by adding 50 μ l of 0.18M H₂SO₄ per well and the absorbances were read at 450nm (See Figure 16). Graphs were plotted to show the absorbances against the varying concentrations of the standards. This was repeated three times and averaged to show reproducibility of the kits.

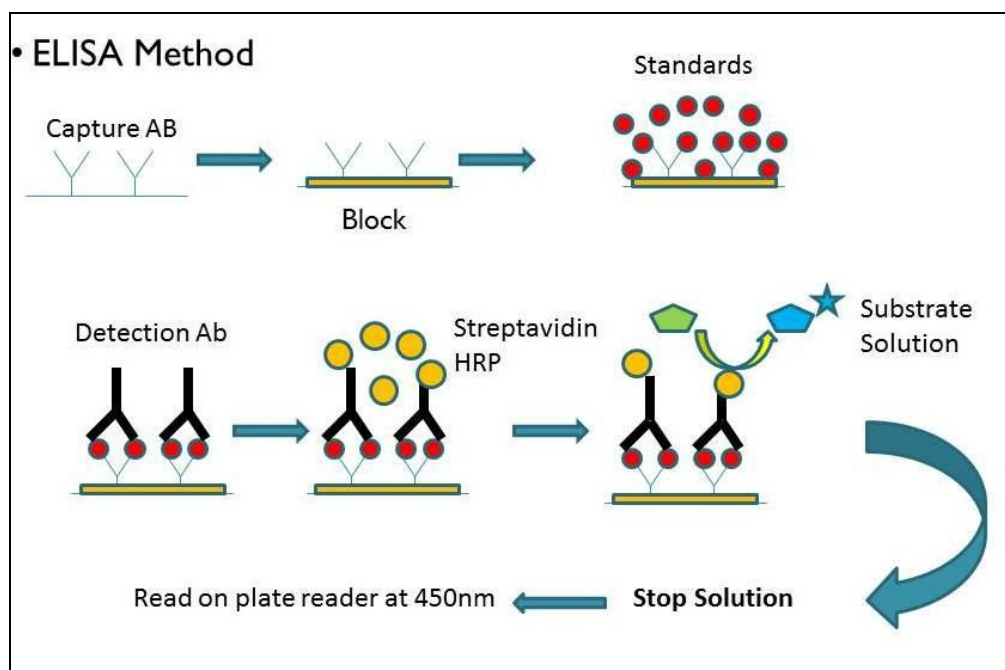


Figure 16: Illustrates the ELISA procedure.

Briefly, ELISA plates are coated with capture antibodies overnight. The plate is washed and blocked. The plate is washed and the standards and samples are added. After a period of 2 hrs the plate is washed again and detection antibodies are added for another 2 hrs. The plate is washed and streptavidin HRP is added for 30 mins and the plate is kept in the dark. The plate is washed three times and substrate peroxidase chromogen was added for 20 mins and finally stopped with 0.18M sulphuric acid. The absorbance is read on a plate reader at 450nm and graphs are plotted with the appropriate standard curve and samples.

2.2.4 Generating Microarray Standard Curves; Initial Protocol

Microarray slides were purchased from ThermoFisher (UK) with epoxysilane surface coatings. The protocol performed is similar to an ELISA. Briefly, diluted capture antibody was loaded onto a 384 well plate (Genetix), and arrayed onto slides at 100µg/ml using a Biorobotics Microgrid II arrayer (Microgrid) and silicon contact pins (Parallel Synthesis Technologies, USA). Printed slides were blocked with either 3% BSA (Sigma) or I-Block (Tropix) for one hour and washed three times with wash buffer (PBS-Tween 0.05%). Standards were made for each cytokine according to manufacturer's instructions and diluted two fold across seven dilutions and added at 100µl per block in ten replicates for two hours. The slide was washed three times and 100µl of appropriately diluted biotinylated detection antibody was added to each block for 90 mins. After washing three times with washing buffer, 100µl of 1:1000 diluted streptavidin-conjugated cy5 (E-Biosciences, UK) was added and incubated at room temperature for 30 mins in the dark. The slide was washed three times and rinsed in ultra-pure water and centrifuged dry (Figure 17).

Slides were spun dried and scanned with a 4200 AL microarray scanner at 635nm (Axon GenePix®). Fluorescence was quantified using the GenePix Pro Software (Axon GenePix®). The experiment was performed as an intra assay and repeated at least three times. As before the median fluorescence of each spot was measured (minus background) and the corrected fluorescence was used to calculate the average fluorescence signal across the standard detectable range (2000pg/ml-12.5pg/ml).

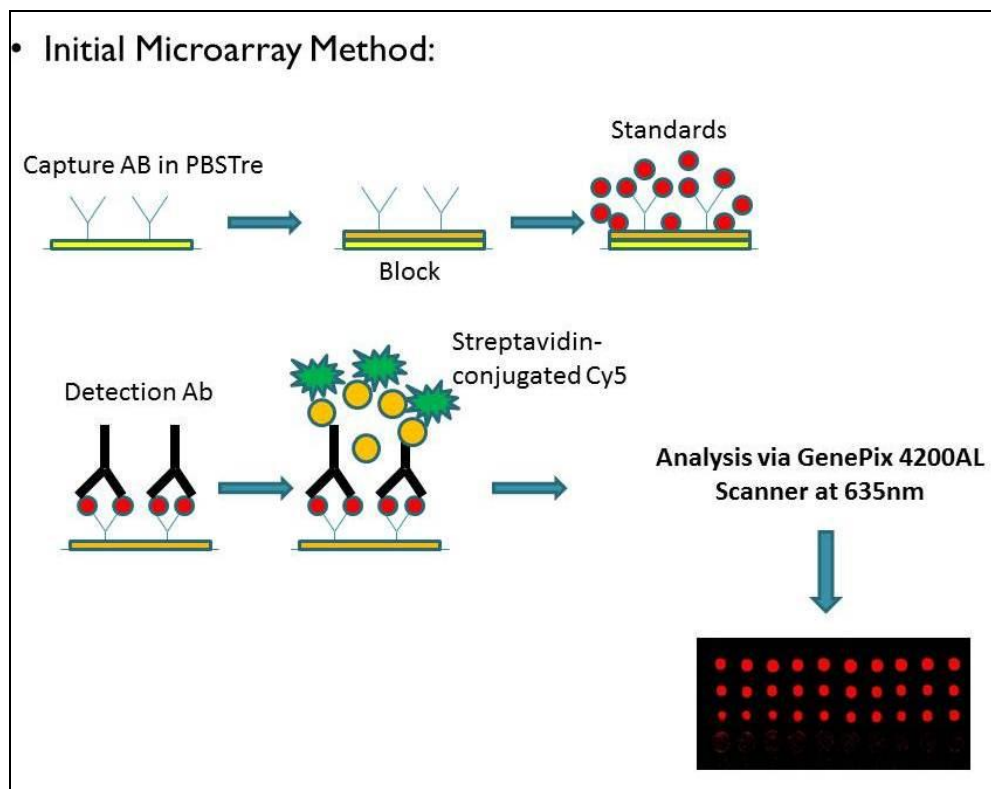


Figure 17: Illustrates the initial microarray method.

Briefly, capture antibodies were mixed with PBS-Tre and printed on slides at 100 μ g/ml. Slides were washed blocked with 3% BSA or I Block for one hour. Slides were then washed and standards/samples were added for 2 hrs. Slides were washed three times again and detection antibodies were added for 90mins. Slides were washed and streptavidin cy5 was added for 30 mins in the dark. The slide was finally washed and dried and scanned on the 4200 AL microarray scanner at 635nm.

2.2.5 Final Optimised Microarray Array Protocol

Printed slides were blocked with I Block (Tropix) for one hour and washed three times with wash buffer (PBS-Tween 0.05%). A calibrated cocktail of standards were made for each cytokine according to manufacturer's instructions and diluted two-fold across eight dilutions and added at 50µl per block for 45mins. Additionally samples were added in corresponding wells on the slide. The slide was washed three times and 50µl of appropriately diluted cocktail of biotinylated detection antibodies were added to each block for 45mins. After washing three times with washing buffer, 50µl of 1:1000 diluted streptavidin-conjugated cy5 (E-Biosciences, UK) was added and incubated at room temperature for 15 mins in the dark. The slide was washed three times and rinsed in ultra-pure water and centrifuged dry.

Slides were spun dried and scanned with a 4200 AL microarray scanner at 635nm (Axon GenePix®). Fluorescence was quantified using the GenePix Pro Software (Axon GenePix®). The experiment was repeated at least twice. As before the median fluorescence of each spot was measured (minus background) and the corrected fluorescence was used to calculate the average fluorescence signal across the standard detectable range.

2.2.6: Amplification

Amplification was performed after the detection stage of the microarray process described above with the addition of 50 μ l of 1:1000 diluted streptavidin-HRP (Bio-RAD, USA) and incubated at room temperature for 15 mins in the dark. The slide was washed and 50 μ l of Bio-Rad Amplification Reagent was added for 10 mins in the dark. The slides were washed three times with 20% DMSO-PBST and subsequently washed three times with wash buffer (see Figure 18). After washing, 50 μ l of 1:1000 diluted streptavidin-conjugated cy5 (E-Biosciences, UK) was added and incubated at room temperature for 15 mins in the dark. The slide was washed three times and rinsed in ultra-pure water and centrifuged dry and analysed as mentioned above.

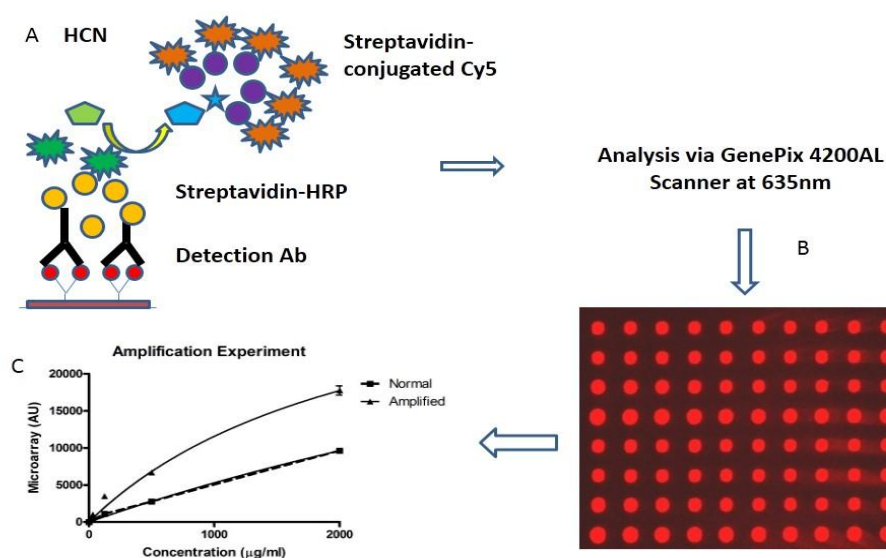


Figure 18: The amplification procedure and the effect it has on a standard curve

The HCN method is used to amplify the standard curve (A). As can be seen on the slide shot the effect of amplification increases the signal intensities of the spots (B). The effect of amplification is beneficial to the microarray platform as it is able to substantially increase the performance and range of the standard curve (C).

2.3 Printing

Slides were used to investigate the effects of dwell time, target height and humidity on spot shape, size and intensity. A slide was taken and was split for print into two. The top half of the slide was kept constant for the slide target height at -0.18mm and the dwell time was varied between 0.00 sec to 4.00 sec. In the second half of the slide the dwell time was kept constant at 0.40sec and the target height was changed between 0.0mm to -0.5mm (Figure 19). This was initially run without humidity (25-30% humidity) and repeated with humidity (60%). Each pad of the 16 pad slide was set to print up to 120 spots. The slide was processed as mentioned in 2.2.5 and signal intensity was measured as well as the number of spots printed per pad.

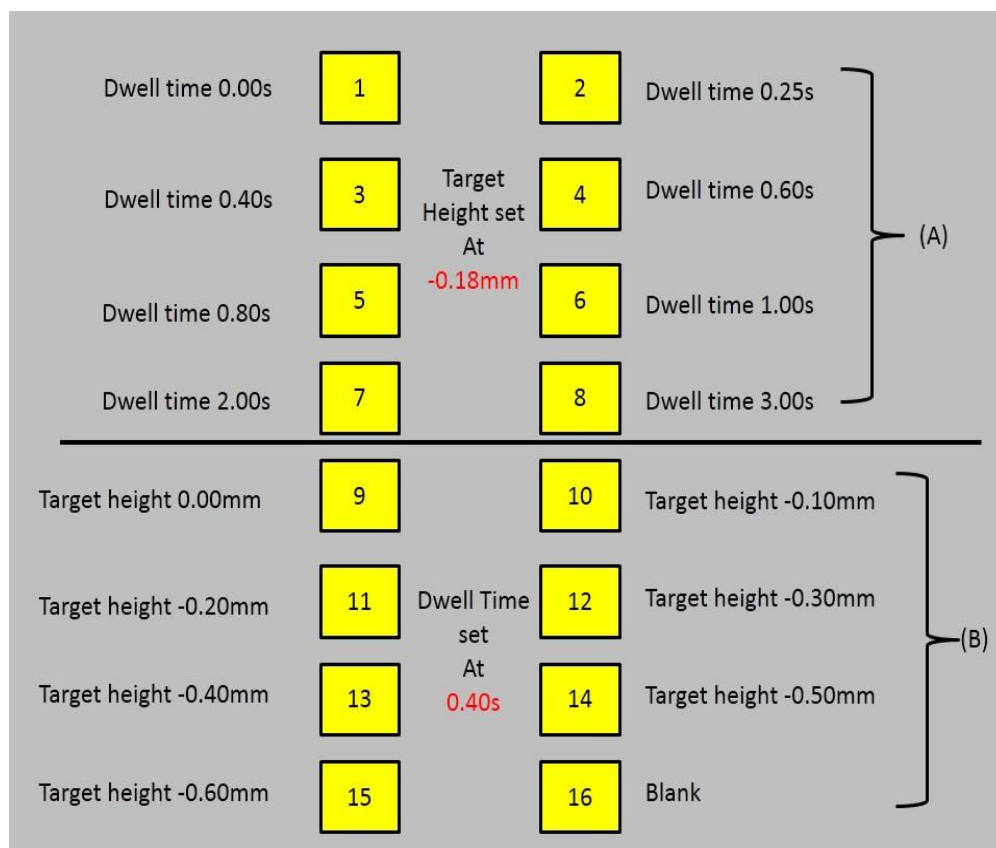


Figure 19: The layout of the print experiment.

In the top half of the slide the target height was kept constant at -0.18mm and the dwell time was varied (A). In the bottom half of the slide the dwell time was kept constant at 0.40sec and the target height was varied (B). Additionally the experiment was run without humidity and then with humidity set at 60% . Note per pad up to 120 spots were expected to be printed.

2.4: Microarray Validation

Due to the lack of guidelines for protein microarray assays the accuracy and reproducibility of the methodology was established based on the guidelines outlined by the Food and Drug Administration (FDA) for pharmacokinetic assay validation where multiple validation experiments were performed including intra- and inter assays. A series of “spike recovery” experiments were also performed. Additionally healthy donors were quantified by both ELISAs and microarrays to see the comparison between techniques. The accepted criteria for this assay for accuracy was between 80-120% and precision at <20% [227].

2.4.1 Intra and Inter-Assay

To determine the precision of the microarray platform, intra-assays and inter-assays were performed. Intra-assays were performed repeatedly over the same slide on the same day and inter-assays performed over a period of three consecutive days. Up to 30 sera from healthy donors were collected and quantified for 16 biomarkers. The mean of the replicates and standard deviation was used to calculate the precision of the microarray methodology.

2.4.2: PBS Spikes and Serum Spikes

PBS was spiked to three known concentrations at 750pg/ml, 188pg/ml and 24pg/ml using recombinant protein standards for each of the 16 biomarkers and quantified using the standard curves generated from the microarrays. These three spikes were set to be above and below the limits of quantification. Accuracy was calculated based on the observed concentration measured against the expected concentration that was spiked (%).

Additionally sera from healthy donors were taken and cytokine levels were quantified for all 16 biomarkers. This serum was then spiked to three known concentration points. The observed concentration was subtracted from background levels to calculate accuracy and precision.

2.4.3 ELISA Vs Microarray Comparison

The microarray technology was compared to a traditional ELISA. 30 sera from healthy donors were obtained and quantified for all 16 biomarkers through microarray and ELISAs. Direct correlations were made between the quantified values between techniques. Additionally Bland-Altman plots were drawn as a means to understand the sensitivity between techniques.

2.4.4: Lower Limit of Detection, Lower Limit of Quantification (LLoQ) and Upper Limit of Quantification (ULoQ)

The lower limit of detection was calculated as the concentration of biomarker required to give a signal that was equal to the background (blank) plus three times the standard deviation of the blank. This was calculated from the average of 3 standard curves for all 16 biomarkers. Additionally the lower limit of quantification (LLOQ) can be calculated to be twice the level of the LOD [243]. However for the limits of quantification, these were the lowest and highest points that could be detected at an acceptable level of accuracy and precision. Hence a series of “spikes” were run at the either end of the standard curves of the 16 biomarkers. The point where the precision fell below 20% was deemed to be LLoQ and 15% for the ULoQ as in line with FDA regulations for assay development.

2.5 Statistical Analysis

For the comparison between ELISA and microarray techniques, paired t-tests were performed (Chapter 4). For the COPD samples where there were three or more groups, Kruskal-Wallis tests were performed and subsequently Dunn's post multiple comparisons tests between each subgroup. Where the software indicated there were significant differences between two groups, Mann-Whitney U tests were performed. For the correlation studies with age and FEV-1 predicted with cytokine concentrations Spearman's r coefficient was performed (Chapter 5). A "p" value of ≤ 0.05 was considered to be statistically significant. Statistics and the generation of graphs were performed using Graphpad Prism 5.01.

Undertaking multiple Kruskal-Wallis tests and correlations also constitutes for multiple testing and therefore needs controlling to avoid the rise in false positive data. Hence this was performed through J-Express Pro 2012 – Build 119 which allows for further proteomic expression analysis. Using this software the "significant analysis of microarrays" or "SAM" was a method chosen to calculate the number of genes that are false positive. This was used on the data to see if any of the significant cytokines that were positively expressed were indeed showing as false-positive.

All heatmaps and hierarchical clustering was performed using MultiExperimentViewer (MEV) version 4.7.4.

Chapter 3: Optimisation of an Antibody Microarray Platform

3.1: Introduction

The ability to measure an array of biomarkers systematically in the same experimental setting is highly desirable. As such, antibody microarrays are regarded as the future of biomarker detection in disease. In the case of multifaceted diseases such as COPD, which involves many immune cells, enzymes and mediators, microarray technology could detect biomarkers which could prove to be useful indicators of the disease process [129, 251-253].

One of the biggest obstacles to this system is the slide surface. The surface chemistry of the slide dictates the mobilisation between the slide surface and the antibody or protein that is to be printed. The physical interaction between proteins and the slide surface by van der Waals, covalent, ionic or hydrophobic interaction needs to be optimised depending on the nature of the protein of interest [218].

Commercially there is a large variety of slide surfaces. These can be split into two main categories; firstly 2D plain slides, which include aminosilane, epoxysilane or poly-L-lysine surfaces that interact by electrostatic or covalent bonds. Secondly, 3D slides that are gel or membrane coated surfaces and include nitrocellulose and agarose slides that interact by physical adsorption [254-257].

Hence there are some important factors that should be considered when choosing the slide surface. These include a binding capacity, a signal-to-noise ratio, the ability to maintain the conformation of the protein that is once bound as well as the reproducibility between slides. The ideal slide would be a combination that enables maximal immobilisation and as well as maintaining the functionality of the antibody.

The spot morphology is often dependant on factors such as the slide surface and the way the capture antibody interacts with the surface chemistry. Poor spot morphology is indicative of low antibody activity and in turn will lead to poor signal intensities [219, 258]. Hence it is important to distinguish which slide surface will provide the best spot morphology but more importantly give higher levels of intensity.

Often the spot size and morphology are dependent on either the slide surface chemistry or the printing buffer. Certain slides surfaces can prevent spot spreading, leading to a reduced spot diameter and better spot morphology [219] [258]. The net result allows for more densely printed arrays.

Prior work in the field has investigated individual parameters such a printing buffers or slides surfaces or blocking buffers across numerous publications. Work conducted by Olle W *et al*, has shown that glycerol to be an efficient printing buffer for printing antibodies [219]. Additionally work by Seurnyck-Servoss *et al* investigated different slides surfaces which showed that both aminosilane and poly-L-lysine surfaces are preferable for antibody microarrays [218]. Finally work by Rimini *et al* investigated different types of blocking buffers onto antibody microarray surfaces which showed that BSA block was effective to in preventing non-specific adsorption [259].

Here we investigate for the first time multiple parameters simultaneously including variety of coating/blocking buffers using four different slide surfaces to investigate the impact on intensity (short and long-term) and spot morphology which provides an more in-depth understanding what is required to build a successful antibody microarray platform.

3.2: Materials and Methods

Briefly slides were purchased from Thermofisher (UK). For the optimisation of slides surfaces, blocking buffers and investigating intensity levels poly-L-lysine, epoxysilane, aldehyde, aminosilane and nitrocellulose slides were used respectively. A variety of 8 in-house coating buffers were used to print on the slide surfaces (see Table 5) and the experiment was run either immediately or one week later. On the day of processing the slides were taken and blocked for an hour with a variety of blocking buffers including I Block, 3% BSA Block, 3% Milk and NAP blocking buffer. The slides were washed and incubated in solutions containing detection antibody conjugated with fluorescent dye for one hour. The slides were washed and spun dry and scanned at 488nm wavelength on the 4200 AL scanner. The intensity levels of these slides were compared against one another to distinguish which would represent the best slide surface for both short and long term use.

For the remainder of the Chapter, poly-lysine slides were used. Due to the low level of sensitivity obtained, these slides were subject to amplification. Briefly, antibody duoset kits were purchased (R&D Systems, MN, USA) and printed on the slide. Slides were processed immediately or after one week. Slides on the day of processing were taken from the vacuum and blocked for an hour with either I Block or 3% BSA block buffer. Standards were made for all 16 cytokines (IL-8, IL-6, IL-1 β , TNF- α , Exotaxin-1, Eotaxin-2, IFN- γ , RAGE, IL-10, IL-4, IL-17, IL-23, MCP-1, VEGF and IP-10) according to manufacturer's instructions and diluted 2 fold across 7 dilutions and added at 100 μ l per block in 10 replicates for two hrs. The slide was washed three times and 100 μ l of appropriately diluted biotinylated detection antibody was added to each block for 90 mins. After washing three times with washing buffer, 100 μ l of 1:1000 diluted streptavidin-conjugated cy5 (E-Biosciences, UK) was added and

incubated at room temperature for 30 mins in the dark. Slides were spun dried and scanned with 4200 AL microarray scanner at 635nm (Axon GenePix®).

For the latter part of this Chapter, and the printing conditions as well as the role Cy5 plays in the detection of antibodies and the detection of cytokines in both plasma and serum were investigated. Slides initially showed a lack of sensitivity at the lowest concentrations of standard curves, hence were subject to tyramide amplification.

Briefly, this was performed after the detection stage of the microarray process described above with the additional of 50µl of 1:1000 diluted streptavidin-HRP (Bio-Rad, USA) in the dark. The slide was washed and 50µl of Bio-Rad Amplification Reagent was added for 10 mins in the dark. The slides were washed three times with 20% DMSO-PBST and subsequently washed thrice with wash buffer. After washing, 50µl of 1:1000 diluted streptavidin-conjugated cy5 (E-Biosciences, UK) was added and incubated at room temperature for 15 mins in the dark. The slide was washed three times and rinsed in ultra-pure water and centrifuged dry and analysed as mentioned above.

3.3: Results

To compare printing buffers, 8 commercially available print buffers were tested across different slide surfaces. Capture antibodies (monoclonal rat anti-mouse IgG1) were mixed with 8 different print buffers (PBS, PBS-T, PBS-GLYc, PBS-GLYc-Tw, PBS-GLYc-TwTre, PBS-Tre, PBS-Tre-Tw and DMSO) and detected with an Alexa Fluor 488 labeled mouse IgG1, isotype control.

The median signal intensities of the spots were calculated. In addition the spot morphology and size were also considered. The final aspect of this investigation was to examine the effect of storage. It is important to find a surface that when stored would produce the same level of intensity when printed freshly and analysed immediately. Hence the correct combination of print buffer and slide surface is sought.

3.3.1 Epoxysilane

Epoxysilane slides provide an epoxy ring that reacts with the amine group on antibodies and proteins that are spotted.

3.3.1.1 Slides surface and coating buffer

The average intensity of 8 printing buffers across concentration of primary antibody ranging from 250 μ g/ml to 0.49 μ g/ml on epoxysilane slides was measured (Figure 3.1.). The average intensity falls quite dramatically after 125 μ g/ml for most buffers. In these conditions on this slide surface PBS-GLYc, PBS-TRE and to a lesser degree PBS perform the best at with the highest intensities measured at over 16000 AU for PBS-Tre and over 12000 AU for both PBSGLY and PBS (Figure 20). PBS-Tre performs the best with both blocking buffers used and is the most consistent printing buffer on this particular slide surface.

Intensity levels could not be maintained at low concentrations in all 8 printing buffers. With both blocking buffers most signal intensities dropped to almost non-recordable levels below 31.25 μ g/ml.

Epoxy silane slides exposed to air lost intensity as the slide surface would interact with the atmosphere and lose reactivity. PBS-Tre could be suggested as a best printing buffer as the average intensity was the highest but subsided sharply with decreasing concentrations of capture antibody printed (at 31.25 μ g/ml).

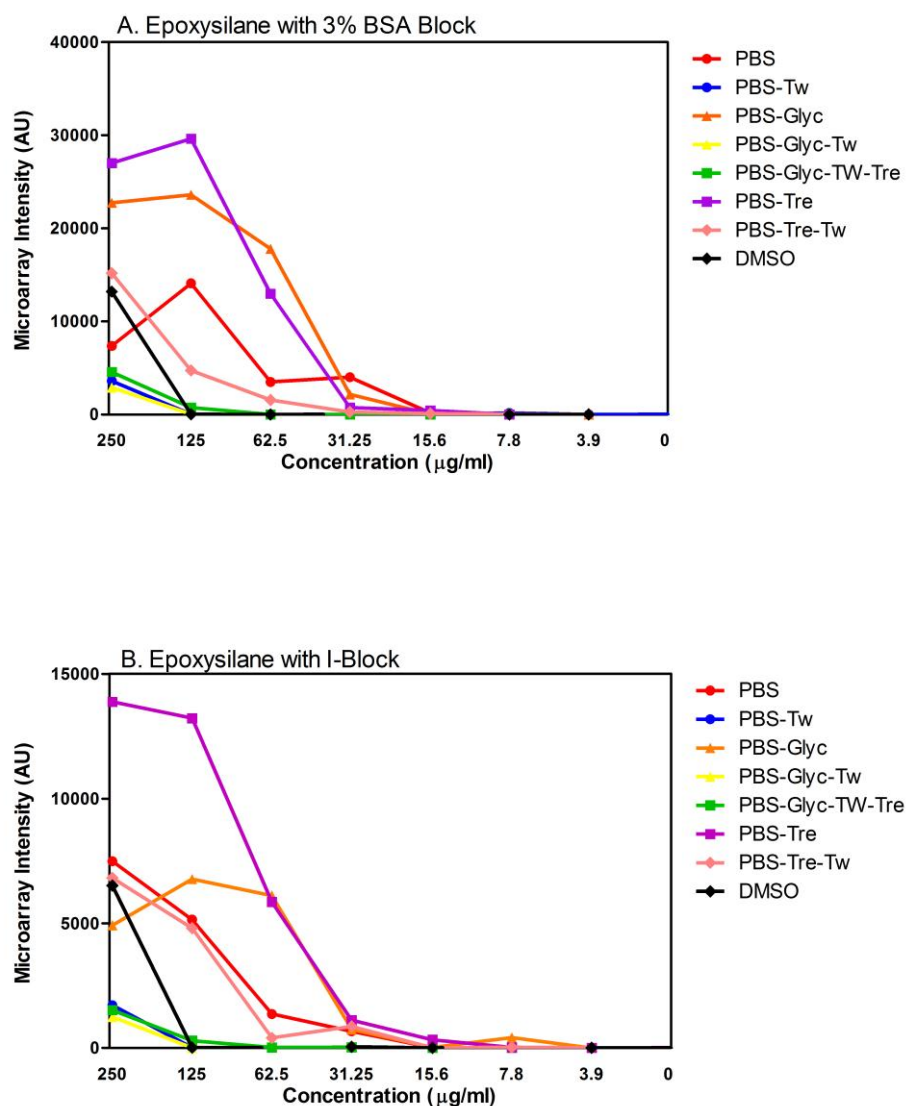


Figure 20: Signal intensity of 8 printing buffers on epoxysilane slides.

The average intensity of 8 printing buffers across monoclonal rat anti-mouse IgG1 serially diluted, ranging from 250 µg/ml to 0 µg/ml with the addition of mouse IgG1 secondary antibody diluted 1:500, then blocked in 3% BSA (A) and I Block (B) on epoxysilane slides was measured. On this slide surface PBS-Tre showed to be the best coating buffer with the highest level of intensity and had the best dynamic range with signals detectable as low as 15.6 µg/ml. Interestingly PBS-Tre performs the best with either blocking reagent where the other 7 buffers are not so consistent (n=3).

3.3.1.2 *Epoxy silane Spot Morphology and Size*

Spot morphology is dependent on a variety of factors including the choice of slide surface and coating buffers. In the case of PBS, the comet like spotting that occurs at the highest concentration indicates there is too much capture antibody loaded onto the spot (Figure 21). As there is so much capture antibody it cannot be sufficiently contained within the coating buffer, and hence tails off as it is “loosely” bound to the surface potentially leading to falsely interpreted results.

The spot morphology for PBSTre was good, so in conjunction with figure 20, PBSTre seemed the most suitable coating buffer for epoxy silane slide surfaces. The next step was to establish the optimum capture antibody concentration to coat a variety of cytokines/antibodies.

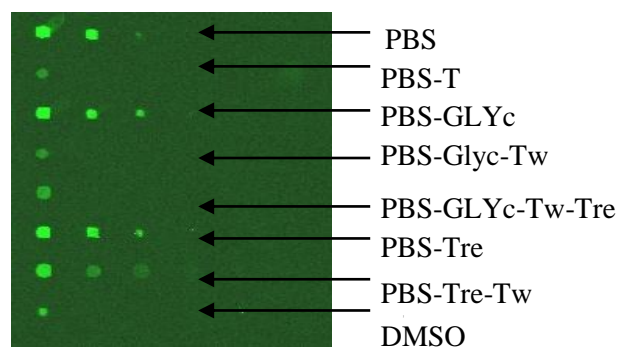


Figure 21: Spot morphology epoxy silane slides when tested with 8 coating buffers.

Of the 8 coating buffers tested only PBS, PBS-GLYc and PBS-Tre and to a lesser degree PBSTreTw produced any signals that could be quantified as shown graphically in Figure 20 showing the suitability of these coating buffers on epoxy silane slide surfaces.

3.3.1.3 Epoxysilane Short vs Long-Term effects of Printing

Antibodies were printed on epoxysilane slide surface. These were processed immediately or one week later once left in dessciated vacuum.

As can be seen there is a big drop in intensities when the slides are processed after one week indicating the slide surface chemistry does not efficiently hold the antibody over a period of time. Specifically, buffers such as PBS, PBS-GLYc, PBS-Tre (starting at 15000 AU immediately and dropping to less than 1000 AU after 1 week) and PBS-Tre-Tw that produced high levels of intensities when processed and analysed immediately all experienced a sharp drop in intensity 1 week later. This shows that this type of slide surface is not ideal when investigating the utility for long-term measurement of biomarkers (Figure 22).

The epoxy slides were tested with I Block to see if a different blocking buffer could produce a higher intensity than 3% BSA. However there were no discernible difference between I Block and 3% BSA block irrespective of spot intensity, morphology or short vs long-term use.

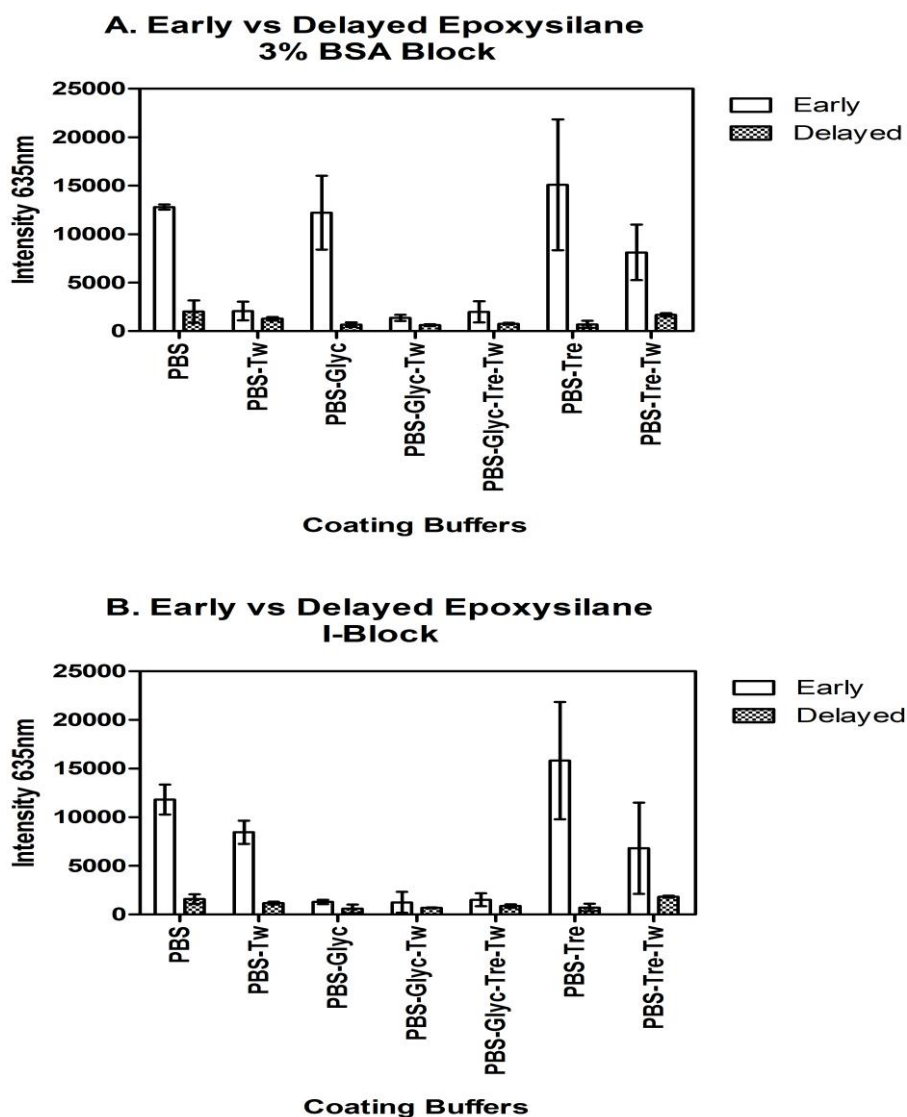


Figure 22: Signal intensity of epoxysilane slides processed immediately or delayed.

The signal intensities between the coating buffers when analysed fresh and analysed after a week once printed. The average intensities were measured at the top end range of 250 $\mu\text{g/ml}$ of capture antibody when blocked with 3 % BSA Block (A) or I Block (B). Buffers such as PBS, PBS-Tre and PBS-Tre-Tw consistently produced high levels of intensities when processed and analysed immediately (with either blocking buffer) but all experienced a sharp drop in intensity when processed one week later. This indicates this is not the best surface for the long-term use of an antibody microarray platform (n=3).

3.3.2 Aminosilane

The aminosilane slide surface provides available amines groups that provide a solid covalent bond between the slide surface and the protein. The composition of the slide surface chemistry provides a high signal to noise ratio [260].

3.3.2.1 Slides surface and coating buffer

The average intensity of 8 printing buffers across concentrations of capture antibody ranging from 250 μ g/ml to 0 μ g/ml with the addition of secondary antibody diluted 1:500, then blocked in 3% BSA on aminosilane slides was measured (Figure 23). The coating buffers, in particular PBS-Tre-Tw and PBS-Glyc produced the best curves. PBS-Tre-Tw had the highest intensity with a peak of 25000 AU (at 250 μ g/ml) and had the most consistent curve with intensities detectable as low as 15.5 μ g/ml. When I-Block was used as a blocking buffer, PBS and PBS-Tre-Tw produced the best curves. PBS had the highest intensity at 15000AU (at 250 μ g/ml) and was the most consistent curve. Note that the overall levels of intensity of the 8 printing buffers were lower when blocked with I-Block compared to 3% BSA.

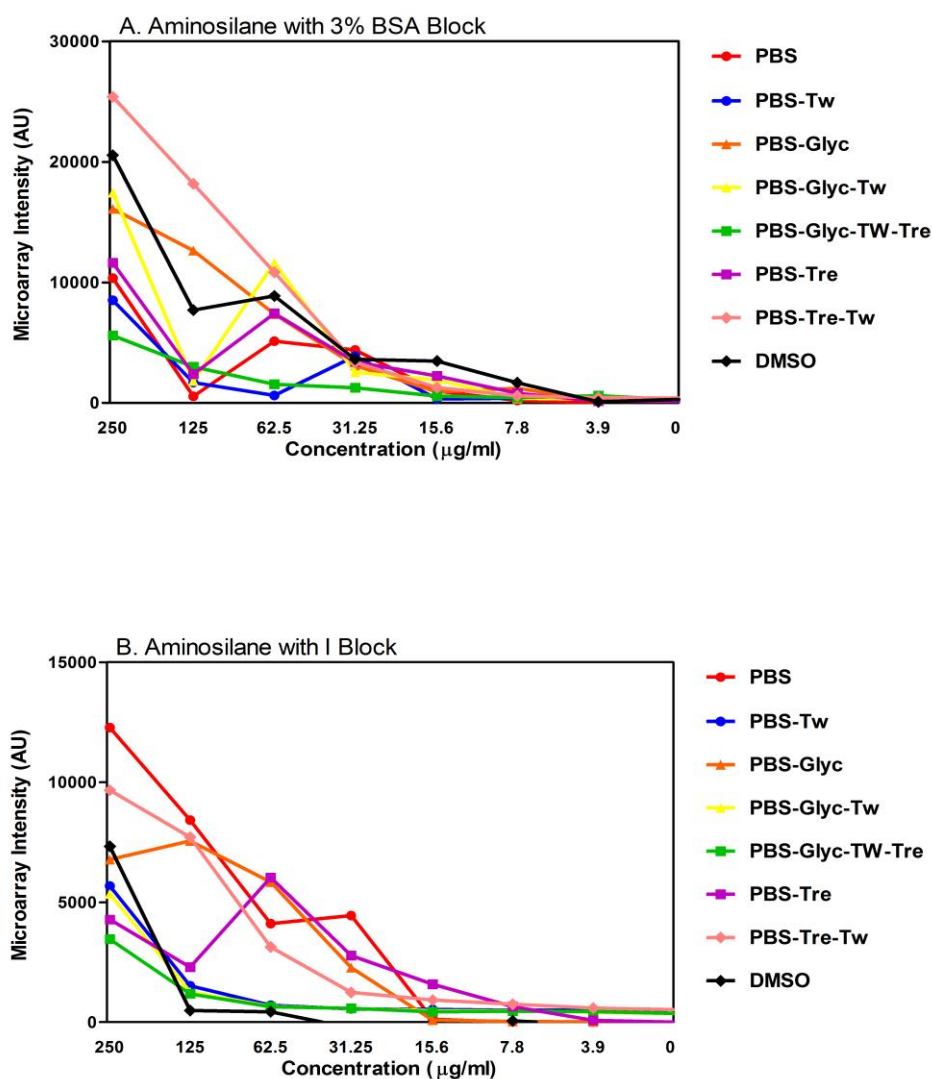


Figure 23: Signal intensities of 8 printing buffers on aminosilane slides.

The average intensity of 8 printing buffers across monoclonal rat anti-mouse IgG1 serially diluted, ranging from 250 µg/ml to 0 µg/ml with the addition of mouse IgG1 secondary antibody diluted 1:500, then blocked in 3% BSA (A) and I Block (B) on aminosilane slides was measured. On this slide surface PBS-Tre-Tw (A) showed to be the ideal coating buffer with the highest level of intensity and had the best dynamic range with signals detectable as low as 15.6 µg/ml. Interestingly PBS performs marginally better than PBSTreTw in I-Block (n=3).

3.3.2.2 Aminosilane Spot Morphology and Size

Aminosilane slides produce nice spot morphology for all printing buffers (Figure 24).

The shape of the spots are round-doughnut and fairly consistent. Note with PBS-Tre the shape of the spot decreases in diameter as the concentration decreases of capture antibody. However DMSO does not spot after 250 μ g/ml, whilst the PBS-T, PBS-Glyc-Tw and PBS-Glyc-Tw-Tre show autofluorescence at the lowest concentration.

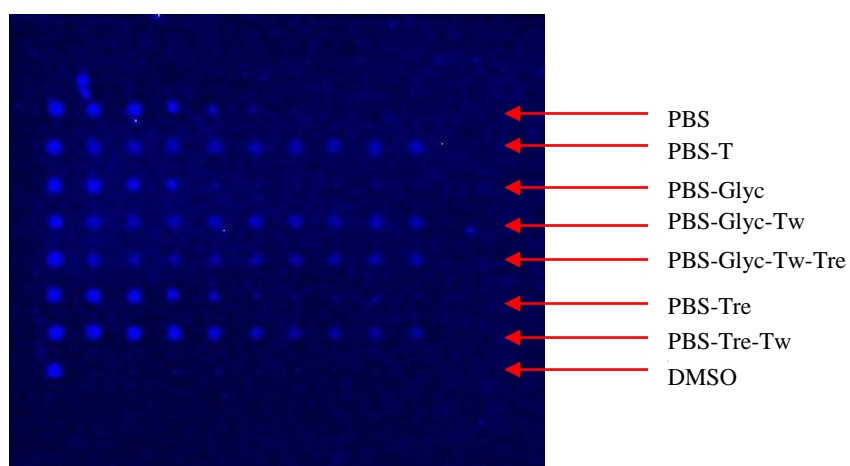


Figure 24: Spot morphology aminosilane slides when tested with 8 coating buffers and blocked with 3% BSA.

Of the 8 coating buffers tested only PBS-Tre-Tw stood out as the print buffer that produced any signals which could be quantified as shown graphically in Figure 23 showing the suitability of these coating buffers on aminosilane slide surfaces.

3.3.2.3 Aminosilane Short vs Long-Term effects of Printing

The short-term vs long-term effects of aminosilane was investigated as described with epoxysilane slides. Aminosilane, like epoxysilane provides a surface chemistry that performs well when processed immediately. Short-term using both 3% BSA block and I Block, aminosilane produce moderate levels of intensity but with high variability, whilst long term the intensity drops dramatically but the variability is reduced with both blocking buffers (Figure 25). This once again indicates whilst short term the slide surface chemistry provides good intensities and spot morphologies, long term it may not be the ideal surface moving forward. Interestingly, PBS-Tre-Tw in I-Block produced a high level of variation indicating this combination of print buffer, slide surface and blocking buffer is unsuitable.

The poor spotting nature of DMSO print buffer on slide surfaces resulted in this buffer being removed in future analysis of the short and long-term effects of printing (Figure 25).

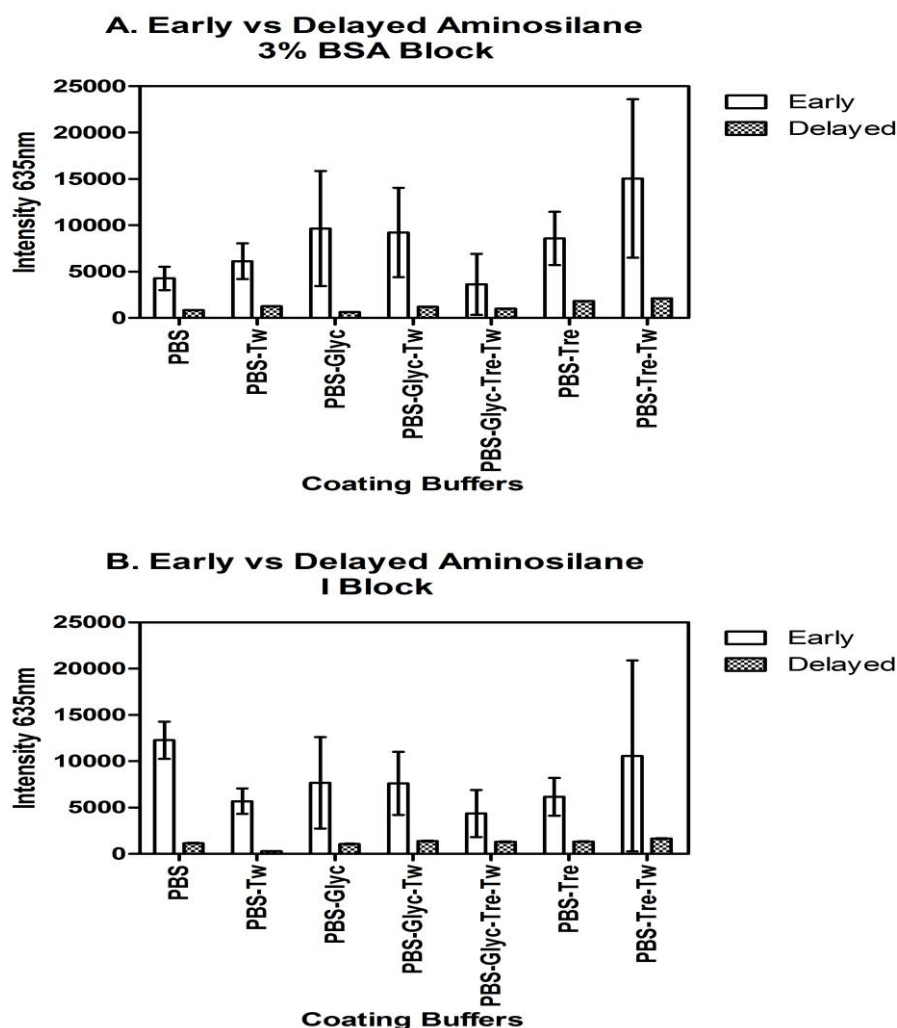


Figure 25: Signal intensity of aminosilane slides processed immediately or delayed

The signal intensities between the coating buffers when analysed fresh and analysed after a week once printed. The average intensities were measured at the top end range of 250 $\mu\text{g/ml}$ of capture antibody when blocked with 3 % BSA Block (A) or I Block (B). The aminosilane surface is not conducive to preserving the formation of the antibodies as shown by a drop of intensity after one week when processed. In all the buffers the intensities have dropped indicating that this slide surface chemistry is unsuitable when used long term when preserving the functionality of the antibody (n=3).

3.3.3 Poly-L-Lysine

Like aminosilane slides, poly-L-lysine slides provide a dense layer of amine groups which are ideal for binding a variety of molecules such as proteins, DNA and oligonucleotides [261].

3.3.3.1 Slides surface and coating buffer

The average intensity of 8 printing buffers across concentrations of primary antibody ranging from 250 μ g/ml to 0.49 μ g/ml with the additional of secondary antibody diluted 1:500 in I-Block on poly-L-lysine slides were measured.

As can be seen PBS-Tre and PBS-Tre-Tw produce the best curve. The consistency of both buffers across the 3 slides surfaces investigated thus far shows their adaptability. The intensity is moderate to high and is detectable as low as 7.8 μ g/ml showing its effectiveness at the lower range (Figure 26). Interestingly, most coating buffers apart from PBS-Tre and PBS-Tre-Tw produced intensities that were too low for detection.

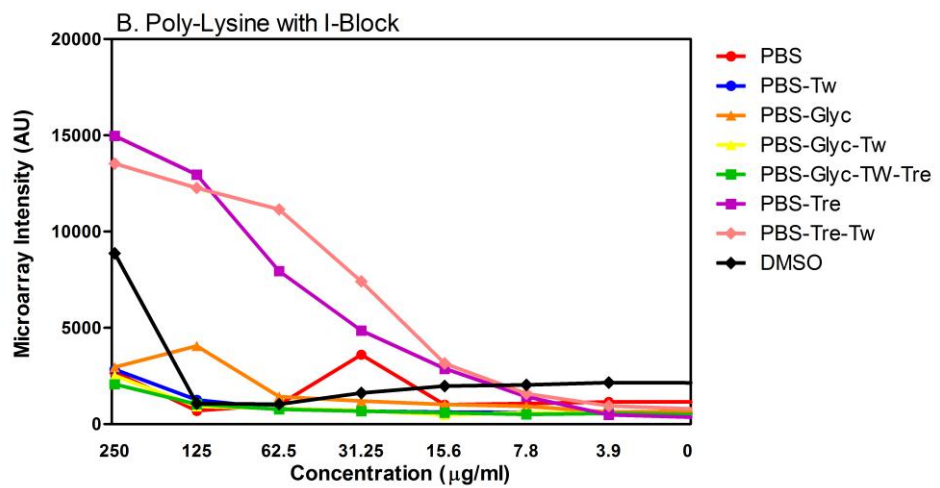
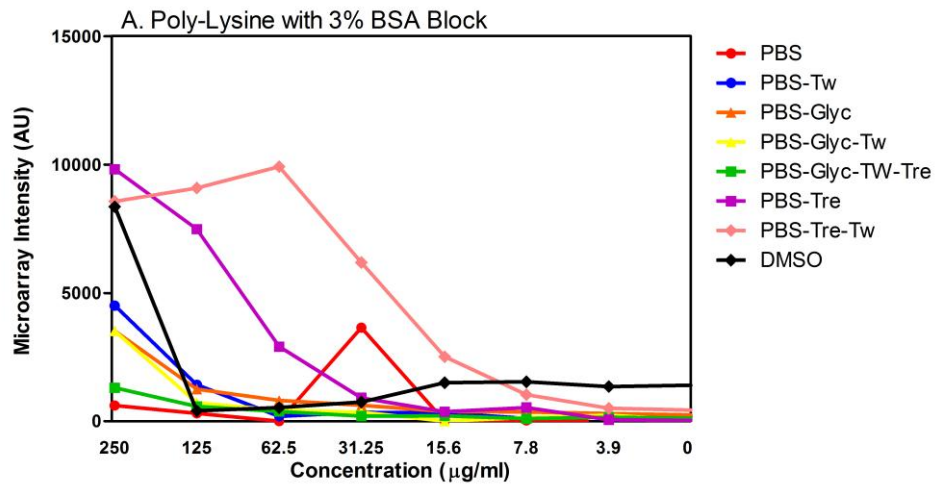


Figure 26: Signal intensities of 8 printing buffers on poly-L-lysine slides.

The average intensity of 8 printing buffers across monoclonal rat anti-mouse IgG1 serially diluted, ranging from 250 μ g/ml to 0 μ g/ml with the addition of mouse IgG1 secondary antibody diluted 1:500, then blocked in 3% BSA (A) and I Block (B) on poly-L-lysine slides was measured. The level of intensity did not vary greatly between 3% BSA Block and I Block. Both PBS-Tre and PBS-Tre-Tw produced the greatest intensities of the buffers (n=3). The shape of both curves are smooth and detectable at the lower range of capture antibody showing both coating buffer has the capacity to work to a broad dynamic range. The intensities for both peaked at approximately 1375 AU (PBS-Tre-Tw) and 15000 AU (PBS-Tre) which is moderate to high in comparison to aminosilane and epoxysilane slides from Thermofisher. Both PBS-Tre and PBS-Tre-Tw have been the most consistent print buffers across the 3 slide surfaces investigated so far showing their efficiency despite changes in slide surface chemistry (n=3).

3.3.3.2 Poly-L-lysine Spot Morphology and Size

The spot morphology did not vary between blocking buffers. Interestingly auto-fluorescence was observed using both block buffers at the lowest capture antibodies concentrations indicating the problem is due to the nature of the slide surface chemistry especially at the lowest concentrations (Figure 27). Additionally for PBS-Tre-Tw the diameter of the spots were approximately 100 microns in size.

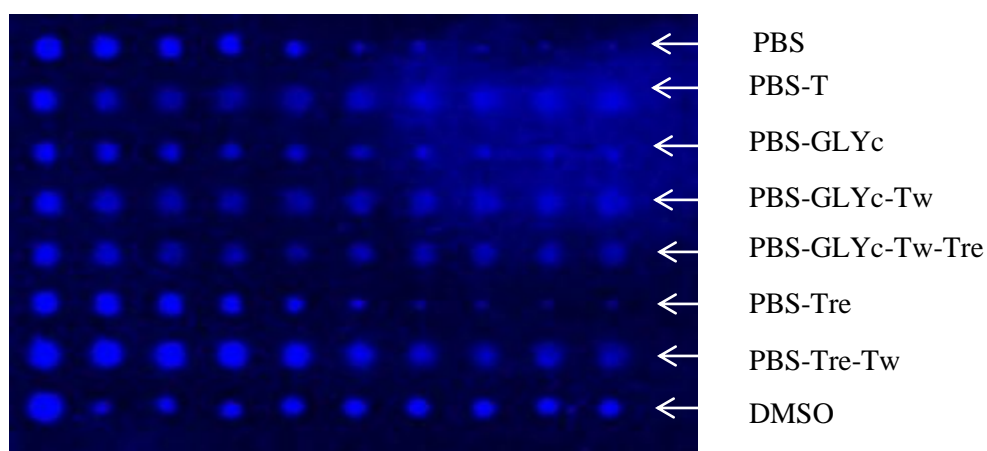


Figure 27: Spot morphology aminosilane slides when tested with 8 coating buffers and blocked with 3% BSA.

Spot morphology poly-L-lysine slides when tested with 8 coating buffers. All 8 printing buffers produced any signals that could be quantified as shown graphically in figure 26 especially PBS, PBS-Tre and PBS-Tre-Tw showing the suitability of these coating buffers on poly-L-lysine slide surfaces.

3.3.3.3 Poly-L-Lysine Short vs Long-Term effects of printing

Antibodies were printed on poly-L-lysine slide surfaces. These were processed immediately or one week later once left in dessciated vacuum. As can be seen with I-Block, the intensity of the slide increased across all 7 buffers, when the slides were printed, stored then analysed one week later. Apart from PBS, the remaining 6 buffers showed an increase in intensity with time. A possible explanation is due to the proteins having sufficient time (7 days) from printing to adsorb to the surface of the slide allowing a greater level of intensity when analysed (Figure 28). Interestingly, when blocked with I Block there is also less variation amongst all 7 buffers suggesting a mixture of I Block and poly-L-lysine could potentially be the optimum combination for printing, storing and maintaining functionally active antibodies.

In the case of PBS, there was a high level of variability over three repetitions leading to high standard deviations and combined with low levels of intensities both immediately processed and delayed, show that this buffer is unsuitable for coating of desired proteins or antibodies. Both PBS-Tre and PBS-Tre-Tw stand out, in particular the latter (with small deviations and high reproducibility) show promise when considering a printing buffer to use long-term (Figure 28).

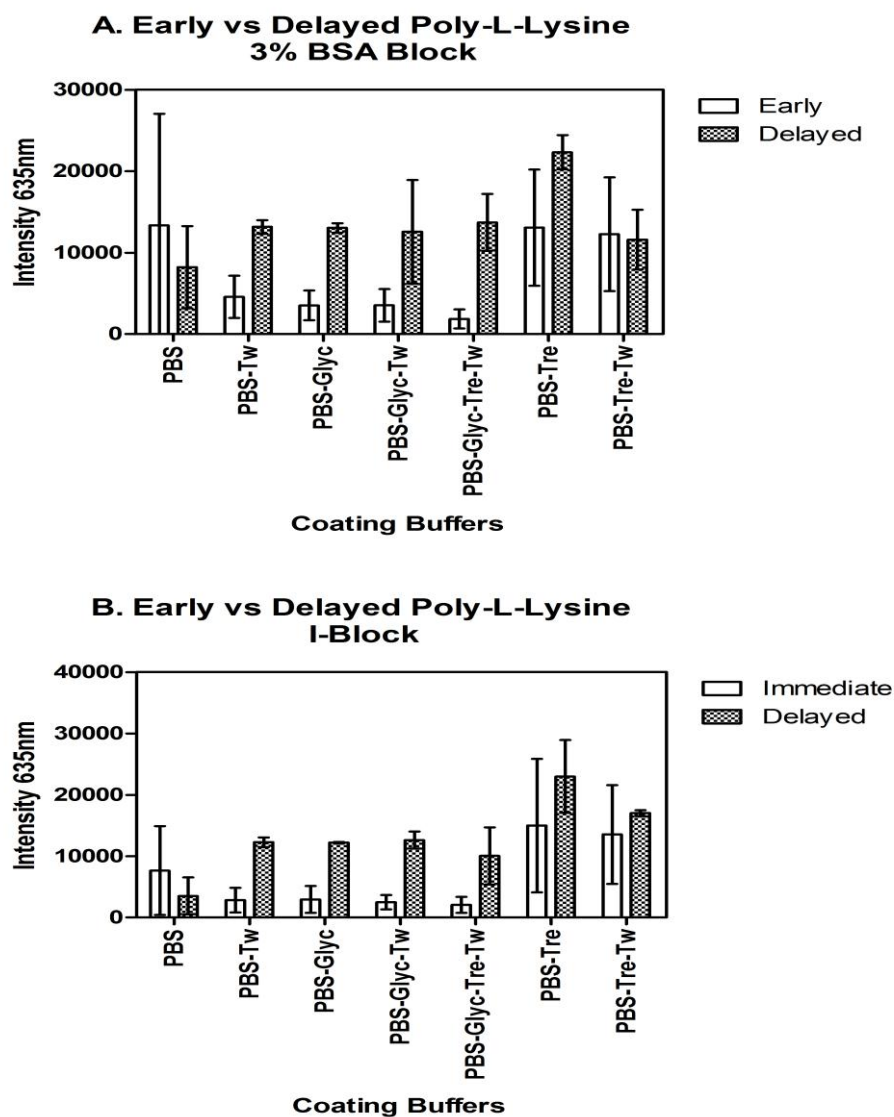


Figure 28: Signal intensity of poly-L-lysine slides processed immediately or delayed.

The signal intensities between the coating buffers when analysed fresh and analysed after a week once printed with 3 % BSA (A) or I Block (B). The average intensities were measured at the top end range of 250 $\mu\text{g/ml}$ of capture antibody. All 7 buffers showed an increase in intensity when processed a week later except in the case of PBS which decreased in intensity. This indicates with the correct print buffer this surface is conducive to long-term storage of slides and can functionally maintain antibodies until processing. Note DMSO was not included in the final analysis due to the variability in print pattern (n=3).

3.3.4 Nitrocellulose

Nitrocellulose slides offer an alternative surface to the slide surfaces described previously. A thin nitrocellulose coating provides a suitable surface that allows for a non-covalent surface for the adhesion of molecules of interest [262]. As this is a coating that does not react with moisture in the atmosphere compared to certain silane surfaces it offers possibly the best alternative to printing the desired capture antibodies which can then be stored over an indefinite time and processed when required. Additionally it has been reported that nitrocellulose slides can offer the lower levels of background and enhanced signal to noise ratios compared to three slides surfaces discussed above.

3.3.4.1 Slides surface and coating buffer

The average intensity of 7 printing buffers across monoclonal rat anti-mouse IgG1 serially diluted, ranging from 250 μ g/ml to 0 μ g/ml with the addition of mouse IgG1 secondary antibody diluted 1:500, then blocked in 3% BSA, I-Block and 3% Milk Block respective on nitrocellulose (Gentel Biosciences) slides were measured. As can be seen from figure 29, irrespective of the blocking buffer used, the vast majority of the printing buffers did not react well with the nitrocellulose surface. In particular buffers that contained glycerol had very low levels of intensity across the three blocking buffers. Additionally the better buffers (PBS and PBS-Tre-Tw) were both inconsistent in shape of their standard curves with neither buffer being smooth. With the shape of the curves being so poor, it was hard to be conclusive about the exact point where the intensity levels dropped beyond measureable levels with certain buffers increasing sporadically as the capture antibody concentration decreased (Figure 29).

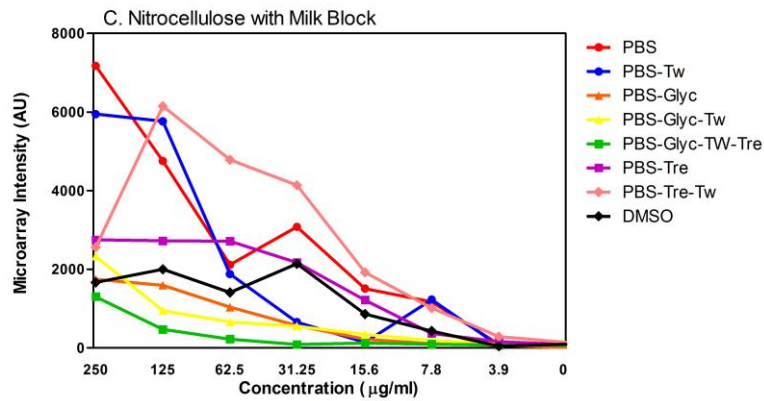
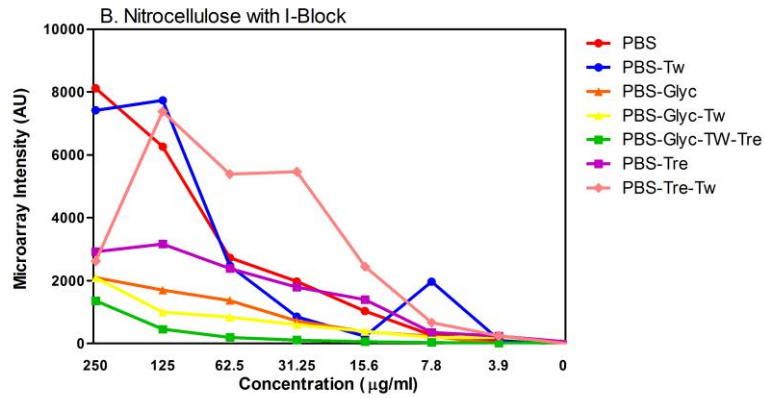
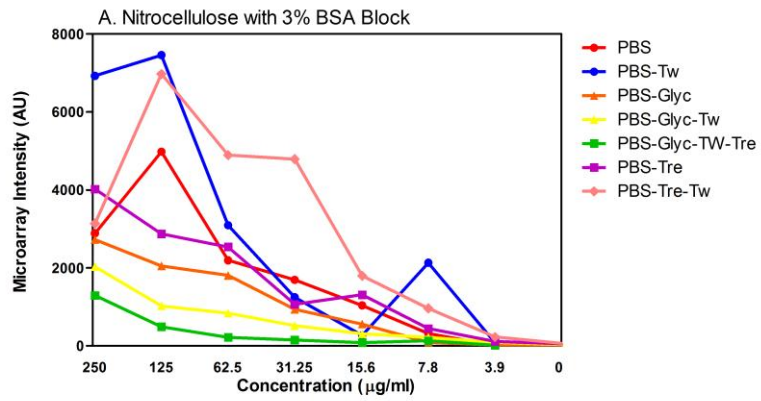


Figure 29: Signal intensity of 8 printing buffers on nitrocellulose slides.

The average intensity of 8 printing buffers across monoclonal rat anti-mouse IgG1 serially diluted, ranging from 250 μ g/ml to 0 μ g/ml with the addition of mouse IgG1 secondary antibody diluted 1:500, then blocked in 3% BSA (A), I Block (B) and Milk Buffer (C) on nitrocellulose slides were measured. As seen in all three graphs, the most consistent print buffers were PBS, PBS-Tw and PBS-Tre-Tw. However most of the printing buffers reacted poorly with the slide surface which coincided with inconsistent graphs, across the three different blocking buffers (n=3). Additionally as noticed on the slide shots, at the highest concentration there was comet like formations, suggesting the problem lies with the amount of capture antibody printed (Figure 30).

3.3.4.2 Nitrocellulose Spot Morphology and Size

With all blocking buffers at the highest concentration of capture antibody, there appears to be a combination of poor spotting or comet like formation indicating at 250 μ g/ml there is an overload of antibody which is not bound to the surface leading to lower than expected signal intensities. It can be noted compared to the poly-L-lysine the spotting is not as distinguished suggesting the coating buffers interact differently with the 4 slide surfaces investigated (Figure 30).

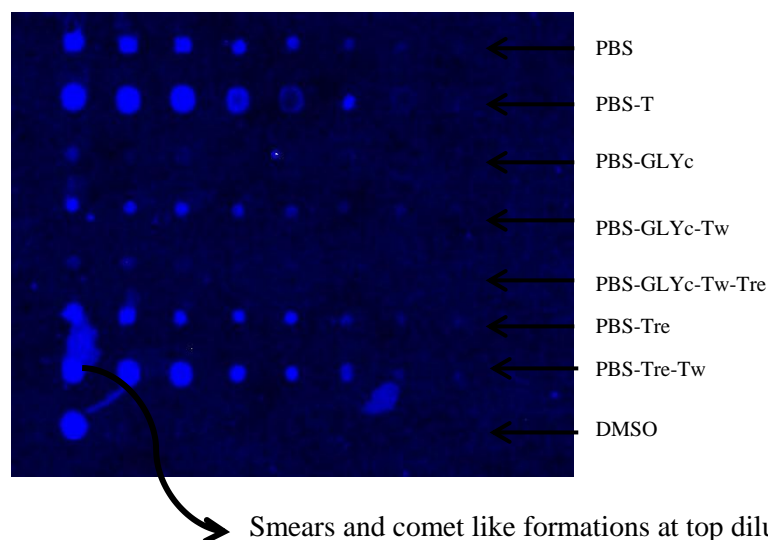


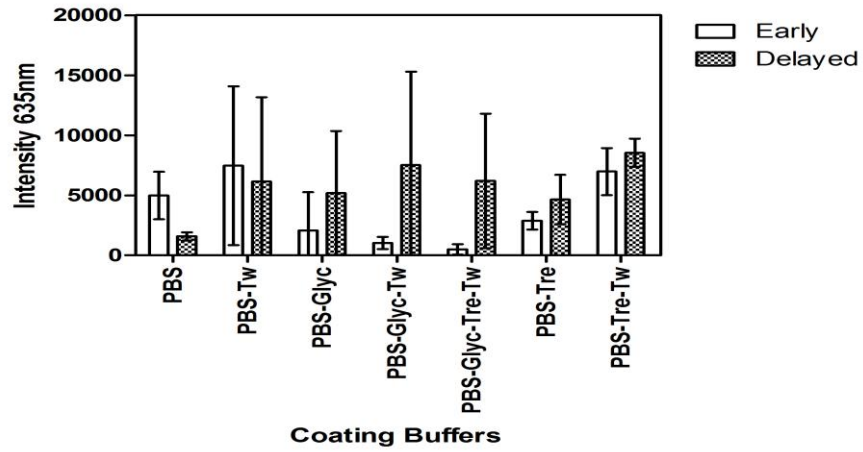
Figure 30: Image to show irregular spotting and smearing of print buffers on nitrocellulose slides when blocked with 3% BSA.

At the top concentration of 250 μ g/ml there was a lot of comet like formations within the spots leading to falsely low intensities indicating at this concentration the antibodies are loosely bound or are too high for the slide surface to hold. Additionally the size and shape of the spots are inconsistent when they are printed and at the lowest concentration signals are not being detected suggesting potential this type of nitrocellulose slide surface may be unsuitable for antibody microarray work.

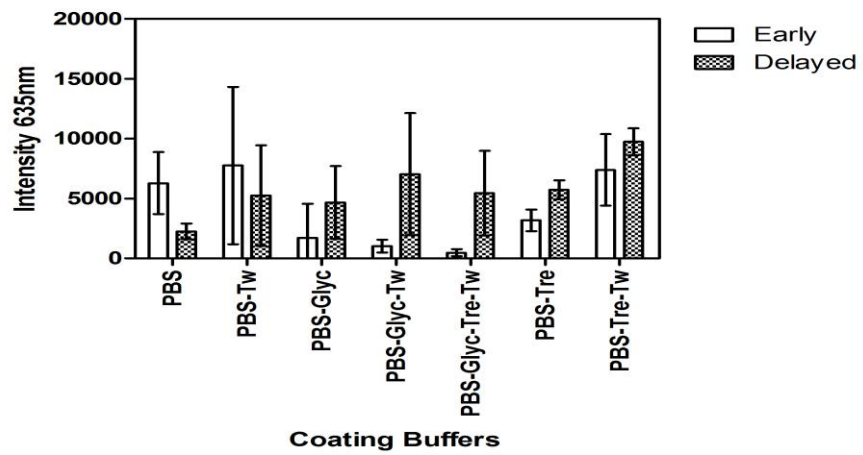
3.3.4.3 Nitrocellulose Short vs Long-Term effect of Printing

The strength of the intensities produced from nitrocellulose slides using the above procedures increases when the slide is analysed after a week compared to when it is processed immediately (Figure 31). When proteins were not given the adequate time to bind to the surface when printed and processed immediately, a large majority of these antibodies are removed during the “wash” phase and thus leads to a lower intensity signals. As shown in Figure 30, DMSO poor spotting pattern led to its exclusion when investigating short versus long-term storage study.

**A. Early vs Delayed Nitrocellulose
3% BSA**



**B. Early vs Delayed Nitrocellulose
I-Block**



**C. Early vs Delayed Nitrocellulose
Milk Block**

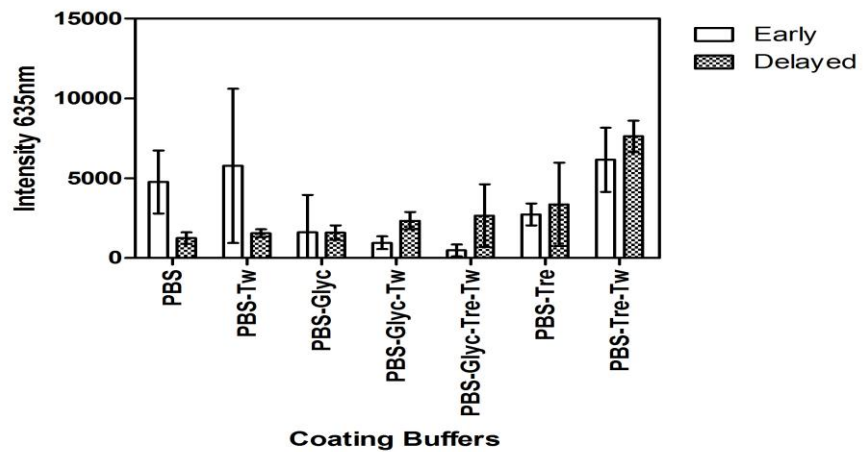


Figure 31: Signal Intensity of nitrocellulose slides processed immediately or delayed.

The average intensity of 7 printing buffers at 125µg/ml of capture antibody when processed and analysed immediately with the additional of secondary antibody diluted 1:500 and stored and analysed 1 week later in 3% BSA blocking buffer (A), I Block (B) and 5% Milk Block (C) (n=3). As can be seen in PBS-Tre-Tw and PBS-Tre there is an increase in intensity when analysed a week later showing that these buffers have the capacity to hold an antibody functionally active over a course of a week. In general the errors bars are much higher than those observed in poly-L-lysine suggesting that this surface despite the ability to hold antibodies better than aminosilane or epoxysilane over a period of a week is not as reproducible as poly-L-lysine.

3.3.5: Milk and NAP Blocking Buffer

NAP Block buffer is a non-animal protein blocking agent used in a vast array of immunodetection assays such as western blots and ELISAs [263, 264]. 5% Milk buffer is a type of casein blocking buffer that is made fresh prior to use. However NAP and 5% milk block buffers led to high background and in certain cases smearing of the slides were noticed when scanned (data not shown). This indicates insufficient blocking. This may indicate that potentially these blocking buffers may be more suitable for 3D planar surfaces such as nitrocellulose compared to the 2D surfaces of epoxysilane, aminosilane or poly-L-lysine. These two blocking buffers subsequently were excluded from future work and not shown in conjunction with the results shown above.

The following table shows a summary of all the four slide surfaces tested. As seen, in terms of consistency and reproducibility, poly-L-lysine slides were the best overall. Despite a better reproducibility in both aminosilane and epoxysilane a week later a dramatic drop in intensity was seen. Only in poly-L-lysine and nitrocellulose slides were there an increase in the level of intensity over time suggesting this slide surfaces is conducive to both short and long term processing. However there was a greater variation in nitrocellulose slides compared to poly-L-lysine slides. Interestingly aldehyde slides were printed with the 8 coating buffers however once processed no spots appeared suggesting that this type of slide surface is not suited for antibody microarray work. Epoxysilane slides offered the highest levels of intensity of all the slide types (Table 11). Hence moving forward to complete the remainder of the antibody microarray work, poly-L-lysine slides were used unless stated otherwise:

Table 11: Summary of the optimisation tests performed across the 5 slide surfaces.

Overall poly-L-lysine slides were the best type of slides surfaces which offered the highest level of consistency. Most encouraging was the increase in intensity levels that was observed in poly-lysine slides over time making them very desirable for future antibody microarray work. Both aminosilane and epoxysilane dropped in intensity when slides were printed after one week making them undesirable for long term use. Nitrocellulose slides produced inconsistent spot morphology with moderate signal intensities which made them undesirable. Hence moving forward poly-L-Lysine slides would be used in future experiments

Slide Surface	Immediate Spot Morphology	Immediate Spot Intensity	Immediate Spot Reproducibility	Spot Intensity after 1 week compared to immediate	Spot Reproducibility after 1 Week compared to immediate
Key:	 = Doughnut shape  = Square shape		* = Poor ** = Fair *** = Very Good **** = Exceptional	 =Increases  =Decreases	* = Poor ** = Fair *** = Very Good **** = Exceptional
Poly-L-Lysine		Moderate-High	***		****
Aminosilane		Moderate	**		****
Epoxysilane	 	Low-Extremely High	***		****
Nitrocellulose		Moderate	***		***

3.3.6 Establishing the optimum capture antibody concentration for printing on poly-L-lysine slides

Poly-L-lysine slides in conjunction with PBS-Tre as the print buffer will be used for future antibody microarray work. The next stage of the investigation was to consider the concentration of capture antibody that is printed on this slide surface that would allow for best signal intensity whilst being consistent in both spot size and morphology. The RANTES duoset kit was used and slides were processed at three capture antibody concentrations (200µg/ml, 100µg/ml and 50µg/ml respectively) Printed slides were blocked for 1 hour in 3% BSA and I-Block. After blocking, slides were washed three times with PBST (containing 0.05% Tween-20) and incubated in solutions containing detection antibody conjugated with fluorescent dye for 1 hour at room temperature on a shaker. Slides were washed with PBST (as described above) and rinsed briefly in ultrapure water. Slides were dried by spinning at 1200 rpm for 5 min and scanned a 4200 AL microarray scanner (Axon GenePix®). Standard curves were drawn to compare the three concentrations of capture antibodies.

As seen from Figure 32 there is little difference in the strength of the standard curves with capture antibody concentrations printed at 200µg/ml compared to 100µg/ml. However it was observed that at 50µg/ml there is a sharp drop in intensity suggesting at this concentration it would be inappropriate to print capture antibodies. Additionally at the lower end of the standard curve (from 100pg/ml) there is no difference between the standard curve printed at 200µg/ml and that printed at 100µg/ml. Additionally the choice of blocking buffer did not have an effect on the signal intensity as the results with I Block were similar to those produced by 3% BSA block (results not shown).

Hence from Figure 32 it was established that printing at 100 μ g/ml would be the optimum concentrations for all future antibodies that are printed on the microarray platform.

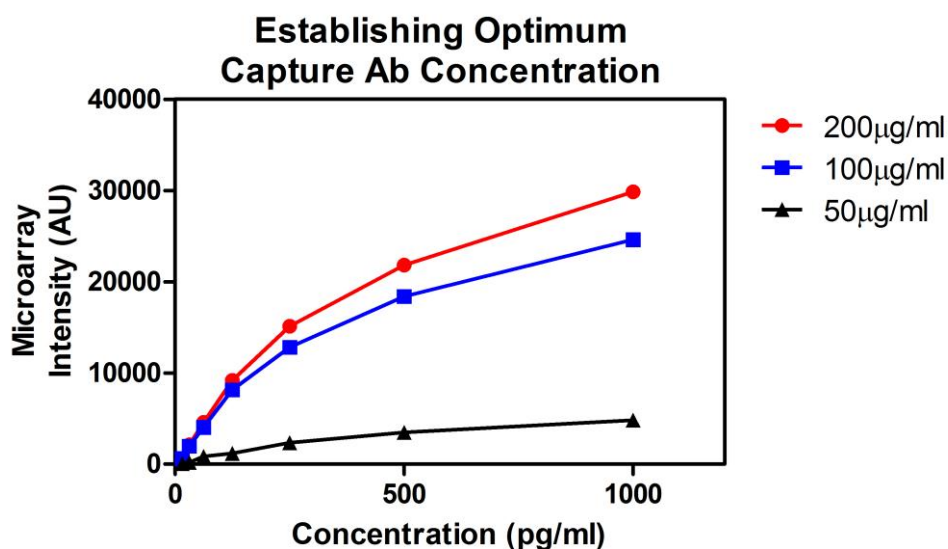


Figure 32: Choosing the optimal concentration of capture antibody that was printed on a poly-L-lysine slide surface and blocked with 3 % BSA.

A substantial drop in intensity was not observed between standard curves printed at 200 μ g/ml and that printed at 100 μ g/ml. However at 50 μ g/ml the standard curve dipped to near undetectable levels at 100pg/ml. The experiment was repeated using I-Block which produced similar trends in the standard curve. This suggested at 100 μ g/ml is the optimal capture antibody concentration for printing antibodies on poly-L-lysine slides.

3.3.7 Poly-L-Lysine Standard Curve Reproducibility

In section 3.3.3.3 we have shown that poly-L-lysine is the ideal surface for both short and long term printing and processing. However this was only applied to capture antibody that was serially diluted. We therefore tested whether the impact of an increase in signal intensity is recorded when standard curves are drawn for TNF- α , Rantes, GMCSF, MCSF, IL-2 and IFN- γ respectively.

These six cytokines were taken and processed as outlined in section 2.2.4. Briefly, standard curves were drawn using poly-L-lysine slides that were processed immediately and delayed without amplification. As can be seen in Figure 33 the highest intensities in the standard curves were spotted when poly-L-lysine slides were processed after a week (delayed). Interestingly the standard curves were higher in poly-L-lysine slides that were processed a week later. This is in-line with the observations noted from Figure 33 where an increase in signal intensity was observed with PBS-Tre when processed a week later. Also it can be seen in figure 33 that there is no major difference between the signal intensities between poly-L-lysine slides processed immediately and those delayed. This shows that poly-L-lysine is a surface that can allow slides to be processed at any given time point which is extremely useful moving forward. So in future for further experiments poly-L-lysine slides were processed immediately unless stated otherwise.

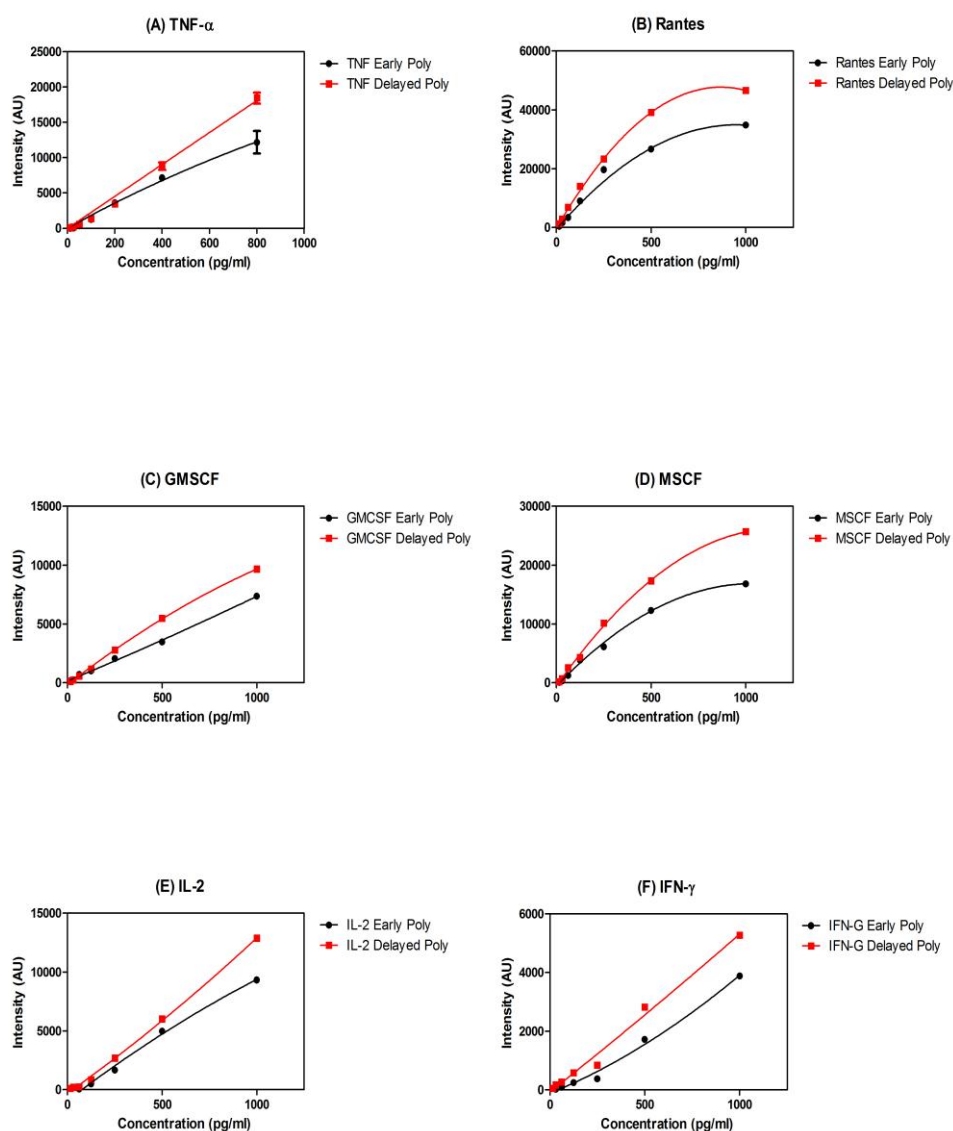


Figure 33: Showing the effect of processing poly-L-lysine slides immediately and delayed on standard curves using six cytokines: (A) TNF- α , (B) Rantes, (C) GMCSF, (D) MSCF, (E) IL-2 and (F) IFN- γ respectively.

When poly-L-lysine slides are printed and processed a week later they produce the highest levels of intensities compared to the same slides that are printed and processed immediately (red vs. black lines). However there is not a big difference between the signal intensities when they are printed immediately or delayed suggesting this surface is suitable for all types of printing and storage.

3.3.8 Sensitivity at the lower end of a standard curve

A key aim of this thesis is the ability to measure multiple biomarkers at very low concentrations. However using the protocol outlined in section 2.2.4, there was a lack of signal intensity at the lowest concentrations of the standard curves (Figure 34). At the lowest concentrations of the 6 cytokines standard curves there is a minimal signal which could cause a problem when measuring low abundant cytokines in serum. This indicates that the poly-L-lysine surface may be incapable of detecting proteins at the lowest concentration. Hence the use of amplification was considered to improve the sensitivity of the lower end of the standard curve.

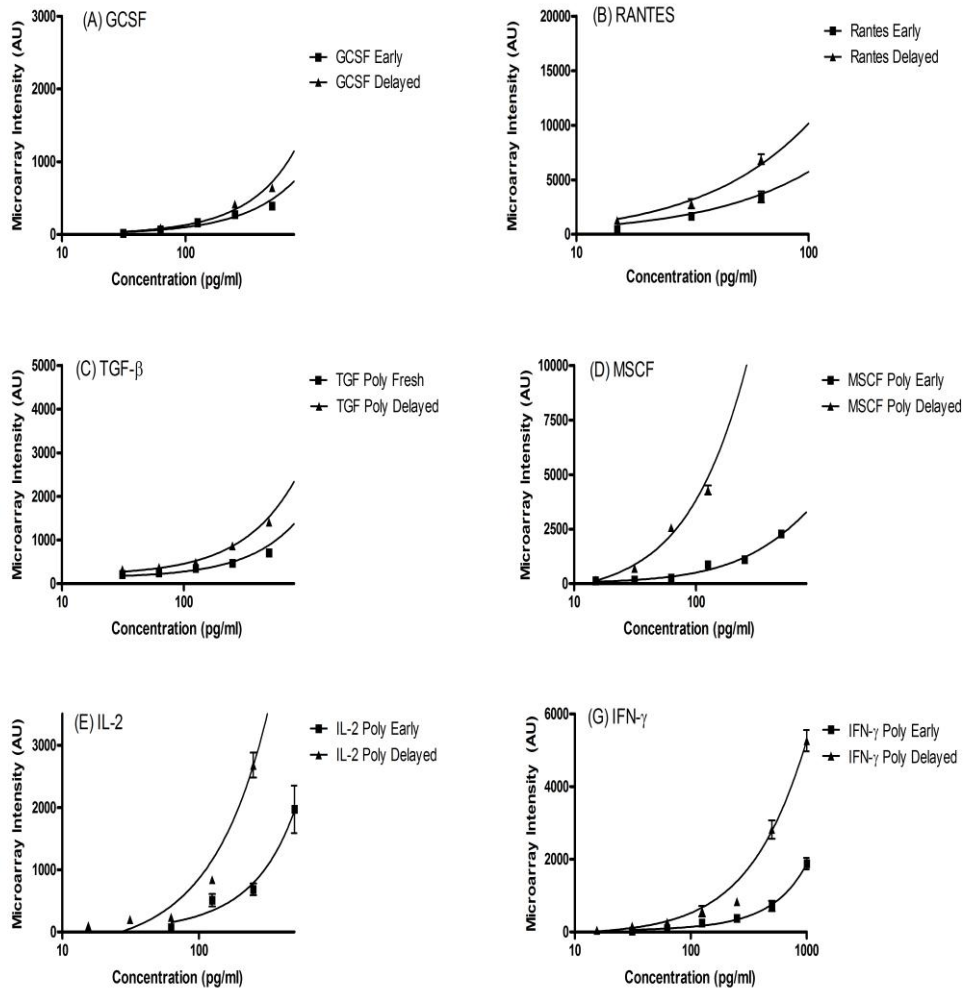


Figure 34: Standard curves for 6 cytokines at the lower end of the standard curve.

As can be seen in all 6 cytokines there is a lack of signal at the lower end of the standard curve. In the case of most cytokines, below 100pg/ml there is very little signal. It is known that most healthy individuals and COPD patients have cytokines concentrations that are equal to or below 100pg/ml, these standard curves will have to be improved through amplification in the future.

3.3.9 Amplification

Amplification was used to improve the sensitivity of the lower range of the standard curves of low abundant cytokines. Figure 35 gives an example of one low abundant cytokine that was investigated (GCSF). Signals were amplified using the BIO-RAD amplification system. Upon amplification the signal intensity is multiplied almost 10 times (Figure 35A). Furthermore with amplification signals can be detected as low as 6pg/ml for GCSF (Figure 35B). Interestingly, the level of background on the slide dropped from an average of 120 AU to 60 AU, which helps enhance the sensitivity of the assay (Figure 35C). The signal to noise ratio was again enhanced upon amplification when the slide is processed normally (Figure 35D). This was found to be the case in all cytokines tested.

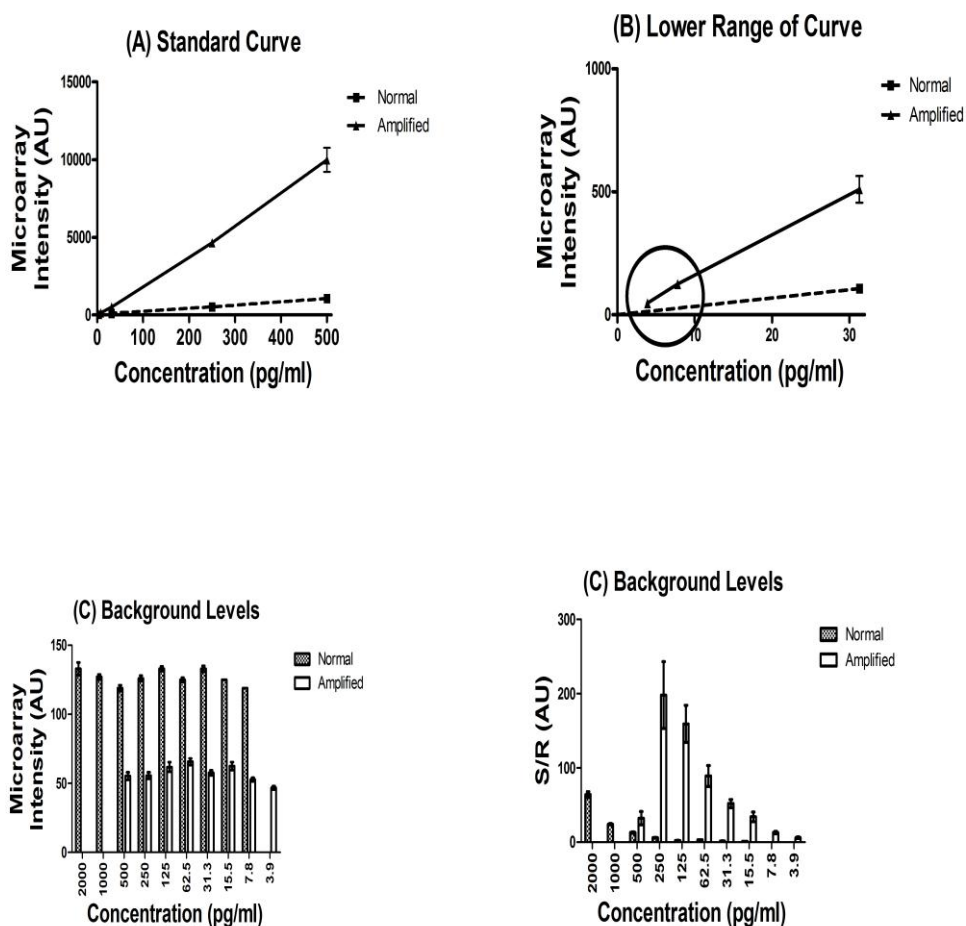


Figure 35: The effect of Bio-Rad amplification is three fold; it allows the raising of the standard curve in general enabling greater sensitivity at the lower concentration.

The difference between a non-amplified and amplified standard curve is shown (A). There is a marked difference at the lowest end of the standard curve with a higher level of intensity observed with the amplified curve compared to the normal curve (B). Additionally the background levels that were previously noticed were reduced (C) and as a result the signal-to-noise ratio of the spots were improved allowing for better detection at the lower concentration (D).

3.3.10: Time Course Experiment to Optimise Cytokine Standard Curves

An important aspect of the microarray protocol was to be quicker than the “gold standard” ELISA. Often ELISAs have 2 hr incubations when standards/samples are added and also after detection antibodies are added, so the process could take up to 8 hours from start to finish. However with the multiplexing nature of the microarray it was important not only to develop a platform that could measure multiple biomarkers but also one that could be fast and deliver a quick turnaround. Subsequently from the original protocol 2.2.4 each procedural step i.e. blocking, adding of standards and detection were continually halved and the signal intensity was measured. It was important to maintain a high level of intensity and also work out the optimal time for each stage of the microarray process. As seen in Figure 36, when the assay was run at half the intended time, the strength of the standard curves were superior than when the assay was run according to the original devised protocol. This may be due to reagents working best within a limited time frame across the slide surface and if left on for longer than required reduces the efficiency of the performance. Additionally, alternative factors like evaporation and exposure to the external environment when running the array are halved which could also have a bearing on the signal intensity.

Subsequently from the data analysed from Figure 36, including previous knowledge gained from understanding both blocking and amplification steps, the protocol was modified and outlined as written in section 2.2.5. This protocol was used for all experiments described hereafter.

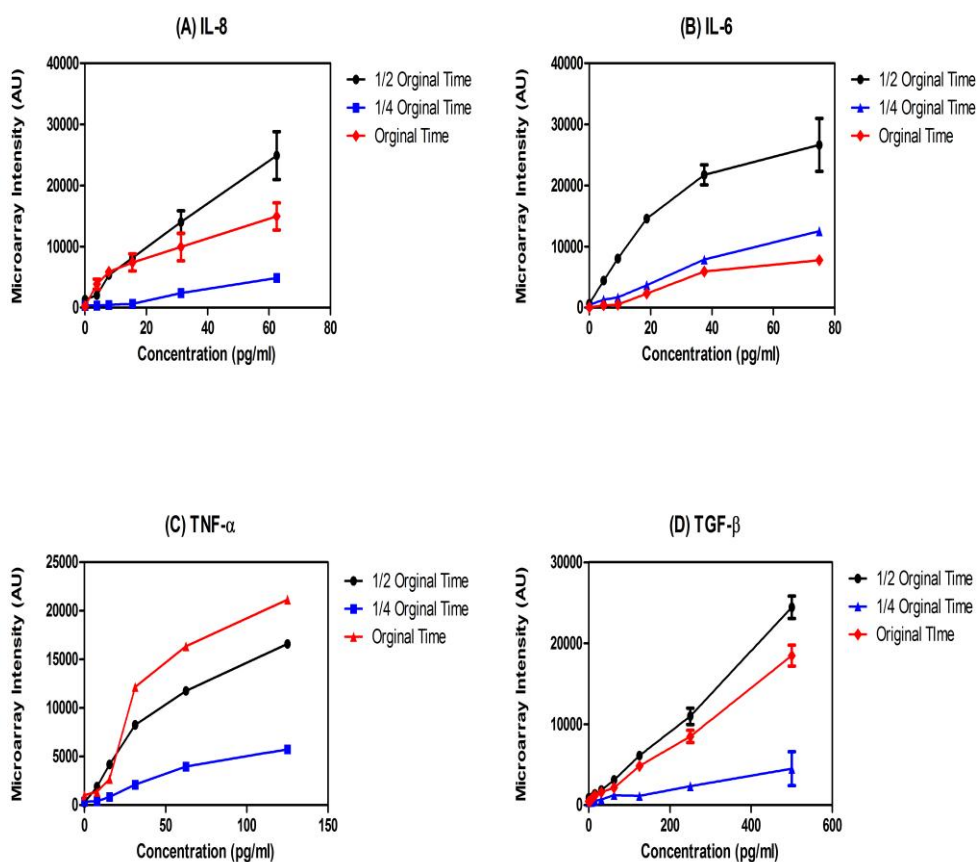


Figure 36: Time course experiment to optimise microarray protocol:

With IL-8 (A), IL-6 (B) and TGF- β (D), when the protocol length was halved from the original time (to 5.5 hours), the strength of the signal is increased whereas in TNF- α (C), this is fairly comparable to the original time. Halving the original time may be the optimal time required for most of the reagents to work at their best. Additionally halving the original time of the protocol maybe what is required to reduce the effect of external environmental factors such as evaporation.

3.3.11 Printing Conditions on Poly-L-Lysine slides

Printing, along with the slide surface, is a crucial step in the microarray process. It is important to get the settings correct for printing as it will allow the optimal size and shape of a spot to be printed. Experiments were subsequently undertaken to investigate the different factors that are involved in the printing procedure. This includes the dwell time (the amount of time the pin spends on each spot) from 0.0 sec to 3 sec and the target height (the distance at which the pin comes from to print on the surface of the slide) from 0.0mm to -0.60mm and also the number of spots the pin can print in the absence or presence of humidity. The number of spots were counted per well and the average calculated upon the experiment being repeated three times.

As seen in Figure 37, there is a major difference between printing with (58%) and without humidity (30%). Firstly when investigating dwell time and the number of spots printed, it can be seen that as the dwell time increases there is a decrease in the number of spots which are printed. This is the general trend observed with/out humidity. However one can see clearly in Figure 37A where there is no humidity there are less spots printed. This is because without humidity the rate of evaporation in the microarray chamber is increased. Therefore capture antibody that is picked up in the pin is more prone to evaporation resulting in less capture antibody that is available to be printed on the slide surface and hence less spots being printed. Additionally when the dwell time is increased, the time between spotting is increased allowing evaporation to take greater effect.

Secondly, when investigating target height a similar trend is observed where humidity aids more spots to be printed; however the effects are not as great as that observed with dwell time. In general, as the target height increases there is not a big difference in the number of spots that were printed. However it has to be noted that at a target height of -0.60mm, the pin did not touch the slide surface enough to allow spots to be printed and were not included in Figure 37 B.

Interestingly when the spot size, shape and diameter were investigated there was no difference in increasing dwell time or target height.

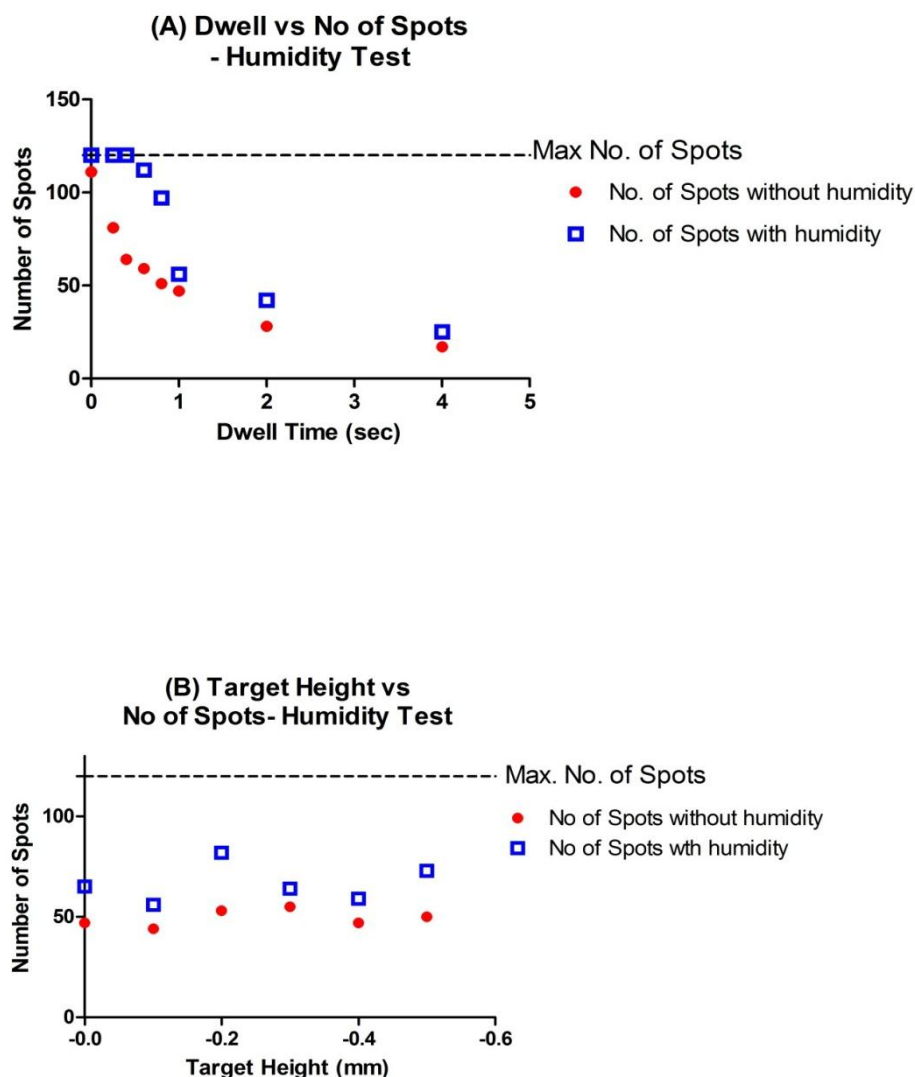


Figure 37: The effect of dwell time and target height on spot printing.

The effect of printing on poly-L-lysine slides was investigated in further depth. Initially the effect of humidity was investigated to see the number of spots that could be printed with humidity (58%) and without humidity (30%). The number of spots are counted per well and the average calculated as the experiment is repeated. As seen humidity enables more spots to be printed irrespective of changes in dwell time or target height. Additionally as dwell time increased there were less spots printed due to evaporation that occurred in the microarray chamber (A). Target height does not affect the number of spots printed except in the case where humidity allows slightly more spots to be printed (B).

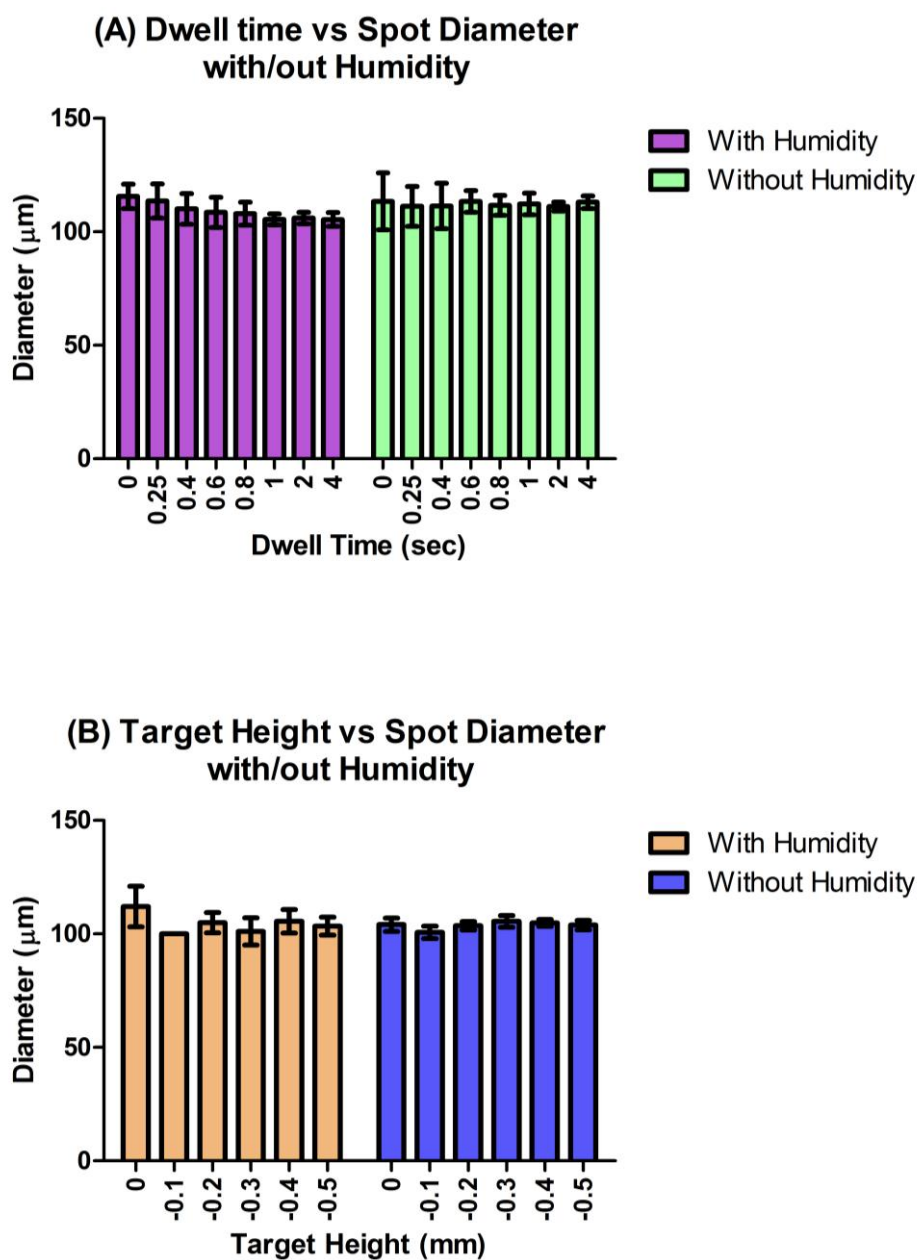


Figure 38: The effect of dwell time and target height on spot diameter/size.

The effect spot diameter was investigated with by varying both the dwell time and target height. The spot diameter was calculated using the 4200AL scanner measuring tool for all spots. The average spot diameter was calculated and plotted above. As seen above, the increase of dwell time or target height does not have an effect of spot diameter or size (A/B) with (58%) or without humidity (30%)

From the data gathered from these experiments, the optimal printing conditions were as follows: dwell time: 0.40sec, target height -0.184mm and the humidity was set to 58%. This is used for all subsequent experiments in thesis.

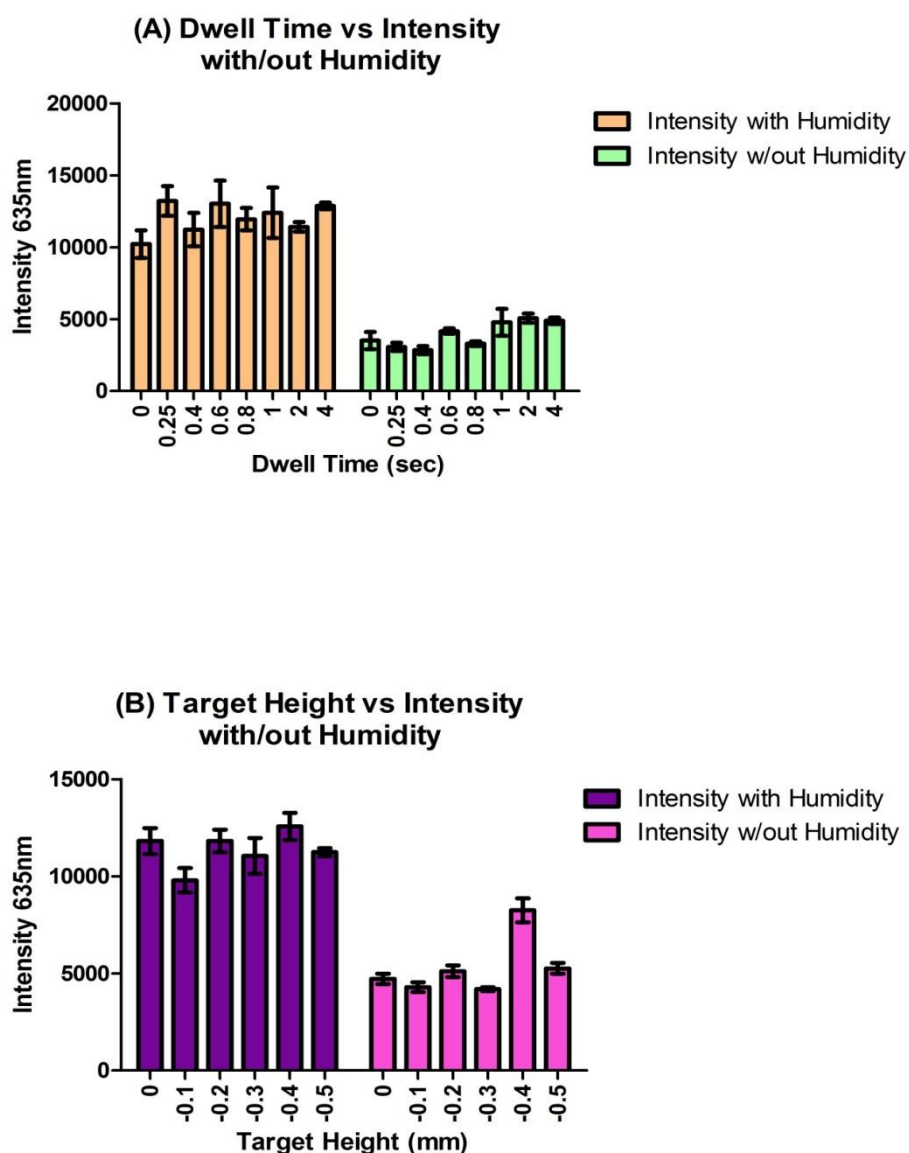


Figure 39: The effect of dwell time and target height on signal intensity.

As seen without humidity, the signal intensity is decreased irrespective of increases in dwell time and target height (A & B). Interestingly, the increase in dwell height and target height does not cause major changes in signal intensities. Humidity causes evaporation which may affect the signal intensity irrespective of the spot size and shape.

3.3.12: Cy5 and the Long terms effects on the slide surface

Here we examined the use of Cy5 for detection on microarray. A major consideration in using cy5 is the possible effect of signal detection over time. Hence the long term effects of cy5 on poly-L-lysine slides were investigated.

Briefly printed slides were blocked with I Block (Tropix) for one hour and washed three times with wash buffer (PBS-Tween 0.05%). A calibrated cocktail of standards (IL-6, IL-17, IP-10 and MCP-1) were made for each cytokine according to manufacturer's instructions and diluted two-fold across eight dilutions and added at 50µl per block for 45mins. The slide was washed three times and 50µl of appropriately diluted cocktail of biotinylated detection antibodies were added to each block for 45mins. After washing three times with washing buffer, 50µl of 1:1000 diluted streptavidin-conjugated cy5 (E-Biosciences, UK) was added and incubated at room temperature for 15 mins in the dark. The slide was washed three times and rinsed in ultra-pure water and centrifuged dry. Slides were spun dried and scanned with a 4200 AL microarray scanner at 635nm.

Subsequently, the processed slide was preserved, protected from light and kept in a vacuum and analysed at repeated intervals over a period of weeks and months. The graphs in figure 40 show that cy5 fluorescence intensity does not drop over time and is consistent over a period of 2 months. This is important in the long term analysis of patient samples, as the slides can be preserved for up to 2 months or more, these samples can be taken re-scanned and recalculated if required. The key to the effectiveness of the cy5 is due to a combination of slide surface and also the print buffer that does not change over time.

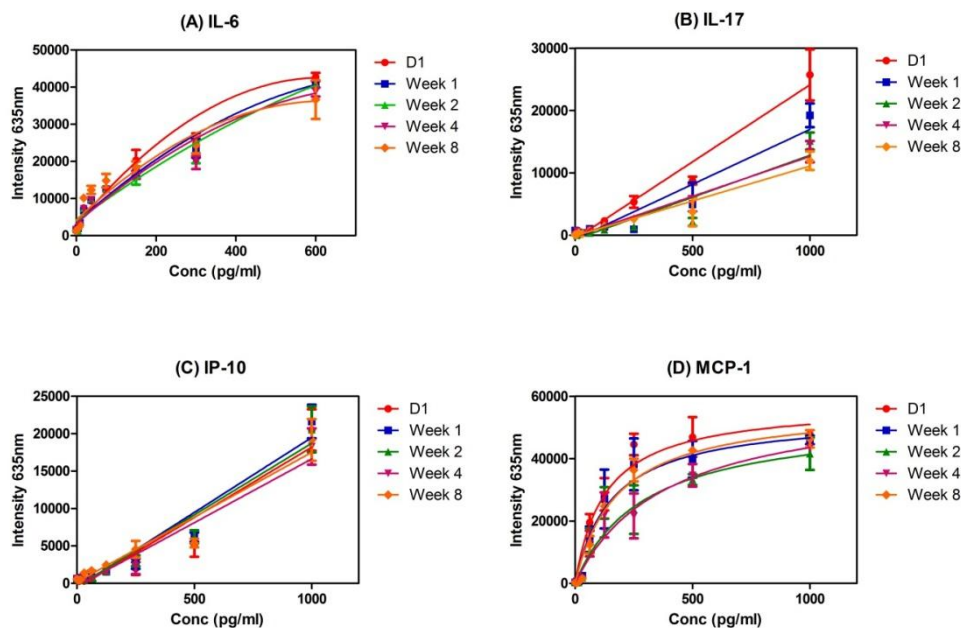


Figure 40: The long terms effects of cy5 on signal intensity.

The durability of cy5 was tested over a period of two months. Processed slides was preserved, protected from light and kept in a vacuum and analysed at repeated intervals over a period of weeks and months. Slides were scanned for 4 cytokines (A-D) and as seen there is no major drop in the strength of the signal over time. This shows the strength of cy5 when stored correctly remain very consistent over a prolonged period of time and can be stored and rescanned if required.

3.3.13: The Effects of Blocking Buffers in Serum/Plasma

Before the validation phase is conducted with serum or plasma, it is important to define the optimum blocking buffer that is to be used on both serum and plasma that contain a variety of proteins that could interfere with the microarray. Initially three serum and plasma were taken from healthy donors and processed.

Serum and plasma was obtained from the sample healthy individuals and the slides were processed and blocked with 3% BSA as described in 2.2.5. Briefly, printed slides were blocked with a blocking buffer for one hour and washed three times with wash buffer (PBS-Tween 0.05%). A calibrated cocktail of standards were made for each cytokine according to manufacturer's instructions and diluted two-fold across eight dilutions and added at 50 μ l per block for 45mins. Additionally samples were added in corresponding wells on the slide. The slide was washed three times and 50 μ l of appropriately diluted cocktail of biotinylated detection antibodies were added to each block for 45mins. After washing three times with washing buffer, 50 μ l of 1:1000 diluted streptavidin-conjugated cy5 (E-Biosciences, UK) was added and incubated at room temperature for 15 mins in the dark. The slide was washed three times and rinsed in ultra-pure water and centrifuged dry. Slides scanned with a 4200 AL microarray scanner at 635nm

Subsequently, the difference in S/N ratio was calculated between serum and plasma in IL-8, TNF- α , IL-1 β , IL-6, TGF- β , MCP-1, VEGF and Eotaxin-1 respectively. Finally 7 different blocking buffers were used to explore the impact on backgrounds levels and S/N in both serum and plasma.

From Figure 41, plasma samples produce higher background levels compared to the sera samples. The biggest problem with this is that low abundance cytokines in plasma are unable to be quantified. Additionally when the signal to noise (S/N) was analysed (see Figure 42), plasma had a much more reduced S/N ratio than serum. In higher abundant cytokines such as MCP-1 and VEGF this may not be a problem as these can be detected much more easily than low abundant markers such as IL-1 β and IL-6 respectively. Hence a variety of factors could contribute to this high background including the slide surface and the type of blocking buffer that is used. Ultimately only one blocking buffer can be used on this microarray system. At present most experiments so far have centred on using either 3% BSA block or I-Block. We shall first look at the effect of using a variety of different blocking buffers on serum then secondly look at plasma to determine which blocking buffer contributes to the least background and produces the highest signal to noise intensity.

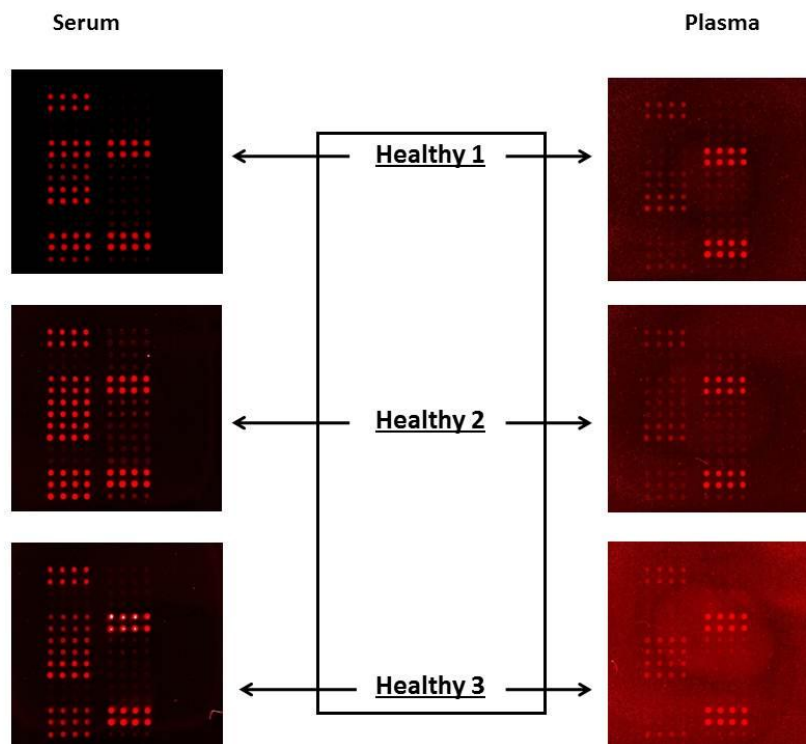


Figure 41: Visual difference between serum and plasma when blocked with 3% BSA.

Serum and plasma was obtained from the sample healthy individuals and the slides were processed to investigate the difference in background levels. From the figure, it can be seen that plasma samples (right) have higher level of background than serum samples (left). There is a greater degree of non-specific binding that occurs in plasma samples leading to higher background levels than in serum. Hence this would make it harder to measure and quantify very low abundance cytokines in plasma than serum samples.

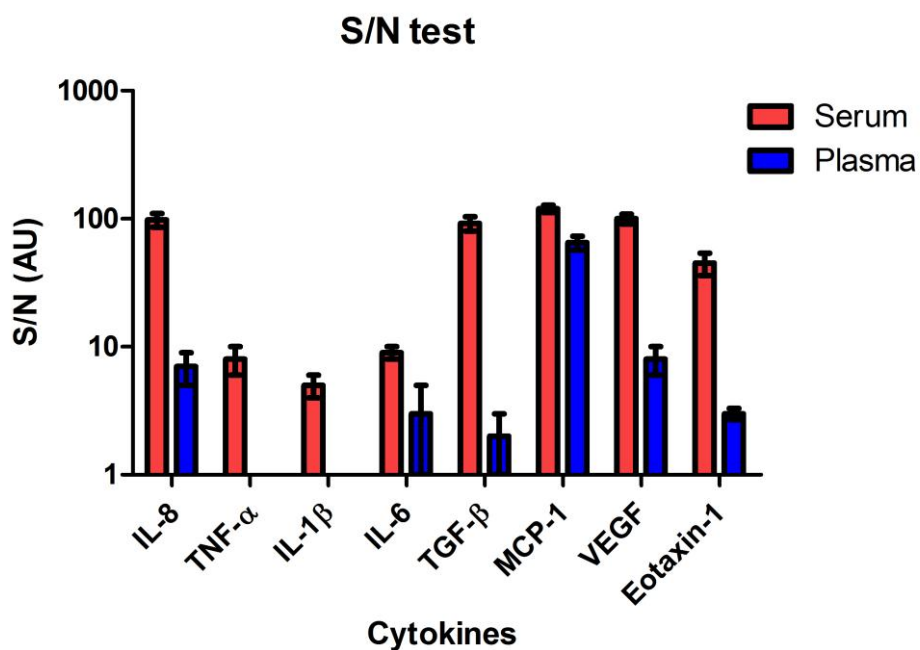


Figure 42: The overall S/N ratio between plasma and serum samples for the 8 cytokines analysed.

The S/N was calculated for 8 cytokines (IL-8, TNF- α , IL-1 β , IL-6, TGF- β , MCP-1, VEGF and MCP-1) between serum and plasma samples. It can be seen that serum has a higher S/N than plasma samples across all 8 cytokines. The superior S/N in serum compared to plasma is especially advantageous in being able to detect low abundance cytokines, such as TNF- α and IL-1 β .

Serum was blocking with 7 different blocking buffers and the S/N and background levels were determined. As can be seen from Figure 43 A, the optimal background levels were produced by 3% BSA, I-Block and also milk blocking buffers and additionally these three buffers also produced the best S/N ratios (B). Interestingly, Smart block and also PVA had some of the highest backgrounds and lowest S/N ratio. 3% BSA Block is slightly better than both I-Block and milk block as it is consistent across all 8 cytokines investigated, especially with low abundant cytokines such as IL-6, IL-1 β and TNF- α , 3% BSA produces a higher S/N ratio than I-Block making this the preferred choice of blocking buffer when investigating serum samples in the future. It has to be noted that milk blocking buffer leaves grain like deposits after the processing of microarray slides making it inconsistent in scanning certain areas of the slide making it less desirable for use than 3% Block or I-Block

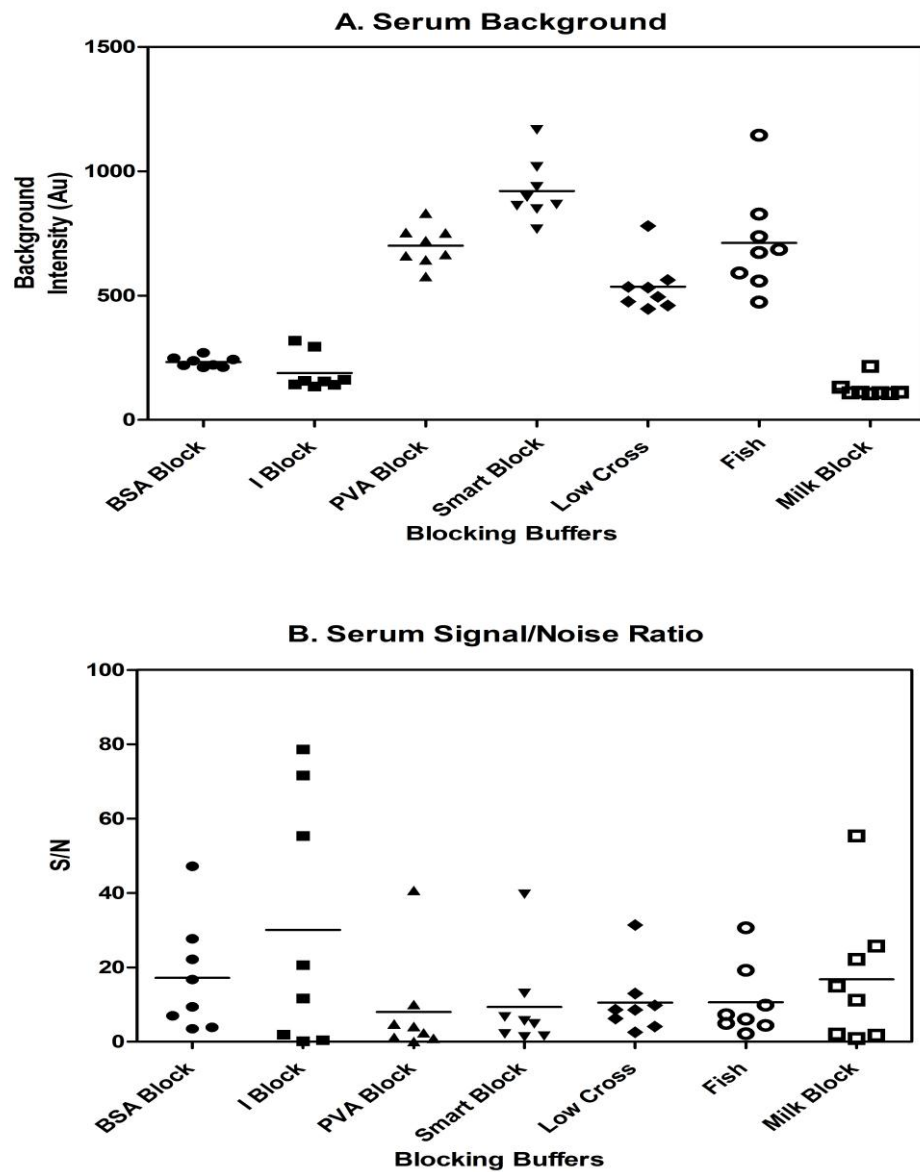


Figure 43: A/B: Investigating the best blocking buffer in serum.

Seven blocking buffers were tested across 8 cytokines in serum. 3% BSA, I Block and milk block produced the best background whereas PVA and Smart block were the highest. Additionally 3% BSA produced the best S/N ratio across all 8 cytokines, especially in low abundant ones such as IL-6 and IL-1 β , suggesting this is the optimum blocking block for serum in this microarray platform. Note in comparison I Block and 3% Milk block has signal intensities that are undetectable.

The same experiment was repeated in plasma to see if the level of background could be reduced. As seen in Figure 44, I-Block had low background levels when tested on plasma and also had the best signal to noise ratios of all the blocking buffers across all the cytokines. However both the background levels and S/N in plasma were far inferior to that produced in serum. This indicates plasma has some components that cause unspecific binding and this contribute to a higher background and poorer signal.

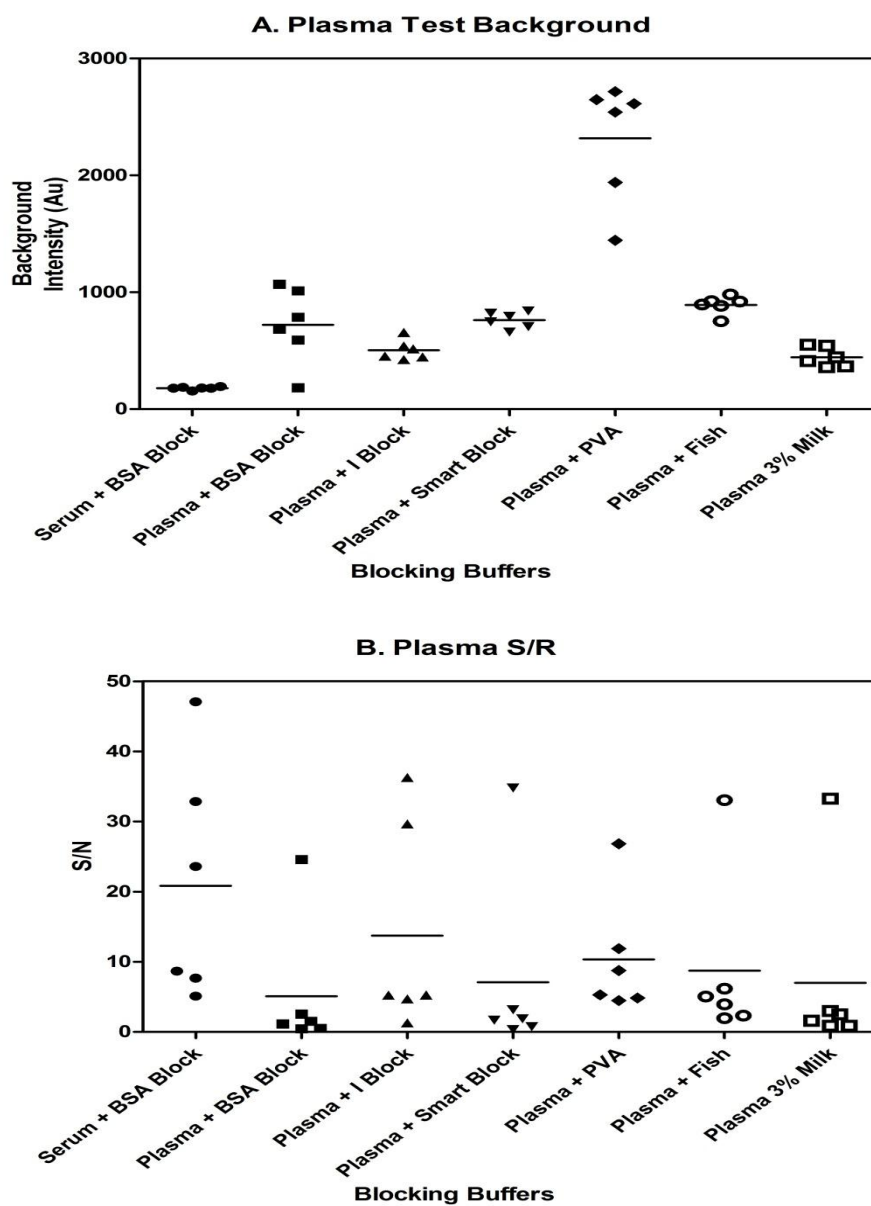


Figure 44: A/B: Investigating the best blocking buffer in plasma.

Plasma was taken and blocked with 6 blocking buffers. As can be seen serum still has the highest S/N ratio and lowest background despite multiple blocking buffers used. Overall I Block has the best combination of lowest background and highest S/N ratio. However the blocking of plasma is not as effective as serum suggesting there are proteins that can contribute to unspecific binding on the microarray platform.

3.3.14: Large and low abundance cytokines

When developing a microarray platform it is desirable to have a platform that is able to measure low (<200pg/ml) and high abundance ($\mu\text{g/ml}$ - mg/ml) cytokines. At present commercial antibody companies such as R&D Systems are able to provide such a platform using chemiluminescence microarrays. Therefore we tested this principle on our microarray system using five cytokines (CRP, MMP-9, RAGE, TIMP-1 and IP-10). These included high abundance cytokines, sera were diluted 1 in 250 and added to the microarray platform and processed with amplification. As seen in Figure 45, by diluting the high abundance cytokines, the low abundance cytokines were too dilute and could barely be detected, in particular IP-10 and RAGE. Hence for it was decided to maintain a platform that could measure cytokines without the need for dilution. Hence the remainder of the chapters; the validation and analysis of COPD samples (Chapter 4 and 5) focusses on the measurement of low abundance to mid-range cytokines.

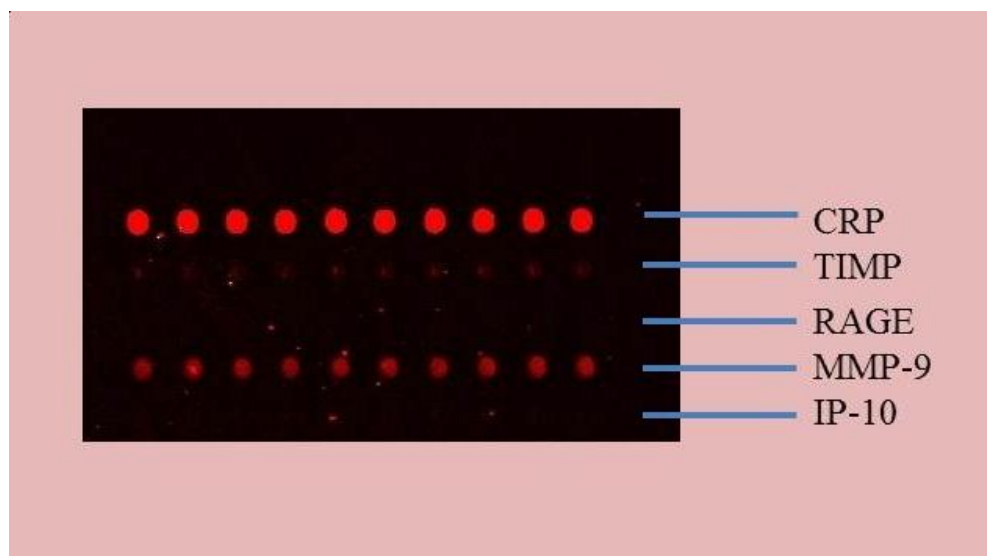


Figure 45: Image to show the microarray incorporating high and small abundance cytokines.

The above image shows illustrates the problems to incorporating high abundance cytokines with low abundance cytokines. CRP required a dilution of 1 in 250 to be used on the microarray platform. However this required diluting all 5 cytokines, 1 in 250 within the same sample and detecting them together, resulting low abundance cytokines being lost into the background which makes it unquantifiable. This suggests the microarray platform can be used to measure low abundance cytokines. Hence for future work only low to mid-range abundance cytokines would be investigated with regards to validation and the screening of COPD patients.

3.4 Discussion

The key aim of the initial part of this project was to establish a print buffer that would provide a platform for capture antibodies to maintain their structure and reactivity both short and long-term. Furthermore it was to compare slide surfaces, working out the best blocking buffer and also to see how the microarray platform performs on biological samples such as serum and plasma.

3.4.1: Printing Buffers

We have shown consistently that PBS-Tre-Tw and PBS-Tre were the best coating buffers. Trehalose in particular is a naturally linked alpha disaccharide that forms a gel like surface on the slide and prevents the antibody from drying out and effectively holds them in position [265-267]. Subsequent rehydration that occurs upon processing the slides allows the antibody to resume its reactivity when it binds to the detection antibody or protein of interest. Tween-20, which is a detergent, also provides additional stability. Hence we can conclude from the evidence gained thus far that PBS-Tre-Tw has the best dynamic standard curve range of all the coating buffers tested. Additionally when this coating buffer was tested across the 4 slide surfaces, it consistently produced the best intensities showing its adaptability across the different slide chemistries.

The second most consistent buffer was PBS-Tre. A combination between PBS and trehalose enabled the antibody to maintain its' functionality especially at the top range of concentrations. However unlike PBS-Tre-Tw, the intensity tended to subside at the lowest concentrations of capture antibody with PBS-Tre.

Looking at all 8 coating buffers, it is possible to say that PBS-Tre-Tw and PBS-Tre were the most consistent buffers which had the highest intensities and could also be detectable at the low range of capture antibody. Thus, PBS-Tre will be used as the preferred print buffer for the remainder of this project.

3.4.2: Slide Surfaces

From the four slides that were used (aminosilane, epoxysilane, poly-L-lysine and nitrocellulose) there are questions regarding reproducibility and storage. Each slide has its own strengths and weaknesses.

3.4.2.1: Epoxysilane

Epoxysilane slides have been very successful in multiplex PCR and DNA microarrays [268-271]. This choice of slide provided the highest level of intensity of all when used fresh and processed almost immediately. However exposure to the moisture in the air results in the surface losing this reactivity and producing very low levels of intensities especially at the lowest concentrations of capture antibody. For this slide to be used consistently over a longer frame of time, it is vital it is stored in a vacuum to prevent exposure to air. Additionally the choice of manufacturer is important as the spot morphology can vary depending on the way the slide is prepared.

As seen previously, when the ThermoFisher slides were stored at room temperature under no vacuum and the slide surface is exposed to the atmosphere led to weak spotting and low signal intensities. It is assumed the ideal storage conditions for epoxysilane slides are in a vacuum and the poor performance of the ThermoFisher slides were due to inadequate preservation of the slide. However when the slides were analysed one week later, the intensity of the spots decreased further with time

suggesting the slide surface chemistry is not compatible with the antibody that was tested in this experiment.

3.4.2.2: Aminosilane

The aminosilane slide surface provides a solid covalent bond between the slide surface and the protein [218, 272] [273]. Aminosilane provides a solid all-round surface that performs well when used short-term. However the intensity levels decrease upon storage of the slides. It produces nice spot morphology and interacts well with PBS-Tre-Tw both short-term and long-term (despite a lack of intensity in the latter).

An important aspect of the project is to have a sufficiently high level of intensity to incorporate the detection of very low abundance proteins in serum of those with irreversible lung disease and healthy controls. Aminosilane does not provide the best surface to enable this detection to occur.

It is thought that this particular slide surface is more suited to the DNA microarrays, however these slides can be used in all conditions whether exposed to air or stored in vacuum. When processed fresh, for long term use this is not the slide surface that would be used for the remainder of the project.

3.4.2.3: Poly-L-Lysine

This surface has been successful in DNA microarrays whereby it provides a positively charged surface to which negatively attached DNA binds to through electrostatic interactions [274, 275] [208]. Overall the intensity of slides increased when they were analysed one week later. This process of “ageing” the slides has been recommended especially in cDNA microarray work [274, 276] [277] and this could be case in our investigation where an increase in intensity was observed with IgG1.

Poly-L-lysine slides provide a platform for moderate to high levels of intensities and a nice spot morphology. The greatest disadvantage is that there is a high degree of autofluorescence that could be misinterpreted as false-positive results. However this is also dependent on the type of coating buffer that is used on the surface and also the concentration of the capture antibody that is printed. As seen previously, PBS-Tre-Tw and PBS-Tre is compatible with the slide surface and the first 5 dilutions produce spots which are not autofluorescing compared to PBS-T or PBS-Glyc-Tw which suggests a combination of coating buffer at the correct concentration of capture antibody could provide a platform for measuring proteins in serum.

3.4.2.4: Nitrocellulose

Nitrocellulose slides are regularly used in antibody microarrays [209, 278, 279]. Nitrocellulose works by providing a thin nitrocellulose coating that allows for a non-covalent yet irreversible surface for the adhesion of molecules of interest [259]. In this investigation we have shown that in nitrocellulose slides, the level of signal intensity increases with time, like poly-L-lysine. However it has been noted that unlike the previous three slide surfaces at 250µg/ml of capture antibody, comet like spot morphology indicated that the slide was overloaded with too much antibody. Subsequent dilutions produced nice round spots and moderate intensities, in particular with PBS-Tre-Tw. The intensities from the nitrocellulose slides at 125µg/ml of capture antibody were comparable to the intensities from aminosilane. Should these slides be required for use on this type of antibody microarray platform, further optimisation will have to be performed.

3.4.3: Blocking Buffers

Different types of blocking buffers can have a significant influence with antibody specificity, signal intensity and background levels [255] [280, 281]. To date, most microarray research focuses on using blocking buffers that reduce non-specific binding that can lead cross reactivity and poor signal intensities. As such the most common used blocking buffers in microarray research include BSA, horse serum as well as varying levels of low fat milk solutions [282] [283, 284].

Overall in this investigation, in terms of blocking buffers there is not much of a difference between 3% BSA Block and I-Block. Depending on the slide surface, one block buffer offered slightly higher levels of intensities than the other but this was marginal in many incidences. However it was noticed on poly-L-lysine slides that were stored in air for 1 week, only the 3% BSA Block produced visible spots that could be analysed as the I-Block, NAP and Milk were affected when the slide was exposed to air and thus did not block as effectively (results not shown).

NAP and 5% milk block buffer led to high background and in certain cases smearing of the slides were noticed when scanned. This indicates insufficient blocking. Overall in terms of blocking buffers there are no differences in the blocking buffers and the intensity was more dependent on the slide surface than the blocking buffer but this will have to be tested across a wide range of proteins of different concentrations and abundances. Whilst the use of varying milk blocking buffers has been used successful in different types of antibodies microarrays, it was deemed incompatible with this poly-L-lysine slide surface.

In the future for most experiments using 3% BSA block and I Block on poly-L-lysine were effective, hence both will continued to be used . However looking forward when investigating serum and plasma the effect of the blocking buffers were investigated in greater depth, serum was much easier to block and generate a signal than plasma. Overall 3% BSA was the best blocking buffer that worked best on the poly-L-lysine surface and also with serum. Plasma proved more difficult with higher background. However if plasma samples were run, I-Block would be the choice of blocking buffer.

I-Block (Tropix) is a purified version of casein that used as a blocking buffer in both western blots and in microarrays [285] [286]. I-Block has been recently been used a prominent blocking buffer in both reverse phase microarrays as well as lysate microarrays [287-289] [290]. I-Block has been used successfully in these antibody microarray experiments where low background levels which can be seen visually on the slide when scanned compared to other milk blocking buffers.

The use of 3% BSA is not uncommon in blocking of antibody microarrays. A study by Rimini *et al*, showed that the blocking with 3% BSA block produced the lowest background signals compared to Superblock and 5% non-fat milk powder in the different sera that were tested [259]. The only difference between the blocking used in their study and the one used in our investigation is that they used 3% BSA in PBS-T whereas just PBS was used here. The data produced in this study, along with the work carried out in their study, which suggests that 3% BSA block produces one of the best S/N ratios.

3.4.4 Amplification

One of the problems that were seen in the initial stages of optimisation was at the lowest end of the standard curves a distinct lack of sensitivity was seen. Knowing that potentially when measuring clinical samples there would be many low abundant cytokines, this presented a problem. Hence one way to overcome this problem was the use of amplification. This additional step is not unusual in antibody microarray as it has been used many years ago by Haab *et al*, [223] and Zhou, *et al* [291] and recently by Chen [292].

In this case tyramide amplification was used. The amplification works by when HRP enzyme (in the presence of a small amount of H_2O_2 on tyramide) causing activation and oxidation of biotinylated tyramide as extremely reactive intermediates and is thought to bind covalently to proteins at electron-rich amino acid residues such as tyrosine. This results in an increased amount of biotin that are present at sites of immune-reactivity, improving the sensitivity of signals leading to enhanced signal to noise ratios. Interestingly the effect of amplification also improves the level of background which almost halved. A possible explanation for this could be when using cy5 by itself without any amplification the PMT laser setting was set at 450 compared to 380-400 PMT with amplification to take in account the enhanced signals. With amplification there is an increase in signal intensity and this makes the background look weaker when it too has been raised compared to a weaker signal and background level without amplification.

3.4.5 Time Course

Ideally a microarray assay has to be sensitive, accurate and precise. However at the same time it should be able to deliver results which are quicker than what is expected of an ELISA. A traditional sandwich ELISA takes up to 8 hrs, hence when designing this stage of the microarray protocol there was an emphasis to build a platform that could take almost half the time of a traditional ELISA. Initially the experimentation started using the same times as that of an ELISA. The average length of the time to perform the assay was continually halved. We noted that half the original time led to the best standard curves. Interestingly the strength of the curve would improve if the experimental length was halved. Leaving reagents on for longer periods of time could lead to unnecessarily structural changes that may reduce the efficiency of the microarray platform than enhance it. Additionally it has to be acknowledged that leaving the slide on for a longer period of time could expose it to evaporation which could also lead to the same problems.

3.4.6: Printing

One of the major problems in printing large multi-cytokine microarrays is that long printing times lead to the increased likelihood of the spot drying over time. To overcome this problem, a study by *MacBeath and Schreiber*, used humidity inside the arrayer [293]. In addition to the correct print buffer, the key is to keep the spot as hydrated as possible during and after printing so that the proteins are not denatured. The different target heights and dwell times did not affect the spot shape or size. That was dependant on the printing buffer. The most important part of printing was the humidity. As the humidity was increased there were more spots that could be printed.

3.4.7 Cy5 Detection

There are multiple ways of obtaining a signal to a microarray experiment. The long term aim is to use a reagent that would provide a signal that could be detected and repeated over time. The use of cy5 enables slides once processed to be scanned repeatedly over a period of 2 months without any apparent drop in signal intensity. This, with a combination of the reagent used in the processing and the slide surface, provides a platform for repeated scanning.

3.5 Conclusion:

In conclusion, multiple parameters were investigated when optimising the microarray platform from the choice of slide surface, to the optimal blocking buffer, the different settings on the microarrayer to print antibodies whilst also considering the need to use amplification to enhance the sensitivity of the platform.

We have shown that PBS-Tre is the best coating buffer when printing a variety of different antibodies. We have also shown that poly-L-lysine slides are an ideal slide surface for antibody microarray use with consistent levels of signals intensities with time making them desirable when slides are printed and analysed both short and long-term. Additionally the use of 3% BSA blocking buffers removes non-specific adsorption leading to enhanced S/N ratio and reduced background allowing for greater detection of low abundance cytokines in serum. The use of amplification allowed enhanced detection of these low abundance cytokines whilst improving both S/N and backgrounds levels. Moving forward these combination of parameters will be used to validate the microarray platform. Ultimately, the aim is to use this optimisation data to help evolve the microarray platform to become both accurate and precise when measuring cytokines in the sera of both healthy and COPD patients.

Chapter 4: Validation of an Antibody Microarray Platform

4.0 Introduction

The measurements of proteins or analytes in biological samples (serum, plasma, sputum etc.) are a key aspect of any bioanalytical method. However for an assay to be deemed suitable, a series of validity tests have to be performed to prove it can be both accurate and reproducible. The validation of a method can be defined by the FDA as “the process by which a method is tested by the developer or user for reliability, accuracy and preciseness for its intended purpose” [227]. Hence a variety of parameters have to be tested that satisfy the above definition. In the case of the validation of this antibody microarray the following parameters are tested;

- A) Limits of Detection,
- B) Limits of Quantification,
- C) Intra and Inter-assays,
- D) Spike Recovery experiments,
- E) Cross-reactivity,
- F) Direct comparison between Microarray and ELISA techniques.

The six points of validation above will serve to provide a robust test into the nature of the antibody microarray technique and should allow one to decide whether it is a reliable method to ultimately measure multiple biological samples in COPD.

Hence the limits of detection (LOD) and lower and upper limits of quantification (LLoQ and ULoQ) are the first tests performed on this microarray platform. The LOD can be defined as lowest level of the analyte that can be detected but cannot be truly quantified [294-297]. Hence one can say that this approach serves to show how low the platform can measure an analyte but this value is both inaccurate and also imprecise. Hence the LLoQ and ULoQ have to be established when measuring biological samples. Both these limits can be defined as the lowest or highest concentration of an analyte that can be reliably measured on a platform such as an ELISA or microarray [227] [243] [294] [298]. This system can then discriminate and exclude values that fall above and below the limits of quantification.

Interestingly in the field of validation and assay optimisation, there are disagreements about how best to measure the LOD and the LLoQ. One approach is to measure the LOD and use this to value to calculate the LoQ. Hence there is more than one experimental way to calculate the LLoQ. The first way centres on an approach used by Armbruster *et al*, whereby doubling the level of the LOD to calculate the LLoQ [243]. The alternative approach used in line with the FDA requirement for bioanalytical validation is to calculate the highest and lowest points of an assay that can be detected and quantified to an acceptable level of accuracy and precision [227]. However it is important to calculate the difference between both the LoD and LLoQ as these will help discriminate between the absence or presence of an analyte in a sample.

Before the LLoQ can be determined it is important to define the parameters that are used to calculate this figure. Initially the limit of the blank (LoB) can be defined as the highest “apparent” signal at a concentration that is found in multiple replicates of a sample that has no analytes (i.e. blank). Whilst the samples may contain no analyte is

it possible that it may give a signal that may or may not be similar to the signal obtained in the lowest concentration of an analyte. The LoB is calculated by measuring multiple replicates of a blank and calculating both the mean and the standard deviation (a).

The LOD can be defined as the lowest concentration of analyte that can be measured and distinguished from the LoB. Although there are various versions of calculating this figure the traditional approach to estimating the limit of detection is defined as “the concentration of the analyte giving a signal equal to the blank plus 3× the standard deviation of the blank (b)” [243].

Often the LLoQ can be equivalent to the LoD but often it is observed to be higher; however it cannot be lower than the LoD (c) [243].

- a) $\text{LoB} = \text{Mean of Blank}$
- b) $\text{LOD} = \text{Blank} + 3\text{SD}(\text{Blank})$
- c) $\text{LLoQ} = 2 \text{LoD}$

Briefly, the LLoQ and ULoQ here are defined as the lowest and highest points that could be detected at an acceptable level of accuracy and precision. When testing standard curves for all 16 cytokines this was applied to calculate a value that is highly accurate and precise as defined from the FDA guidelines on bioanalytical method validation.

Accuracy can be defined as how close a measurement is to a true value and precision can be defined as the reproducibility of the values with regard to how close the values are to one another [238] [299]. This is often known as the coefficient of variation (CV %). Both the intra and inter-assays are key parameters in determining the performance and characteristic of the microarray platform. Additionally these parameters are used to calculate accuracy include spike recovery experiments. It is important to calculate the accuracy so to take into account how true the value is and if not calculate the level of inaccuracy. Both accuracy and precision can be calculated by analysing quality control (QC) samples at 3 concentrations (low, medium and high) which should represent the range of the standard curve.

The level of accuracy from commercially available microarray kits range from 70-130% dependent on the number of cytokines investigated and type of biological sample tested. Additionally precision (CV %) is often less than or equal to 20-30% dependent on the nature of the assay. The efficiency of an analytical system depends upon high levels of accuracy and precision recorded over multiple test experiments.

One of the biggest issues with microarray platforms when using a mixture of different antibodies and reagents is the problem of cross-reactivity. If cross-reactivity exists between different capture and detection antibodies, this will then limit the number of proteins that can be tested on an array. Cross reactivity between detection antibodies and capture antibodies as well as a non-specific analytes limits the number of proteins that can be used on a multiplexing platform.

However it is not only antibodies alone that can lead to cross-reactivity. It is thought that other reagents in which antibodies are diluted could be involved as a source of interference in the assay [300] [301]. Non-specific binding may lead to a large background signal, therefore decreasing the sensitivity of the assay. However there are

reagents which may cause changes in proteins due to varying ionic strength, pH or hydrophobicity that may irreversibly change the structure of the protein leading to potential cross-reactivity and hence reducing the efficiency of the microarray platform [302]. A study by Pflieger *et al*, showed that use of different diluents in antibodies contribute significantly to both signal intensity and assay performance [303].

Other factors in assay development, such as the temperature the microarray is run, the length of incubations, the number of wash steps and concentrations of the reagents, may all contribute to cross-reactivity and have to be optimised in order to improve the performance of the microarray.

In this Chapter a direct comparison is made between ELISA and microarray. The antibody microarray is developed originally from the ELISA model for protein detection. Here the standard curves of both techniques are compared against one another to see the level of correlation. However this alone is not adequate to measure how comparable both techniques are so a selection of consenting healthy controls were recruited and serum measured for all 16 cytokines on the microarray and also on the ELISA.

4.2 Materials and Methods

For the validation Chapter, poly-lysine slides were used. Due to the low level of sensitivity obtained, these slides were subject to amplification. Briefly, antibody duoset kits were purchased (R&D Systems, MN, USA) and printed on poly-L-lysine slides. Slides were processed immediately or after one week. Slides on the day of processing were taken from the vacuum and blocked for an hour with either I-Block or 3% BSA block buffer. Standards were made for all 16 cytokines (IL-8, IL-6, IL-1 β , TNF- α , Exotaxin-1, Eotaxin-2, IFN- γ , RAGE, IL-10, IL-4, IL-17, IL-23, MCP-1, VEGF and IP-10) according to manufacturer's instructions and diluted 2 fold across 7 dilutions and added at 50 μ l per well in 10 replicates for 45 mins. Additionally healthy human sera were added to the corresponding well on the slides. The slide was washed three times and 50 μ l of appropriately diluted biotinylated detection antibody was added to each block for 45 mins. Slides were subjected to tyramide amplification. Briefly, this was performed after the detection stage of the microarray process described above with the additional of 50 μ l of 1:1000 diluted streptavidin-HRP (Bio-Rad, USA) in the dark. The slide was washed and 50 μ l of Bio-Rad Amplification Reagent was added for 10 mins in the dark. The slides were washed three times with 20% DMSO-PBST and subsequently washed thrice with wash buffer. After washing, 50 μ l of 1:1000 diluted streptavidin-conjugated cy5 (E-Biosciences, UK) was added and incubated at room temperature for 15 mins in the dark. The slide was washed three times and rinsed in ultra-pure water and centrifuged dry and scanned with the 4200 AL microarray scanner at 635nm (Axon GenePix®). Fluorescence was quantified using the GenePix Pro Software (Axon GenePix®). The experiment was repeated at least twice. The median fluorescence of each spot was measured (minus

background) and the corrected fluorescence was used to calculate the average fluorescence signal across the standard detectable ranges.

ELISAs were performed using the R&D systems duoset kits (listed in the previous section and used in the microarray) as described by the manufacturer's instructions. Briefly, plates were coated with 1-4 μ g/ml of capture antibody and incubated overnight at room temperature. The plates were washed 3 times with PBS-Tween 0.05% (Sigma) and blocked with Reagent Diluent (1% BSA in PBS) for 1 hour and washed three times. Standards were made in Reagent Diluent at the top concentration (according to kit instructions) and diluted 2 fold (across seven points) at 100 μ l per well in duplicates for 2 hrs. The plate was washed three times and 100 μ l of appropriately diluted biotinylated detection antibody was added to each well for 2 hrs. After washing three times with washing buffer, 100 μ l of diluted streptavidin-HRP was added and incubated at room temperature for 30 mins in the dark. Wells were washed three times and the enzyme substrate peroxidase chromogen was added. After incubation for 30 mins at room temperature the reaction was stopped by adding 50 μ l of 0.18M H₂SO₄ per well and the absorbances were read at 450nm.

To determine the precision of the microarray platform, intra- and inter assays were performed. Intra-assays were performed repeatedly over the same slide on the same day and inter-assays were performed over a period of three consecutive days. Up to 30 healthy volunteers sera were collected and the 16 biomarkers were quantified. The mean of the replicates and the standard deviation was used to calculate the precision of the microarray methodology.

PBS was also spiked to three known concentrations (750pg/ml, 188pg/ml and 24pg/ml) using recombinant protein standards for each of the 16 biomarkers and quantified using the standard curves generated from the microarrays. These three spikes were set

to be above and below the limits of quantification. Accuracy (%) was calculated based on the observed concentration measured against the expected concentration.

To identify any effects that serum proteins may have on the assay system, sera from healthy donors were taken and cytokine levels were quantified for all 16 biomarkers. This serum was then spiked to the three known concentrations points mentioned above. The observed concentration was subtracted from background levels to calculate accuracy and precision.

Finally to compare both ELISAs and microarrays, a group of healthy individuals were chosen and quantified for all 16 cytokines on the ELISA and microarray to determine the similarity between both methods.

4.3 Results

4.3.1 Limits of Detection and Quantification

The limits of detection and quantification were calculated first. This was done in three stages. The first was to calculate LOD. The LOD is defined as the lowest level of the analyte that can be detected but cannot be truly quantified [227]. This is calculated by drawing standard curves for all 16 biomarkers and using the curve to work out the standard deviation of the blank. Then the following equation is applied to calculate the LOD:

$$\text{LOD} = 3\text{SD (mean Blank)} + \text{mean Blank.}$$

For the limits of quantification, these were the lowest and highest points that could be detected at an acceptable level of accuracy and precision. Hence a series of “spikes” were run at the either end of the standard curves of the 16 biomarkers. The point where the precision fell below 20% was deemed to be LLoQ and 15% for the ULoQ as in line with FDA regulations for assay development.

Table 12 illustrates the limits of detection and quantification for all 16 cytokines. This shows that with low abundance cytokines such as IL-6 and IL-8 the microarray system was able to measure signals as low as 1.5pg/ml, where in slightly higher abundant cytokines such as RAGE and eotaxin-2, the LLoQ was 5.9pg/ml. This shows the microarray platform can measure to a low level of sensitivity.

Whilst the LOD is very low, often it is not chosen as the limit to measure proteins in biological samples. As these LOD values are very low, at these concentrations there is a higher degree of variability between samples. Additionally the ULoQ takes into account the high abundance cytokines in this 16 cytokine panel such as RAGE,

Eotaxin-2 and IL-23 and makes the necessary adjustments. Furthermore, in future studies, biological samples that fall above and below the LLoQ and ULoQ are included as follows: those that fall below the LLoQ are deemed to be undetectable (zero); and the ULoQ is the highest analyte concentration that can be quantified with acceptable precision and accuracy.

The lower limit of detection is calculated as the concentration of biomarker required to give a signal that is equal to the background (blank) plus three times the SD of the blank [243]. The LLOQ can be defined as twice the level of the LOD [243] or the lowest analyte concentration that can be quantified with acceptable precision and accuracy as in line with FDA regulations for assay development [227].

Table 12: Shows the LOD, LLoQ and ULoQ for 16 cytokines.

Cytokines	Limits of Detection & Quantification		
	LOD (pg/ml)	LLoQ (pg/ml)	ULoQ (pg/ml)
IL-8	0.535	1.5	750
IL-6	0.683	1.5	750
TNF- α	1.126	1.5	750
IL-1 β	0.404	2.9	750
VEGF	0.744	1.5	750
EOTAXIN-1	1.863	2.9	750
IFN- γ	0.108	2.9	750
IL-17	0.445	5.9	750
EOTAXIN-2	0.739	5.9	1900
IP-10	0.458	5.9	750
RAGE	0.968	5.9	1900
MCP-1	0.284	5.9	750
IL-4	0.6	2.9	750
IL-10	0.503	2.9	750
TGF- β	0.398	2.9	750
IL-23	0.612	5.9	1900

Table 12 illustrates the LOD, LLoQ and ULoQ for all 16 cytokines on poly-L-lysine slides. The lower limit of detection is calculated as the concentration of biomarker required to give a signal that is equal to the background (blank) plus three times the standard deviation of the blank. The lower limit of quantification (LLOQ) is defined as twice the level of the LOD or the point where the CV, as a measure of precision, falls below 20% is deemed to be LLoQ in line with FDA regulations for assay development.

The lower limit of detection varied from 0.284 to 1.9pg/ml for the 16 biomarkers investigated. The lower limit of quantification ranged between 1.5-5.9pg/ml and the upper limit of quantification between 750-1900pg/ml for the 16 biomarkers respectively.

4.3.2: Cross Reactivity

Cross reactivity testing is an important validity parameter in cytokine binding based assays such as ELISAs and in this case, the antibody microarray platform.

Hence to determine if cross reactivity occurs in this microarray platform the following experiments were conducted; (I) A microarray panel was printed with a variety of capture antibodies and a single protein standard was added to which a complete cocktail of detection antibodies were added (Figure 46 & 47), and (II) a microarray panel was printed with a variety of capture antibodies and no protein standards were added and a complete cocktail of detection antibodies were added and processed as normal (Figure 48 & 49), and finally (III) a microarray panel was printed with a variety of capture antibodies and a cocktail of recombinant protein standards and a complete cocktail of detection antibodies with 1 antibody removed to detect if cross reactivity occurs between detection antibodies and specific cytokines (Figure 50 & 51).

No cross-reactivity was observed in all three experiments. In the first experiment a single protein standard was added to a combination of a full set of capture and detection antibodies and as expected only the protein that was added showed an observable signal (Figure 46 & 47). In the second experiment a full set of a selection capture antibodies were printed and added with the complimentary version of the detection antibodies without any protein standards and as expected no signals were detected (Figure 48 & 49).

The third experiment is the most decisive to show a lack of cross-reactivity. When all 16 capture antibodies are printed and their protein standards added with all but one detection antibody all 15 spots show signals except for the set of spots that have no specific detection antibody. As an example, eotaxin-1 was not added and in Figure 50 & 51 there was no signal observed, showing the microarray platform to be highly specific for the remaining 15 cytokines.

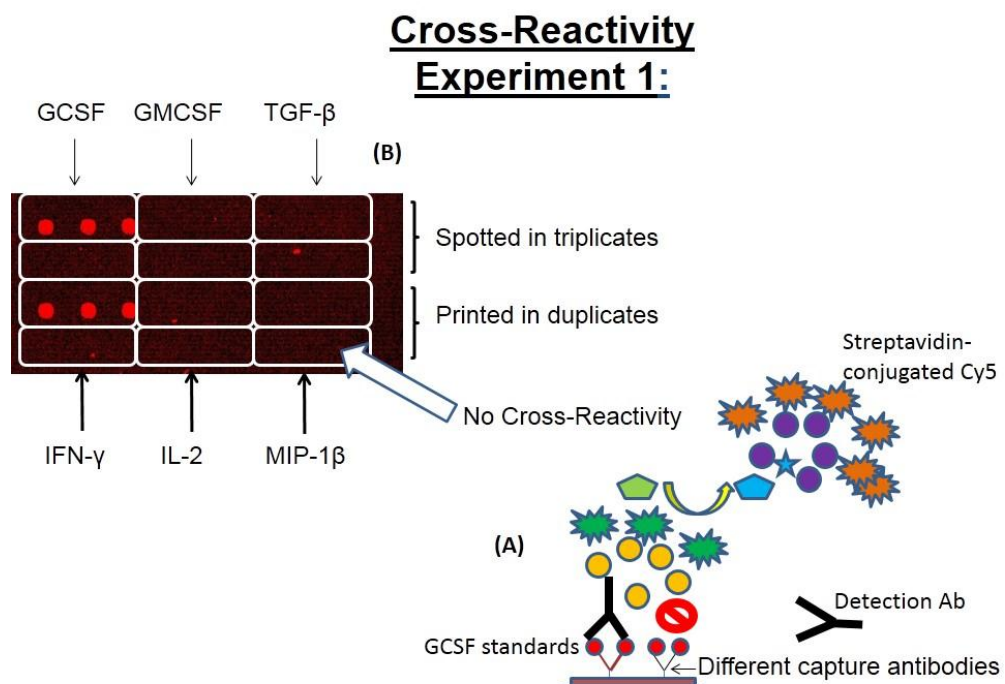


Figure 46: Cross reactivity experiment 1; a complete selection of capture antibodies are added and only 1 protein standard is added with a complete cocktail of detection antibodies.

As seen from the cartoon, a microarray panel was printed with a variety of different capture antibodies and a single protein standard (GCSF) was added to which a complete cocktail of detection antibodies were added including GCSF detection antibody and developed by streptavidin cy5 (A). This is reflected when the slide was scanned, as GCSF spots appear to be detected, whilst the remaining cytokines (GMCSF, TGF- β , IFN- γ , IL-2 and MIP-1 β) that were also printed where not detected in the other panels, hence showing no cross-reactivity (B).

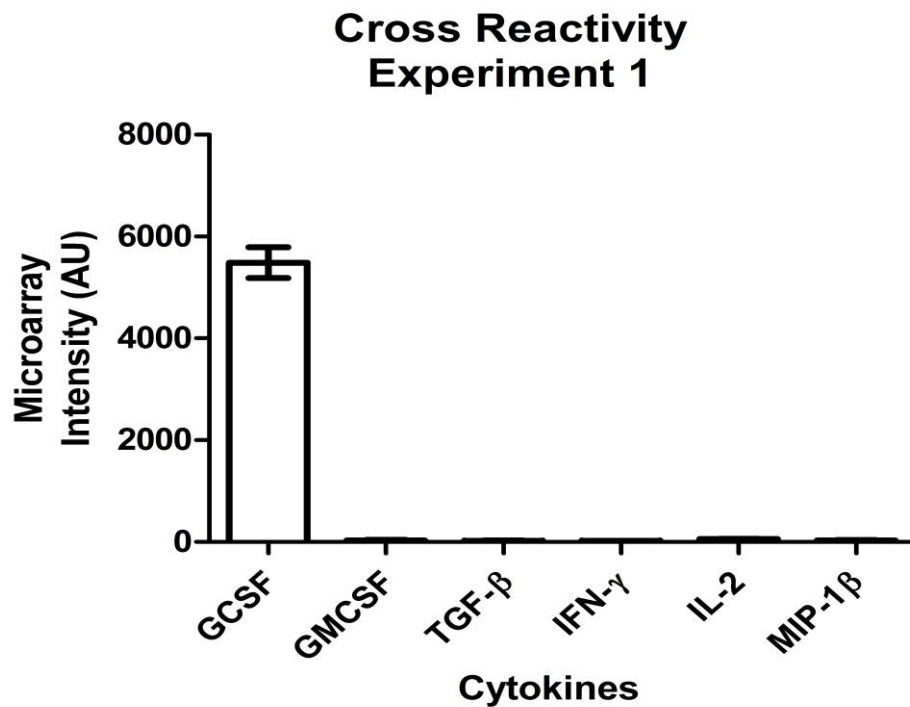


Figure 47: Cross reactivity experiment 1; A graphical representation of the experiment where a selection of capture antibodies are added and only 1 protein standard is added with a complete cocktail of detection antibodies.

A graphical representation of the experiment is shown where a microarray panel was printed with a variety of different capture antibodies and a single protein standard (GCSF) was added to which a complete cocktail of detection antibodies were added including GCSF detection antibody. This is reflected when the slide was scanned, as GCSF spots appear to be detected, as shown by an increase in signal intensity whilst the remainder of the cytokines (GMCSF, TGF-β, IFN-γ, IL-2 and MIP-1β) that were also printed were not detected, as shown, where no signal intensity was observed.

Cross-Reactivity Experiment 2

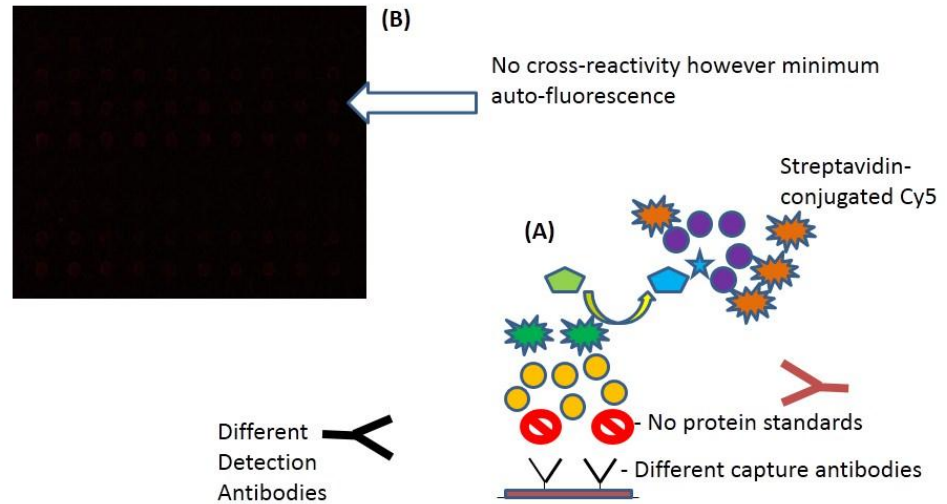


Figure 48: Cross reactivity experiment; a complete selection of capture antibodies are added with no recombinant protein standards and a complete cocktail of detection antibodies.

As seen from the cartoon, a microarray panel was printed with a variety of capture antibodies and no protein standards were added and a complete cocktail of detection antibodies were added and developed by streptavidin cy5 (A). This is reflected when the slide was scanned, when no spots were detected, except for a minimal amount of autofluorescence (B).

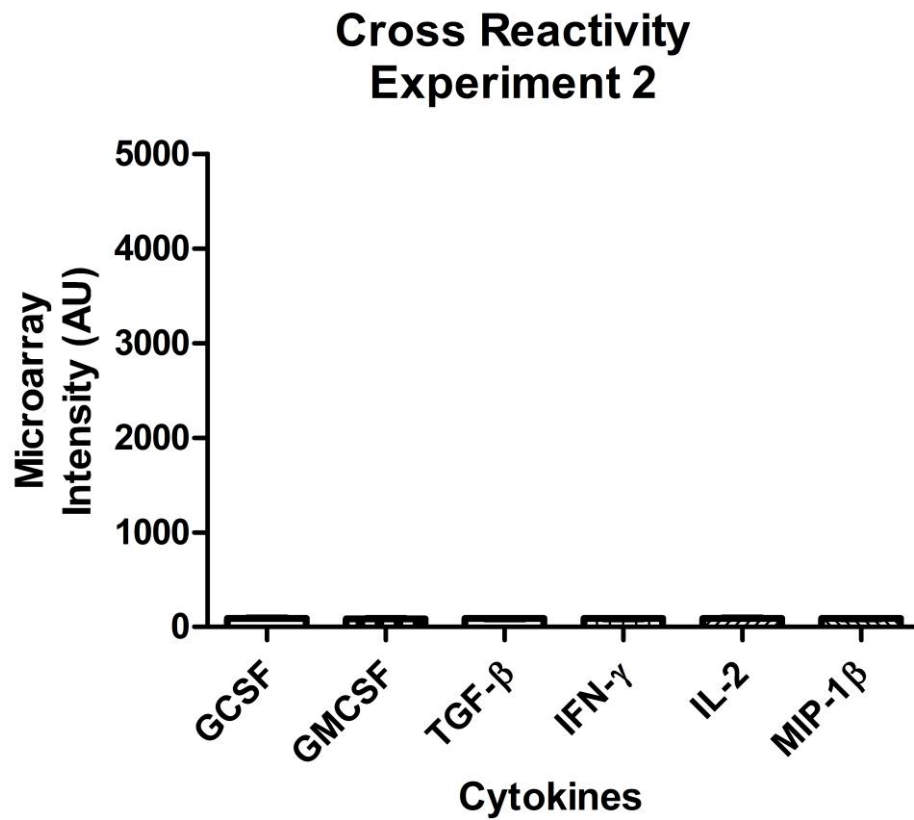


Figure 49: Cross reactivity experiment 2; a graphical representation of the experiment complete selection of capture antibodies are added with no protein standards and a complete cocktail of detection antibodies.

A graphical representation of the experiment is shown where a microarray panel was printed with a variety of different capture antibodies and no recombinant protein standards were added to which a complete cocktail of detection antibodies were added. This is reflected when the slide was scanned, and no spots were detected as shown by trace levels of signal intensity for the six cytokines detected.

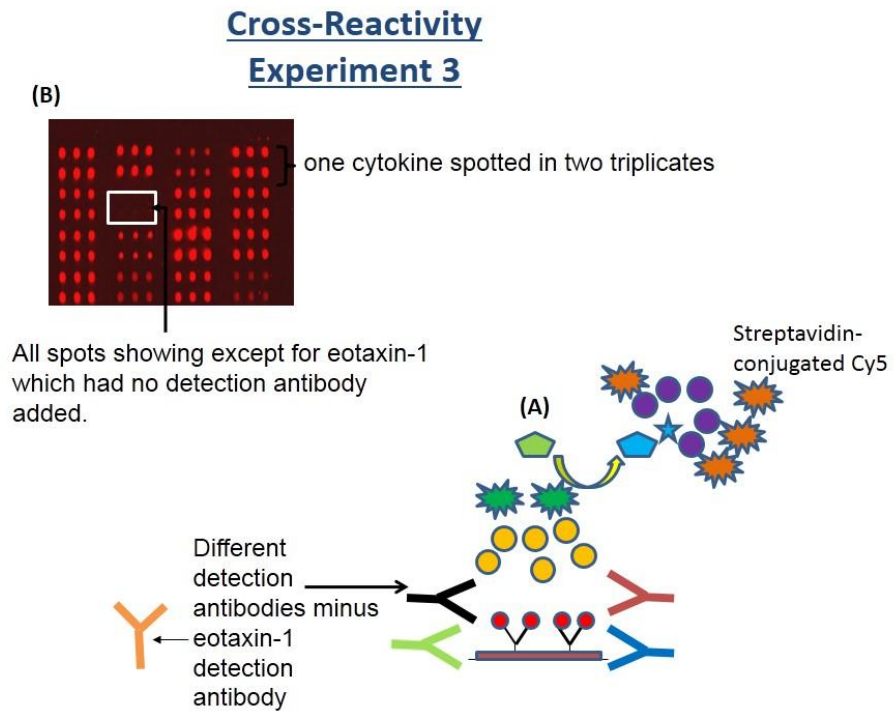


Figure 50: Cross reactivity experiment 3; 16 capture antibodies are printed and added with a complete set of 16 protein standards and with a 15 detection antibodies except for eotaxin-1 antibody

As seen from the cartoon, a microarray panel was printed with a variety of capture antibodies (16) and a cocktail of recombinant protein standards (16) and a complete cocktail of detection antibodies with 1 antibody removed to detect if cross reactivity occurs between detection antibodies and specific cytokines (A). In this case eotaxin-1 detection antibody was removed from the cocktail of detection antibodies. This is reflected when the slide was scanned, and spots are detected for all the remaining 15 cytokines except for eotaxin-1 as highlighted in the white box where no spots are seen, indicating the microarray system does not display cross-reactivity (B).

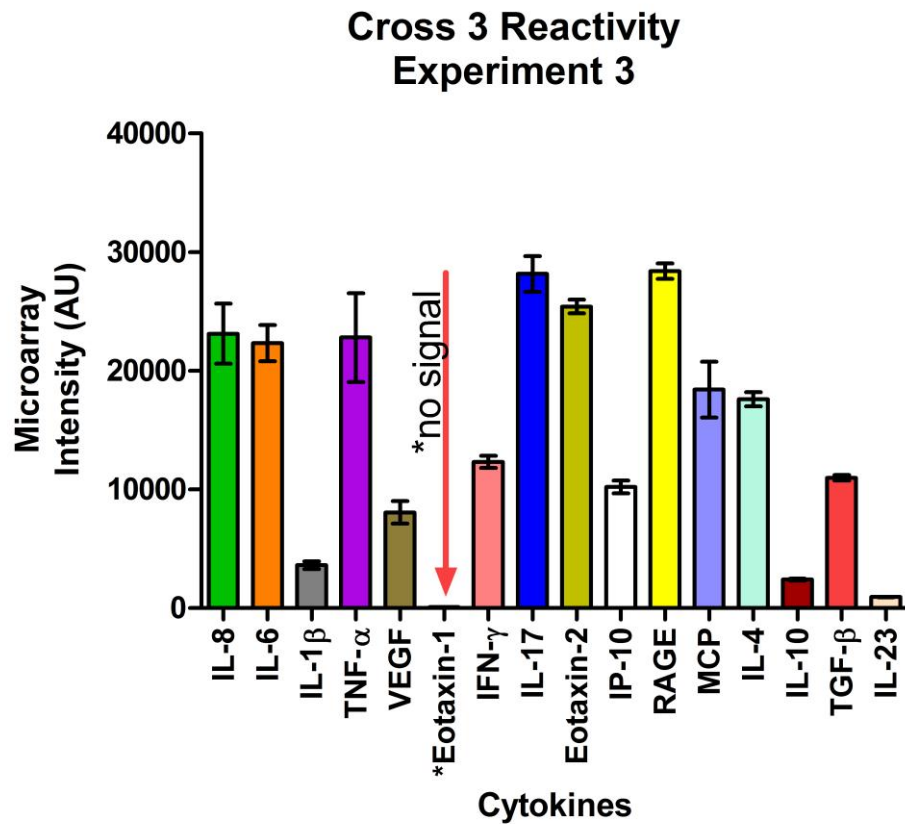


Figure 51: Cross reactivity experiment 3; a graphical representation of the experiment where 16 capture antibodies are printed and added with a complete set of 16 protein standards and with a 15 detection antibodies except for eotaxin-1 antibody

A graphical representation of the experiment is shown where a microarray panel was printed with a variety of capture antibodies (16) and a cocktail of recombinant protein standards (16) and a complete cocktail of detection antibodies with 1 antibody removed to detect if cross reactivity occurs between detection antibodies and specific cytokines. In this case eotaxin-1 detection antibody was removed from the cocktail of detection antibodies. This is reflected when the slide was scanned, and no signal is observed for eotaxin-1, whilst signals can be observed for all other 15 cytokines indicating there is no cross-reactivity in this microarray platform.

4.3.3 PBS and Serum Spike recovery

PBS was also spiked to three known concentrations (750pg/ml, 188pg/ml and 22pg/ml) using recombinant protein standards for each of the 16 biomarkers (IL-8, IL-6, IL-1 β , TNF- α , Exotaxin-1, Eotaxin-2, IFN- γ , RAGE, IL-10, IL-4, IL-17, IL-23, MCP-1, VEGF and IP-10) and quantified using the standard curves generated from the microarrays. These three spikes were set to be above and below the limits of quantification. Accuracy (%) was calculated based on the observed concentration measured against the expected concentration. To identify any effects that serum proteins may have on the assay system, sera from healthy donors were taken and cytokine levels were quantified for all 16 biomarkers. This serum was then spiked to the three known concentration points mentioned above. The observed concentration was subtracted from background levels to calculate accuracy and precision (Figure 52).

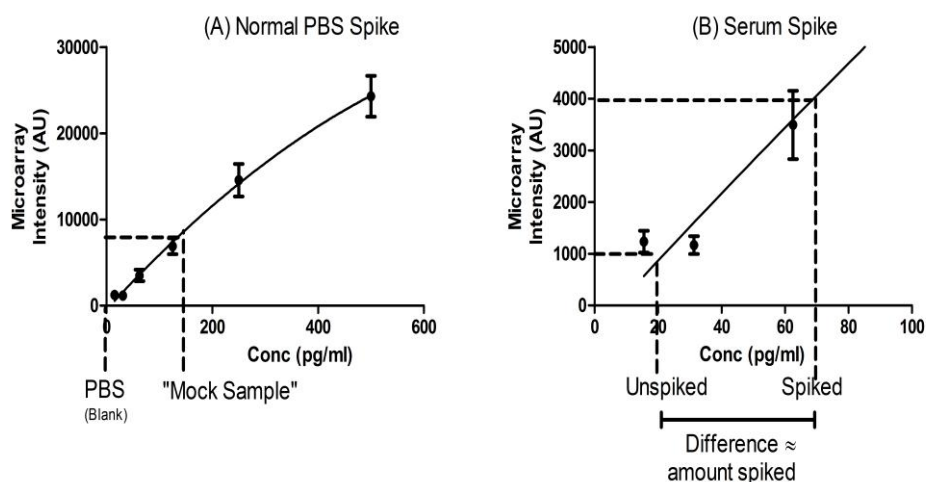


Figure 52: Microarray assay validation using PBS and serum samples spiked with known concentrations of cytokines.

Sixteen cytokines were quantified in PBS (IL-8, IL-6, IL-1 β , TNF- α , Exotaxin-1, Eotaxin-2, IFN- γ , RAGE, IL-10, IL-4, IL-17, IL-23, MCP-1, VEGF and IP-10). Three different known concentrations of cytokine (750 pg/ml, 188 pg/ml, 22 pg/ml) were then added to aliquots of PBS. The difference between blank PBS and spiked PBS was determined by the microarray assay (A).

Additionally these sixteen cytokines were quantified in the serum of a healthy volunteer. Three different known concentrations of cytokine (750 pg/ml, 188 pg/ml, 22 pg/ml) were then added to aliquots of the serum, and the concentration difference between the original and spiked serum samples was determined by microarray assay (B).

4.3.4 Target Concentration Spiked in PBS or Serum

For all 16 biomarkers, PBS and serum spike recovery (accuracy and precision) were tested at three targeted concentrations; namely at 750pg/ml, 188pg/ml and 22pg/ml (Figure 53A). For all three targeted concentration points the observed concentration of all 16 cytokines (mean) was in line with the actual concentration spiked. As seen in Figs 53B/C, all biomarkers fall in the acceptance criteria for spike accuracy (80-120%) and precision ($\leq 20\%$).

If this is broken down into individual cytokines it can be seen in both serum and PBS spikes. For all three targeted concentration points the observed concentrations of all 16 cytokines fall within the acceptable criteria in relation to the expected concentration (Figure 54A/B). Also in the accuracy and precision of all 16 cytokines the majority of the cytokines are within the acceptable parameters (Figure 55 & 56). However it has to be acknowledged that are certain cytokines that fall slightly below the acceptable levels. This occurs in the lower abundant cytokines such as IL-8, IL-6 and IP-10 which were found in very low levels in healthy subjects and the variation at these low levels have led to greater levels of inaccuracy and imprecision. However these values are comparable to those reported in Wood *et al*, [28], and Anderson *et al*, [29]. This shows that the microarray platform developed is both precise and accurate.

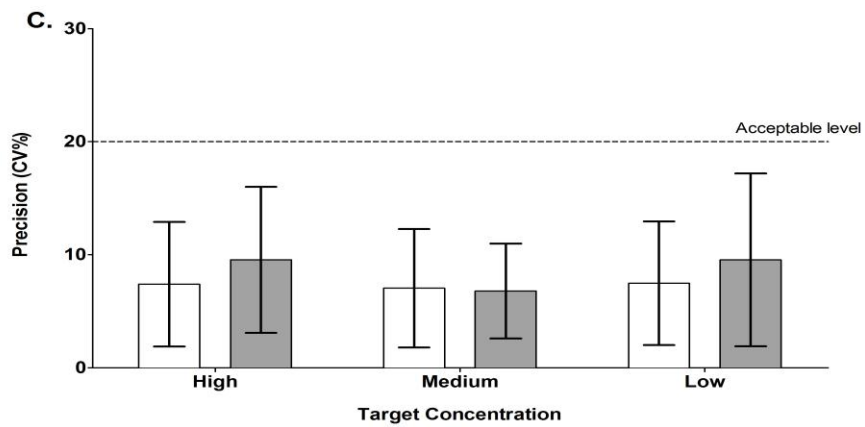
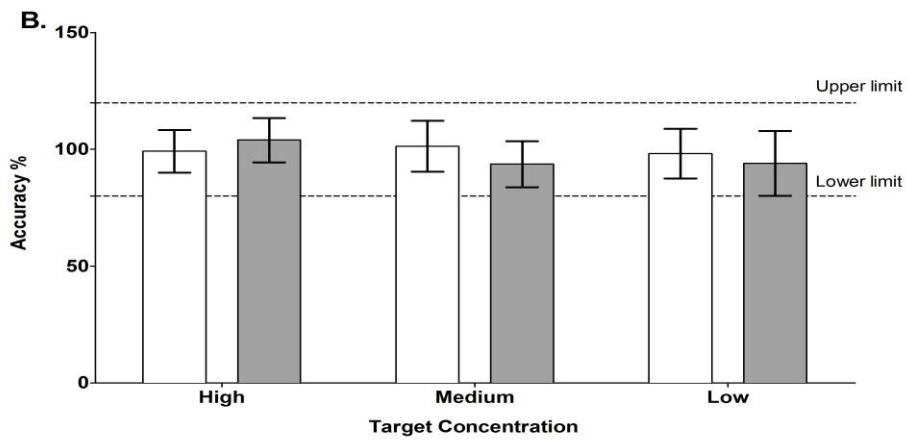
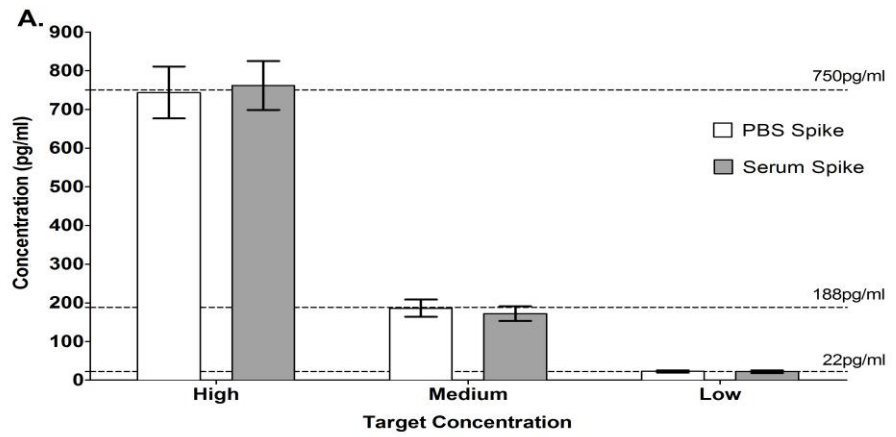


Figure 53: Accuracy and precision of cytokine concentration determination by microarray assay.

Cytokine concentrations in spiked PBS and serum samples determined by microarray assay (mean \pm SD for 16 cytokines) (A). The actual concentrations are indicated by the dashed lines. (B) The percentage accuracy of cytokine concentration determination by microarray assay (mean \pm SD for 16 cytokines) relative to the acceptable limits for variation in accuracy prescribed by the FDA. (C) The coefficient of variation of cytokine concentration determination by microarray assay (mean \pm SD for 16 cytokines) in spiked PBS and serum samples.

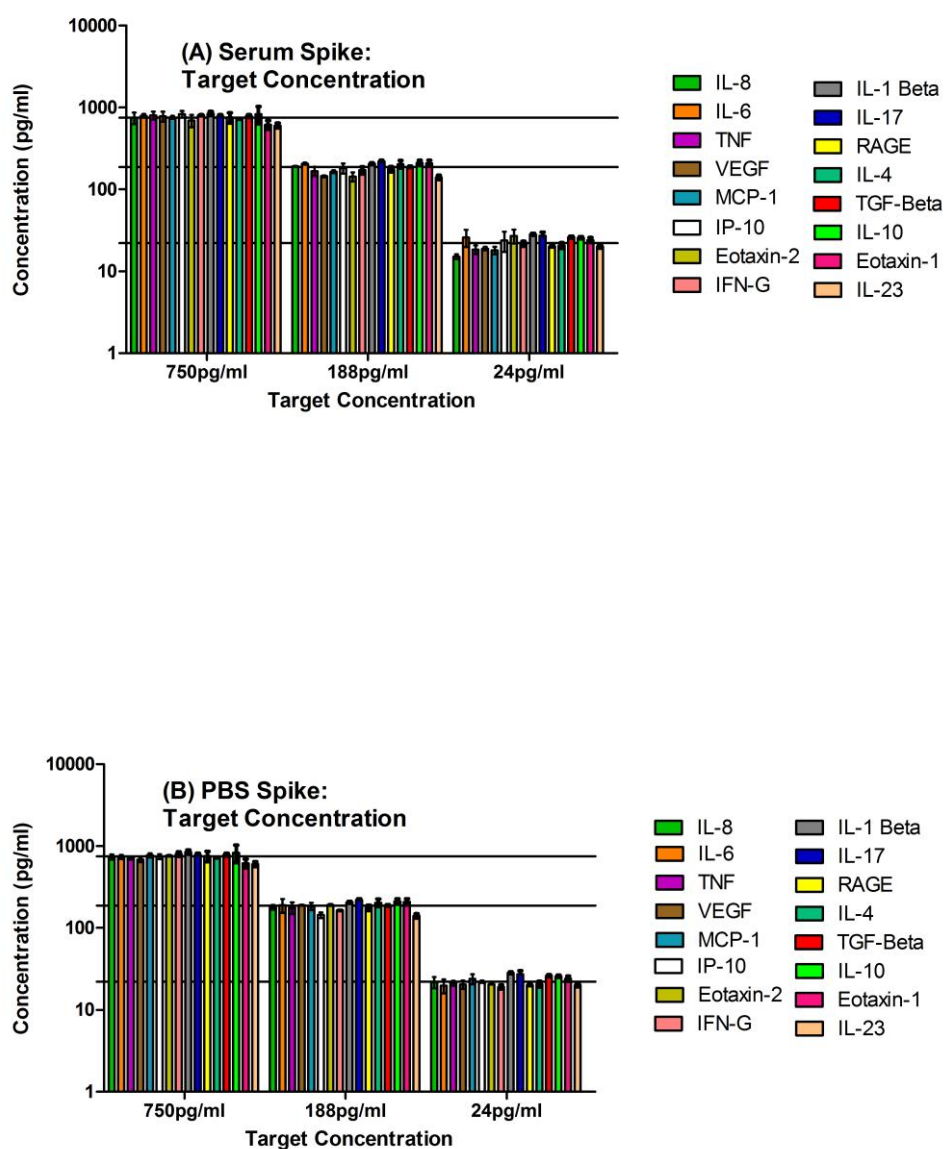


Figure 54: PBS and serum were spiked at three known concentration across all 16 biomarkers (A & B).

Cytokine concentrations in spiked PBS and spiked serum determined by microarray assay (mean \pm SD for 16 cytokines) (A + B). The actual concentrations are indicated by the solid lines. As seen from the figure, the observed concentrations from the spike experiments for both PBS and serum are close in relation to the actual concentration with the exception of low abundance cytokines such as IL-8 and IL-6.

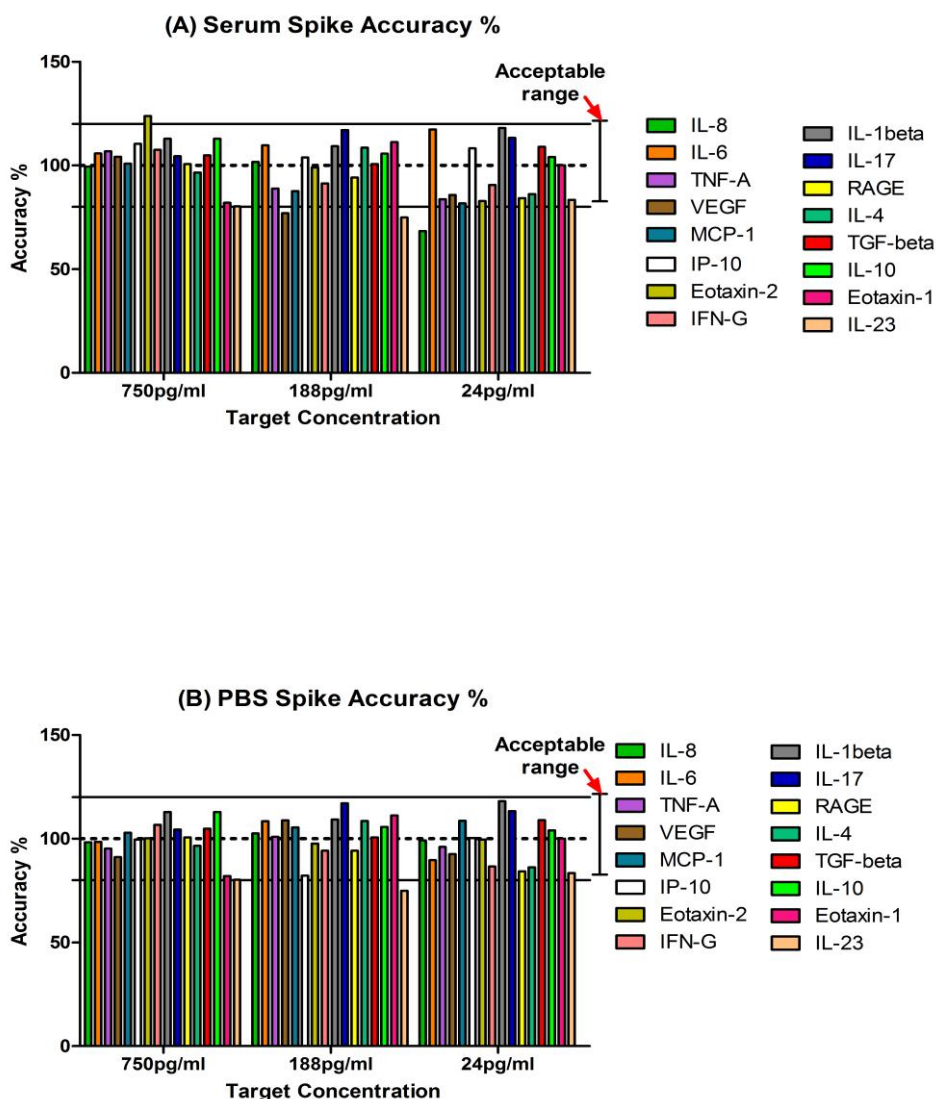


Figure 55: The observed mean concentration was recorded and compared with the expected concentration to calculate the mean accuracy.

The percentage accuracy of each of the 16 cytokines concentration determination by microarray assay (IL-8, IL-6, IL-1 β , TNF- α , Exotaxin-1, Eotaxin-2, IFN- γ , RAGE, IL-10, IL-4, IL-17, IL-23, MCP-1, VEGF and IP-10) relative to the acceptable limit for variation in accuracy prescribed by the FDA. As seen, with the exception of IL-8 and IL-23 the remaining 14 cytokines would fall between the accuracy levels set between 80-120%.

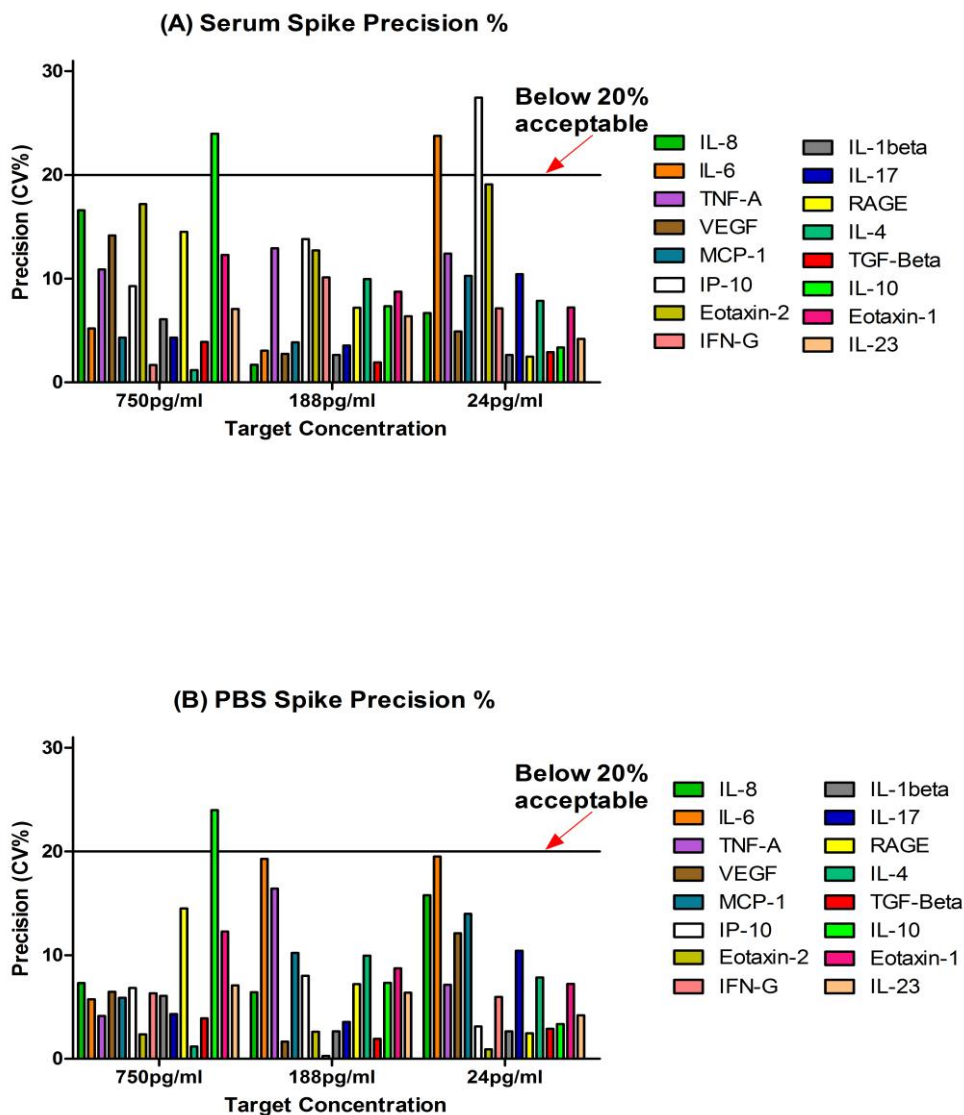


Figure 56: The precision of the assay of all 16 cytokines are shown was calculated (A &B).

The coefficient of variation each of the 16 cytokines concentration determination by microarray assay (IL-8, IL-6, IL-1 β , TNF- α , Exotaxin-1, Eotaxin-2, IFN- γ , RAGE, IL-10, IL-4, IL-17, IL-23, MCP-1, VEGF and IP-10) relative to the acceptable limit for variation in accuracy prescribed by the FDA. However it was noted that in low abundance cytokines, such as IL-8 and IL-6 and IP-10, the accuracy and precision were lower than is considered acceptable.

4.3.5: Intra and Inter assay precision

For the intra assay variation, 13 out of 16 biomarkers were within the acceptable limits for precision. However, a lower level of precision was achieved in the inter assay variation (11 out of 16 biomarkers within acceptable levels of precision) (Figure 57A). This is probably due to the greater variation that occurs at the lowest concentration in the very low abundance cytokines in healthy sera (for example IL-10). From the microarray assay data for the 16 cytokines on up to 30 healthy volunteer's sera (see section 4.3.6 below), the cytokines were split into three groups - low abundance cytokines with serum concentrations ≤ 50 pg/ml (IL-1beta, IL-4, IL-6, IL-8, IL-10 and TNF-alpha), mid-abundance cytokines with concentrations 50-200 pg/ml (VEGF, MCP-1, Eot-1, IFN-gamma, TGF-beta, IL-17) and high abundance cytokines with concentrations ≥ 200 pg/ml (Eot-2, IL-23, IP-10 and RAGE). As expected there is a greater level of variation in the low abundance cytokines compared to the mid and high abundance cytokines as the level of CV% is higher in the former (Figures 57). The precision of the low, mid and high abundance groups was compared by Kruskal-Wallis test; there was no significant difference between the three groups for intra-assay CV, although the median CV for the low abundance group was on the limit for acceptable precision (CV ~20%) and the range of CVs was greatest for this group (Figure 57B). As anticipated, the inter-assay CVs were higher than the intra-assay CVs, although the median CVs for the mid and high abundance cytokines again similar and well within the acceptable limit (Figure 57C). However, the median intra-assay CV for the low abundance cytokines was above the acceptable limit of precision and was significantly higher than for either the mid or high abundance groups (as shown by a post-hoc Dunn's Multiple Comparison Test) (Figure 57C).

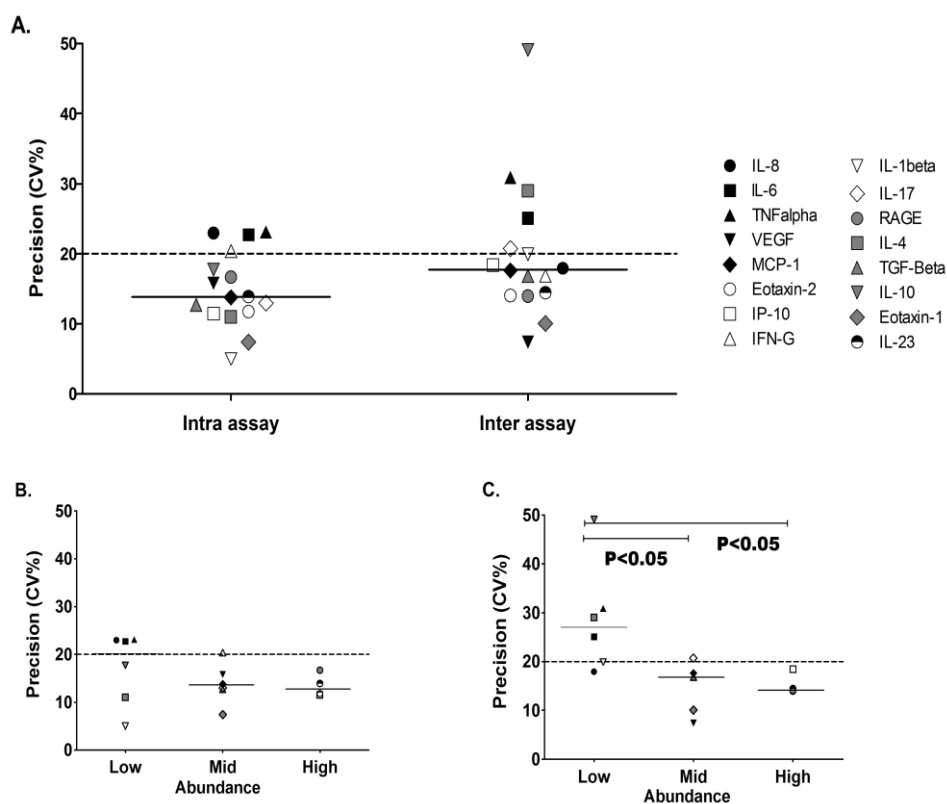


Figure 57: The intra- and inter-assay precision.

(A) The intra- and inter-assay CV% for the quantification of 16 cytokines. (B) The intra-assay coefficient of variation for low, mid and high abundance cytokines. (C) The inter-assay coefficient of variation for low, mid and high abundance cytokines. The dashed lines represent the acceptable limit of precision ($CV \leq 20\%$). The solid lines represent the median for each group. Significant differences between low, mid and high groups in (B) and (C) were determined by Kruskal-Wallis test with a post-hoc Dunn's Multiple Comparison test. The definition of low, mid and high abundance cytokines was based on the samples shown in Figure 53, giving the following cut-offs: low abundance < 50 pg/ml; mid abundance 50-200 pg/ml; high abundance > 200 pg/ml.

4.3.6 Comparison of Microarray technology with ELISA

The next stage was to compare between both ELISA and microarray methodology to see if the standard curves were positively correlated. When directly comparing methods, four cytokines (MIP-1 β , Rantes, GM-CSF and M-CSF) were investigated and showed there were positive correlations between both the methods (using Spearman's Rank correlation for each cytokine) showing that multiplex microarray technology does compare well to "traditional" ELISAs (Figure 58A-D). Both technologies show a strong degree of correlation which was statistically significant with regard to their respective standard curves with r values above 0.9865 for all 4 cytokines tested.

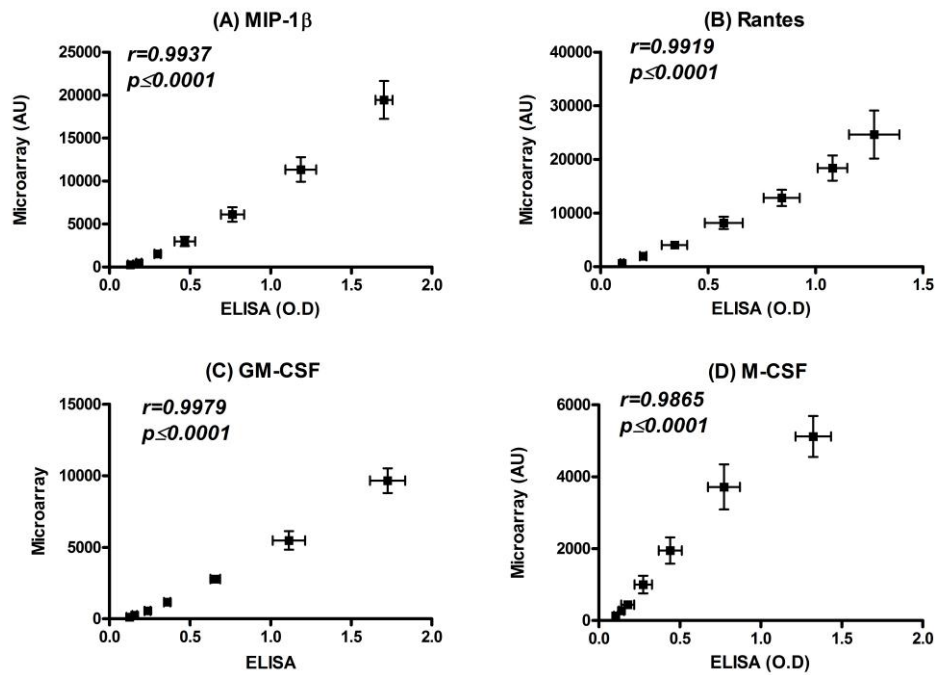


Figure 58: A-D: This shows that multiplex microarray technology significantly correlates with the “traditional” ELISAs.

Shows correlation between individual “traditional” ELISAs (n=3) and multiplex microarrays (n=10) of cytokines. The individual values each cytokine was plotted with microarray values on the Y-axis and ELISA values on the X-axis. The errors bars are calculated as SD. Note there is a strong correlation between all the 4 cytokines investigated (MIP-1β: $r=0.9937$, $p \leq 0.0018$, Rantes: $r=0.9919$, $p \leq 0.0001$, GMCSF: $r=0.9979$, $p \leq 0.0002$ and MSCF: $r=0.9865$, $p \leq 0.0001$ respectively).

However the comparison of standard curves alone is insufficient to prove conclusively that both methods comparable. Ultimately another test was performed to see how similar two methods compare to one another as well as the quantification of clinical samples. Hence a comparison between the quantitative aspects of both methods was tested. Thirty sera was obtained from healthy individuals and quantified for all 16 biomarkers using both microarray and ELISAs. The direct correlations are shown in Figure 59. This shows that across all 16 biomarkers there were no significant differences between techniques ($0.3404 \leq P \leq 0.0997$). Additionally Bland Altman plots were drawn to see if there was an agreement between techniques (Figure 60). The level of bias is dictated by the thin dotted line either side of the zero. In the Bland-Altman plot, with IL-8, TNF- α and VEGF there is not so much deviation from the zero (as indicated by the bias line) (Figure 60). However with IL-1 β there is a bias towards the microarray system and further indicates that when investigating very low abundance cytokines like IL-1 β , the microarray technology has an advantage over an ELISA as it is able to detect more sensitively at low concentrations.

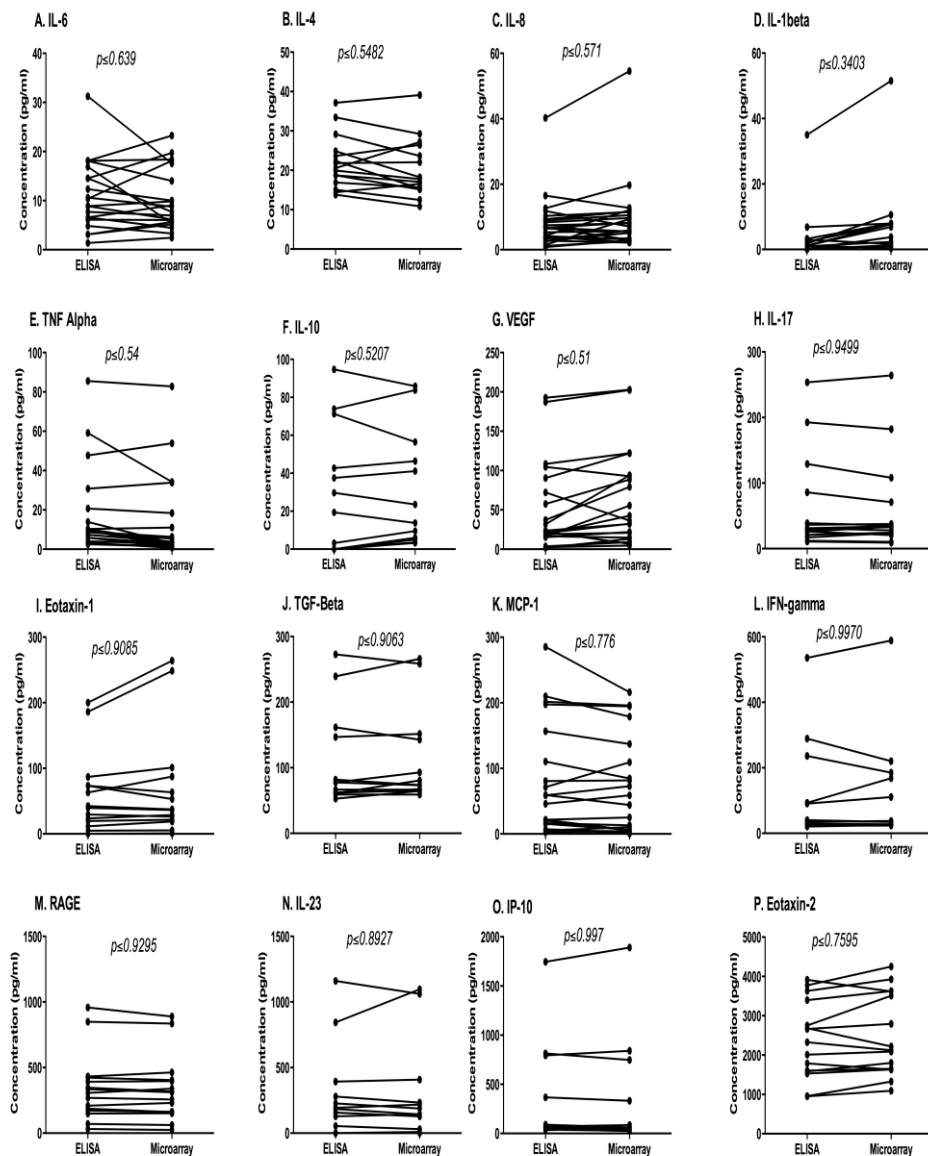


Figure 59: Correlation between microarray and ELISA techniques.

Thirty sera were quantified by ELISA and microarray assay for 16 cytokines to see how well both techniques correlate to one another. The microarray technology was compared to traditional ELISA. Sera were obtained from 30 healthy individuals and quantified for all 16 cytokines using both microarray and ELISA. Across the 16 biomarkers tested, there were no significant differences between techniques ($0.3404 \leq P \leq 0.997$)

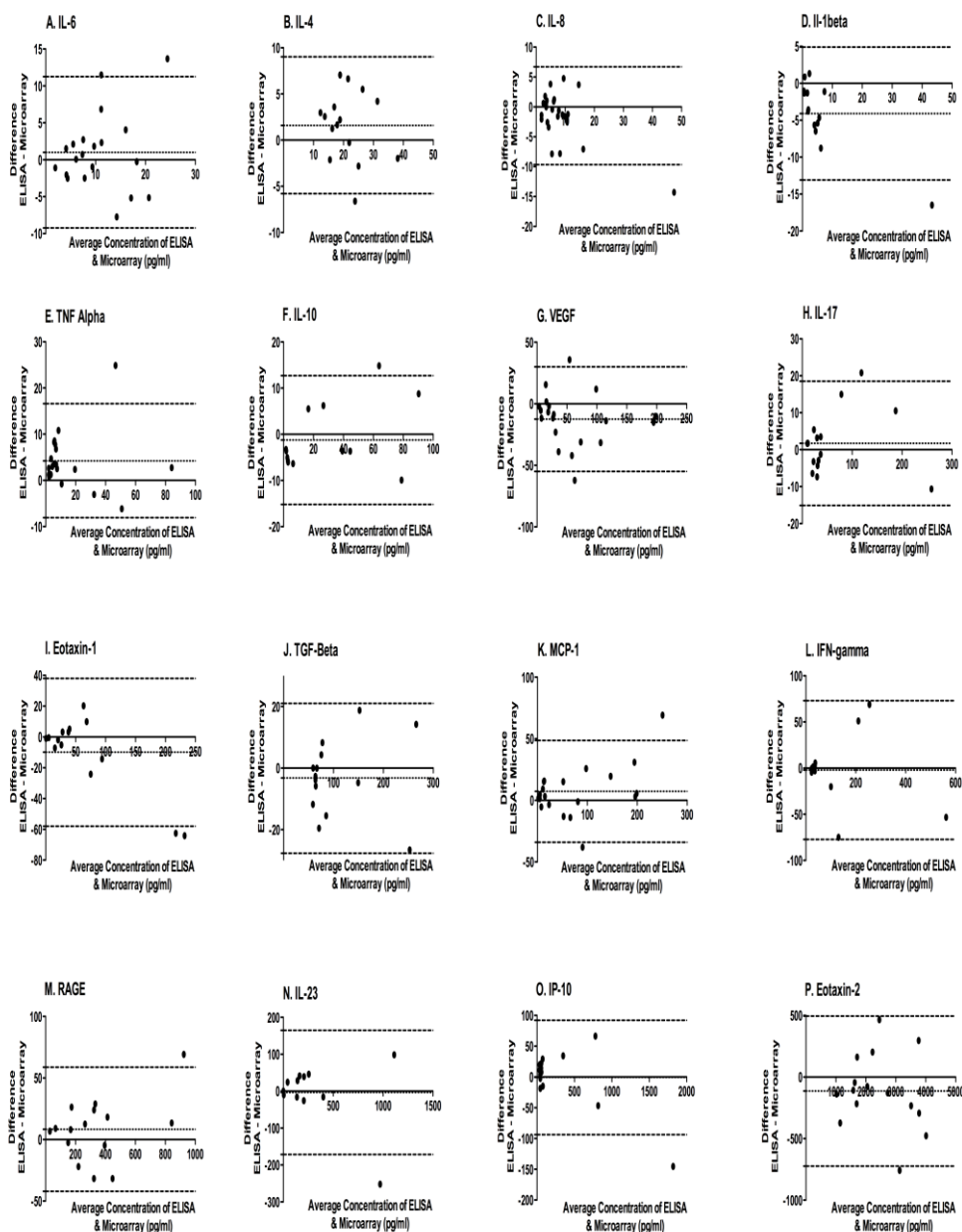


Figure 60: Bland Altman graphs to show difference between two ELISAs and Microarrays.

Bland Altman plots were drawn to see if there was an agreement between both ELISAs and microarrays. Bland Altman plots further highlight the agreement between these techniques since, for most cytokines, the bias in favour of one or other technique was negligible. However it was noticed that, for lower abundance cytokines such as IL-1 β (D), the microarray platform is slightly more sensitive than the ELISA.

Table 13 shows a summary of the values gathered from the variety of validity experiments undertaken. In the vast majority of cytokines, the values fall well within the levels of accuracy and precision outlined by the FDA guidelines for bioanalytical method validation. The majority of exceptions arise often in the low abundant cytokines where at the lowest level there is variation when samples are repeated multiple times; ie intra and inter assays. This can now be compensated through the calculation of both the lower and upper limits of quantification. This allows users to decide whether those falling outside these limits are to be included when performing a large population study comparing multiple groups.

Table 13: Summary of the data from all the validity tests.

Tests:	Intra Assay (CV%)	Inter assay (CV%)	LOD (pg/ml)	LLOQ (pg/ml)	PBS Spike Accuracy (%)	PBS Spike CV%	Serum Spike Accuracy (%)	Serum Spike Precision (%)
IL-1 β	5.002	19.92	0.404	2.9	113.34	3.794	99.856	3.74
IL-17	12.96	20.71	0.445	5.9	111.55	6.015	103.48	6.09
IL-4	10.99	28.98	0.600	2.9	97.047	6.337	95.81	6.33
IL-10	17.74	*49.07	0.503	2.9	107.49	11.56	101.56	11.5
IL-8	22.95	17.91	0.535	1.5	100.04	9.838	89.88	8.32
TNF- α	23.11	30.89	1.126	1.5	97.485	9.225	93.12	12
IL-6	22.72	25.08	0.683	1.5	98.85	14.38	110.95	10.64
IFN- γ	20.39	16.84	0.108	2.9	95.8	4.197	96.425	6.31
Eot-1	7.39	10.06	1.863	2.9	97.71	9.411	89.973	9.42
IL-23	13.89	14.44	0.612	5.9	79.5	5.864	88.356	5.84
RAGE	16.66	13.95	0.968	5.9	93.03	8.037	97.128	8.05
TGF- β	12.71	16.82	0.398	2.9	104.37	2.915	100.49	2.95
MCP-1	13.76	17.61	0.284	5.9	105.69	10.61	90.072	6.13
Eot-2	11.76	14.04	0.739	5.9	99.1	1.984	101.86	16.3
VEGF	15.08	7.4	0.744	1.5	97.5	6.754	88.957	7.27
IP-10	11.45	18.4	0.458	5.9	94	5.983	107.57	16.8

* Samples below detection limits

This includes –intra, inter-assays, the limits of detection and quantification as well as the spiked experiments. Most of the values fall within the FDA derived guidelines for bioanalytical validation. Those that fall below the expected guidelines are discussed below.

4.4 Discussion

At present there are no comprehensive guidelines for the validation of microarray protein biomarker studies. It is thus highly desirable that such criteria are established to ensure work can be standardized across research institutions [304] [305]. Consequently, for this study, the optimisation and validation of the microarray protocol was based upon the FDA guidelines for pharmacokinetic immunoassays.

The limits of quantification are defined as the lowest and highest points in an assay that can be detected and quantified to an acceptable level of accuracy and precision. Both the LLoQ and ULoQ like the LOD are expressed as a concentration limit on the microarray platform. Therefore in association with the LoD/LLoQ established for all 16 biomarkers, the microarray has the advantage of being able to detect the lowest concentrations. Whilst the LOD shown here is very low, often it is not chosen as the limit to measure proteins in biological samples, as at this concentration there is a higher degree of variability between samples and thus the LLoQ is chosen when using microarray technology as it is the lowest analyte concentration that can be quantified to an acceptable level with both accuracy and precision.

A spike recovery test was conducted across 3 days to investigate the accuracy and precision of the methodology across both control samples (PBS) and biological samples (serum) for 16 biomarkers of interest. We show that, in the majority of biomarkers (14 out of 16), the accuracy is between 80-120% and the precision $\leq 20\%$ CV, which is in accordance with data published in recent literature [126] [306] [307] [308]. Additionally inter- and intra-assays were both reproducible and precise with 11 of the 16 cytokines falling within the aforementioned criteria. However it was noted that in low abundance cytokines, such as IL-8 and IL-10, the accuracy and precision were lower than is considered acceptable. This is due to greater calculated percentage

differences and as such should be reflected under different guidelines. Nevertheless, the biological and clinical relevance of very low serum levels of cytokines/chemokines has yet to be determined.

Having shown that the majority of biomarker measurements fall within the FDA guidelines for pharmacokinetic immunoassays we then wanted to show that the assays were as reproducible and sensitive as the ELISA, the “gold standard” of immunoassay quantification [309] [310]. We show that when both ELISA and microarray were used to quantify a biomarker in serum there was no significant difference in the cytokine concentrations calculated. However, for some low abundance biomarkers, such as IL-1beta and IL-6, there is less agreement between techniques and this may be due to the lower sensitivity of the ELISA compared to the microarray, as in microarrays the standard curves were plotted 2 dilution points lower than in the ELISA.

One caveat to the comparison between ELISA and microarray is that the microarray platform is measured by fluorescence intensity compared to that of the optical density used in an ELISA. Using fluorescence for detection gives the microarray a scale that is measurable over many 10,000s AU compared to the discrete 0-3 OD scale used in an ELISA. This clearly offers greater scope for the detection of biomarkers using microarrays.

Currently there are many commercially available protein microarray platforms, however, the high cost of purchasing these kits makes it unattainable for most [299] [311]. The microarray protocol established here shows the stages required for optimisation that enables detection of multiple biomarkers at a lower running cost. This detection is not limited to the 16 biomarkers that are shown here but indeed can be expanded as required.

The in-house sandwich microarray workflow developed here demonstrates that multiple biomarkers can be quantified with relative ease, using reduced quantity of sample volume than required for ELISAs of equal biomarker number.

Chapter 5: Application of an Antibody Microarray as a Diagnostic Platform for COPD

5.1 Introduction

COPD is defined as “a preventable and treatable disease state that is characterised by airflow limitation that is not fully irreversible. The airflow limitation is progressive over time and is associated by an abnormal inflammatory response to noxious gaseous particles, in particular those from cigarette fumes” [1, 312].

The detection of early COPD in patients with respiratory disease is highly desirable. However, diagnosing COPD is difficult as there is no single “GOLD standard” procedure available. Physical characteristics such as wheezing, chronic cough, breathlessness and sputum production have been implicated in the diagnosis of COPD. Additionally, other physical attributes such as use of accessory muscles, increased paradoxical abdominal movement and monitoring weight are used as predictors of disease outcome [313-316].

Currently, the common measurements of physical symptoms of the disease include spirometric airflow tests, which measures FEV₁ and FVC. FEV₁ is defined as the volume of air a patient can expire in one second following a full intake of breath, whilst FVC can be defined as the total maximum volume of air that a patient can exhale following full inspiration [1, 317, 318]. If the ratio of FEV₁/FVC falls below 0.7, allied with a FEV₁ <80%, the individual is defined as having COPD [319, 320]. However, spirometry alone may not suggest an individual may have COPD. Chest radiography may also aid in the differential diagnosis of COPD. Also pulse oximetry can be undertaken to calculate the saturation of oxygen that is present in an individual

at rest and at sleep to determine if he/she may have hypoxia, which is a common characteristic in COPD [321-325]. Finally, a test can be performed for α 1-antitrypsin deficiency, which is a hereditary genetic disorder caused by an abnormality in chromosome 14. A lack of α 1-antitrypsin production by the liver leads to a lack of control of neutrophil elastases in the lungs; leads to symptoms associated with emphysema.

Hence, a system that would allow physicians to detect the different stages of the disease is highly desirable, but is presently unavailable [326-328]. It is vital to have a diagnostic platform, or combination of platforms, that would aid the diagnosis of sufferers more effectively, and help them improve their treatment according to the type of disease they have.

The previous two chapters have shown the development/optimisation (Chapter 3), and the validation (Chapter 4), of a microarray platform. This section focuses on applying this microarray platform to screen a selection of individuals that have COPD compared to non-smoking controls and smokers without symptoms of COPD.

The microarray has been developed to measure up to 16 biomarkers simultaneously; all of these were measured to see if there are distinguishable patterns which could lead to improved understanding of the disease. An ultimate goal would be to be able to use these biomarkers in the early diagnosis of COPD development in 'healthy' smokers.

5.2 Materials and Methods

Briefly, antibody duoset kits were purchased (R&D Systems, MN, USA) and printed on poly-L-lysine slides. Slides were processed immediately or after one week. Slides on the day of processing were taken from the vacuum and blocked for an hour with either I-Block or 3% BSA block buffer. Standards were made for all 16 cytokines (IL-8, IL-6, IL-1 β , TNF- α , Exotaxin-1, Eotaxin-2, IFN- γ , RAGE, IL-10, IL-4, IL-17, IL-23, MCP-1, VEGF and IP-10) according to manufacturer's instructions and diluted 2 fold across 7 dilutions and added at 50 μ l per well in 10 replicates for 45 mins. Additionally healthy human sera and COPD human sera were added to the corresponding well on the slides. The slide was washed three times and 50 μ l of appropriately diluted biotinylated detection antibody was added to each block for 45 mins. Slides were subjected to tyramide amplification. Briefly, this was performed after the detection stage of the microarray process described above with the additional of 50 μ l of 1:1000 diluted streptavidin-HRP (Bio-Rad, USA) in the dark. The slide was washed and 50 μ l of Bio-Rad Amplification Reagent was added for 10 mins in the dark. The slides were washed three times with 20% DMSO-PBST and subsequently washed thrice with wash buffer. After washing, 50 μ l of 1:1000 diluted streptavidin-conjugated cy5 (E-Biosciences, UK) was added and incubated at room temperature for 15 mins in the dark. The slide was washed three times and rinsed in ultra-pure water and centrifuged dry and scanned with the 4200 AL microarray scanner at 635nm (Axon GenePix®). Fluorescence was quantified using the GenePix Pro Software (Axon GenePix®). The experiment was repeated three times. The median fluorescence of each spot was measured (minus background) and the corrected fluorescence was used to calculate the average fluorescence signal across the standard detectable ranges.

5.3: Results

5.3.1: The effect of COPD on cytokine levels in Non Smoking Controls, Smoking Controls and COPD individuals

Sera from non-smoking controls, healthy smoking controls and COPD individuals were analysed on the microarray platform. As shown in Figures 61 and 62, there are no significant differences between groups for serum concentrations of most cytokines, except for eotaxin-2 and MCP-1, where there are significant differences between all three groups ($p \leq 0.0326$; Figure 63 and $p \leq 0.0167$; Figure 64, respectively). However for other remaining cytokines (IL-8, IL-1 β , TNF- α , IL-6, IFN- γ , IP-10, IL-4, IL-10, IL-23, IL-17, RAGE, eotaxin-1 TGF- β , and VEGF, there were no significant differences between all three groups.

A line was drawn on all graphs at the 95 percentile of the healthy control group. Interestingly certain cytokines such as VEGF, MCP-1 and IL-23 showed values in both the healthy smoker group and COPD group to be well above the 95th percentile.

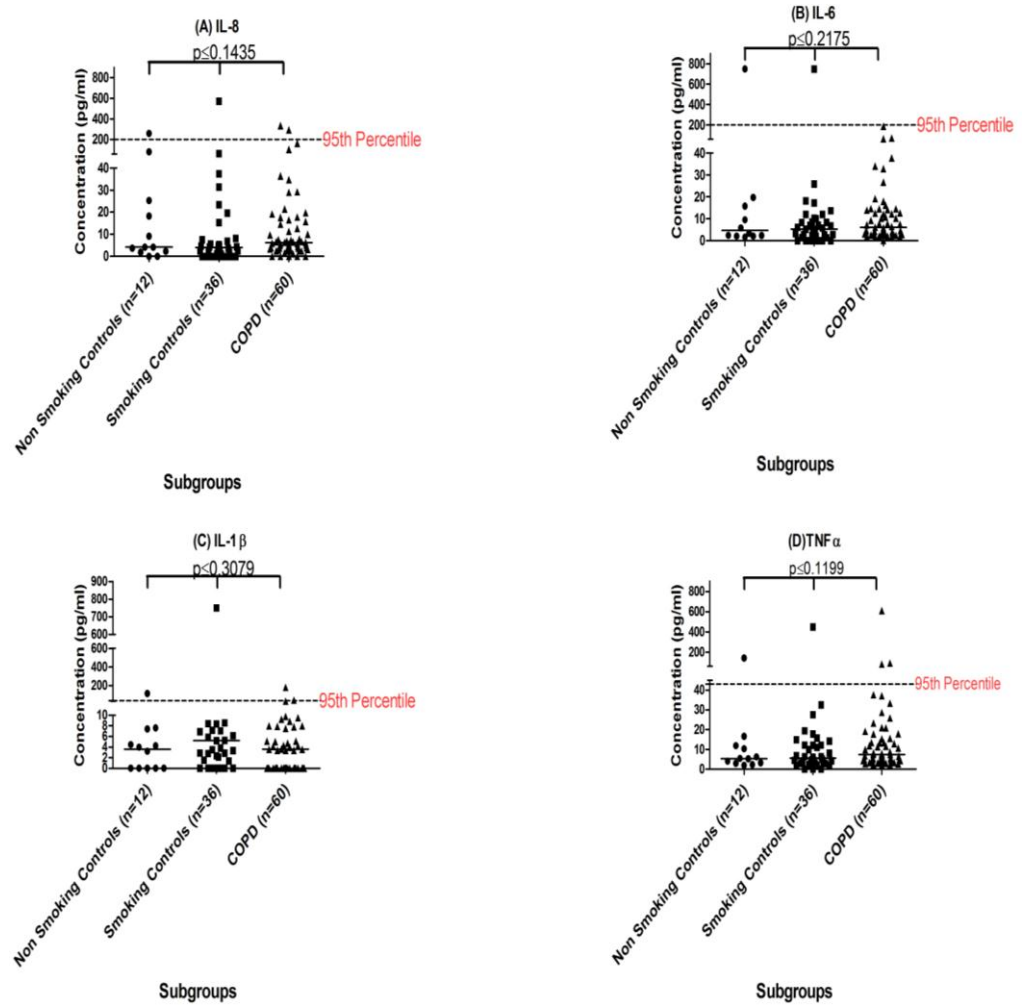


Figure 61: Differences in cytokine expressions in subjects with COPD, healthy smoking controls and non-smoking controls: IL-8, IL-6, IL- β and TNF- α (A-D, respectively).

The difference in cytokine expression was investigated for the in those with COPD, healthy smoking controls and non-smoking controls in IL-8 (A), IL-6 (B), IL-1 β (C) and TNF- α (D) respectively. Kruskal-Wallis tests were performed to compare all three patient cohorts, and subsequently Dunn's post multiple comparisons tests between each subgroup which showed no significant differences between all three groups for each of the 4 cytokines. However in general the results were negative with no differences in groups seen.

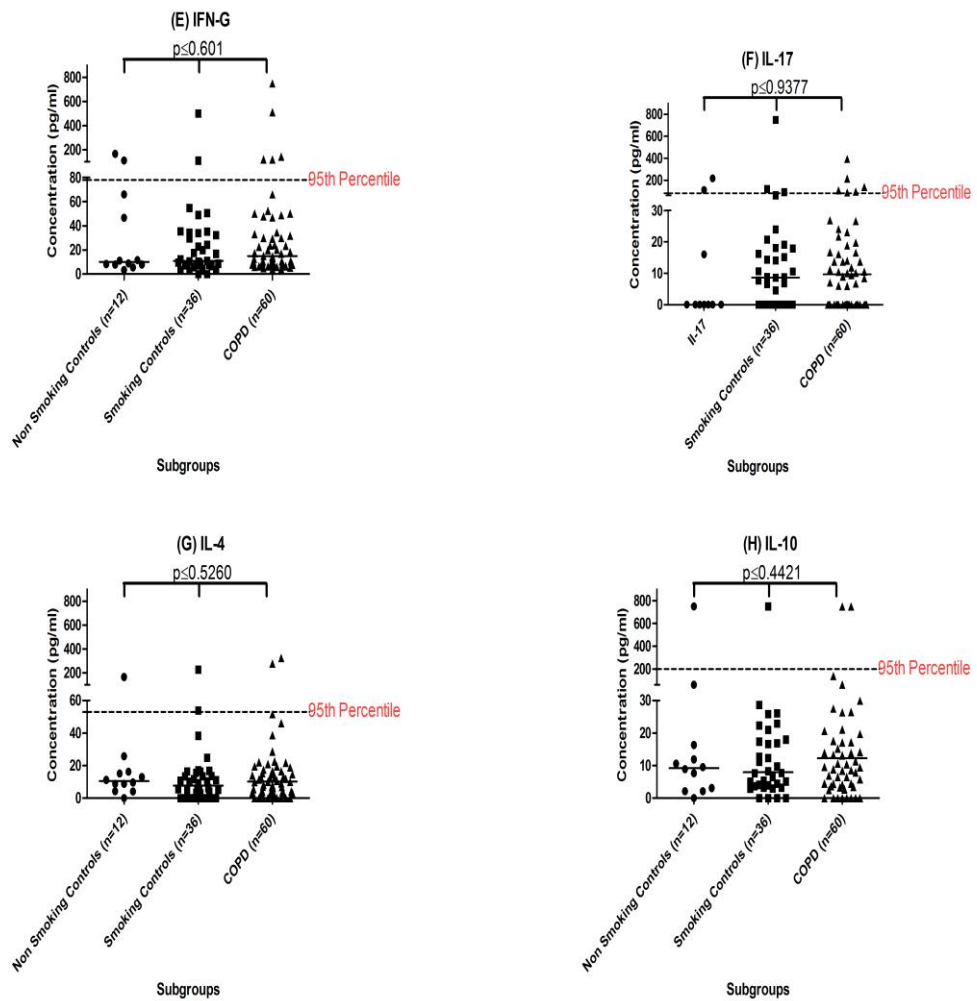


Figure 62: Differences in cytokine expressions in subjects with COPD, healthy smoking controls and non-smoking controls: IFN- γ , IL-17, IL-4 and IL-10 (E-H, respectively).

The difference in cytokine expression was investigated for the in those with COPD, healthy smoking controls and non-smoking controls in IFN- γ (E), IL-17 (F), IL-4 (G) and IL-10 (H) respectively. Kruskal-Wallis tests were performed to compare all three patient cohorts and subsequently Dunn's post multiple comparisons tests between each subgroup which showed no significant differences between all three groups for each of the 4 cytokines. However in general the results were negative with no differences in groups seen.

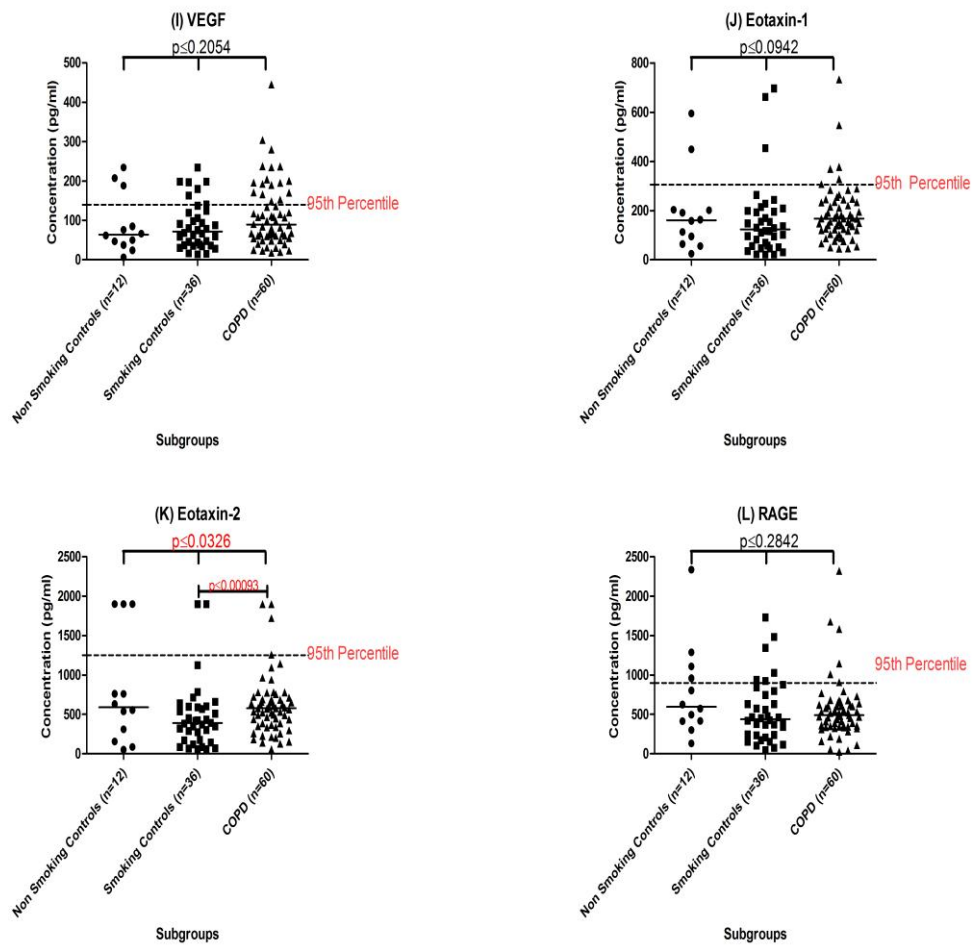


Figure 63: Differences in cytokine expressions in subjects with COPD, healthy smoking controls and non-smoking controls: VEGF, Eotaxin-1, Eotaxin-2 and RAGE (I-L, respectively).

The difference in cytokine expression was investigated for the in those with COPD, healthy smoking controls and non-smoking controls in VEGF (I), eotaxin-1 (J), eotaxin-2 (K) and RAGE (L) respectively. Kruskal-Wallis tests were performed to compare all three patient cohorts and subsequently Dunn's post multiple comparisons tests between each subgroup which showed no significant differences between all three groups for VEGF (I), eotaxin-1 (J) and RAGE (L). However, in the case of eotaxin-2 (K), there is a significant difference between all three groups ($p \leq 0.0326$), in particular between the smoker control and COPD group when Mann Whitney tests were performed ($p \leq 0.00093$) shows an increase in eotaxin-2 expression in the COPD group compared to the smoking controls.

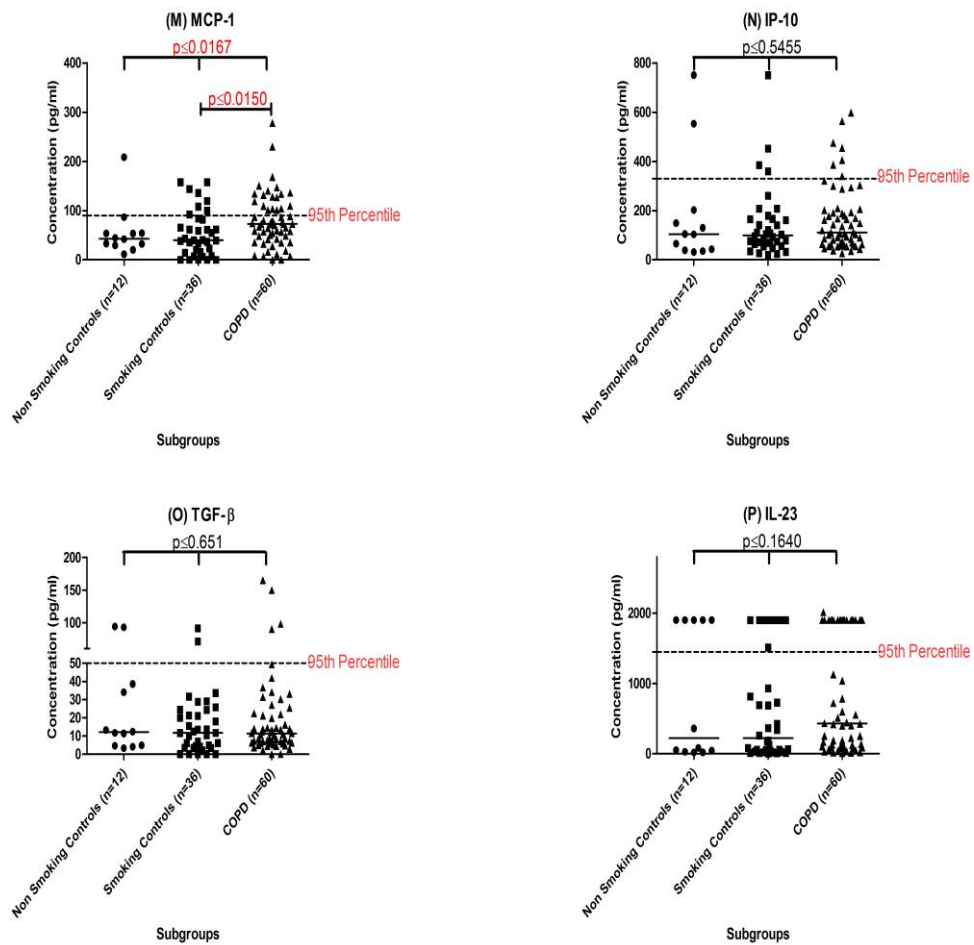


Figure 64: Differences in cytokine expressions in subjects with COPD, healthy smoking controls and non-smoking controls: MCP-1, IP-10, TGF- β and IL-23 (M-P, respectively).

The difference in cytokine expression was investigated for the in those with COPD, healthy smoking controls and non-smoking controls in MCP (M), IP-10 (N), TGF- β (O) and IL-23 (P) respectively. Kruskal-Wallis tests were performed to compare all three patient cohorts and subsequently Dunn's post multiple comparisons tests between each subgroup which showed no significant differences between all three groups for IP-10, TGF-beta and IL-23. In the case of MCP-1 (M) there is a significant difference between all three groups, in particular between the non-smoking control and COPD group when Mann Whitney tests were performed ($p \leq 0.0144$) shows an increase in MCP-1 expression in COPD compared to the non-smoking controls.

5.3.2: The effect of smoking status on the likelihood of developing COPD

The healthy smokers and COPD patients could be further subdivided into current smoking and ex-smoking groups to see whether the effect of smoking could possibly indicate a pattern of how COPD may arise from those who are healthy smokers. As seen in Table 13, there were no significant differences between all 5 groups except in the case of MCP-1, Kruskal-Wallis tests were performed to compare all five patient cohorts and subsequently Dunn's post multiple comparisons tests between each subgroup, which showed there is a trend towards a progressive increase in this cytokine across all five groups from never-smokers to COPD current smokers. Mann Whitney tests performed showed a significant increase in MCP-1 between the healthy ex-smoking group and the COPD ex-smoking group ($p \leq 0.0021$).

Table 14 Investigates the effect of smoking status of developing COPD in healthy non-smoking individuals, ex healthy smokers, current healthy smokers, COPD ex-smokers and COPD current smokers

Cytokine	Kruskal-Wallis P Value
IL-8	0.1460
IL-6	0.5183
IL-1 β	0.7472
TNF- α	0.2854
VGEF	0.5247
Eotaxin-1	0.0997
IFN- γ	0.8544
IL-17	0.9938
Eotaxin-2	0.0854
IP-10	0.04698
RAGE	0.6311
MCP-1	0.0120
IL-4	0.6984
IL-10	0.5870
TGF- β	0.5106
IL-23	0.4545

Table 14 aims to show if there is a significant difference between the effects of smoking and the cessation of smoking in those who are healthy smokers and COPD patients. Kruskal-Wallis tests were performed to compare all five patient cohorts (in healthy individuals and subsequently Dunn's post multiple comparisons tests between each subgroup; ex healthy smokers, current healthy smokers, COPD ex-smokers and COPD current smokers) which showed no significant differences between all five groups in each of the 16 cytokines except for MCP-1 where there was a significant difference between all groups ($p \leq 0.0120$). With MCP-1 there was trend towards a progressive increase in MCP-1 across all five groups from non-smoking individuals to COPD current smokers (data not shown).

5.3.3: The correlation between cytokine expression and FEV% in those with COPD

The FEV% predicted was initially evaluated to see if there was a relationship between this variable and the expression of cytokines. As can be seen in figures 65-69, the correlation between these two variables were analysed by Spearman's Rank correlation, which showed no significant correlations for any of the 16 cytokines. Overall all 16 cytokines displayed negative results when FEV% correlation was investigated.

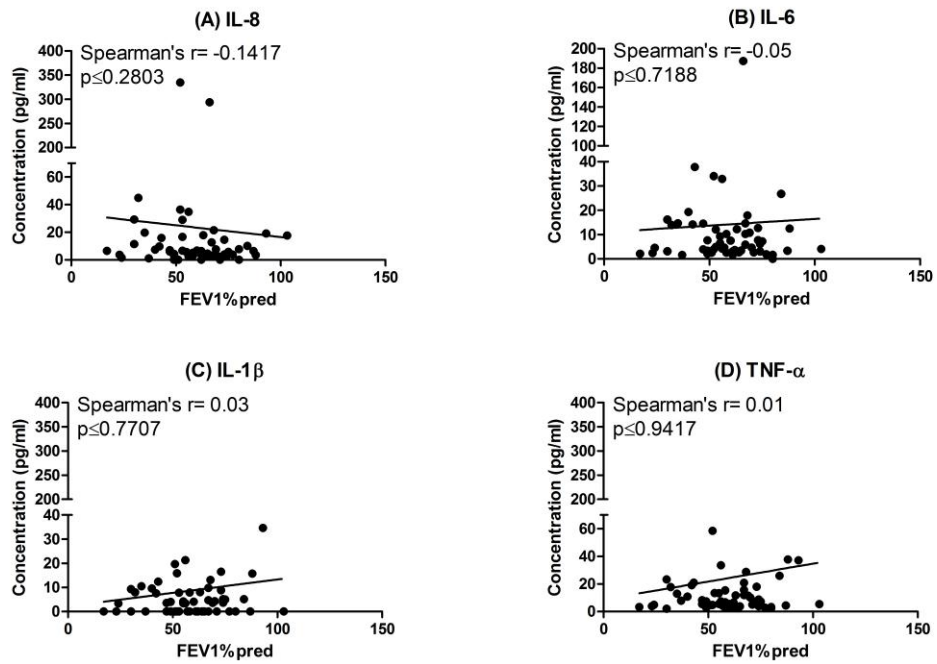


Figure 65: Correlation between FEV-1 predicted and cytokine concentration: IL-8, IL-6, IL-1 β and TNF- α (A-D, respectively).

Spearman's Rank correlation tests were performed to compare the relationship between the FEV-1% predicted against the concentration of the respective cytokines IL-8 (A), IL-6 (B), IL-1 β (C) and TNF- α (D), in patients with COPD which showed no significant correlations. In general all four cytokines showed negative results in correlation to FEV-1% pred.

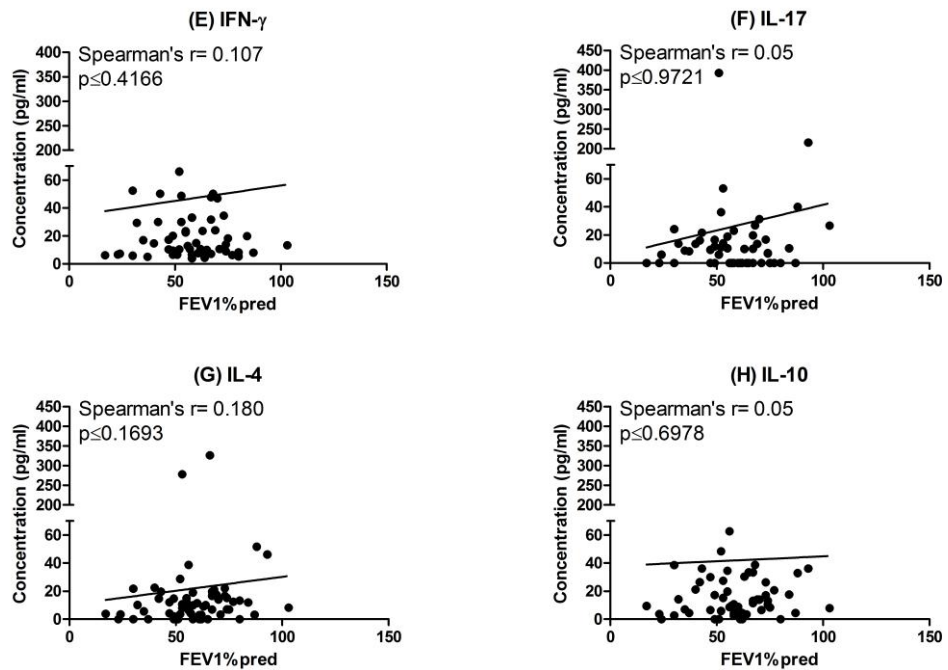


Figure 66: Correlation between FEV-1 predicted and cytokine concentration: IFN- γ , IL-17, IL-4, IL-10 (E-H, respectively).

Spearman's Rank correlation tests were performed to compare the relationship between the FEV-1% predicted against the concentration of the respective cytokines, IFN- γ (E), IL-17 (F), IL-4 (G), and IL-10 (H) in patients with COPD, which showed no significant correlations. In general all four cytokines showed negative results in correlation to FEV-1% pred.

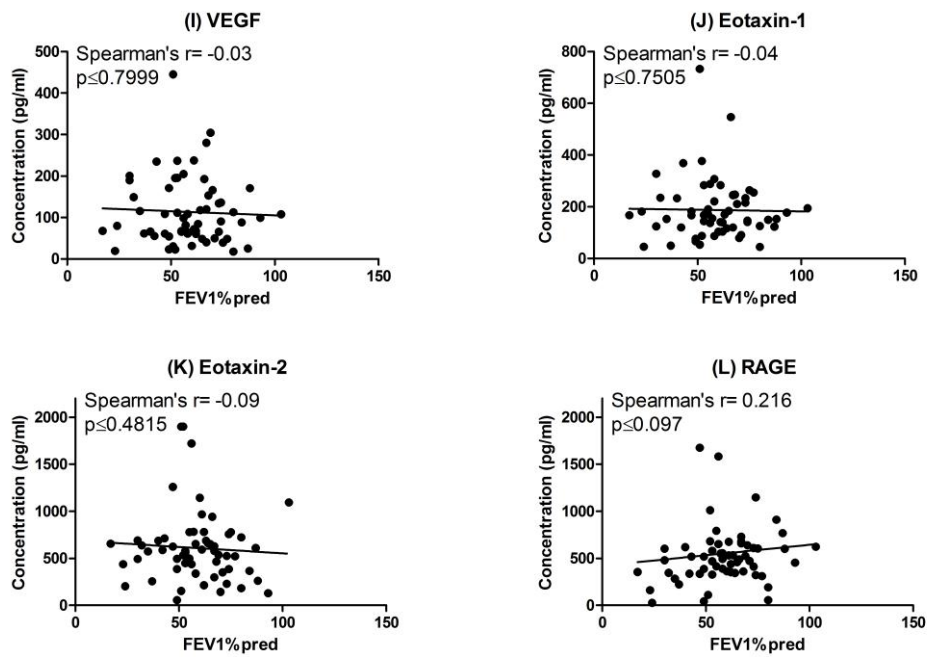


Figure 67: Correlation between FEV-1 predicted and cytokine concentration: VEGF, Eotaxin-1, Eotaxin-2 and RAGE (I-L, respectively).

Spearman's Rank correlation tests were performed to compare the relationship between the FEV-1% predicted against the concentration of the respective cytokines, VEGF (I), Eotaxin-1 (J), Eotaxin-2 (K) and RAGE (L) in patients with COPD which showed no significant correlation for all four cytokines. In general all four cytokines showed negative results in correlation to FEV-1% pred.

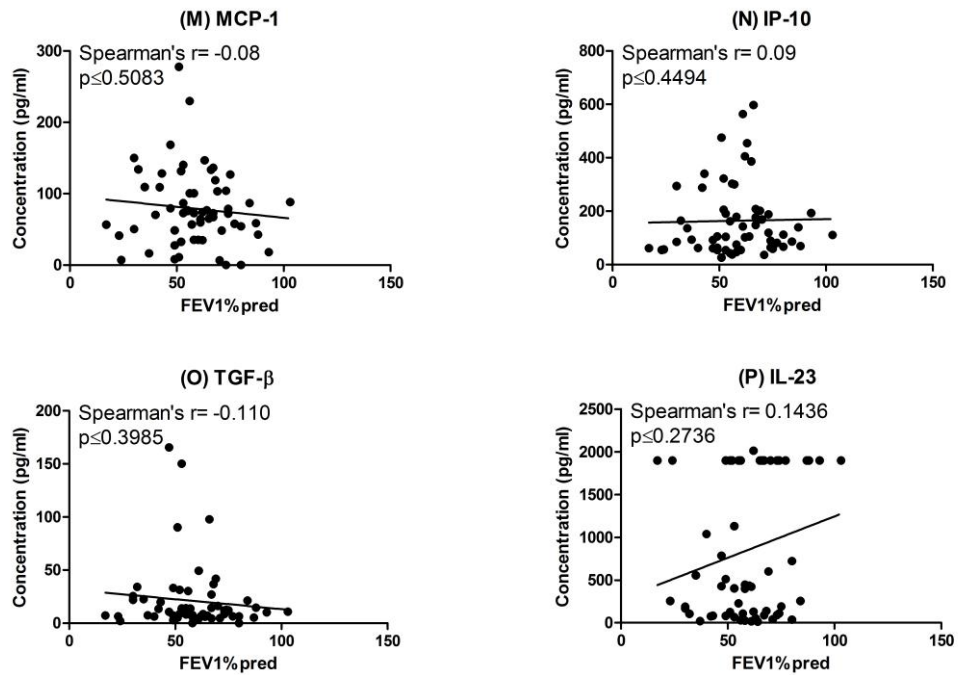


Figure 68: Correlation between FEV-1 predicted and cytokine concentration: MCP-1, IP-10, TGF-Beta and IL-23 (M-P, respectively).

Spearman's Rank correlation tests were performed to compare the relationship between the FEV-1% predicted against the concentration of the respective cytokines, MCP-1 (M), IP-10 (N), TGF- β (O) and IL-23 (P) in patients with COPD which showed no significant correlation in all 4 cytokines. In general all four cytokines showed negative results in correlation to FEV-1%pred.

5.3.4: The effect of gender on the cytokine expression in those with COPD

The difference in gender were investigated between the 3 cohorts (healthy controls, smoking controls and COPD subjects) to see if there were significant differences between males and females amongst those who smoked and had COPD and those that smoked and did not have COPD. Kruskal-Wallis tests were performed and subsequently Dunn's post multiple comparisons tests between each subgroup;

- i) Male Healthy Non-Smokers,
- ii) Female Healthy Non-Smokers,
- iii) Male Healthy Smokers,
- iv) Female Healthy Smokers,
- v) Male COPD Subjects,
- vi) Female COPD Subjects

However the results for all 16 cytokines (IL-8, IL-6, IL-1 β , TNF- α , VEGF, Eotaxin-1, Eotaxin-2, RAGE, MCP-1, IL-4, IL-10, TGF- β , IP-10, IFN- γ , IL-17 and IL-23) were all negative indicating in this study there is no difference between gender in this study (data not shown)

5.3.5: The GOLD stages of COPD

COPD severity is divided into four categories according to international guidelines outlined by the Global Initiative for Chronic Obstructive Lung Disease (GOLD). This is often known as stage 1 (mild), stage 2 (moderate), stage 3 (severe) and stage 4 (very severe). This is based on the forced expiratory volume per second (FEV-1%) outlined in Table 1 (chapter 1). Hence graphs were plotted to show the mean concentration and standard deviation against the four stages of GOLD. As one might expect, there were variations between all samples in all groups. Additionally as the severity of COPD increases, inflammatory markers and growth factors also increase in expression. However in the graphs plotted (Figure 69-72) due to the unequal distribution of numbers in each group a general trend in all 16 biomarkers were not established. Additionally a “REF” group was added to the each graph. This were the normal healthy controls, which served as a reference point to which the split COPD cohorts were compared.

Finally the means of all the 16 cytokines for each GOLD stage was grouped to see whether there was a cumulative difference between groups. In Figure 73 it could be seen that the expression of cytokines was the lowest in stage 4 and highest in stages 2/3. This may indicate that at GOLD stage 4 the immune response was suppressed as shown by the lowest expression of nearly all 16 cytokines. Interestingly only the expression of IL-23 increased in GOLD stage 4. However one has to be cautious when making definitive assumptions from this data not knowing the medication those in the most severe group (stage 4) are undertaking.

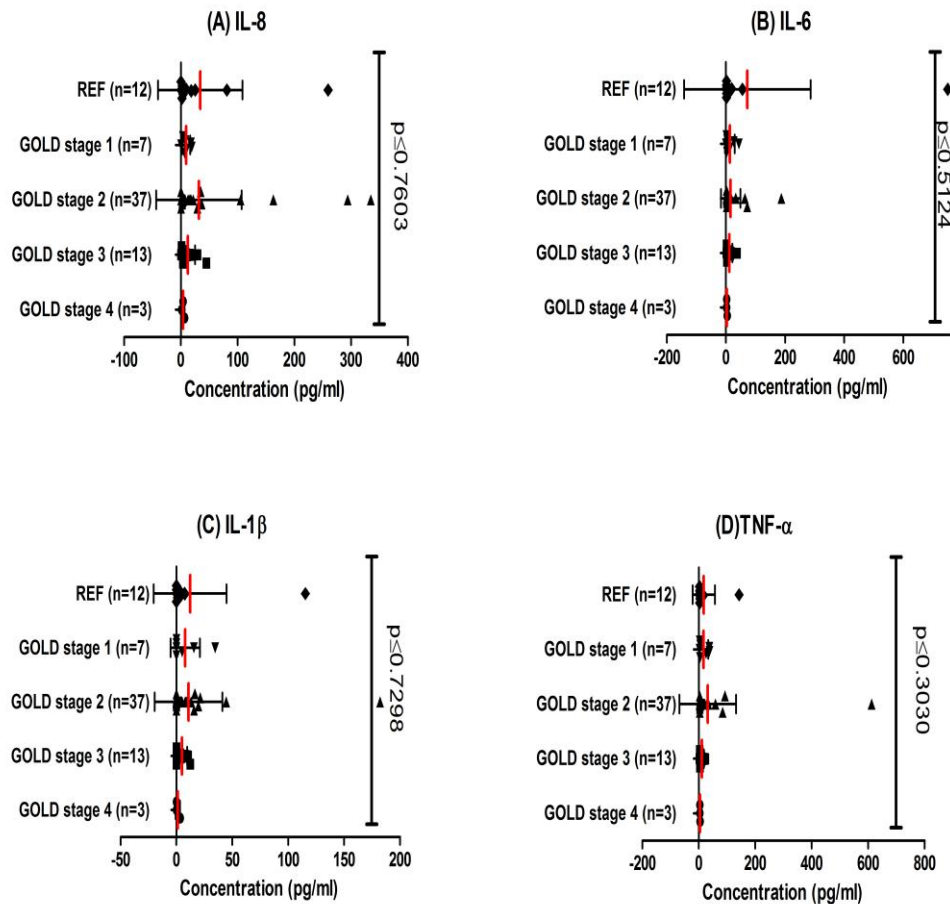


Figure 69: Graph to show how the concentration of cytokine varies with the Global Initiative for Chronic Obstructive Lung Disease (GOLD) stage for IL-8, IL-6, IL-1 β and TNF- α respectively (A-D).

All cytokines are expressed as mean concentration (pg/ml). Kruskal-Wallis test were performed and subsequently Dunn's post multiple comparisons tests between each subgroup to compare all 5 groups across all 4 cytokines that showed no significant differences. A general trend seemed to show the level of cytokine concentration increasing as the severity rating of GOLD increases. A "REF" group are healthy non-smoking control used as a comparison. Note at GOLD stage 4, the immune system could potentially be suppressed as indicated by low expressions of all 4 cytokines.

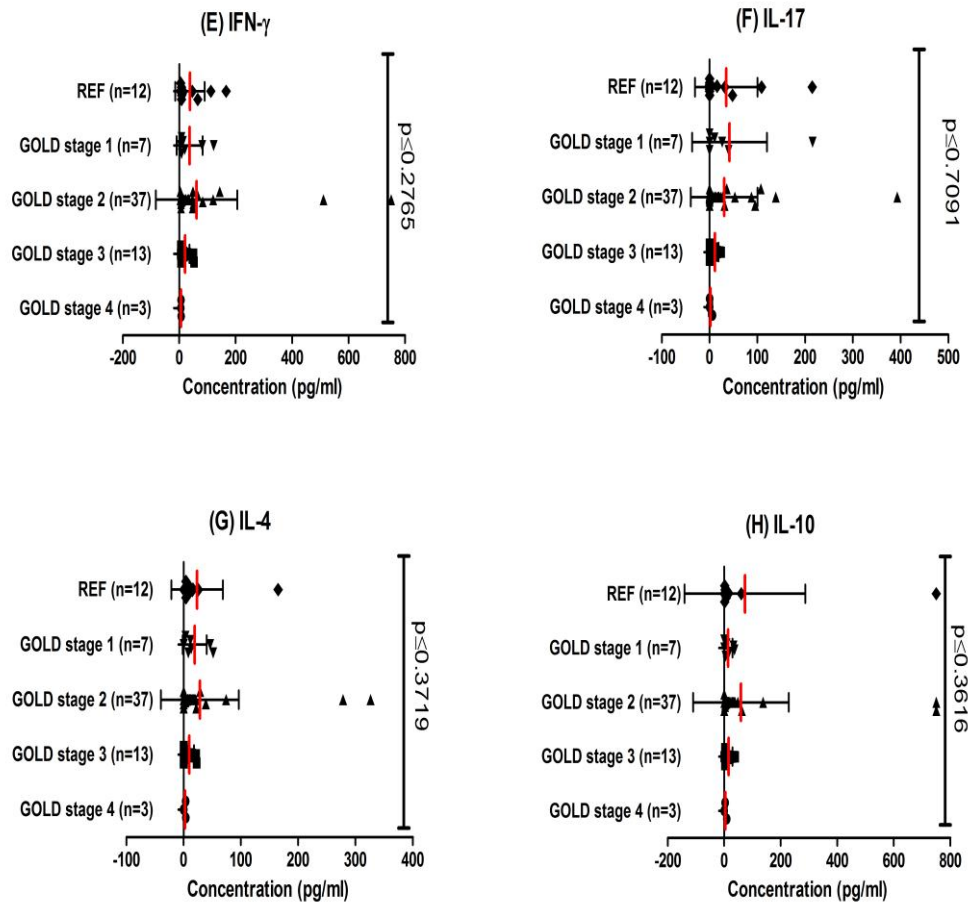


Figure 70: Graph to show how the concentration of cytokine varies with the Global Initiative for Chronic Obstructive Lung Disease (GOLD) stage for IFN- γ , IL-17, IL-4 and IL-10 respectively (E-H).

All cytokines are expressed as mean concentration (pg/ml). Kruskal-Wallis test were performed and subsequently Dunn's post multiple comparisons tests between each subgroup to compare all 5 groups across all 4 cytokines that showed no significant differences. A general trend seemed to show the level of cytokine concentration increasing as the severity rating of GOLD increases. A "REF" group are healthy non-smoking control used as a comparison. Note at GOLD stage 4, the immune system could potentially be suppressed as indicated by low expressions of all 4 cytokines. However it has to be acknowledged that there are 3 subjects in GOLD stage 4 and the medication they are on is unknown which could influence the data.

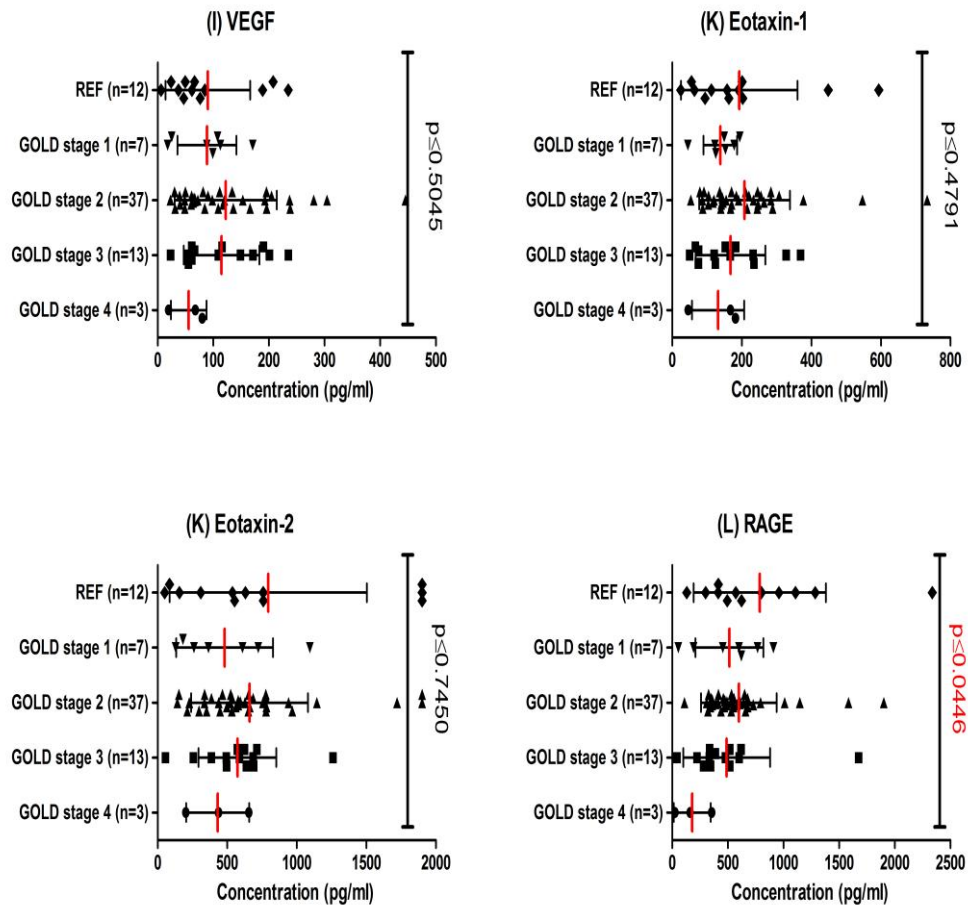


Figure 71: Graph to show how the concentration of cytokine varies with the Global Initiative for Chronic Obstructive Lung Disease (GOLD) stage for VEGF, Eotaxin-1, Eotaxin-2 and RAGE respectively (I-L).

All cytokines are expressed as mean concentration (pg/ml). Kruskal-Wallis test were performed and subsequently Dunn's post multiple comparisons tests between each subgroup to compare all 5 groups across all 4 cytokines showed significant differences across all groups in RAGE ($p \leq 0.0446$) only. The immune system appears to be most active at stage 3 in the above cytokines, whilst at GOLD stage 4 the immune system seems suppressed as indicated by low expressions of all 4 cytokines. However it has to be acknowledged that there are 3 subjects in GOLD stage 4 and the medication they are on is unknown which could influence the data.

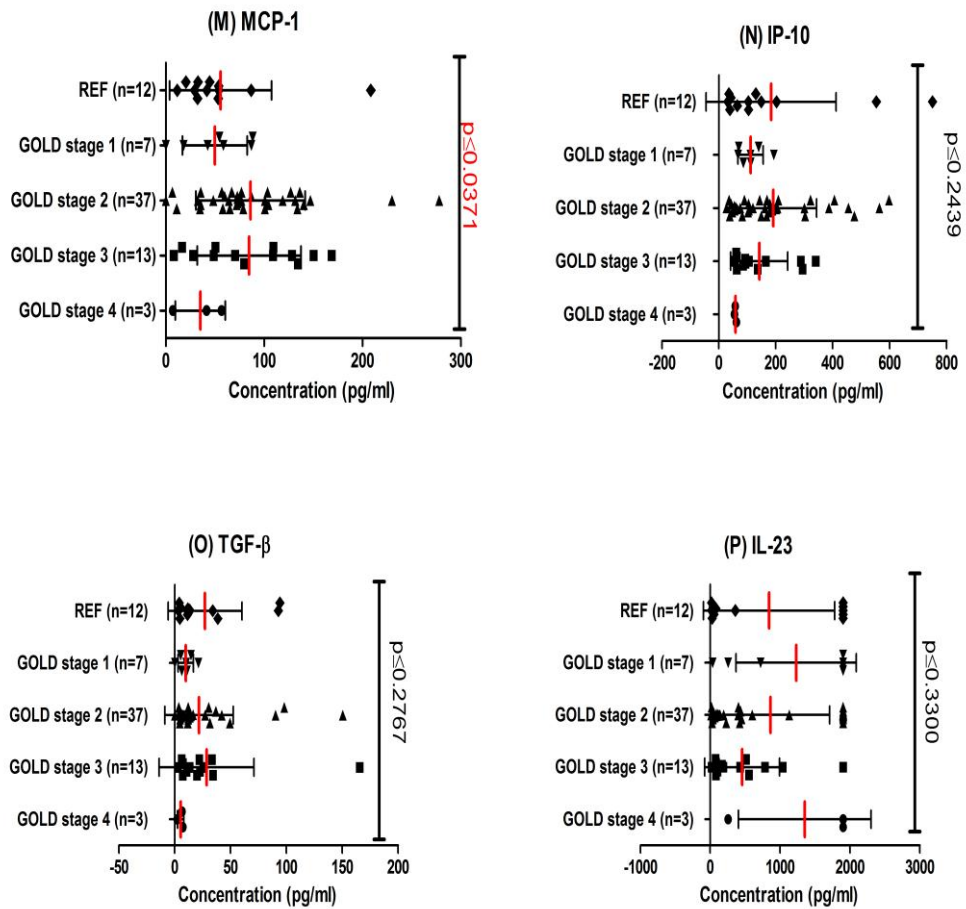


Figure 72: Graph to show how the concentration of cytokine varies with the Global Initiative for Chronic Obstructive Lung Disease (GOLD) stage for MCP-1, IP-10, TGF-beta and IL-23 respectively (M-P).

All cytokines are expressed as mean concentration (pg/ml). Kruskal-Wallis test were performed and subsequently Dunn's post multiple comparisons tests between each subgroup to compare all 5 groups across all 4 cytokines that showed significant differences all groups in MCP-1 ($p \leq 0.0371$) only. The lowest expression of cytokines was observed at GOLD stage 4 as in line with the other 12 cytokines above except for IL-23 which is increased (P). However it has to be acknowledged that there are 3 subjects in GOLD stage 4 and the medication they are on is unknown which could influence the data.

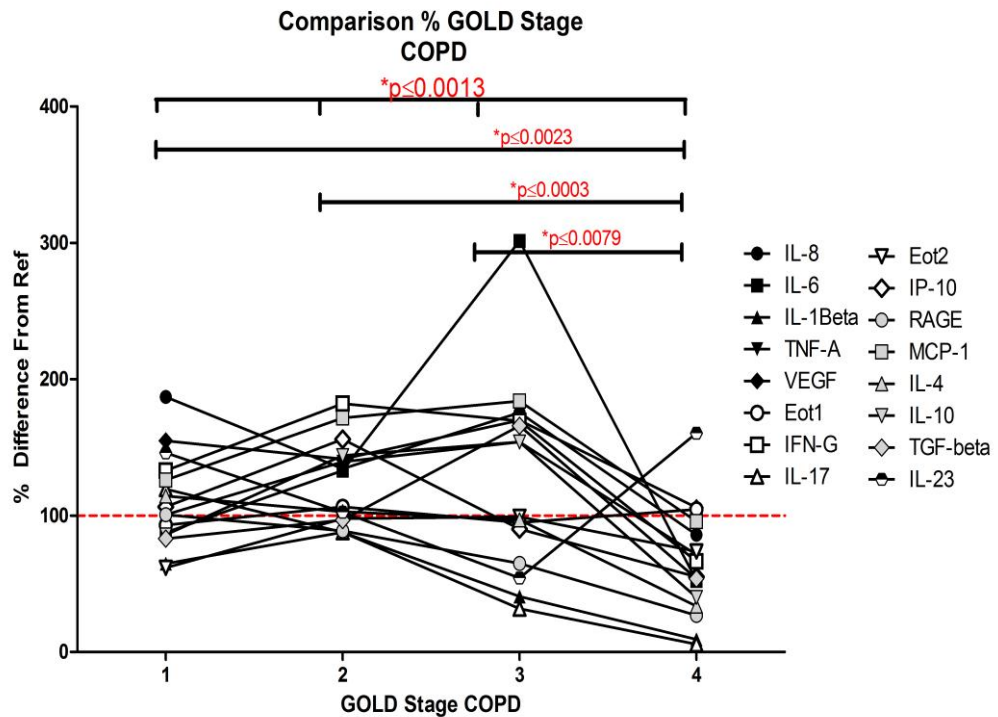


Figure 73: Dot plot to show the mean cytokine expression of all 16 cytokines across the 4 stages of GOLD.

As can be seen above the immune system is most active between stages 2 and 3 of GOLD. However at GOLD stage 4 where the FEV-1% drops less than 30%. It appears a potential explanation for this drop in the level of cytokines (with the exception of IL-23 which has increased expression at GOLD stage 4) could be that the immune system is suppressed significant compared to the other stages. However it has to be acknowledged that there are 3 subjects in GOLD stage 4 and the medication they are on is unknown which could influence the data which could negatively impact the nature of this finding.

5.3.6: Relationship between Age and FEV-1%

The relationship between FEV-1 and age was investigated. Over time healthy individuals experience a reduction in FEV-1% and this is exacerbated in those with COPD and who smoke. However it seems to be no correlation between both variables in this study. This suggests both variables are independent of each other (Figure 74). Additionally the data was split to see if there was a difference between age/FEV-1 % compared to those who were current smokers and those who were ex-smokers. The data (not shown) shows that there is no correlation between COPD current and ex-smokers in relation to age and FEV-1 predicted.

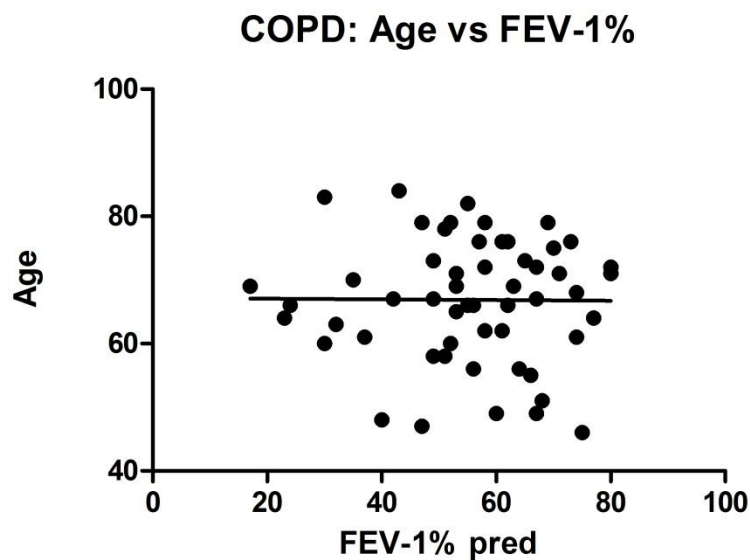


Figure 74: The relationship between “age” and predicted FEV-1% in COPD individuals.

There is no correlation between these two variables. Interestingly, the range of the COPD variables for age was between 46-84 and FEV-1 between 17-122%. This indicates there is no relationship between the two variables suggesting both are independent of one another.

5.3.7: The effect of Age on COPD

An interesting aspect of this study was to investigate the impact of age on the progression of COPD. The ages of the COPD patients ranged from 46 to up 83 years (figures 84-87). As seen in Figure 87, only for IP-10 did age correlate significantly with serum concentration of the cytokines. There was an increase in IP-10 associated with an increase in age ($p \leq 0.0162$). Additionally VEGF showed a trend towards positive correlation with age ($p \leq 0.06$). The remainder of the cytokines tested showed no significant correlations with age.

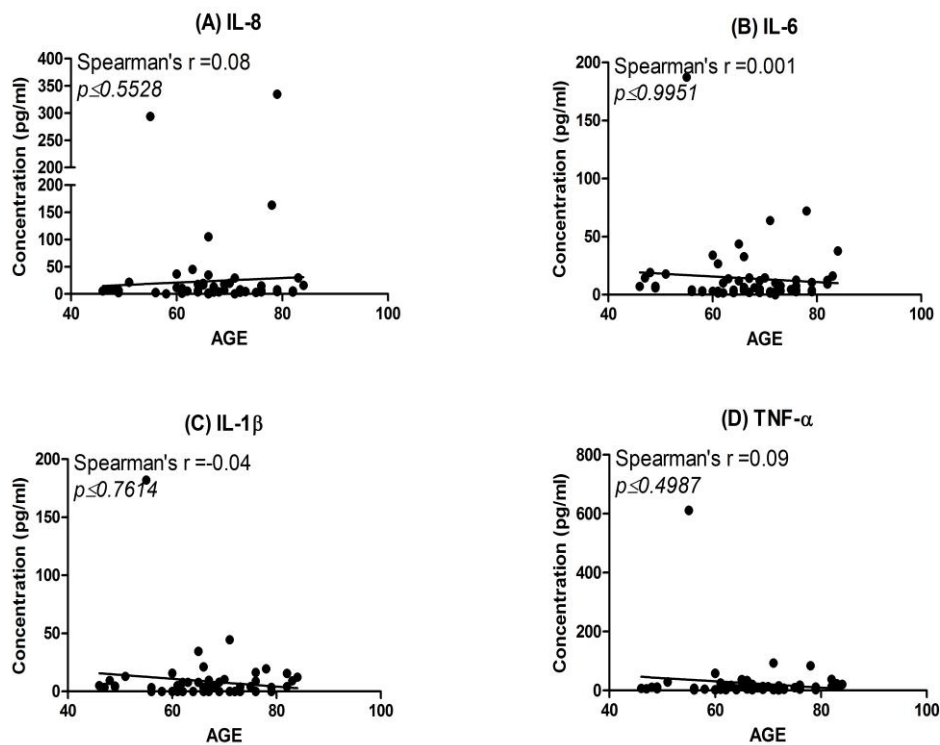


Figure 75: Correlation between “age” and cytokine concentration: IL-8, IL-6, IL-1 β and TNF- α respectively (A-D, respectively).

Spearman's Rank correlation tests were performed to compare the relationship between the “age” against the concentration of the respective cytokines; IL-8 (A), IL-6 (B) IL-1 β (C) and TNF- α (D), which showed no significant correlation in those with COPD.

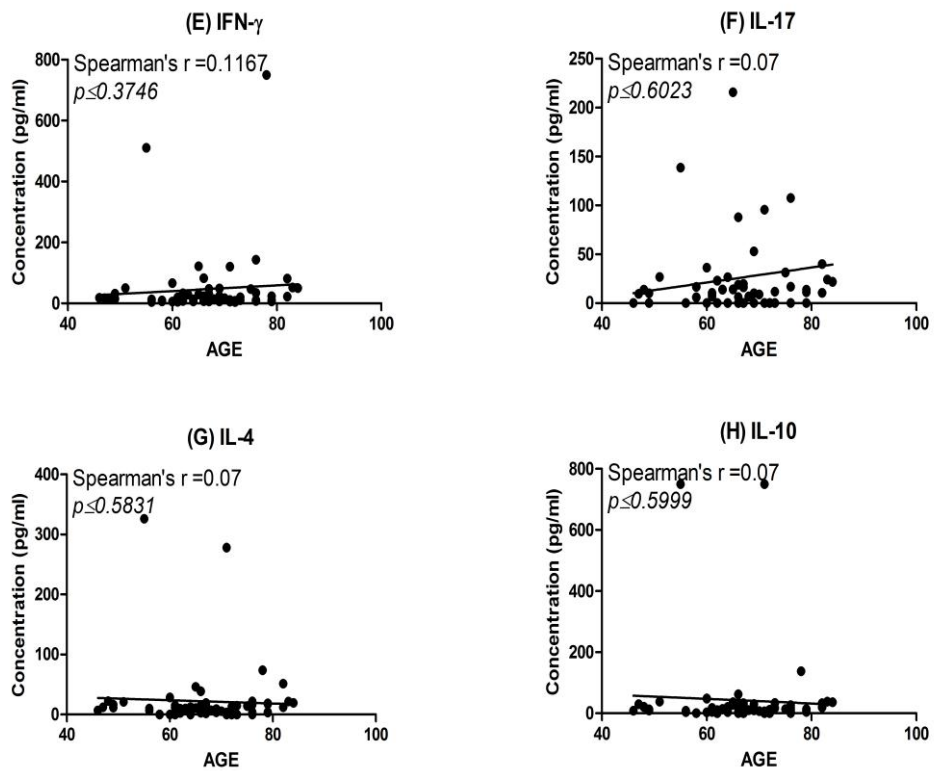


Figure 76: Correlation between “age” and cytokine concentration: IFN- γ , IL-17, IL-4 and IL-10 (E-H, respectively).

Spearman’s Rank correlation tests were performed to compare the relationship between the “age” against the concentration of the respective cytokines; IFN- γ (E), IL-17 (F), IL-4 (G) and IL-10 (H) which showed no significant correlation in those with COPD.

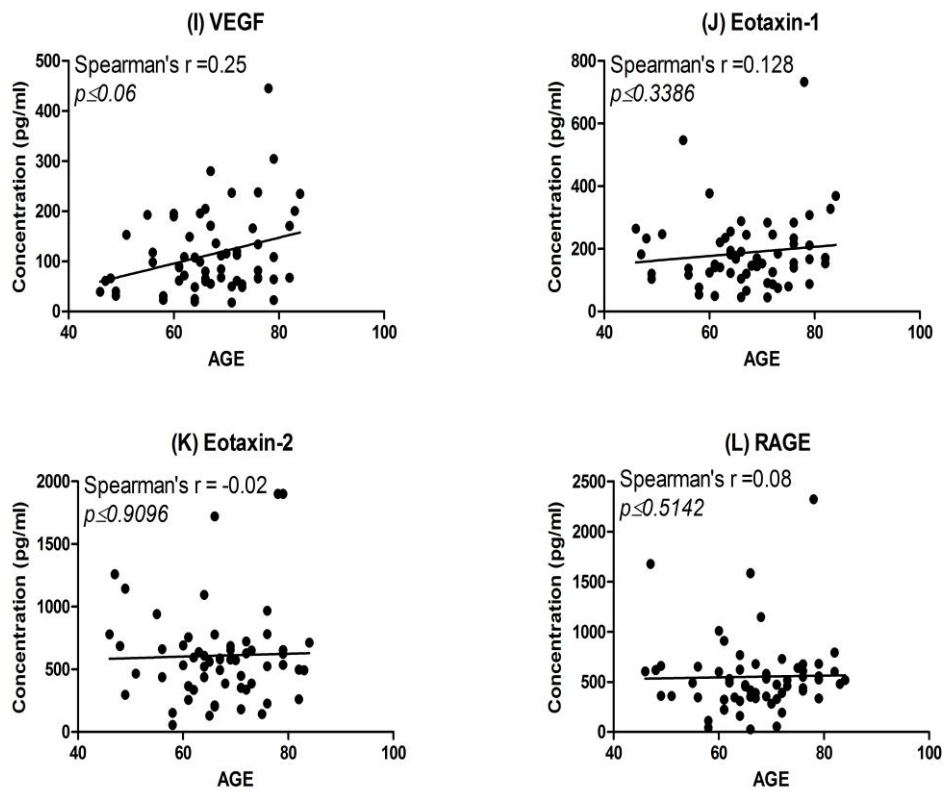


Figure 77: Correlation between “age” and cytokine concentration: VEGF, Eotaxin-1, Eotaxin-2 and RAGE (I-L, respectively).

Spearman’s Rank correlation tests were performed to compare the relationship between “age” and the concentration of the respective cytokines; eotaxin-1 (J), eotaxin02 (K) and RAGE (L) which showed no significant correlation. VEGF (I) concentration showed a trend towards a significant positive correlation with age ($p \leq 0.06$) in those with COPD.

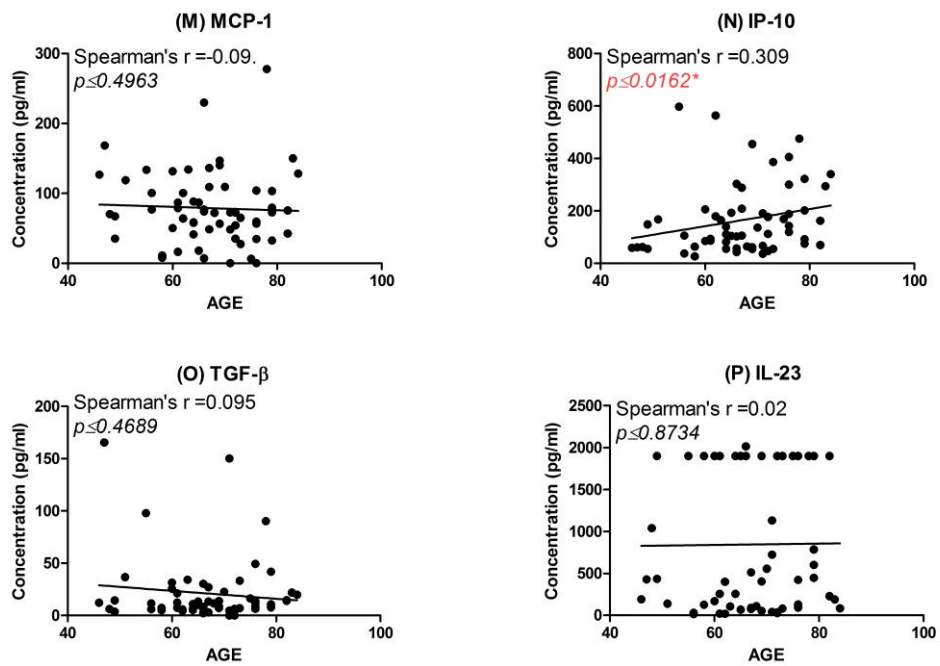


Figure 78: Correlation between “age” and cytokine concentration: MCP-1, IP-10, TGF- β , IL-23 (M-P, respectively).

Spearman’s Rank correlation tests were performed to compare the relationship between “age” and the concentration of the respective cytokines; MCP-1 (M), TGF- β (O) and IL-23 (P). IP-10 concentration showed a significant positive correlation with age ($p \leq 0.0162$) in those with COPD.

5.3.8: Clustering of Microarray Data

Due to the large sample size and the 16 biomarkers used, the data was analysed further in Multiple Experiment Viewer 4.7.4 (MEV). MEV is a Java tool that allows for complex proteomic data analysis. This was used to see if there were any new correlations or significant differences to the graphs previously shown in this chapters. An advantage of using MEV is that it avoids producing multiple graphs of the data when it can be represented as just one whole data set. This is shown in figure 87 where a heat-map is drawn to show the expression of all 16 biomarkers and also to see visually the difference between all three patient cohorts.

Interestingly when the heat-map is hierarchical clustered, the expression of the 16 biomarkers is not dependant on the FEV-1 levels. Immediate differences in the cytokines patterns between patient cohorts are not seen in the heatmap (Figure 79A) however when the statistical analysis was undertaken on the heatmap both MCP-1 ($p \leq 0.018$) and eotaxin-2 ($p \leq 0.034$) showed a significant difference between all three groups illustrated in Figure 79B which was in line with the results shown in section 5.3.1.

Figure 79: Heat-map to show the expression of all 16 biomarkers across all the samples which are subdivided into the three patient cohorts.

The heat-map above shows a hierarchical clustering of the levels of expression of the 16 biomarkers studied in sera of COPD, healthy smoking (S) controls and healthy controls (NS). The multiple different proteins are outlined on the vertical axis, and the patient cohorts on the horizontal axis. Red and blue colours indicate high and low protein expression respectively (A). When Kruskal-Wallis test were performed to compare differences between all patient cohorts both MCP-1 ($p \leq 0.018$) and eotaxin-2 ($p \leq 0.034$) were deemed statistically significant (B) which was in line with data produced in section 5.3.1.

5.3.9 False Discovery:

Undertaking multiple Kruskal-Wallis tests and correlations also constitutes for multiple testing and therefore needs controlling to avoid the rise in false positive data. Hence this was performed through J-Express Pro 2012 – Build 119 which allows for further proteomic expression analysis. Using this software the “significant analysis of microarrays” or “SAM” was a method chosen to calculate the number of genes that are false positive. As both MCP-1 and eotaxin-2 both expressed significant between healthy non-smokers, healthy smoking controls and COPD patients, SAM was used to see if these were either true results or in fact false positive results.

Table 15 below shows the results from SAM analysis. Interesting it has shown that only eotaxin-2 (highlighted in yellow) to be a truly positive result (FDR=0 and q value=0). MCP-1 (highlighted in orange) that was shown up early in Chapter 5 as being significant is shown to have a FDR and q-value of 25. Like p-values, q-values can be assigned of cut of 5% or $q \leq 0.05$. Therefore as seen from Table 15, MCP-1 is defined as being false positive ($\geq 25\%$) and this has to be acknowledged when analysing the data. Therefore one can presume that eotaxin-2 is the only significant cytokine that could have a bearing on COPD from the data generated from this study.

Table 15: To show the significant analysis of microarrays” or “SAM” method used to discover false-positive results amongst all 16 cytokines

Number:	Cytokine:	False Discovery Rate (FRD):	Q value:
1	Eotaxin-2	0	0
2	RAGE	37.5	25
3	MCP-1	25	25
4	IL-6	37.5	37.5
5	VEGF	60	60
6	IL-23	75	75
7	Eotaxin-1	75	75
8	IL-1 β	93.75	75
9	IL-10	91.667	75
10	IP-10	82.5	75
11	TGF- β	88.636	75
12	Il-17	87.5	75
13	IFN- γ	80.769	75
14	IL-4	80.357	75
15	IL-8	75	75
16	TNF- α	75	75

Table 15 shows the use of the SAM method to discover false-positive data. Previously in Chapter 5, MCP-1 ($p \leq 0.0167$) and Eotaxin-2 ($p \leq 0.0326$) were discovered to be statistically significant when comparing healthy non-smoking controls, healthy smoking controls and COPD patients. When this data was analysed by SAM, which serves to assume each null hypothesis is true for each cytokine, it was shown that only eotaxin-2 can be regarded as a truly positive result. Like p-values, q-values have a cut-off point of 5% or 0.05 and therefore whilst MCP-1 was considered significant when analysed by Kruskal-Wallis testing, the repeated nature of performing that test across 16 cytokines has led to a false positive result. Therefore it has to be acknowledged moving forward from the data in this study, the only eotaxin-2 is a significant cytokine and could play a role in the pathogenesis of COPD.

5.4 Discussion

5.4.1 Biomarkers in COPD

Our study shows that none of the 16 biomarkers completely correlates to all the factors outlined in the patient demographics. In general apart from eotaxin-2, the remaining of the data across the different variables were largely negative. Indeed when SAM analysis was performed on the dataset, only eotaxin-2 was shown to have truly positive data, meaning the significant data produced by MCP-1 has to be regarded as an obsolete. Therefore only eotaxin-2 can be considered as a cytokine which has significance in this study.

However eotaxin-2 was not correlated significantly to FEV-1% despite being significant differences between the COPD group and both the smoking and non-smoking control groups. Hence eotaxin-2 may be important biomarker in distinguishing between those that have COPD and those who are healthy smokers.

Many of the inflammatory markers measured in COPD patients in this study, such as IL-6, IL-1 β and TNF- α , were not significantly different to the healthy smoker controls. Similarly, it is known that IL-8 plays an important role in the recruitment of neutrophils to the site of inflammation; however in this study there were no significant differences in IL-8 levels between all 3 groups investigated.

MCP-1 is a chemoattractant that is responsible for the recruitment of monocytes that can differentiate into macrophages. Currently there are few publications that directly implicate a role for MCP-1 in COPD. Liu *et al*, showed there to be an increase in the level of MCP-1 with low levels of FEV1% predicted in stable COPD patients [137]. However in this investigation no trend was seen between the FEV-1% and MCP-1 concentrations. CCR₂ is a receptor that is specific for MCP-1 that is present on all

monocytes, macrophages and T-lymphocytes [330, 331]. Increased MCP-1 levels in BAL fluid have been implicated in those with chronic bronchitis who smoke, suggesting that this chemokine plays a role in the inflammatory process in association with cigarette smoke [332, 333].

Similarly it is thought that MCP-1 is secreted by alveolar macrophages which are exposed to noxious particles present in cigarette smoke. This may enter the circulation of the pulmonary capillaries in and around the lungs that could contribute to higher levels of MCP-1 in the serum of those that have COPD compared to the healthy controls [144]. This suggests that analysing MCP-1 in serum is perhaps futile in comparison to investigating it in BAL fluid.

Eotaxins, mainly comprising of eotaxin-1,-2 and -3, are strong chemoattractants for eosinophils. Usually this chemokine and its receptor are known to be associated in allergic reactions [334, 335]. It is postulated that eotaxins cause an influx of eosinophils into the bronchoalveolar lavage of those with asthma [336-339]. It has been reported that eosinophils can also influence other immune effector cells such as macrophages and T-lymphocytes [187] [340] [341]. However a mechanism for the role of eotaxins in COPD has yet to be postulated.

In this study we have shown that, of all the 16 biomarkers investigated, eotaxin-2 correlated significantly between the three patient cohorts. As mentioned in chapter one, as COPD is often described as a multicomponent disease including both emphysema and asthma, one can postulate that those whose have overlapping symptoms associated with asthma are represented in this study through the elevated expression of both eotaxin-1 and eotaxin-2 in the COPD cohort compared to the healthy smoking controls. Whilst it has never been proven that eotaxins have a

positive role in the pathogenesis of COPD, the results of this study indicate that these chemokines may play a role in the recruitment and activation of other immune effector cells such as macrophages which in turn play a role in the disease.

It is worth noting the inflammatory cytokines such as IL-6, TNF- α and IL-1 β showed no significant differences between these cytokines across the different patient subgroups which is contrary to results in the field that suggest that these three cytokines could play a role in the inflammatory processes in COPD. TNF- α in particular is secreted by macrophages, mast cells and epithelial cells [342] [343] [344]. IL-1 β is known to activate macrophages in those with COPD which in turn contribute to the inflammatory process by release chemokines and activating the metalloproteinases [345]. IL-6 has been found to be elevated in the sputum and plasma of COPD patients who have known to have an exacerbation of the disease. IL-6 is known to increase the inflammatory effect of COPD by releasing CRP from the liver [346].

Here we show that neither of these three inflammatory markers are elevated in this study, however, information is not available whether the COPD patients have had recent exacerbations prior to giving a blood sample. However going by results, it looks unlikely that the COPD patients would have had any exacerbations. Additionally it is unlikely that these exacerbations would be noticed in serum compared to BAL fluid. As a caveat it has to be acknowledged that information about the treatment that these COPD patients are no available which would have a significant bearing on the expression of these cytokines.

Interestingly the body's response to any inflammatory processes that occur is to produce anti-inflammatory cytokines that could perhaps counteract the effect of inflammation that is present in COPD. To this end, this study included the measurement of IL-10 which is a known anti-inflammatory marker [347]. Specifically IL-10 has the ability to suppress T_H1 cytokines such as TNF- α and IL-1 β , hence possibly the reason why the inflammatory cytokines were not as significantly different between the patient cohorts [348] [349]. However from the data in this study there was no significant increase in the expression of IL-10 in the COPD cohort compared to both the control cohorts.

IL-17 is also known as IL17A. It is a glycosylated cytokines; approximately 25kDa in size that is produced by T_H17 cells [350] [351, 352]. The role of IL-17 and the T_H17 cells in COPD are yet to be fully understood. It is thought that IL-17 may play a role in the pathogenesis of COPD through the stimulation and chemokine production [108] [107] [353]. Specifically a role for IL-17A involves the production of chemokines such as IL-8 and GM-CSF which can lead to neutrophilic inflammation in COPD. In this study, no increase of serum IL-17 was observed in the COPD cohort compared to the healthy smoker cohort. Additionally it is thought that IL-17 may have a role in the production of metalloproteinases, in particular MMP-9 which contributes to epithelial tissue damage that ultimately leads to emphysema [105].

As with IL-17, the exact role of IL-23 is not known. It is thought in mouse models involving cigarette smoke IL-23 induces the production of IFN- γ and also the proliferation of memory T-cells [354]. However it is thought that IL-23 has a positive influence on the expression of IL-17. IL-23 is thought to induce T_H17 cells to produce IL-17 working by a positive feedback system [355, 356]. In this investigation it can be

seen that both IL-17 and IL-23 are both up-regulated in the COPD cohort compared to the normal healthy cohort. Interestingly a large population of IL-23 is highly expressed as shown in the heatmap. A plausible explanation to this could be a polymorphism in the IL-23 gene which is better recognised in certain samples than others when using this particular duoset kit.

In studies of severe COPD patients (without a history of asthma), bronchoscopy of airway smooth muscle has shown an increase in size compared to that of those whom didn't suffer from the disease [357] [358]. It is also thought that the expression of contractile proteins such as calponin and myosin are lower in COPD patients. This reduces the elasticity of lung fibres which induces airflow resistance [57]. It is believed that the growth factors such TGF- β plays a pivotal role in increasing the expression of ASM contractile proteins such as α -actin and calponin in patients with COPD compared to asymptomatic smokers [57].

In subsequent studies it has been shown that there is an increase in the size of airway smooth muscle (ASM) in the peripheral airways of those who smoke and are diagnosed with COPD. Additionally there is a positive correlation in increased ASM and decreased FEV₁ levels. This supports the growing assertion that airway smooth muscle remodelling may be accountable for chronic airflow limitation. It is hypothesised that cigarette smoke may be responsible for either the growth of ASM or specifically increasing ASM tones [57].

In airway remodelling, mucosal thickening can augment the effect of mucosal restriction against elastic load. In a study in 2004, Baraldo and colleagues further supported the case that an increase in airflow limitation was in parallel with abnormalities that occur in airway remodelling of ASM cells. This resulted in a

thickening of the mucosal epithelial walls, which causes a narrowing of the airway lumen compared to normal airways [359]. However, in this study it can be seen that TGF- β there was no difference between the three patient cohorts suggesting if there was any airway remodelling in the lung there is no overspill into the pulmonary system as shown by the results.

Interestingly the other growth factor in this biomarker study was VEGF. The actual role of VEGF and its receptors are not fully understood in COPD. In this study we have shown that expression of VEGF was not significantly increased in the COPD cohort compared to the both the healthy control cohorts. Additionally serum VEGF level correlated negatively with a decline in predicted FEV-1%. In a study by Kierszniewska-Stepien *et al*, it was shown that there was an increase in serum VEGF in those with mild COPD compared to healthy controls and there was a similar correlation with their FEV-1% predicted level. Additionally they reported there were no significant increases in serum VEGF in severe COPD patients. They suggest that alveolar damage that occurs due to emphysema may result in impaired VEGF production from lung epithelial cells in those with severe COPD [360].

In addition to the measurement of standardised biomarkers in COPD, like those involved in inflammation and tissue remodelling, a new emphasis has been placed on discovering potential new biomarkers that could help distinguish those who have COPD from healthy controls. These biomarkers could help understand how the disease could progress compared to the standardised biomarkers. Hence for this investigation, the receptor for advanced glycation end-products (RAGE) was used as a potential novel biomarker. Work carried out in the field has shown that RAGE could influence a variety of different immune processes including cell/tissue injury as well

as being involved in oxidative stress and hypoxia which are two hallmarks of COPD [138, 165]. Work on murine models has shown that the treatment with sRAGE has shown to reverse the effect of inflammation. In humans it is thought that low levels of RAGE in blood may have a regulatory role in diseases such as rheumatoid arthritis and coronary heart disease, hence suggesting that low levels of this cytokine could be an indicator of poor inflammatory control [138, 139, 165]. Though it has been known that RAGE has been expressed in lung tissue of normal healthy controls, the exact role of this cytokine is not completely understood.

Specifically in relation to RAGE in blood, a study by Smith *et al* showed that plasma sRAGE was significantly lower in stable COPD patients compared to healthy controls. They also noticed a significant positive correlation with FEV-1% predicted and plasma sRAGE [361]. In this investigation we have shown that there are no significant differences between the three patient subgroups investigated as well as there being no significant correlations with respect to “age” and FEV-1%.

5.4.2: Gender differences in COPD

Over many years, there has seen a rise in the number of women developing tobacco related diseases such as COPD and lung cancer [362] [363] [364] . Compared to men who have similar levels of airway obstruction women are reported to develop worse dyspnea and have poorer quality of life scores [365] [366]. Despite COPD being well studied, there seems to be a lack of knowledge about the gender differences between men and women in serum biomarkers in those with the disease. In this investigation we looked closely at the difference between the expression of 16 cytokines across both genders in the three patient cohorts.

No significant differences were observed in the expression of the biomarkers between sexes in all three groups. Overall, the data showed no skew favouring either gender apart from those mentioned above.

However it has to be acknowledged that there are limitations in the present study. Ideally it would be beneficial to have exactly the same numbers of both females and males in each cohort. For all the 16 cytokines studied, there were more males than females, which may have skewed the data favouring male cytokine expression especially for VEGF (m=35, f=26). Additionally if information was available with regard to BODE, BMI and also smoking pack year history, further analyses could be performed in relation to gender and the expression of the 16 biomarkers. One can hypothesise at this stage that possibly the smoking pack year history could contribute to the higher expression of VEGF in males compared to females. A plausible mechanism for the role in VEGF could be directly related to the number of cigarettes that is smoked by an individual. Increased smoking could lead to impaired VEGF production that leads to airway obstruction and, ultimately, emphysema.

5.4.3: Age differences in COPD

In the third part of this study, the effect of age was investigated in relation to the expression of cytokines. One of the earliest studies was conducted by CM Fletcher *et al*, which studied the FEV-1 % in a group of west London men to show the different stages of GOLD severity introduced by GOLD [367]. Their study showed that over a period of 75 years of an individual's life, FEV-1% falls irrespective of smoking. However their study noted that smoking did increase the drop in FEV-1%. However it was thought that, whilst the measurements such as FEV-1% and FVC% can be good indicators of airflow limitation, they fail to distinguish between airflow limitation caused by small airway obstruction and emphysema. Hence, in this study, the majority

of the cytokines in this microarray panel did not show a significant correlation with FEV-1% apart from IP-10. Only IP-10 showed a positively significant relationship with FEV-1% and age. IP-10 is a chemokine that is secreted by a variety of immune effector cells such as bronchial epithelial cells and neutrophils in response to both IFN- γ and TNF- α [368] [369] is known to be up-regulated in those who have an exacerbation in COPD compared to healthy controls [146]. However there is very little to show the relationship between the expression of this chemokine in relation to age in those with COPD. Additionally within the COPD samples, the direct relationship between age and FEV-1 showed there to be no correlation in the data.

Chapter 6: General Discussion, Future Work & Conclusion

6.1 General Discussion

There is increasing evidence that COPD is associated with prolonged systematic inflammation in both the airways and the lung. Previously ELISA work has shown that there are biomarkers, such as CRP, IL-8 and TNF- α , that significantly increased in COPD patients compared to healthy smoking and non-smoking controls [342] [370] [371] [372]. However the ELISA methodology is limited by the ability to measure one protein in one sample at any one time.

The main aim of this thesis was develop a microarray platform that would allow multiple biomarkers to be quantified. Initially a number of variables that can potentially affect the microarray ranging from printing buffers, blocking buffer, slide surface etc were examined (Chapter 3). Initially the print buffer was assessed in combination with different slide surfaces. It was imperative to have a print buffer that could hold the conformational shape of the capture antibody intact so the sandwich microarray process would function. Additionally the print buffer had to interact well with the chemically modified surfaces of the different slide types. Finally the combination of slide surface and print buffer would have to provide a high level of reproducibility and signal strength both short and long term.

In this stage of the investigation trehalose was diluted in PBS and printed on poly-L-lysine slides was the best choice for this antibody microarray platform. Trehalose in particular is a naturally linked alpha disaccharide that forms a gel like surface on the slide and prevents the antibody from drying out and effectively holds them in position [212] [265] [267] [373]. Subsequent rehydration that occurs upon processing the slides allows the antibody to resume its reactivity when it binds to the detection antibody or protein of interest.

Poly-L-lysine is not novel in terms of its use in microarrays. In particular this slide surface has been used readily in cDNA work [211] [214] [374]. Of all the slide surfaces tested, poly-L-lysine was the best type of slide surface for long term processing of the slide. A key aim when developing this project was to have a microarray platform that could process and quantify blood immediately and if required at a later date. The natural ageing of poly-L-lysine coated slides means that the strength of the signal is consistent over time and in parts the signal may in fact improve with time making it an ideal surface for running antibody microarrays [219] [275].

One of the findings of our initial work with the generation of standard curves using normal sandwich ELISAs on the microarray was that at the lowest concentration of all 16 cytokines tested there was a lack of sensitivity. A lot of research groups have had the same problem with sensitivity and resort to amplification to improve this issue. For example work by Zhou *et al*, used two-colour rolling-circle amplification to improve sensitivity in their serum antibody microarrays [291] without noticing any cross-reactivity. More recently Meany *et al*, have used tyramide signal amplification in their lectin microarrays [375]. This study used an opti-4CN amplification module

that is often used in western blots and lysate microarray as shown in a study by Chan *et al*, to amplify signals [376]. In our study amplification has a two-fold effect on the microarray slides; firstly the level of background is almost halved and secondly the signal to noise ratio is enhanced. An explanation for both could be amplification adds an extra layer to the antibody microarray process which could remove non-specific binding, increasing sensitivity and thus leading to less background and hence enhancing the signal around each spot printed. Additionally amplification did not lead to any cross reactivity.

The choice of blocking buffer was then considered. It was shown that only 3% BSA and I-Block were effective on poly-L-lysine slide surfaces. 3% BSA may have contributed to a slightly higher level of background than I-Block but it was able to provide the best signal to noise ratio (S/N) which is was vital in being able to detect very low abundant cytokines.

The main aim of the validation chapter (Chapter 4) was to run a series of experiments that would examine the robustness of the antibody microarray platform that was optimised in the previous chapter. The use of microarrays have been prevalent over the last decade with a lot of focus built on developing a platform that is both robust and accurate and satisfies the accepted criteria outlined by different assay developmental federations. However different research groups follow different acceptable criteria for their own microarray technology. Work carried out by Urbanoswa *et al* developed an antibody microarray platform that had accuracy level between 70-130% and precision levels as high as 30% [126]. These were at the time in accordance with the FDA for analytical method validation. However more recently these parameters set by the FDA for accuracy and precision seem to have been revised

to fit tighter criteria (accuracy 80-120%) and precision ($\leq 20\%$) [227]. Interestingly, other companies, namely Affymetrix base their guidelines on the Luminex bead based assay, where they have accuracy levels between 70-130% and have precision levels $\leq 20\%$ [377]. No universal level is in place for accuracy and precision for analytical method validation remains unclear. A consensus needs to be established whereby in microarray technology a set of criteria are followed that any research group or company wanting to undertake and develop such a platform can adhere to. By allowing research groups or companies to adopt their own approach to setting acceptable accuracy and precision levels doesn't offer universal standardization with regard to microarray quantification and validation. Ideally a quantitative microarray approach should have the parameters for accuracy as close to 100% as possible and the level of precision as low as possible. In this investigation we adopted an approach whereby the level of accuracy cumulatively of all 16 biomarkers to be between 80-120% as in line with FDA regulations and tried to make sure that the level of precision was below 20%. However the problem that was identified and has to be accepted as a limitation in this study is, at the very lowest concentrations (below 1pg/ml) for many cytokines there were higher than acceptable variations that occur in some sera. However to compensate for this lack of accuracy the lower limits of quantification were established. This enabled the study to reject and remove values which even though were quantified were actually below or above the accepted level of accuracy and precision for the assay. Hence the overall effect is to improve the microarray platform.

The two main objectives in this PhD were to firstly to develop an antibody microarray technology that would enable cytokines to be quantified in sera. This involved the optimisation and validation of the microarray technology. The second objective was to quantify biomarkers in serum samples from both COPD patients and healthy controls. The ultimate aim of this thesis was thus to use the microarray platform developed to produce a biomarker profile that can be used for diagnostic purposes.

This study has shown that compared to traditionally sandwich ELISA, the microarray system that has been developed can be used to identify potential biomarkers that have been implicated in the pathogenesis of COPD. In addition clinical variables such as smoking history, age and FEV-1% predicted were compared to see if there were correlations between these parameters.

The main aim of the COPD chapter (chapter 5) was to use the microarray system to have sera quantify biomarkers for a selection of age-matched individuals that were either diagnosed as having COPD, were healthy smoking controls or non-smoking healthy controls. Within both the COPD and healthy smoking cohorts were current and ex-smokers. The results of this study showed that whilst certain inflammatory cytokines were not significantly more up-regulated in the COPD cohort compared to both the other two control cohorts. Only eotaxin-2 and MCP-1 showed significant differences between the three groups suggesting these were possibly key biomarkers in the disease. However one of the problems with multiple Kruskal-Wallis testing allows for potentially false positive results to be generated. When this was tested using the SAM method via J-Express Pro, this showed that only eotaxin-2 was only true result (FDR and q-value=0) and MCP-1 gave a false-positive result (FDR and q-

value $\geq 25\%$). This therefore meant that the significant MCP-1 result between the 3 subgroups investigated was invalid.

Interestingly it was observed that at GOLD stage 4 of the study there was a significant drop in the expression of 15 of the 16 biomarkers investigated. This suggested that at this stage of COPD, the immune system may potentially be immunosuppressed. It has to be acknowledged that with just three patients in GOLD stage 4 it would be difficult to make definitive assumptions about why these cytokines are decreased compared to the previous stages. Additionally it has to be acknowledged and discussed that the medication that the COPD patients were on were not available prior to analysis. It has to be taken into account that patients at GOLD stages 3 and 4 could be likely to be on a high dose of inhaled corticosteroids, which are immunosuppressive which would lead to drop in the 15 cytokines observed. However without the information available, this cannot be definitive to make such conclusions.

Overall the data generated from this study were largely negative with the exception of eotaxin-2, which therefore unlikely to be much use for research and diagnosis of COPD. It therefore is worth considering whether serum itself may not be the best biological fluid that can be used when investigating COPD as much of pathogenesis of the disease occurs within the lungs and therefore using BAL fluid or induced sputum instead may become more beneficial.

6.2: Future Work

There are a number of areas where the microarray work could be taken in the future. One of the problems that were encountered was the potential for antibodies in the duosets to lose sensitivity over time, reflected in the strength of the standard curve signal diminishing over time. Specifically this affects the bottom end of the standard curve meaning that much needed sensitivity to measure low abundant cytokines is no longer available, reducing the efficiency of the microarray platform.

This problem was overcome in this study as most of the optimisation and validation were completed with a batch of cytokines kits purchased at the start of the investigation. A new set of kits were then purchased in during the last steps of the investigation and for running the COPD samples. In most laboratories the purchasing of multiple kits is often unattainable. Hence improving the shelf life of cytokine kits have to be addressed in order to prevent loss of signal over time. This issue was partially addressed when the second batch of cytokine kits were purchased. All 16 cytokine kits were split in capture, detection and protein standard and almost all the contents were aliquoted into smaller storage tubes that can be frozen until use. However another problem that arose from the storing of the samples in the freezer came through the problem of multiple freeze-thaw cycles. If this occurs over at least four to five times, the signal strength starts to decrease over time suggesting that the antibody is suffering damage to its structure through multiple changes in temperature. To possibly address this problem it may be worth adding a cryoprotective agent, such as trehalose, to the neat concentrations of antibodies that may prevent the issue of loss of signal over time or avoiding freeze-thawing if possible. One of the biggest strengths of the microarray is also one of its biggest weaknesses in that so little reagent is used, there needs to be a better way of storing antibodies and reagents that

can be used over many months. These kits are purchased to run approximately 20 ELISAs per kit. As the microarrays in this investigation use only a fraction of these reagents during any one slide the requirement is to make a kit last over the recommended storage shelf life. Hence cryoprotective like trehalose will prevent the antibody from actually freezing and could thus extend the shelf life. If further time was available it would have been interesting to run a series of tests that could have shown whether this would work.

Whilst the sandwich microarray platform established here was highly successful in being able to quantify cytokines in sera to a high level of accuracy and precision, the procedure lasts up to 5 hours including analysis. Additionally depending on the number of samples and cytokines tested the analysis could take longer. Moving forward it is important that if this microarray technology is to be introduced to a greater clinical audience that a centralised computer programme may have to be developed to analyse the data much quicker.

It may also be worth considering whether there could be a quicker qualitative approach whereby the strength of the signal of a spot could indicate whether someone has a low or high level of cytokine in blood. This would employ a type of reverse phase microarray system whereby sera would be directly printed on the slide surface instead of the capture antibody and directly detected using biotinylated secondary antibody that could be developed by fluorescence. Initial work had begun on this concept which showed that the printing of sera on poly-L-lysine slides were unsuitable and the addition of streptavidin cy5 was insufficient in developing a consistent signal. It was then shown that nitrocellulose slides allow the absorption of sera better to the surface than poly-L-lysine. Serum prints poorly on poly-L-lysine

slides, however on nitrocellulose there were indication that the spot morphology and consistency of spotting was better. Streptavidin infra-red was used instead of streptavidin cy5 which showed an improved level of sensitivity especially with the nitrocellulose slide compared with cy5 which leads to many background problems. The objective of running this reverse phase approach allows the whole process to be completed within 3 hrs once the sera have been printed on the slide. One can directly print sera from healthy individuals next to COPD or disease type individuals which would make it easier to see differences between both cohorts.

Additionally, for the quantification of cytokines developed here, a 16 pad slide was used. For the reverse phase sera assay there is potential to use more pads on a slide which would allow for more detection antibodies to be tested. Whilst it is important to be able to quantify proteins in biological samples it is just as important to be able to pick out differences between different disease cohorts as soon as possible and this potential reverse phase sera microarray could potentially become a more faster approach to help diagnose multiple samples with further optimisation and validation.

Whilst the use of this microarray platform has been useful in distinguishing between COPD, healthy smoking and non-smoking healthy cohorts in sera it would have been more informative if more biological samples could have been investigated. Other biological samples such as urine, bronchoalveolar lavage (BAL), plasma and cerebral spinal fluid were also tested on this microarray platform. One of the problems noticed with plasma compared to sera was that there was a higher level of background in plasma that could be reduced by using a different blocking buffer. However in BAL fluid, due to the scarcity of low abundant proteins, it made it slightly more difficult to quantify these 16 biomarkers. However it was noticed that compared to both plasma

and sera, BAL fluid produced some of the best background levels and subsequently these samples have been tried on a parallel project using this microarray technology. In the context of this project it would have been interesting if there were complimentary BAL, sputum or plasma samples that would have been available to the sera samples that were obtained in this study. As the sera are from the circulation in those with COPD, it does not reveal completely the mechanisms of change that are occurring at the sites of inflammation. For example a combination of BAL samples and lung biopsies would help provide a more in depth study of the pathogenesis of COPD.

Furthermore, in this study, only three variables (age, sex and FEV-1%) were available as a tool for analysis. In previous COPD studies other variables such as BMI, BODE scale and smoking pack year history have also been used for additional purposes. For example with the availability of the smoking pack year history or the BODE scale, correlations could have been performed with the cytokine data to see if there a trend, in particular with MCP-1 and eotaxin-2 which were the most prominent of all the 16 biomarkers.

Additionally as mentioned in the previous chapters, the microarray study chooses to investigate 16 cytokines which were considered to be important in the pathogenesis of COPD. However as mentioned previously, this microarray platform is not just restricted to these 16 cytokines and if the resources were available there is the potential to look further and include many more cytokines. Cytokines not included in this study that have been included in Table 2 (Chapter 1) could be incorporated in any future work. Additionally over time one would expect novel cytokines to be

implicated in COPD and it is important that more, less common cytokines are investigated in this disease setting.

Finally one of the biggest limitations of this microarray platform that needs to be addressed is the ability to measure high abundance cytokines with low abundant cytokines. When high abundance cytokines were incorporated with small cytokines, a dilution of the samples resulted in small abundant cytokines being diluted too much making them unquantifiable. Realistically it would be impossible to be able to quantify a high abundance cytokine such as CRP with a low abundant cytokine IL-beta. Indeed this is the case in many leading microarray commercial companies which often try to limit their dynamic range where very large abundant cytokines are run on a different microarray platform to low abundant cytokines. The dynamic range for the 16 biomarkers in this thesis is between 0-2000pg/ml. The potential may be to push this dynamic range up to 10,000pg/ml which would enable more cytokines that can be investigated. This would require further optimisation and validation.

This microarray technology could have multiple implications in both research and management of those with COPD. At present there is no specific medication that is offered to those with COPD. In future the microarray technology could be used in a hospital setting where physicians could use the technology to monitor a drug treatment plan over a period of time.

6.3 Concluding Remarks

In conclusion, this thesis has shown that an in-house antibody microarray system has been optimised and validated testing many parameters that allows for accurate and precise detection of up to 16 biomarkers thought to be involved in COPD. The investigation using the microarray technology on the COPD samples have shown that eotaxin-2 could potentially be an important biomarker of COPD in sera. They may work through the recruitment of immune effector cells into the lungs that secrete further cytokines and contribute to the inflammatory cascade that occurs in disease. Further future optimisation and validation would allow for more biomarkers to be tested on this antibody microarray that would allow this platform to be a useful diagnostic tool. This would enable this microarray system to be used in any disease setting.

Bibliography

1. Mannino, D.M., *Chronic obstructive pulmonary disease: definition and epidemiology*. *Respir Care*, 2003. **48**(12): p. 1185-91; discussion 1191-3.
2. Mannino, D.M. and S. Braman, *The epidemiology and economics of chronic obstructive pulmonary disease*. *Proc Am Thorac Soc*, 2007. **4**(7): p. 502-6.
3. Barnes, P.J., *Chronic obstructive pulmonary disease: a growing but neglected global epidemic*. *PLoS Med*, 2007. **4**(5): p. e112.
4. Barnes, P.J., *Mediators of chronic obstructive pulmonary disease*. *Pharmacol Rev*, 2004. **56**(4): p. 515-48.
5. Cosio Piqueras, M.G. and M.G. Cosio, *Disease of the airways in chronic obstructive pulmonary disease*. *Eur Respir J Suppl*, 2001. **34**: p. 41s-49s.
6. Mannino, D.M. and A.S. Buist, *Global burden of COPD: risk factors, prevalence, and future trends*. *Lancet*, 2007. **370**(9589): p. 765-73.
7. Chapman, K.R., et al., *Epidemiology and costs of chronic obstructive pulmonary disease*. *Eur Respir J*, 2006. **27**(1): p. 188-207.
8. Jones, P.W., et al., *Health-related quality of life in patients by COPD severity within primary care in Europe*. *Respir Med*, 2011. **105**(1): p. 57-66.
9. Agusti, A.G., et al., *Systemic effects of chronic obstructive pulmonary disease*. *Eur Respir J*, 2003. **21**(2): p. 347-60.
10. Agusti, A., *Systemic effects of chronic obstructive pulmonary disease: what we know and what we don't know (but should)*. *Proc Am Thorac Soc*, 2007. **4**(7): p. 522-5.
11. Bourdin, A., et al., *Recent advances in COPD: pathophysiology, respiratory physiology and clinical aspects, including comorbidities*. *Eur Respir Rev*, 2009. **18**(114): p. 198-212.
12. Rodriguez-Roisin, R., *The airway pathophysiology of COPD: implications for treatment*. *COPD*, 2005. **2**(2): p. 253-62.
13. Arne, M., et al., *How often is diagnosis of COPD confirmed with spirometry?* *Respir Med*, 2010. **104**(4): p. 550-6.
14. Joo, M.J., T.A. Lee, and K.B. Weiss, *Geographic variation of spirometry use in newly diagnosed COPD*. *Chest*, 2008. **134**(1): p. 38-45.
15. Poels, P.J., T.R. Schermer, and C. van Weel, *Underuse of spirometry in the diagnosis of COPD*. *Monaldi Arch Chest Dis*, 2005. **63**(4): p. 234; author reply 234-5.
16. Gorska, K., et al., *Comparison of cellular and biochemical markers of airway inflammation in patients with mild-to-moderate asthma and chronic obstructive pulmonary disease: an induced sputum and bronchoalveolar lavage fluid study*. *J Physiol Pharmacol*, 2008. **59 Suppl 6**: p. 271-83.
17. Gorska, K., et al., *Eosinophilic airway inflammation in chronic obstructive pulmonary disease and asthma*. *J Physiol Pharmacol*, 2008. **59 Suppl 6**: p. 261-70.
18. Guerra, S., *Asthma and chronic obstructive pulmonary disease*. *Curr Opin Allergy Clin Immunol*, 2009. **9**(5): p. 409-16.
19. Wood, A.M. and R.A. Stockley, *The genetics of chronic obstructive pulmonary disease*. *Respir Res*, 2006. **7**: p. 130.
20. Briggs, D.D., Jr., *Chronic obstructive pulmonary disease overview: prevalence, pathogenesis, and treatment*. *J Manag Care Pharm*, 2004. **10**(4 Suppl): p. S3-10.

21. Shapiro, S.D. and E.P. Ingenito, *The pathogenesis of chronic obstructive pulmonary disease: advances in the past 100 years*. Am J Respir Cell Mol Biol, 2005. **32**(5): p. 367-72.
22. Miller, A., et al., *Dual-energy X-ray absorptiometry is the method of choice to assess body composition in COPD*. Respirology, 2009. **14**(3): p. 411-8.
23. Dewan, N.A., *COPD exacerbations: to X-ray or not to X-ray*. Chest, 2002. **122**(4): p. 1118-21.
24. Waatevik, M., et al., *Different COPD disease characteristics are related to different outcomes in the 6-minute walk test*. COPD, 2012. **9**(3): p. 227-34.
25. Brown, C.D. and R.A. Wise, *Field tests of exercise in COPD: the six-minute walk test and the shuttle walk test*. COPD, 2007. **4**(3): p. 217-23.
26. Chiba, H. and S. Abe, *[The environmental risk factors for COPD--tobacco smoke, air pollution, chemicals]*. Nihon Rinsho, 2003. **61**(12): p. 2101-6.
27. Criner, G.J. and B.R. Celli, *Advanced COPD: pathogenesis, evaluation, and treatment*. Semin Respir Crit Care Med, 2010. **31**(3): p. 255.
28. Alifano, M., et al., *Treatment of COPD: from pharmacological to instrumental therapies*. Eur Respir Rev, 2010. **19**(115): p. 7-23.
29. Usmani, O.S., *Unravelling the small airways: structure-function-treatment relationships in asthma and COPD*. Respiration, 2012. **84**(1): p. 1-3.
30. Hoshino, T., R. Toda, and H. Aizawa, *Pharmacological treatment in asthma and COPD*. Allergol Int, 2009. **58**(3): p. 341-6.
31. Berger, W.E. and D.C. Cline, *Asthma and COPD: definitions, epidemiology, and treatment guidelines*. Postgrad Med, 2005. **118**(6 Suppl Acute): p. 2-8.
32. Telenga, E.D., et al., *Inhaled corticosteroids in chronic obstructive pulmonary disease: a review*. Expert Opin Pharmacother. **11**(3): p. 405-21.
33. Cosio, B.G., et al., *Theophylline restores histone deacetylase activity and steroid responses in COPD macrophages*. J Exp Med, 2004. **200**(5): p. 689-95.
34. Barnes, P.J., *Theophylline for COPD*. Thorax, 2006. **61**(9): p. 742-4.
35. Schweiger, T.A. and M. Zdanowicz, *Systemic corticosteroids in the treatment of acute exacerbations of chronic obstructive pulmonary disease*. Am J Health Syst Pharm. **67**(13): p. 1061-9.
36. Gan, W.Q., S.F. Man, and D.D. Sin, *Effects of inhaled corticosteroids on sputum cell counts in stable chronic obstructive pulmonary disease: a systematic review and a meta-analysis*. BMC Pulm Med, 2005. **5**: p. 3.
37. Fens, N., et al., *Exhaled breath profiling enables discrimination of chronic obstructive pulmonary disease and asthma*. Am J Respir Crit Care Med, 2009. **180**(11): p. 1076-82.
38. Barnes, P.J., *ABC of chronic obstructive pulmonary disease. Future treatments*. BMJ, 2006. **333**(7561): p. 246-8.
39. Bergren, D.R., *Environmental tobacco smoke exposure and airway hyperresponsiveness*. Inflamm Allergy Drug Targets, 2009. **8**(5): p. 340-7.
40. Gompertz, S., et al., *Relationship between airway inflammation and the frequency of exacerbations in patients with smoking related COPD*. Thorax, 2001. **56**(1): p. 36-41.
41. Martin, P., H. Glasgow, and J. Patterson, *Chronic obstructive pulmonary disease (COPD): smoking remains the most important cause*. N Z Med J, 2005. **118**(1213): p. U1409.
42. Kaminsky, D.A. and T.W. Marcy, *COPD and smoking cessation motivation*. Chest, 2004. **125**(5): p. 1958; author reply 1958-9.
43. Zaher, C., et al., *Smoking-related diseases: the importance of COPD*. Int J Tuberc Lung Dis, 2004. **8**(12): p. 1423-8.

44. Churg, A., M. Cosio, and J.L. Wright, *Mechanisms of cigarette smoke-induced COPD: insights from animal models*. Am J Physiol Lung Cell Mol Physiol, 2008. **294**(4): p. L612-31.
45. Kent, L., et al., *Cigarette smoke extract induced cytokine and chemokine gene expression changes in COPD macrophages*. Cytokine, 2008. **42**(2): p. 205-16.
46. Suzuki, M., et al., *Decreased airway expression of vascular endothelial growth factor in cigarette smoke-induced emphysema in mice and COPD patients*. Inhal Toxicol, 2008. **20**(3): p. 349-59.
47. Loukides, S., P. Bakakos, and K. Kostikas, *Oxidative stress in patients with COPD*. Curr Drug Targets, 2011. **12**(4): p. 469-77.
48. Joppa, P., et al., *Oxidative stress in patients with COPD and pulmonary hypertension*. Wien Klin Wochenschr, 2007. **119**(13-14): p. 428-34.
49. Kinnula, V.L. and M. Myllarniemi, *Oxidant-antioxidant imbalance as a potential contributor to the progression of human pulmonary fibrosis*. Antioxid Redox Signal, 2008. **10**(4): p. 727-38.
50. Kinnula, V.L. and J.D. Crapo, *Smoking and COPD-mechanisms and prevention*. COPD, 2009. **6**(4): p. 231-3.
51. Tantucci, C. and D. Modena, *Lung function decline in COPD*. Int J Chron Obstruct Pulmon Dis, 2012. **7**: p. 95-9.
52. Barnes, P.J., *Histone deacetylase-2 and airway disease*. Ther Adv Respir Dis, 2009. **3**(5): p. 235-43.
53. Cavalcante, A.G. and P.F. de Bruin, *The role of oxidative stress in COPD: current concepts and perspectives*. J Bras Pneumol, 2009. **35**(12): p. 1227-37.
54. Bhowmik, A., *Histone deacetylase activity and COPD*. N Engl J Med, 2005. **353**(5): p. 528-9; author reply 528-9.
55. Barnes, P.J., *Reduced histone deacetylase in COPD: clinical implications*. Chest, 2006. **129**(1): p. 151-5.
56. St-Laurent, J., et al., *Influence of smoking on airway inflammation and remodelling in asthma*. Clin Exp Allergy, 2008. **38**(10): p. 1582-9.
57. Chung, K.F., *The role of airway smooth muscle in the pathogenesis of airway wall remodeling in chronic obstructive pulmonary disease*. Proc Am Thorac Soc, 2005. **2**(4): p. 347-54; discussion 371-2.
58. Chung, K.F., *Inflammatory mediators in chronic obstructive pulmonary disease*. Curr Drug Targets Inflamm Allergy, 2005. **4**(6): p. 619-25.
59. Menezes, A.M. and P.C. Hallal, *Role of passive smoking on COPD risk in non-smokers*. Lancet, 2007. **370**(9589): p. 716-7.
60. Van Overveld, F.J., et al., *Differences in responses upon corticosteroid therapy between smoking and non-smoking patients with COPD*. J Physiol Pharmacol, 2006. **57 Suppl 4**: p. 273-82.
61. Camp, P.G., D.E. O'Donnell, and D.S. Postma, *Chronic obstructive pulmonary disease in men and women: myths and reality*. Proc Am Thorac Soc, 2009. **6**(6): p. 535-8.
62. Sertogullarindan, B., et al., *Frequency of pulmonary hypertension in patients with COPD due to biomass smoke and tobacco smoke*. Int J Med Sci, 2012. **9**(6): p. 406-12.
63. Salvi, S. and P.J. Barnes, *Is exposure to biomass smoke the biggest risk factor for COPD globally?* Chest, 2010. **138**(1): p. 3-6.
64. Ekici, A., et al., *Obstructive airway diseases in women exposed to biomass smoke*. Environ Res, 2005. **99**(1): p. 93-8.
65. Fullerton, D.G., N. Bruce, and S.B. Gordon, *Indoor air pollution from biomass fuel smoke is a major health concern in the developing world*. Trans R Soc Trop Med Hyg, 2008. **102**(9): p. 843-51.

66. Po, J., *Respiratory disease associated with solid biomass fuel exposure in rural women and children ; a systemic review and meta-analysis*. Am J Respir Crit Care Med, 2009. **179**(A4740).
67. Regalado, J., et al., *The effect of biomass burning on respiratory symptoms and lung function in rural Mexican women*. Am J Respir Crit Care Med, 2006. **174**(8): p. 901-5.
68. Moran-Mendoza, O., et al., *Wood smoke-associated lung disease: a clinical, functional, radiological and pathological description*. Int J Tuberc Lung Dis, 2008. **12**(9): p. 1092-8.
69. Blanc, P.D. and K. Toren, *Occupation in chronic obstructive pulmonary disease and chronic bronchitis: an update*. Int J Tuberc Lung Dis, 2007. **11**(3): p. 251-7.
70. Rodriguez, E., et al., *Impact of occupational exposure on severity of COPD*. Chest, 2008. **134**(6): p. 1237-43.
71. Blanc, P.D., et al., *Occupational exposures and the risk of COPD: dusty trades revisited*. Thorax, 2009. **64**(1): p. 6-12.
72. Boschetto, P., et al., *Chronic obstructive pulmonary disease (COPD) and occupational exposures*. J Occup Med Toxicol, 2006. **1**: p. 11.
73. Ramirez-Venegas, A., et al., *Survival of patients with chronic obstructive pulmonary disease due to biomass smoke and tobacco*. Am J Respir Crit Care Med, 2006. **173**(4): p. 393-7.
74. Zhou, Y., et al., *COPD in Chinese nonsmokers*. Eur Respir J, 2009. **33**(3): p. 509-18.
75. Steinkamp, G., *[COPD, the systemic disease: nutrition - an underestimated and unresolved problem]*. Pneumologie, 2003. **57**(11): p. 681-9.
76. Wouters, E.F., et al., *Systemic and local inflammation in asthma and chronic obstructive pulmonary disease: is there a connection?* Proc Am Thorac Soc, 2009. **6**(8): p. 638-47.
77. Jeffery, P.K., *Remodeling and inflammation of bronchi in asthma and chronic obstructive pulmonary disease*. Proc Am Thorac Soc, 2004. **1**(3): p. 176-83.
78. Borger, P., et al., *Beyond the Immune System: The Role of Resident Cells in Asthma and COPD*. J Allergy (Cairo), 2012. **2012**: p. 968039.
79. Maeno, T., *[The role of CD8+ T cells in the pathogenesis of COPD]*. Nihon Kokyuki Gakkai Zasshi, 2008. **46**(3): p. 268-9.
80. Morissette, M.C., J. Parent, and J. Milot, *Perforin, granzyme B, and FasL expression by peripheral blood T lymphocytes in emphysema*. Respir Res, 2007. **8**: p. 62.
81. Paats, M.S., et al., *Systemic CD4+ and CD8+ T-cell cytokine profiles correlate with GOLD stage in stable COPD*. Eur Respir J, 2012. **40**(2): p. 330-7.
82. Tetley, T.D., *Macrophages and the pathogenesis of COPD*. Chest, 2002. **121**(5 Suppl): p. 156S-159S.
83. Barnes, P.J., *Alveolar macrophages in chronic obstructive pulmonary disease (COPD)*. Cell Mol Biol (Noisy-le-grand), 2004. **50 Online Pub**: p. OL627-37.
84. Olesiejuk, R., K. Danielak-Rybka, and B. Wojnarowicz-Dmitruk, *[Emphysema connected with Alpha-1 anti-trypsin deficiency]*. Pneumonol Alergol Pol, 2003. **71**(7-8): p. 344-8.
85. Miravittles, M., *Alpha1-anti-trypsin deficiency: epidemiology and incidence*. Respir Med, 2002. **96**(3): p. 205.
86. Jeffery, P.K., *Remodeling in asthma and chronic obstructive lung disease*. Am J Respir Crit Care Med, 2001. **164**(10 Pt 2): p. S28-38.

87. Ilumets, H., et al., *Transient elevation of neutrophil proteinases in induced sputum during COPD exacerbation*. Scand J Clin Lab Invest, 2008. **68**(7): p. 618-23.
88. Demedts, I.K., et al., *Role of apoptosis in the pathogenesis of COPD and pulmonary emphysema*. Respir Res, 2006. **7**: p. 53.
89. Urbanowicz, R.A., et al., *Altered effector function of peripheral cytotoxic cells in COPD*. Respir Res, 2009. **10**: p. 53.
90. Tosiek, M.J., et al., *CD4+CD25+Foxp3+ regulatory T cells are dispensable for controlling CD8+ T cell-mediated lung inflammation*. J Immunol, 2011. **186**(11): p. 6106-18.
91. Saetta, M., et al., *Increased proportion of CD8+ T-lymphocytes in the paratracheal lymph nodes of smokers with mild COPD*. Sarcoidosis Vasc Diffuse Lung Dis, 2003. **20**(1): p. 28-32.
92. Huang, H., et al., *CD4+ Th1 cells promote CD8+ Tc1 cell survival, memory response, tumor localization and therapy by targeted delivery of interleukin 2 via acquired pMHC I complexes*. Immunology, 2007. **120**(2): p. 148-59.
93. Lim, S.C., et al., *Apoptosis of T lymphocytes isolated from peripheral blood of patients with acute exacerbation of chronic obstructive pulmonary disease*. Yonsei Medical Journal, 2011. **52**(4): p. 581-7.
94. Rufino, R., et al., *Quantitative assessment of elastic fibers in chronic obstructive pulmonary disease*. J Bras Pneumol, 2007. **33**(5): p. 502-9.
95. Urbanowicz, R.A., et al., *Enhanced effector function of cytotoxic cells in the induced sputum of COPD patients*. Respir Res, 2010. **11**: p. 76.
96. Gupta, J., et al., *T lymphocyte subset profile and serum alpha-1-antitrypsin in pathogenesis of chronic obstructive pulmonary disease*. Clin Exp Immunol, 2007. **149**(3): p. 463-9.
97. Plumb, J., et al., *Increased T-regulatory cells within lymphocyte follicles in moderate COPD*. Eur Respir J, 2009. **34**(1): p. 89-94.
98. Barcelo, B., et al., *Phenotypic characterisation of T-lymphocytes in COPD: abnormal CD4+CD25+ regulatory T-lymphocyte response to tobacco smoking*. Eur Respir J, 2008. **31**(3): p. 555-62.
99. Smyth, L.J., et al., *CD4-regulatory cells in COPD patients*. Chest, 2007. **132**(1): p. 156-63.
100. Demoor, T., et al., *Increased T-regulatory cells in lungs and draining lymph nodes in a murine model of COPD*. Eur Respir J, 2010. **35**(3): p. 688-9.
101. Castellani, M.L., et al., *IL-35, an anti-inflammatory cytokine which expands CD4+CD25+ Treg Cells*. J Biol Regul Homeost Agents, 2010. **24**(2): p. 131-5.
102. Qiu, S.L., et al., *[CD(4)(+)Foxp3(+) regulatory T cells in inflammation and emphysema after smoking cessation in rats]*. Zhonghua Jie He He Hu Xi Za Zhi, 2010. **33**(9): p. 688-92.
103. Roos-Engstrand, E., et al., *Expansion of CD4+CD25+ helper T cells without regulatory function in smoking and COPD*. Respir Res, 2011. **12**: p. 74.
104. Chen, K., et al., *IL-17RA is required for CCL2 expression, macrophage recruitment, and emphysema in response to cigarette smoke*. PLoS One, 2011. **6**(5): p. e20333.
105. Alcorn, J.F., C.R. Crowe, and J.K. Kolls, *TH17 cells in asthma and COPD*. Annu Rev Physiol, 2010. **72**: p. 495-516.
106. Hong, S.C. and S.H. Lee, *Role of th17 cell and autoimmunity in chronic obstructive pulmonary disease*. Immune Netw, 2010. **10**(4): p. 109-14.

107. Zhang, X., et al., *Increased interleukin (IL)-8 and decreased IL-17 production in chronic obstructive pulmonary disease (COPD) provoked by cigarette smoke*. Cytokine, 2011. **56**(3): p. 717-25.
108. Pridgeon, C., et al., *Regulation of IL-17 in chronic inflammation in the human lung*. Clin Sci (Lond), 2011. **120**(12): p. 515-24.
109. Ling Ye, X.W., Meiling Jin, *Role of Airway Epithelial Cells in Development of Chronic Obstructive Pulmonary Disease*. Journal of Epithelial Biology and Pharmacology, 2009. **2**: p. 44-50.
110. Reynolds, P.R., M.G. Cosio, and J.R. Hoidal, *Cigarette smoke-induced Egr-1 upregulates proinflammatory cytokines in pulmonary epithelial cells*. Am J Respir Cell Mol Biol, 2006. **35**(3): p. 314-9.
111. Wang, I.J., C.Y. Wu, and F.R. Hu, *Effect of proinflammatory cytokines on the human MUC5AC promoter activity in vitro and in vivo*. Clin Ophthalmol, 2007. **1**(1): p. 71-7.
112. McManus, T.E., et al., *Acute and latent adenovirus in COPD*. Respir Med, 2007. **101**(10): p. 2084-90.
113. Gandhi, A., et al., *Factors associated with symptomatic rhinovirus infection in patients with COPD*. J Clin Virol, 2012.
114. Glader, P., et al., *Cigarette smoke extract modulates respiratory defence mechanisms through effects on T-cells and airway epithelial cells*. Respir Med, 2006. **100**(5): p. 818-27.
115. Comer, D.M., et al., *Airway epithelial cell apoptosis and inflammation in COPD, smokers and nonsmokers*. Eur Respir J, 2013. **41**(5): p. 1058-67.
116. Puchelle, E., et al., *Airway epithelial repair, regeneration, and remodeling after injury in chronic obstructive pulmonary disease*. Proc Am Thorac Soc, 2006. **3**(8): p. 726-33.
117. Li, W., Y. Xu, and Z. Zhang, *Activity of matrix metalloproteinase in airway epithelial cells of COPD patients*. J Huazhong Univ Sci Technolog Med Sci, 2005. **25**(2): p. 151-4.
118. Sethi, S., et al., *Airway bacterial concentrations and exacerbations of chronic obstructive pulmonary disease*. Am J Respir Crit Care Med, 2007. **176**(4): p. 356-61.
119. Working, G., *Biomarkers Definitions Working G. Biomarkers and surrogate endpoints: preferred definitions and conceptual framework*. Clinical pharmacology and therapeutics. 2001. **69**(3): p. 89-95.
120. Sin, D.D. and J. Vestbo, *Biomarkers in chronic obstructive pulmonary disease*. Proc Am Thorac Soc, 2009. **6**(6): p. 543-5.
121. Rosenberg, S.R. and R. Kalhan, *Biomarkers in chronic obstructive pulmonary disease*. Transl Res, 2012. **159**(4): p. 228-37.
122. Martinez, F.J., et al., *Sex differences in severe pulmonary emphysema*. Am J Respir Crit Care Med, 2007. **176**(3): p. 243-52.
123. Nicholas, B.L., C.D. O'Connor, and R. Djukanovic, *From proteomics to prescription-the search for COPD biomarkers*. COPD, 2009. **6**(4): p. 298-303.
124. Taylor, D.R. and I.D. Pavord, *Biomarkers in the assessment and management of airways diseases*. Postgrad Med J, 2008. **84**(998): p. 628-34; quiz 633.
125. Frangogiannis, N.G., *Biomarkers: hopes and challenges in the path from discovery to clinical practice*. Transl Res, 2012. **159**(4): p. 197-204.
126. Urbanowska, T., et al., *Protein microarray platform for the multiplex analysis of biomarkers in human sera*. J Immunol Methods, 2006. **316**(1-2): p. 1-7.

127. Higashimoto, Y., et al., *Serum biomarkers as predictors of lung function decline in chronic obstructive pulmonary disease*. *Respir Med*, 2009. **103**(8): p. 1231-8.
128. Richens, J.L., et al., *Systems biology coupled with label-free high-throughput detection as a novel approach for diagnosis of chronic obstructive pulmonary disease*. *Respir Res*, 2009. **10**: p. 29.
129. Pinto-Plata, V., et al., *Profiling serum biomarkers in patients with COPD: associations with clinical parameters*. *Thorax*, 2007. **62**(7): p. 595-601.
130. Vestbo, J., et al., *Evaluation of COPD Longitudinally to Identify Predictive Surrogate End-points (ECLIPSE)*. *Eur Respir J*, 2008. **31**(4): p. 869-73.
131. Agusti, A., et al., *Characterisation of COPD heterogeneity in the ECLIPSE cohort*. *Respir Res*, 2010. **11**: p. 122.
132. Garcia-Rio, F., et al., *Systemic inflammation in chronic obstructive pulmonary disease: a population-based study*. *Respir Res*, 2010. **11**: p. 63.
133. Ropcke, S., et al., *Repeatability of and relationship between potential COPD biomarkers in bronchoalveolar lavage, bronchial biopsies, serum, and induced sputum*. *PLoS One*, 2012. **7**(10): p. e46207.
134. Pinto-Plata, V., et al., *Inflammatory and repair serum biomarker pattern. Association to clinical outcomes in COPD*. *Respir Res*, 2012. **13**: p. 71.
135. Di Stefano, A., et al., *T helper type 17-related cytokine expression is increased in the bronchial mucosa of stable chronic obstructive pulmonary disease patients*. *Clin Exp Immunol*, 2009. **157**(2): p. 316-24.
136. Gasse, P., et al., *IL-1 and IL-23 mediate early IL-17A production in pulmonary inflammation leading to late fibrosis*. *PLoS One*, 2011. **6**(8): p. e23185.
137. Liu, S.F., et al., *Correlation between serum biomarkers and BODE index in patients with stable COPD*. *Respirology*, 2009. **14**(7): p. 999-1004.
138. Sukkar, M.B., et al., *Soluble RAGE is deficient in neutrophilic asthma and COPD*. *Eur Respir J*, 2012. **39**(3): p. 721-9.
139. Young, R.P., B.A. Hay, and R.J. Hopkins, *Does RAGE protect smokers from COPD?* *Eur Respir J*, 2011. **38**(3): p. 743-4; author reply 744.
140. Nadigel, J., et al., *IL-8 production in response to cigarette smoke is decreased in epithelial cells from COPD patients*. *Pulm Pharmacol Ther*, 2013.
141. Gao, J. and B. Zhan, *The effects of Ang-1, IL-8 and TGF-beta1 on the pathogenesis of COPD*. *Mol Med Rep*, 2012. **6**(5): p. 1155-9.
142. D'Armiento, J.M., et al., *Eosinophil and T cell markers predict functional decline in COPD patients*. *Respir Res*, 2009. **10**: p. 113.
143. Fujimoto, K., et al., *Airway inflammation during stable and acutely exacerbated chronic obstructive pulmonary disease*. *Eur Respir J*, 2005. **25**(4): p. 640-6.
144. Traves, S.L., et al., *Increased levels of the chemokines GROalpha and MCP-1 in sputum samples from patients with COPD*. *Thorax*, 2002. **57**(7): p. 590-5.
145. Aaron, S.D., et al., *Multi analyte profiling and variability of inflammatory markers in blood and induced sputum in patients with stable COPD*. *Respir Res*, 2010. **11**: p. 41.
146. Quint, J.K., et al., *Serum IP-10 as a biomarker of human rhinovirus infection at exacerbation of COPD*. *Chest*, 2010. **137**(4): p. 812-22.
147. Quint, J.K. and J.A. Wedzicha, *The neutrophil in chronic obstructive pulmonary disease*. *J Allergy Clin Immunol*, 2007. **119**(5): p. 1065-71.
148. Lappalainen, U., et al., *Interleukin-1beta causes pulmonary inflammation, emphysema, and airway remodeling in the adult murine lung*. *Am J Respir Cell Mol Biol*, 2005. **32**(4): p. 311-8.

149. Pauwels, N.S., et al., *Role of IL-1alpha and the Nlrp3/caspase-1/IL-1beta axis in cigarette smoke-induced pulmonary inflammation and COPD*. Eur Respir J, 2011. **38**(5): p. 1019-28.
150. Rupp, J., et al., *Imbalanced secretion of IL-1beta and IL-1RA in Chlamydia pneumoniae-infected mononuclear cells from COPD patients*. Eur Respir J, 2003. **22**(2): p. 274-9.
151. Ishii, T., et al., *Neither IL-1beta, IL-1 receptor antagonist, nor TNF-alpha polymorphisms are associated with susceptibility to COPD*. Respir Med, 2000. **94**(9): p. 847-51.
152. Eagan, T.M., et al., *TNF-alpha is associated with loss of lean body mass only in already cachectic COPD patients*. Respir Res, 2012. **13**(1): p. 48.
153. Deveci, Y., et al., *[Serum ghrelin, IL-6 and TNF-alpha levels in patients with chronic obstructive pulmonary disease.]*. Tuberk Toraks, 2010. **58**(2): p. 162-72.
154. Daldegan, M.B., M.M. Teixeira, and A. Talvani, *Concentration of CCL11, CXCL8 and TNF-alpha in sputum and plasma of patients undergoing asthma or chronic obstructive pulmonary disease exacerbation*. Braz J Med Biol Res, 2005. **38**(9): p. 1359-65.
155. Basyigit, I., et al., *[Body mass index and serum and sputum TNF-alpha levels relation in asthma and COPD]*. Tuberk Toraks, 2004. **52**(3): p. 256-61.
156. Cordoba-Lanus, E., et al., *Association of IL-6 gene polymorphisms and COPD in a Spanish population*. Respir Med, 2008. **102**(12): p. 1805-11.
157. Grubek-Jaworska, H., et al., *IL-6 and IL-13 in induced sputum of COPD and asthma patients: correlation with respiratory tests*. Respiration, 2012. **84**(2): p. 101-7.
158. Vogiatzis, I., et al., *Effects of rehabilitative exercise on peripheral muscle TNFalpha, IL-6, IGF-I and MyoD expression in patients with COPD*. Thorax, 2007. **62**(11): p. 950-6.
159. Hodge, S., et al., *Interleukin-4 and tumour necrosis factor-alpha inhibit transforming growth factor-beta production in a human bronchial epithelial cell line: possible relevance to inflammatory mechanisms in chronic obstructive pulmonary disease*. Respiriology, 2001. **6**(3): p. 205-11.
160. Zhu, J., et al., *Plasma cells and IL-4 in chronic bronchitis and chronic obstructive pulmonary disease*. Am J Respir Crit Care Med, 2007. **175**(11): p. 1125-33.
161. Imaoka, H., et al., *Interleukin-18 production and pulmonary function in COPD*. Eur Respir J, 2008. **31**(2): p. 287-97.
162. Hardaker, E.L., et al., *Regulation of TNF-alpha- and IFN-gamma-induced CXCL10 expression: participation of the airway smooth muscle in the pulmonary inflammatory response in chronic obstructive pulmonary disease*. FASEB J, 2004. **18**(1): p. 191-3.
163. Torvinen, M., H. Campwala, and I. Kilty, *The role of IFN-gamma in regulation of IFN-gamma-inducible protein 10 (IP-10) expression in lung epithelial cell and peripheral blood mononuclear cell co-cultures*. Respir Res, 2007. **8**: p. 80.
164. Boutou, A.K., et al., *Levels of inflammatory mediators in chronic obstructive pulmonary disease patients with anemia of chronic disease: a case-control study*. QJM, 2012. **105**(7): p. 657-63.
165. Wu, L., et al., *Advanced glycation end products and its receptor (RAGE) are increased in patients with COPD*. Respir Med, 2011. **105**(3): p. 329-36.

166. Wu, Q., et al., *IL-23-dependent IL-17 production is essential in neutrophil recruitment and activity in mouse lung defense against respiratory Mycoplasma pneumoniae infection*. *Microbes Infect*, 2007. **9**(1): p. 78-86.
167. Zhang, L., et al., *Expression of Interleukin (IL)-10, IL-17A and IL-22 in Serum and Sputum of Stable Chronic Obstructive Pulmonary Disease Patients*. *COPD*, 2013.
168. Demeo, D.L., et al., *IL10 polymorphisms are associated with airflow obstruction in severe alpha1-antitrypsin deficiency*. *Am J Respir Cell Mol Biol*, 2008. **38**(1): p. 114-20.
169. Ceyhan, B.B., F.Y. Enc, and S. Sahin, *IL-2 and IL-10 levels in induced sputum and serum samples of asthmatics*. *J Investig Allergol Clin Immunol*, 2004. **14**(1): p. 80-5.
170. Mak, J.C., et al., *Elevated plasma TGF-beta1 levels in patients with chronic obstructive pulmonary disease*. *Respir Med*, 2009. **103**(7): p. 1083-9.
171. Pavlisa, G., et al., *Serum levels of VEGF and bFGF in hypoxic patients with exacerbated COPD*. *Eur Cytokine Netw*, 2010. **21**(2): p. 92-8.
172. Chung, K.F., *Cytokines in chronic obstructive pulmonary disease*. *Eur Respir J Suppl*, 2001. **34**: p. 50s-59s.
173. Tomaki, M., et al., *Decreased expression of antioxidant enzymes and increased expression of chemokines in COPD lung*. *Pulm Pharmacol Ther*, 2007. **20**(5): p. 596-605.
174. Seifart, C., et al., *TNF-alpha-, TNF-beta-, IL-6-, and IL-10-promoter polymorphisms in patients with chronic obstructive pulmonary disease*. *Tissue Antigens*, 2005. **65**(1): p. 93-100.
175. Ferroni, P., et al., *Rebuttal to circulating IL-6 levels in chronic obstructive pulmonary disease*. *Thromb Haemost*, 2001. **85**(2): p. 373.
176. Hannink, J.D., et al., *Non-invasive ventilation abolishes the IL-6 response to exercise in muscle-wasted COPD patients: A pilot study*. *Scand J Med Sci Sports*, 2012.
177. Lin, J.C., et al., *Mechanism of cigarette smoke-induced kinin B(1) receptor expression in rat airways*. *Peptides*, 2010. **31**(10): p. 1940-5.
178. Antoniu, S.A., *Challenges in targeting TNF alpha in asthma and COPD*. *Curr Opin Investig Drugs*, 2009. **10**(5): p. 404-6.
179. Karadag, F., et al., *Biomarkers of systemic inflammation in stable and exacerbation phases of COPD*. *Lung*, 2008. **186**(6): p. 403-9.
180. Ogawa, Y., E.A. Duru, and B.T. Ameredes, *Role of IL-10 in the resolution of airway inflammation*. *Curr Mol Med*, 2008. **8**(5): p. 437-45.
181. Barnes, P.J., *The cytokine network in asthma and chronic obstructive pulmonary disease*. *J Clin Invest*, 2008. **118**(11): p. 3546-56.
182. Kang, M.J., et al., *IL-18 induces emphysema and airway and vascular remodeling via IFN-gamma, IL-17A, and IL-13*. *Am J Respir Crit Care Med*, 2012. **185**(11): p. 1205-17.
183. Kang, M.J., et al., *IFN-gamma-dependent DNA injury and/or apoptosis are critical in cigarette smoke-induced murine emphysema*. *Proc Am Thorac Soc*, 2006. **3**(6): p. 517-8.
184. Barczyk, A., et al., *Cytokine production by bronchoalveolar lavage T lymphocytes in chronic obstructive pulmonary disease*. *J Allergy Clin Immunol*, 2006. **117**(6): p. 1484-92.
185. Siva, R., et al., *Eosinophilic airway inflammation and exacerbations of COPD: a randomised controlled trial*. *Eur Respir J*, 2007. **29**(5): p. 906-13.
186. Saha, S. and C.E. Brightling, *Eosinophilic airway inflammation in COPD*. *Int J Chron Obstruct Pulmon Dis*, 2006. **1**(1): p. 39-47.

187. Jahnz-Royk, K., T. Plusa, and J. Mierzejewska, *Eotaxin in serum of patients with asthma or chronic obstructive pulmonary disease: relationship with eosinophil cationic protein and lung function*. *Mediators Inflamm*, 2000. **9**(3-4): p. 175-9.
188. Qiu, Y., et al., *Biopsy neutrophilia, neutrophil chemokine and receptor gene expression in severe exacerbations of chronic obstructive pulmonary disease*. *Am J Respir Crit Care Med*, 2003. **168**(8): p. 968-75.
189. Noguera, A., et al., *Enhanced neutrophil response in chronic obstructive pulmonary disease*. *Thorax*, 2001. **56**(6): p. 432-7.
190. Profita, M., et al., *Chronic obstructive pulmonary disease and neutrophil infiltration: role of cigarette smoke and cyclooxygenase products*. *Am J Physiol Lung Cell Mol Physiol*, 2010. **298**(2): p. L261-9.
191. Hollander, C., et al., *Serum and bronchial lavage fluid concentrations of IL-8, SLPI, sCD14 and sICAM-1 in patients with COPD and asthma*. *Respir Med*, 2007. **101**(9): p. 1947-53.
192. Eickmeier, O., et al., *Sputum biomarker profiles in cystic fibrosis (CF) and chronic obstructive pulmonary disease (COPD) and association between pulmonary function*. *Cytokine*, 2010. **50**(2): p. 152-7.
193. Minton, K., *T cell signalling: Balancing regulatory and self-reactive T cells*. *Nat Rev Immunol*, 2012. **12**(10): p. 685.
194. Bordon, Y., *T cell signalling: heavy metal rocks T cells*. *Nat Rev Immunol*, 2011. **11**(5): p. 300-1.
195. Wilkinson, B., H. Wang, and C.E. Rudd, *Positive and negative adaptors in T-cell signalling*. *Immunology*, 2004. **111**(4): p. 368-74.
196. Greenlee, K.J., Z. Werb, and F. Kheradmand, *Matrix metalloproteinases in lung: multiple, multifarious, and multifaceted*. *Physiol Rev*, 2007. **87**(1): p. 69-98.
197. Polosukhin, V.V., et al., *Hypoxia-inducible factor-1 signalling promotes goblet cell hyperplasia in airway epithelium*. *J Pathol*, 2011. **224**(2): p. 203-11.
198. Marillier, R.G., et al., *IL-4/IL-13 independent goblet cell hyperplasia in experimental helminth infections*. *Bmc Immunology*, 2008. **9**: p. 11.
199. Horsnell, W.G., et al., *Delayed goblet cell hyperplasia, acetylcholine receptor expression, and worm expulsion in SMC-specific IL-4Ralpha-deficient mice*. *PLoS Pathog*, 2007. **3**(1): p. e1.
200. Makris, D., *Tc2 response at the onset of COPD exacerbations*. *CHEST*, 2008. **134**(3): p. 483-8.
201. Costa, C., et al., *CXCR3 and CCR5 chemokines in induced sputum from patients with COPD*. *Chest*, 2008. **133**(1): p. 26-33.
202. Islam, L.N. and P.C. Wilkinson, *Chemotactic factor-induced polarization, receptor redistribution, and locomotion of human blood monocytes*. *Immunology*, 1988. **64**(3): p. 501-7.
203. Konigshoff, M., N. Kneidinger, and O. Eickelberg, *TGF-beta signaling in COPD: deciphering genetic and cellular susceptibilities for future therapeutic regimen*. *Swiss Med Wkly*, 2009. **139**(39-40): p. 554-63.
204. Santibanez, J.F., M. Quintanilla, and C. Bernabeu, *TGF-beta/TGF-beta receptor system and its role in physiological and pathological conditions*. *Clin Sci (Lond)*, 2011. **121**(6): p. 233-51.
205. Filippi, C.M., et al., *Transforming growth factor-beta suppresses the activation of CD8+ T-cells when naive but promotes their survival and function once antigen experienced: a two-faced impact on autoimmunity*. *Diabetes*, 2008. **57**(10): p. 2684-92.

206. Kubiczikova, L., et al., *TGF-beta -- an excellent servant but a bad master*. J Transl Med, 2012. **10**(1): p. 183.
207. Carlsson, A., et al., *Serum proteome profiling of metastatic breast cancer using recombinant antibody microarrays*. European Journal of Cancer, 2008. **44**(3): p. 472-480.
208. Yu, X., et al., *Protein microarrays: effective tools for the study of inflammatory diseases*. Methods Mol Biol, 2009. **577**: p. 199-214.
209. Ingvarsson, J., et al., *Detection of pancreatic cancer using antibody microarray-based serum protein profiling*. Proteomics, 2008. **8**(11): p. 2211-9.
210. Orzechowski, R., et al., *Antibody microarray profiling reveals individual and combined serum proteins associated with pancreatic cancer*. Cancer Res, 2005. **65**(23): p. 11193-202.
211. Angenendt, P., et al., *Toward optimized antibody microarrays: a comparison of current microarray support materials*. Anal Biochem, 2002. **309**(2): p. 253-60.
212. Wu, P. and D.W. Grainger, *Toward immobilized antibody microarray optimization: print buffer and storage condition comparisons on performance*. Biomedical Sciences Instrumentation, Vol 40, 2004. **449**: p. 243-248.
213. Lee, C.S. and B.G. Kim, *Improvement of protein stability in protein microarrays*. Biotechnology Letters, 2002. **24**(10): p. 839-844.
214. Seurnyck-Servoss, S.L., et al., *Evaluation of surface chemistries for antibody microarrays*. Analytical Biochemistry, 2007. **371**(1): p. 105-115.
215. Sobek, J., C. Aquino, and R. Schlapbach, *Quality considerations and selection of surface chemistry for glass-based DNA, peptide, antibody, carbohydrate, and small molecule microarrays*. Methods Mol Biol, 2007. **382**: p. 17-31.
216. Altman, N., *Replication, variation and normalisation in microarray experiments*. Appl Bioinformatics, 2005. **4**(1): p. 33-44.
217. Hessner, M.J., et al., *Immobilized probe and glass surface chemistry as variables in microarray fabrication*. BMC Genomics, 2004. **5**(1): p. 53.
218. Servoss, S.L., et al., *High-throughput analysis of serum antigens using sandwich ELISAs on microarrays*. Methods Mol Biol, 2009. **520**: p. 143-50.
219. Olle, E.W., et al., *Comparison of antibody array substrates and the use of glycerol to normalize spot morphology*. Exp Mol Pathol, 2005. **79**(3): p. 206-9.
220. Lee, Y., et al., *Micropatterned assembly of silica nanoparticles for a protein microarray with enhanced detection sensitivity*. Biomed Microdevices, 2010. **12**(3): p. 457-64.
221. Wingren, C. and C.A. Borrebaeck, *Antibody microarray analysis of directly labelled complex proteomes*. Current Opinion in Biotechnology, 2008. **19**(1): p. 55-61.
222. Mo, X.Y., et al., *The effects of different sample labelling methods on signal intensities of a 60-mer diagnostic microarray*. J Virol Methods, 2006. **134**(1-2): p. 36-40.
223. Haab, B.B., *Methods and applications of antibody microarrays in cancer research*. Proteomics, 2003. **3**(11): p. 2116-22.
224. Espina, V., et al., *Protein microarray detection strategies: focus on direct detection technologies*. J Immunol Methods, 2004. **290**(1-2): p. 121-33.

225. Karsten, S.L., et al., *An evaluation of tyramide signal amplification and archived fixed and frozen tissue in microarray gene expression analysis*. Nucleic Acids Res, 2002. **30**(2): p. E4.
226. Bansal, S. and A. DeStefano, *Key elements of bioanalytical method validation for small molecules*. AAPS J, 2007. **9**(1): p. E109-14.
227. Administration, F.a.D., *Guidance for Industry: Bioanalytical Method Validation*. www.fda.gov/downloads/Drugs/.../Guidances/ucm070107.pdf, 2001.
228. Smolec, J., et al., *Bioanalytical method validation for macromolecules in support of pharmacokinetic studies*. Pharm Res, 2005. **22**(9): p. 1425-31.
229. James, C.A., M. Breda, and E. Frigerio, *Bioanalytical method validation: a risk-based approach?* J Pharm Biomed Anal, 2004. **35**(4): p. 887-93.
230. Shah, V.P., et al., *Bioanalytical method validation--a revisit with a decade of progress*. Pharm Res, 2000. **17**(12): p. 1551-7.
231. Smith, G., *Review of the 2008 European Medicines Agency concept paper on bioanalytical method validation*. Bioanalysis, 2009. **1**(5): p. 877-81.
232. Jacobson, R.H., *Validation of serological assays for diagnosis of infectious diseases*. Rev Sci Tech, 1998. **17**(2): p. 469-526.
233. Boterman, M., et al., *Recommendations on the interpretation of the new European Medicines Agency Guideline on Bioanalytical Method Validation by Global CRO Council for Bioanalysis (GCC)*. Bioanalysis, 2012. **4**(6): p. 651-60.
234. Srinivas, N.R., *Bioanalytical assay validation parameters re-visited: perspectives on stability studies*. Biomedical Chromatography, 2009. **23**(10): p. 1031-3.
235. Kricka, L.J. and S.R. Master, *Validation and quality control of protein microarray-based analytical methods*. Mol Biotechnol, 2008. **38**(1): p. 19-31.
236. Kandasamy, K., et al., *Bioanalytical method development, validation and quantification of flupirtine maleate in rat plasma by liquid chromatography-tandem mass spectrometry*. Arzneimittelforschung, 2011. **61**(12): p. 693-9.
237. Xue, Y.J., et al., *An integrated bioanalytical method development and validation approach: case studies*. Biomedical Chromatography, 2012. **26**(10): p. 1215-27.
238. Gonzalez, A.G., M.A. Herrador, and A.G. Asuero, *Intra-laboratory assessment of method accuracy (trueness and precision) by using validation standards*. Talanta, 2010. **82**(5): p. 1995-8.
239. Bayley, D.L., et al., *Validation of assays for inflammatory mediators in exhaled breath condensate*. Eur Respir J, 2008. **31**(5): p. 943-8.
240. Tignon, M., et al., *Development and inter-laboratory validation study of an improved new real-time PCR assay with internal control for detection and laboratory diagnosis of African swine fever virus*. J Virol Methods, 2011. **178**(1-2): p. 161-70.
241. Binsaeed, A.A., et al., *A validation study comparing the sensitivity and specificity of the new Dr. KSU H1N1 RT-PCR kit with real-time RT-PCR for diagnosing influenza A (H1N1)*. Annals of Saudi Medicine, 2011. **31**(4): p. 351-5.
242. Vessman, J., *Selectivity or specificity? Validation of analytical methods from the perspective of an analytical chemist in the pharmaceutical industry*. J Pharm Biomed Anal, 1996. **14**(8-10): p. 867-9.
243. Armbruster, D.A. and T. Pry, *Limit of blank, limit of detection and limit of quantitation*. Clin Biochem Rev, 2008. **29 Suppl 1**: p. S49-52.

244. Choi, D.H., et al., *Validation of a method for predicting the precision, limit of detection and range of quantitation in competitive ELISA*. *Anal Sci*, 2007. **23**(2): p. 215-8.
245. Anderson, M., et al., *Evaluation of Multiplex Immunoassay Results*. *Genetic Engineering & Biotechnology News*, 2011. **31**(8): p. 24-25.
246. Fang, L., et al., *Estimating area under the curve and relative exposure in a pharmacokinetic study with data below quantification limit*. *J Biopharm Stat*, 2011. **21**(1): p. 66-76.
247. Guo, Y., O. Harel, and R.J. Little, *How well quantified is the limit of quantification?* *Epidemiology*, 2010. **21 Suppl 4**: p. S10-6.
248. Bergstrand, M. and M.O. Karlsson, *Handling data below the limit of quantification in mixed effect models*. *AAPS J*, 2009. **11**(2): p. 371-80.
249. Wang, X., S. Ghosh, and S.W. Guo, *Quantitative quality control in microarray image processing and data acquisition*. *Nucleic Acids Res*, 2001. **29**(15): p. E75-5.
250. Petrov, A.S., S, *Microarray Image Processing and Quality Control*. *Journal of VLSI Signal Processing*, 2004. **38**: p. 211-226.
251. Koutsokera, A., et al., *Systemic biomarkers in exacerbations of COPD: the evolving clinical challenge*. *Chest*, 2012. **141**(2): p. 396-405.
252. Al-shair, K., et al., *Biomarkers of systemic inflammation and depression and fatigue in moderate clinically stable COPD*. *Respir Res*, 2011. **12**: p. 3.
253. Cazzola, M. and G. Novelli, *Biomarkers in COPD*. *Pulm Pharmacol Ther*, 2010. **23**(6): p. 493-500.
254. Gong, P., G.M. Harbers, and D.W. Grainger, *Multi-technique comparison of immobilized and hybridized oligonucleotide surface density on commercial amine-reactive microarray slides*. *Anal Chem*, 2006. **78**(7): p. 2342-51.
255. Lv, L.L., et al., *Construction of an antibody microarray based on agarose-coated slides*. *Electrophoresis*, 2007. **28**(3): p. 406-13.
256. Cretich, M., et al., *High sensitivity protein assays on microarray silicon slides*. *Anal Chem*, 2009. **81**(13): p. 5197-203.
257. Darr, C.M., et al., *A comparative evaluation of microarray slides as substrates for the development of protease assay biosensors*. *Exp Mol Pathol*, 2011. **91**(3): p. 714-7.
258. Moran-Mirabal, J.M., et al., *Controlling microarray spot morphology with polymer liftoff arrays*. *Anal Chem*, 2007. **79**(3): p. 1109-14.
259. Rimini, R., et al., *Validation of serum protein profiles by a dual antibody array approach*. *J Proteomics*, 2009. **73**(2): p. 252-66.
260. Metwalli, E., et al., *Surface characterizations of mono-, di-, and tri-aminosilane treated glass substrates*. *J Colloid Interface Sci*, 2006. **298**(2): p. 825-31.
261. Wu, Q.H., et al., *[Oligonucleotide microarray preparation using enhanced poly-L-lysine glass slides]*. *Di Yi Jun Yi Da Xue Xue Bao*, 2004. **24**(11): p. 1236-41.
262. Liu, Y., et al., *Neoglycolipid-based oligosaccharide microarray system: preparation of NGLs and their noncovalent immobilization on nitrocellulose-coated glass slides for microarray analyses*. *Methods Mol Biol*, 2012. **808**: p. 117-36.
263. Subramaniam, R., et al., *A multivalent Mannheimia-Bibersteinia vaccine protects bighorn sheep against Mannheimia haemolytica challenge*. *Clin Vaccine Immunol*, 2011. **18**(10): p. 1689-94.

-
264. Price, K.E., N.G. Greene, and A. Camilli, *Export requirements of pneumolysin in Streptococcus pneumoniae*. J Bacteriol, 2012. **194**(14): p. 3651-60.
265. Wu, P. and D.W. Grainger, *Comparison of hydroxylated print additives on antibody microarray performance*. J Proteome Res, 2006. **5**(11): p. 2956-65.
266. Preininger, C., et al., *Optimizing processing parameters for signal enhancement of oligonucleotide and protein arrays on ARChip Epoxy*. Bioelectrochemistry, 2005. **67**(2): p. 155-62.
267. Momose, Y., et al., *Comparative analysis of transcriptional responses to the cryoprotectants, dimethyl sulfoxide and trehalose, which confer tolerance to freeze-thaw stress in Saccharomyces cerevisiae*. Cryobiology, 2010. **60**(3): p. 245-61.
268. Sauer, U., L. Bodrossy, and C. Preininger, *Evaluation of substrate performance for a microbial diagnostic microarray using a four parameter ranking*. Anal Chim Acta, 2009. **632**(2): p. 240-6.
269. Yu, L., et al., *High-performance UV-curable epoxy resin-based microarray and microfluidic immunoassay devices*. Biosens Bioelectron, 2009. **24**(10): p. 2997-3002.
270. Giraud, G., et al., *Fluorescence lifetime imaging of quantum dot labeled DNA microarrays*. Int J Mol Sci, 2009. **10**(4): p. 1930-41.
271. Jia, M., et al., *Development of a sensitive microarray immunoassay for the quantitative analysis of neuropeptide Y*. Anal Chem, 2012. **84**(15): p. 6508-14.
272. Pollack, J.R., *DNA microarray technology. Introduction*. Methods Mol Biol, 2009. **556**: p. 1-6.
273. Sip, M., et al., *Detection of viral infections by an oligonucleotide microarray*. J Virol Methods, 2010. **165**(1): p. 64-70.
274. Redkar, R.J., et al., *Signal and sensitivity enhancement through optical interference coating for DNA and protein microarray applications*. J Biomol Tech, 2006. **17**(2): p. 122-30.
275. Balboni, I., et al., *Evaluation of microarray surfaces and arraying parameters for autoantibody profiling*. Proteomics, 2008. **8**(17): p. 3443-9.
276. Kimura, N., et al., *Site-specific, covalent attachment of poly(dT)-modified peptides to solid surfaces for microarrays*. Bioconjug Chem, 2007. **18**(6): p. 1778-85.
277. Tomizaki, K.Y., K. Usui, and H. Mihara, *Protein-protein interactions and selection: array-based techniques for screening disease-associated biomarkers in predictive/early diagnosis*. FEBS J, 2010. **277**(9): p. 1996-2005.
278. Garcia, B.H., 2nd, et al., *Antibody microarray analysis of inflammatory mediator release by human leukemia T-cells and human non small cell lung cancer cells*. J Biomol Tech, 2007. **18**(4): p. 245-51.
279. Bohm, D., et al., *Antibody microarray analysis of the serum proteome in primary breast cancer patients*. Cancer Biol Ther, 2011. **12**(9): p. 772-9.
280. Kusnezow, W., et al., *Antibody microarrays: an evaluation of production parameters*. Proteomics, 2003. **3**(3): p. 254-64.
281. Cho, E.J., et al., *Optimization of aptamer microarray technology for multiple protein targets*. Anal Chim Acta, 2006. **564**(1): p. 82-90.
282. Karoonuthaisiri, N., et al., *Development of antibody array for simultaneous detection of foodborne pathogens*. Biosens Bioelectron, 2009. **24**(6): p. 1641-8.

283. Kuno, A., et al., *Focused differential glycan analysis with the platform antibody-assisted lectin profiling for glycan-related biomarker verification*. Mol Cell Proteomics, 2009. **8**(1): p. 99-108.
284. Lian, W., et al., *Sensitive detection of multiplex toxins using antibody microarray*. Anal Biochem, 2010. **401**(2): p. 271-9.
285. Longo, C., et al., *A novel biomarker harvesting nanotechnology identifies Bak as a candidate melanoma biomarker in serum*. Exp Dermatol, 2011. **20**(1): p. 29-34.
286. Signore, M. and K.A. Reeder, *Antibody validation by Western blotting*. Methods Mol Biol, 2012. **823**: p. 139-55.
287. Aguilar-Mahecha, A., et al., *Development of reverse phase protein microarrays for the validation of clusterin, a mid-abundant blood biomarker*. Proteome Sci, 2009. **7**: p. 15.
288. Espina, V., et al., *Reverse phase protein microarrays for monitoring biological responses*. Methods Mol Biol, 2007. **383**: p. 321-36.
289. Gallagher, R.I., et al., *Reverse phase protein microarrays: fluorometric and colorimetric detection*. Methods Mol Biol, 2011. **723**: p. 275-301.
290. Pierobon, M., et al., *Reverse-phase protein microarrays*. Methods Mol Biol, 2012. **823**: p. 215-35.
291. Zhou, H., et al., *Two-color, rolling-circle amplification on antibody microarrays for sensitive, multiplexed serum-protein measurements*. Genome Biol, 2004. **5**(4): p. R28.
292. Chen, Q., et al., *Amplified in breast cancer 1 enhances human cholangiocarcinoma growth and chemoresistance by simultaneous activation of Akt and Nrf2 pathways*. Hepatology, 2012. **55**(6): p. 1820-9.
293. MacBeath, G. and S.L. Schreiber, *Printing proteins as microarrays for high-throughput function determination*. Science, 2000. **289**(5485): p. 1760-3.
294. Iwaki, K. and Y. Hayashi, *[Method for estimating the precision and detection limit for ELISA]*. Nihon Yakurigaku Zasshi, 2009. **134**(4): p. 207-11.
295. van den Heuvel, E., *Estimation of the limit of detection for quantal response bioassays*. Pharm Stat, 2011. **10**(3): p. 203-12.
296. Huang, S., T. Wang, and M. Yang, *The Evaluation of Statistical Methods for Estimating the Lower Limit of Detection*. Assay Drug Dev Technol, 2012.
297. Longford, N.T., *Handling the limit of detection by extrapolation*. Stat Med, 2012. **31**(26): p. 3133-46.
298. Xue, Y.J., et al., *An integrated bioanalytical method development and validation approach: case studies*. Biomed Chromatogr, 2012. **26**(10): p. 1215-27.
299. JG, W., *Protein Microarrays: Reduced Autofluorescence and improved LOD*. ENG Life Sci, 2010. **10**(2): p. 103-108.
300. Kricka, L.J., *Interferences in immunoassay--still a threat*. Clin Chem, 2000. **46**(8 Pt 1): p. 1037-8.
301. Martins, T.B., et al., *Heterophile antibody interference in a multiplexed fluorescent microsphere immunoassay for quantitation of cytokines in human serum*. Clin Diagn Lab Immunol, 2004. **11**(2): p. 325-9.
302. Tate, J. and G. Ward, *Interferences in immunoassay*. Clin Biochem Rev, 2004. **25**(2): p. 105-20.
303. Pflieger, C., N. Schloot, and F. ter Veld, *Effect of serum content and diluent selection on assay sensitivity and signal intensity in multiplex bead-based immunoassays*. J Immunol Methods, 2008. **329**(1-2): p. 214-8.

304. Valentin, M.A., et al., *Validation of immunoassay for protein biomarkers: bioanalytical study plan implementation to support pre-clinical and clinical studies*. J Pharm Biomed Anal, 2011. **55**(5): p. 869-77.
305. Ellington, A.A., et al., *Measurement and quality control issues in multiplex protein assays: a case study*. Clin Chem, 2009. **55**(6): p. 1092-9.
306. Wood, B.A., et al., *Microsphere immunoassay for the detection of cytokines in domestic cat (*Felis catus*) plasma: elevated IL-12/23 in acute feline immunodeficiency virus infections*. Vet Immunol Immunopathol, 2012. **145**(3-4): p. 604-10.
307. Binnicker, M.J., D.J. Jespersen, and J.A. Harring, *Evaluation of three multiplex flow immunoassays compared to an enzyme immunoassay for the detection and differentiation of IgG class antibodies to herpes simplex virus types 1 and 2*. Clin Vaccine Immunol, 2010. **17**(2): p. 253-7.
308. Dietrich, H., et al., *Safety, tolerability, and pharmacokinetics of a single dose of pasireotide long-acting release in healthy volunteers: a single-center Phase I study*. Eur J Endocrinol, 2012. **166**(5): p. 821-8.
309. Elshal, M.F. and J.P. McCoy, *Multiplex bead array assays: performance evaluation and comparison of sensitivity to ELISA*. Methods, 2006. **38**(4): p. 317-23.
310. Leng, S.X., et al., *ELISA and multiplex technologies for cytokine measurement in inflammation and aging research*. J Gerontol A Biol Sci Med Sci, 2008. **63**(8): p. 879-84.
311. Knight, P.R., et al., *Development of a sensitive microarray immunoassay and comparison with standard enzyme-linked immunoassay for cytokine analysis*. Shock, 2004. **21**(1): p. 26-30.
312. Viegi, G., et al., *Definition, epidemiology and natural history of COPD*. Eur Respir J, 2007. **30**(5): p. 993-1013.
313. Espinosa de los Monteros, M.J., et al., *Variability of respiratory symptoms in severe COPD*. Arch Bronconeumol, 2012. **48**(1): p. 3-7.
314. Tashkin, D.P., et al., *Lung function and respiratory symptoms in a 1-year randomized smoking cessation trial of varenicline in COPD patients*. Respir Med, 2011. **105**(11): p. 1682-90.
315. Agusti, A., et al., *Night-time symptoms: a forgotten dimension of COPD*. Eur Respir Rev, 2011. **20**(121): p. 183-94.
316. Voll-Aanerud, M., et al., *Respiratory symptoms in adults are related to impaired quality of life, regardless of asthma and COPD: results from the European community respiratory health survey*. Health Qual Life Outcomes, 2010. **8**: p. 107.
317. Celli, B.R., et al., *Predictors of Survival in COPD: more than just the FEV1*. Respir Med, 2008. **102 Suppl 1**: p. S27-35.
318. van Dijk, W.D. and T.R. Schermer, *Change in FEV1 over time in COPD*. N Engl J Med, 2011. **365**(26): p. 2540; author reply 2541.
319. Celli, B.R. and R.J. Halbert, *Point: should we abandon FEV(1)/FVC <0.70 to detect airway obstruction? No*. Chest, 2010. **138**(5): p. 1037-40.
320. Mohamed Hoesein, F.A., P. Zanen, and J.W. Lammers, *Lower limit of normal or FEV1/FVC < 0.70 in diagnosing COPD: an evidence-based review*. Respir Med, 2011. **105**(6): p. 907-15.
321. Kent, B.D., P.D. Mitchell, and W.T. McNicholas, *Hypoxemia in patients with COPD: cause, effects, and disease progression*. Int J Chron Obstruct Pulmon Dis, 2011. **6**: p. 199-208.

322. Krieger, A.C., et al., *Respiratory disturbance during sleep in COPD patients without daytime hypoxemia*. *Int J Chron Obstruct Pulmon Dis*, 2007. **2**(4): p. 609-15.
323. Vonk-Noordegraaf, A., et al., *Early changes of cardiac structure and function in COPD patients with mild hypoxemia*. *Chest*, 2005. **127**(6): p. 1898-903.
324. Sabit, R., et al., *The effects of hypoxia on markers of coagulation and systemic inflammation in patients with COPD*. *Chest*, 2010. **138**(1): p. 47-51.
325. Burtscher, M., et al., *Intermittent hypoxia increases exercise tolerance in patients at risk for or with mild COPD*. *Respir Physiol Neurobiol*, 2009. **165**(1): p. 97-103.
326. Blasi, F. and E.E. Guffanti, *Chronic obstructive pulmonary disease in the elderly: identifying the knowledge gaps to support research and clinical practice guidelines*. *Curr Opin Pulm Med*, 2011. **17 Suppl 1**: p. S55.
327. Incalzi, R.A., et al., *From Global Initiative for Chronic Obstructive Lung Disease (GOLD) guidelines to current clinical practice : an overview of the pharmacological therapy of stable chronic obstructive pulmonary disorder*. *Drugs Aging*, 2006. **23**(5): p. 411-20.
328. Pierson, D.J., *Clinical practice guidelines for chronic obstructive pulmonary disease: a review and comparison of current resources*. *Respir Care*, 2006. **51**(3): p. 277-88.
329. Tusher, V.G., R. Tibshirani, and G. Chu, *Significance analysis of microarrays applied to the ionizing radiation response*. *Proc Natl Acad Sci U S A*, 2001. **98**(9): p. 5116-21.
330. Jee, Y., et al., *Upregulation of monocyte chemotactic protein-1 and CC chemokine receptor 2 in the central nervous system is closely associated with relapse of autoimmune encephalomyelitis in Lewis rats*. *J Neuroimmunol*, 2002. **128**(1-2): p. 49-57.
331. Deshmane, S.L., et al., *Monocyte chemoattractant protein-1 (MCP-1): an overview*. *J Interferon Cytokine Res*, 2009. **29**(6): p. 313-26.
332. de Boer, W.I., et al., *Monocyte chemoattractant protein 1, interleukin 8, and chronic airways inflammation in COPD*. *J Pathol*, 2000. **190**(5): p. 619-26.
333. Tanino, M., et al., *Increased levels of interleukin-8 in BAL fluid from smokers susceptible to pulmonary emphysema*. *Thorax*, 2002. **57**(5): p. 405-11.
334. Matsuura, H., et al., *Elevation of plasma eotaxin levels in children with food allergy*. *Nihon Rinsho Meneki Gakkai Kaishi*, 2009. **32**(3): p. 180-5.
335. Williams, T.J. and P.J. Jose, *Role of eotaxin and related CC chemokines in allergy and asthma*. *Chem Immunol*, 2000. **78**: p. 166-77.
336. Zietkowski, Z., et al., *Eotaxin-1 in exhaled breath condensate of stable and unstable asthma patients*. *Respir Res*, 2010. **11**: p. 110.
337. Krisiukeniene, A., et al., *Smoking affects eotaxin levels in asthma patients*. *J Asthma*, 2009. **46**(5): p. 470-6.
338. Paplinska, M., H. Grubek-Jaworska, and R. Chazan, *[Role of eotaxin in the pathophysiology of asthma]*. *Pneumonol Alergol Pol*, 2007. **75**(2): p. 180-5.
339. Hemelaers, L. and R. Louis, *[Eotaxin: an important chemokine in asthma]*. *Rev Med Liege*, 2006. **61**(4): p. 223-6.
340. Sabroe, I., et al., *Differential regulation of eosinophil chemokine signaling via CCR3 and non-CCR3 pathways*. *J Immunol*, 1999. **162**(5): p. 2946-55.
341. Ferland, C., et al., *IL-16 activates plasminogen-plasmin system and promotes human eosinophil migration into extracellular matrix via CCR3-chemokine-mediated signaling and by modulating CD4 eosinophil expression*. *J Immunol*, 2004. **173**(7): p. 4417-24.

342. Petrescu, F., S.C. Voican, and I. Silosi, *Tumor necrosis factor-alpha serum levels in healthy smokers and nonsmokers*. *Int J Chron Obstruct Pulmon Dis*, 2010. **5**: p. 217-22.
343. Franciosi, L.G., et al., *Markers of exacerbation severity in chronic obstructive pulmonary disease*. *Respir Res*, 2006. **7**: p. 74.
344. Pitsioui, G., et al., *Tumor necrosis factor-alpha serum levels, weight loss and tissue oxygenation in chronic obstructive pulmonary disease*. *Respir Med*, 2002. **96**(8): p. 594-8.
345. Singh, B., S. Arora, and V. Khanna, *Association of severity of COPD with IgE and interleukin-1 beta*. *Monaldi Arch Chest Dis*, 2010. **73**(2): p. 86-7.
346. He, J.Q., et al., *Associations of IL6 polymorphisms with lung function decline and COPD*. *Thorax*, 2009. **64**(8): p. 698-704.
347. Sharma, G., N.A. Hanania, and Y.M. Shim, *The aging immune system and its relationship to the development of chronic obstructive pulmonary disease*. *Proc Am Thorac Soc*, 2009. **6**(7): p. 573-80.
348. Akdis, C.A. and K. Blaser, *Mechanisms of interleukin-10-mediated immune suppression*. *Immunology*, 2001. **103**(2): p. 131-6.
349. Taylor, A., et al., *Mechanisms of immune suppression by interleukin-10 and transforming growth factor-beta: the role of T regulatory cells*. *Immunology*, 2006. **117**(4): p. 433-42.
350. Doe, C., et al., *Expression of the T helper 17-associated cytokines IL-17A and IL-17F in asthma and COPD*. *Chest*, 2010. **138**(5): p. 1140-7.
351. Miossec, P., *IL-17 and Th17 cells in human inflammatory diseases*. *Microbes Infect*, 2009. **11**(5): p. 625-30.
352. Korn, T., et al., *IL-17 and Th17 Cells*. *Annu Rev Immunol*, 2009. **27**: p. 485-517.
353. Zhang, J., et al., *Increased expression of CD4(+)IL-17(+) cells in the lung tissue of patients with stable chronic obstructive pulmonary disease (COPD) and smokers*. *Int Immunopharmacol*, 2013. **15**(1): p. 58-66.
354. Oppmann, B., et al., *Novel p19 protein engages IL-12p40 to form a cytokine, IL-23, with biological activities similar as well as distinct from IL-12*. *Immunity*, 2000. **13**(5): p. 715-25.
355. Hirahara, K., et al., *Signal transduction pathways and transcriptional regulation in Th17 cell differentiation*. *Cytokine Growth Factor Rev*, 2010. **21**(6): p. 425-34.
356. Ivanov, II, L. Zhou, and D.R. Littman, *Transcriptional regulation of Th17 cell differentiation*. *Semin Immunol*, 2007. **19**(6): p. 409-17.
357. Gosens, R., et al., *Muscarinic receptor signaling in the pathophysiology of asthma and COPD*. *Respir Res*, 2006. **7**: p. 73.
358. Pera, T., et al., *Cigarette smoke and lipopolysaccharide induce a proliferative airway smooth muscle phenotype*. *Respir Res*, 2010. **11**: p. 48.
359. Baraldo, S., et al., *Neutrophilic infiltration within the airway smooth muscle in patients with COPD*. *Thorax*, 2004. **59**(4): p. 308-12.
360. Kierszniewska-Stepien, D., et al., *Serum vascular endothelial growth factor and its receptor level in patients with chronic obstructive pulmonary disease*. *Eur Cytokine Netw*, 2006. **17**(1): p. 75-9.
361. Smith, D.J., et al., *Reduced soluble receptor for advanced glycation end-products in COPD*. *Eur Respir J*, 2011. **37**(3): p. 516-22.
362. Greaves, L.J. and L.A. Richardson, *Tobacco use, women, gender, and chronic obstructive pulmonary disease: are the connections being adequately made?* *Proc Am Thorac Soc*, 2007. **4**(8): p. 675-9.

-
363. Rahmanian, S.D., P.T. Diaz, and M.E. Wewers, *Tobacco use and cessation among women: research and treatment-related issues*. J Womens Health (Larchmt), 2011. **20**(3): p. 349-57.
364. Punturieri, A., et al., *Lung cancer and chronic obstructive pulmonary disease: needs and opportunities for integrated research*. J Natl Cancer Inst, 2009. **101**(8): p. 554-9.
365. Rosi, E. and G. Scano, *Cigarette smoking and dyspnea perception*. Tob Induc Dis, 2004. **2**(1): p. 35-42.
366. Celli, B., et al., *Sex differences in mortality and clinical expressions of patients with chronic obstructive pulmonary disease. The TORCH experience*. Am J Respir Crit Care Med, 2011. **183**(3): p. 317-22.
367. Fletcher, C.P., R., *The natural history of chronic bronchitis and emphysema*. New York: Oxford, 1976. **Pr**.
368. Barnes, P.J. and M.G. Cosio, *Characterization of T lymphocytes in chronic obstructive pulmonary disease*. PLoS Med, 2004. **1**(1): p. e20.
369. Spurrell, J.C., et al., *Human airway epithelial cells produce IP-10 (CXCL10) in vitro and in vivo upon rhinovirus infection*. Am J Physiol Lung Cell Mol Physiol, 2005. **289**(1): p. L85-95.
370. Tanni, S.E., et al., *Smoking status and tumor necrosis factor-alpha mediated systemic inflammation in COPD patients*. J Inflamm (Lond), 2010. **7**: p. 29.
371. Dentener, M.A., et al., *Differences in local versus systemic TNFalpha production in COPD: inhibitory effect of hyaluronan on LPS induced blood cell TNFalpha release*. Thorax, 2006. **61**(6): p. 478-84.
372. Sarioglu, N., et al., *Relationship between BODE index, quality of life and inflammatory cytokines in COPD patients*. Multidiscip Respir Med, 2010. **5**(2): p. 84-91.
373. Kusnezow, W., et al., *Antibody microarray-based profiling of complex specimens: systematic evaluation of labeling strategies*. Proteomics, 2007. **7**(11): p. 1786-99.
374. Miller, J.C., et al., *Antibody microarray profiling of human prostate cancer sera: antibody screening and identification of potential biomarkers*. Proteomics, 2003. **3**(1): p. 56-63.
375. Meany, D.L., et al., *Tyramide signal amplification for antibody-overlay lectin microarray: a strategy to improve the sensitivity of targeted glycan profiling*. J Proteome Res, 2011. **10**(3): p. 1425-31.
376. Chan, S.M., et al., *Protein microarrays for multiplex analysis of signal transduction pathways*. Nat Med, 2004. **10**(12): p. 1390-6.
377. Affymetrix, I., *Assay Qualifications*. http://www.panomics.com/products/luninex-assays/index.php?id=product_64, 2012.